Journal of Pharmacy and Pharmacology

The Pharmaceutical Society of Great Britain

British Pharmaceutical Conference
One Hundred and Seventh Meeting
Leeds, September 1970

Volume 22 Supplement December 1970

British Pharmaceutical Conference

LEEDS

September 14-18, 1970

CHAIRMAN

J. M. ROWSON

Journal of Pharmacy and Pharmacology

17 Bloomsbury Square, London, W.C.1.

Journal of Pharmacy and Pharmacology

British Pharmaceutical Conference

Supplement

Editor: D. W. Mathieson, B.Sc., Ph.D., F.R.I.C.
Press Editor: J. R. Fowler, B.Pharm., F.P.S.

December 1970 **Vol. 22**

SCIENCE PAPERS

SCIENCE PAPERS

J. Pharm. Pharmac., 1970, **22**, *Suppl.*, 1 S-7 S *Received February* 6, 1970

Science Papers

The compression properties of lactose

OYA ALPAR, J. A. HERSEY*, AND E. SHOTTON

*Department of Pharmaceutics, The School of Pharmacy, University of London, Brunswick Square, London, W.C.*1, *U.K.*

The tabletting characteristics of crystalline and spray dried lactose under direct compression have been examined together with the effect of particle size, shape and storage of the powders. The results indicated that the particle size had little effect, although there was a general tendency for the compact strength to increase as the particle size decreased. On the other hand, the particle shape and storage of the powder influenced the strength of the tablets and the force lost to the die wall. The 22 μm and 35 μm fractions of spray dried lactose—especially the latter—were almost entirely very regular spherical particles which resulted in the strongest tablets, whereas fractions below or above contained many more angular particles resulting in weaker tablets. Storage of the small particle size fraction of the crystalline material appeared to induce aggregation, and on compaction, a harder tablet was formed, accompanied by a decrease in the force lost to the die wall.

Lactose is widely used in tablet formulations, but little work has been reported in the literature on its compression characteristics. Higuchi, Elowe & Busse (1954) using a grade of crystalline lactose, measured the surface area, porosity, hardness and disintegration times of tablets compressed at various pressures. Subsequently, Gunsel & Lachman (1963) compared the use of similarly sized crystalline lactose and spray dried lactose in various formulations. They were able to demonstrate an increase in the tablet hardness when prepared from the formulation containing spray-dried lactose. Fell & Newton (1968) measured the tensile strength of tablets prepared from the two forms of lactose and showed that, for particles of 150–210 μm, the conventional crystalline lactose tablets were harder; for smaller sized fractions, the spray dried lactose tablets were harder. For both forms, the tablet strength increased as the particle size decreased.

Hersey, Bayraktar & Shotton (1967) previously reported on the effect of particle size on the strength of sodium chloride tablets prepared at several different pressure levels and it was anticipated that a similar approach would be useful in a comparison of the spray-dried and crystalline forms of lactose.

EXPERIMENTAL

Crystalline lactose and spray-dried lactose, which were hydrated, were size fractionated using a Lavino Alpine Air-Jet Sieve. For each material, a sub-sieve fraction

* Present address: Sandoz A.G., CH-4002 Basle, Switzerland.

was obtained by feeding the original material through a Gem fluid energy mill operating at 100 psig using a feed rate of about 5 g min^{-1}.

The size fractions were subjected to microscopic size analysis, moisture determination, apparent density and angle of repose determinations. Microscopic size analysis was by the British Standard method (No 3406 Part A, 1963). After allowing the fraction to equilibrate with the atmosphere, the moisture content was determined immediately before compression using the Cahn Gram Electrobalance as described by Shotton & Rees (1966). The bulk density of the powders was determined by pouring a sample, at 45°, into a tared 25 ml measuring cylinder. The angle of repose, was measured with reseived material by the tilting table method described by Train (1958).

After sieving, some material from each size fraction was immediately examined as above and then compressed, whilst an aliquot of the crystalline sample was stored in a screw-capped jar for twelve months before testing. The stored material was subsequently resieved before testing as the crystalline lactose had caked badly. Comparative experiments with stored spray dried lactose showed no visible caking had occurred. Material sufficient to produce a 0·4 cm long tablet in the 1 cm diameter die at zero porosity, 0·6895 g, was introduced into the die cavity by hand and compressed using a power driven tablet machine instrumented in a manner similar to that described by Shotton & Ganderton (1960). The apparent density of the tablet was obtained from the dimensions of the ejected tablet and the crushing strength of the tablet immediately determined by the method of Shotton & Ganderton (1960).

RESULTS

For the sieved fractions, the moisture content and the mean size obtained by microscopic examination is given in Table 1 and these were unaffected by storage. The relative densities of tablets prepared under different pressures is given in Table 2.

Table 1. *Particle size of fractions and moisture content.* Average of three determinations

Aperture size of sieves (μm) Milled		Crystalline lactose			Spray dried lactose	
		Mean particle size (μm)	Moisture content % Stored	Fresh	Mean particle size (μm)	Moisture content %
		2	4·65	4·81	2	4·74
—32		22	3·15	5·00	22	5·00
+32	—40	34	4·92	5·01	35	4·92
+40	—45	43	—	4·47	41	4·58
+45	—63	59	4·57	4·47	54*	—
+63	—76	69*	—	—	71	4·66
+76	—105	82	4·35	—	90*	—
+105	—125	110	4·14	4·50	119	4·60

* Mean sieve aperture
(Lactose monohydrate contains 5·0014% Water)

To compare die wall friction effects of the different materials, two of the fractions of spray dried, freshly sifted and stored crystalline lactose were chosen. These were the +32/−40 μm size fraction and the +105/−125 μm size fraction. Results of force lost to die wall for these powders are plotted respectively in Fig. 1A and B. Results of ejection force for the former size are given in Fig. 2A and for the latter size in Fig. 2B.

Table 2. *Bulk densities of powders and relative* densities of tablets.* Average of 5 results at arbitrary pressures PI–PIV.

Substance	Lactose														
	Crystalline			Crystalline			Crystalline			Crystalline			Crystalline		
	S.D.	Fresh	Stored	S.D.	Fresh	Stored	S.D.	Fresh	Stored	S.D.	Fresh	Stored	S.D.	Fresh	Stored
Aperture size of sieves (μm)	Bulk density of powder			PI			PII			PIII			PIV		
							Average compression force (kg) †								
	0	0	0	666	494	592	895	782	874	1362	1213	1328	1800	1763	1859
Milled	0·49	0·31	0·36	0·74	0·74	0·74	0·79	0·78	0·77	0·83	0·83	0·83	0·86	0·86	0·87
−32	0·56	0·44	0·40	0·71	0·74	0·75	0·76	0·79	0·77	0·81	0·82	0·82	0·84	0·85	0·86
+32 −40	0·64	0·65	0·61	0·75	0·75	0·74	0·79	0·78	0·78	0·83	0·82	0·82	0·85	0·86	0·86
+40 −45	0·70	0·71	—	0·75	0·75	—	0·80	0·79	—	0·84	0·82	—	0·87	0·87	—
+45 −63	—	0·73	0·66	—	0·75	0·74	—	0·79	0·78	—	0·83	0·82	—	0·88	0·86
+63 −76	0·70	—	—	0·74	—	—	0·79	—	—	0·83	—	—	0·87	—	0·87
+76 −105	—	—	0·67	—	—	0·75	—	—	0·79	—	—	0·83	—	—	—
+105 −125	0·70	0·74	0·72	0·75	0·75	0·75	0·79	0·79	0·80	0·83	0·84	0·85	0·88	0·88	0·89

S.D. = Spray dried
Stored = Powders stored for 12 months
Fresh = Powders used immediately after sieving
• = Apparent densities of tablets based on physical measurements of tablets.
(True density of lactose = 1·525)
†Comparative range in S.I. ≈ 4·5 — 17·5 kN

In Fig. 3A-C results for the strength of the tablets prepared from the different particle size fractions at the four pressure levels are given for freshly sifted crystalline lactose, the stored crystalline lactose and for the spray-dried material respectively. In each case, the result given in the mean of five determinations.

DISCUSSION

The method of moisture determination of Shotton & Rees (1966) used measures the free and bound water in the lactose sample. Since lactose is in the form of the monohydrate, it contains about 5% bound water. The results in Table 1 indicate that there was no free water in the lactose samples used and the lower percentages indicate a content of anhydrous lactose in many of the fractions consistent with the findings of Gunsel & Lachman (1963).

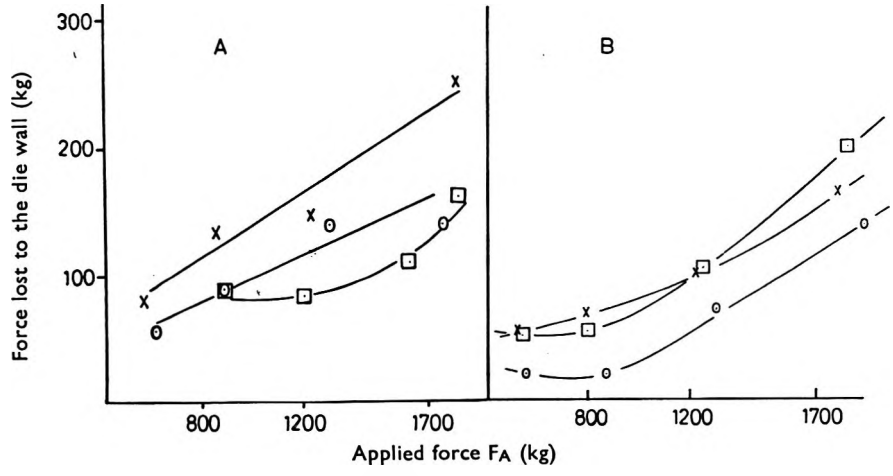

FIG. 1. Effect of applied force on the force lost to the die wall. A. Size fraction +32/−40 μm. B. Size fraction +105/−125 μm. × Crystalline lactose—freshly sieved. ○ Crystalline lactose—stored. □ Spray dried lactose.

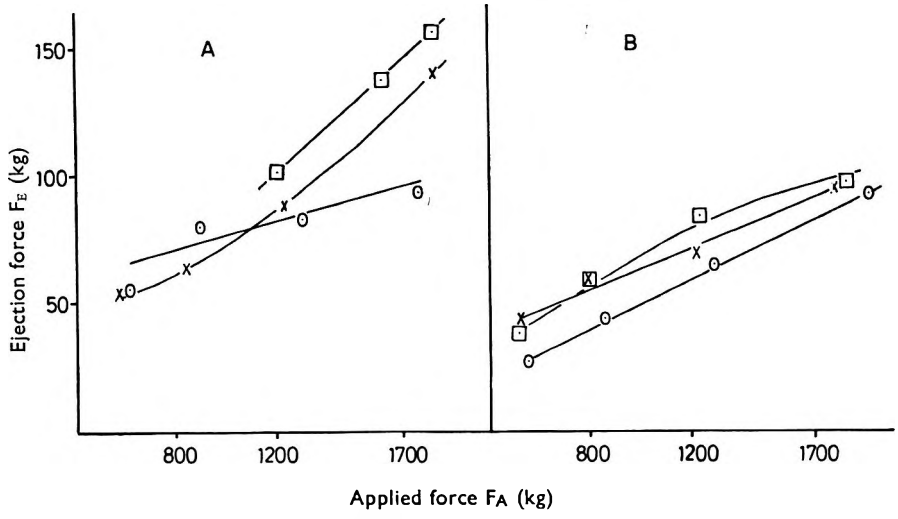

FIG. 2. Effect of applied force on the ejection force. A. Size fraction $+32/-40\,\mu$m. B. Size fraction $+105/-125\,\mu$m. × crystalline lactose—freshly sieved. ○ Crystalline lactose—stored. □ Spray dried lactose.

The bulk density before compaction is dependent upon the previous history of the lactose. The stored crystalline lactose fractions after sieving exhibited a lower density than the freshly sifted crystalline material. This suggests that the material formed loose aggregates during storage and which were not completely broken down by sieving. Evidence of aggregation is also inferred from the generally higher angles of repose of the stored material compared with the freshly sifted crystalline lactose. When the stored material was mounted in liquid paraffin aggregation was not seen under the microscope, indicating that the process completely destroyed the aggregate structure.

Comparison of Fig. 1A and 1B shows that spray dried lactose has a lower die wall friction at $+32/-40\,\mu$m size fraction than the freshly sieved crystalline material whereas at $+105/-125\,\mu$m size fraction there is little difference between the two materials. At both chosen particle size levels, the die wall friction is lower using stored material than when using freshly sieved crystalline material. These observations may also be explained by the shape difference between the particles. At 35 μm, the spray dried material consists almost entirely of spherical particles (Fig. 4). This fraction, which gives the lowest angle of repose, Table 3, will have a small contact area with the die wall and thus frictional resistance will be smaller than for the irregular crystalline variety. At the higher size range, the spray-dried material is largely crystalline and there is therefore little difference between the two fractions. The stored crystalline fractions consisting of loosely bound agglomerates will also have less die wall contact and therefore has a lower frictional resistance than the freshly-seived material at both size fractions.

Results similar to those occuring and the die wall during compression occur on ejection of the compacts (Fig. 2A and B) except that the 35 μm spray-dried fraction has a much higher ejection force than might be expected. This may be due to the fact that the spherical particles on compaction will fracture, thereby increasing the frictional resistance on subsequent ejection.

Figs 3A-C show the effect of particle size on the strength of lactose compacts

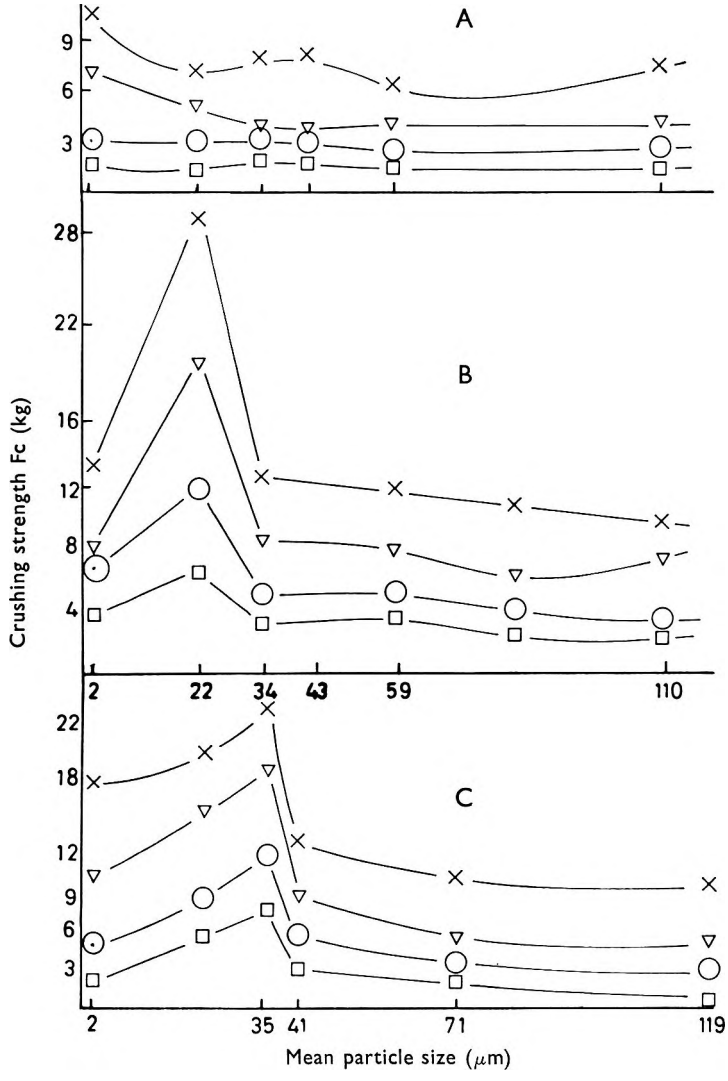

FIG. 3. Effect of mean particle size on the crushing strength of A, freshly sieved, and B, stored crystalline and C, spray dried lactose tablets, Machine setting to arbitrary pressures of □ PI. ○ PII. ▽ PIII. × PIV.

Table 3. *Angles of repose of various lactose fractions (Means of 7 experiments)*

Aperture size of sieves (μm)		Angle of repose °		
		Crystalline stored	Crystalline fresh	Spray dried
Milled		(no flow)	(no flow)	(no flow)
−32		(no flow)	(no flow)	40
+32	−40	50	46	37
+40	−45	—	42	39
+45	−63	65	41	—
+63	−76	—	—	38
+76	−105	45	—	—
+105	−125	42	44	40

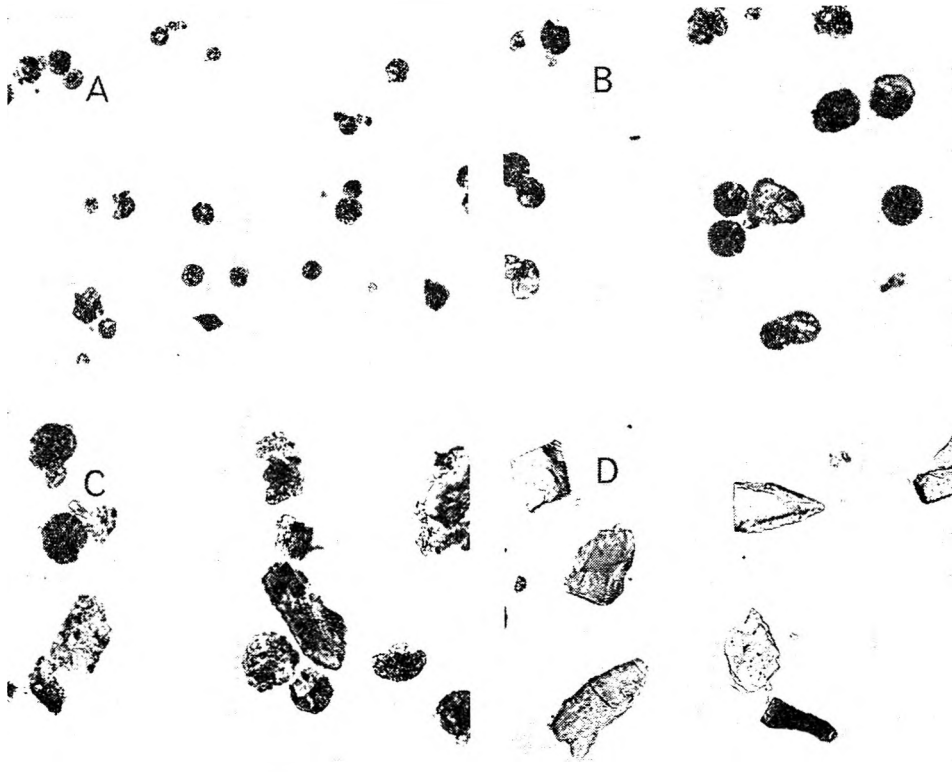

FIG. 4. Photomicrographs of lactose: spray dried 22 μm (A), 35 μm (B), 41 μm (C) and crystalline 34 μm.

prepared at different pressures. Fig. 3A shows that with the freshly-sieved material, particle size has little effect, although there is a general tendency for the compact strength to increase as the particle size is reduced. This tendency is also shown in Fig. 3B for stored lactose and Fig. 3C for spray-dried material, however, in both of these cases, a maxima is observed. The strength of tablets prepared from spray-dried material (Fig. 3C) is greater than that of tablets prepared from freshly sieved crystalline lactose, as found by Gunsel & Lachman (1963) and Fell & Newton (1968), but is less than the strength of tablets prepared from stored, crystalline material (Fig. 3B).

This increase of strength shown by the stored-lactose may be due to the weak agglomerate formation as shown by bulk-density and angle of repose determinations. These loose agglomerates are deemed equivalent to weak granules, which occupy a larger volume of the die with fewer contacts at the die wall. On compression, these aggregates must break down and there will be much local shear within the particle mass leading to a stronger tablet. Since there are also fewer die wall contacts, the effective frictional force will also be reduced (Fig. 1A and B) and the compression force will be more advantageously utilized. The very high value for the crushing strength of the 22 μm stored fraction is an exaggeration of these effects possibly due to the tendency of this fraction to agglomerate more readily than the other size fractions. In Table 2, it can be seen that this fraction has a lower bulk density than either of the other two powders examined, however, on compaction, this material forms, at least, equally dense tablets.

Further examination of Table 2 shows that the 2 μm fraction of stored material is in fact more dense than the freshly sieved variety, which suggests that this material does not aggregate, or conversely, that the freshly sifted material is more readily agglomerated and on storage, these agglomerates break down. Thus it should be anticipated that there will be little difference between these two fractions at the 2 μm level, as shown by Fig. 3A and B. Loss of aggregate structure on milling spray-dried material, also accounts for the fact that similar strength values for 2 μm spray-dried fraction material.

Examination of the effect of mean compaction force on the crushing strength of the 2 μm fraction of freshly sieved lactose produced the strongest tablets possibly due to the high surface area available for bonding. On storage it would appear that with the 22 μm size fraction, and to a decreasing extent with increasing particle size, the tendency to form loose aggregates is manifest in a stronger compact. With the spray-dried material, departures from sphericity either above or below the 35 μm spherical particle used in this batch is consistent with a decrease in tablet strength. Fig. 4A–D is included so that the extent of the change of particle shape between the different fractions can be seen. The 22 μm (Fig. 4A) and 35 μm (Fig. 4B) spraydried particles are almost entirely spherical, but the 41 μm spraydried particles (Fig. 4C) contained a large proportion of angular material similar to the crystalline lactose shown in Fig. 4D.

With lactose powder, it appears that particle shape, whether as spheres or angular crystals, or weak aggregates formed on storage, has a considerable effect upon tablet strength.

Acknowledgements

We should like to thank British Whey Products Ltd. and McKessor-Robbins Ltd., for the samples of crystalline and spray-dried lactose used in this investigation and the Turkish Government for the financial support of one of us (H.O.A.) which enabled this work to be undertaken. We also wish to thank Mr. P. Herman, Sandoz Ltd. for the photographs in Fig. 4.

REFERENCES

FELL, J. T. & NEWTON, J. M. (1968). *J. Pharm. Pharmac.*, **20**, 657–658.
GUNSEL, W. C. & LACHMAN, L. (1963). *J. pharm. Sci.*, **52**, 178–182.
HERSEY, J. A. and BAYRAKTAR, G. & SHOTTON, E. (1967). *J. Pharm. Pharmac.*, **19**, 24S–30S.
HIGUCHI, T. ELOWE, L. N. & BUSSE, L. W. (1954). *J. Am. pharm. Ass.*, 43, 685–689.
SHOTTON, E. & GANDERTON, D. (1960). *J. Pharm. Pharmac.*, **12**, *Suppl.*, 87T–92T.
SHOTTON, E. & REES, J. E. (1966). *Ibid.*, **18** Suppl., 160S–167S.
TRAIN, D. (1958). *Ibid.*, **10**, 127T–135T.

J. Pharm. Pharmac., 1970, **22**, *Suppl.*, 8 S–10 S

Received March 18, 1970

SHORT COMMUNICATION

The compaction of magnesium carbonate

N. A. ARMSTRONG AND R. F. HAINES-NUTT

Welsh School of Pharmacy, University of Wales Institute of Science and Technology, Cardiff, Wales, U.K.

Compaction is essentially a two-stage process. As pressure is applied, re-arrangement of powder particles takes place within the die, so that large voids are filled and interparticulate friction may be sufficient to cause fragmentation of the weaker particles. Further increase in pressure is believed to cause elastic and plastic deformation of the particles, which results in the particles being brought into close physical contact; this in turn may permit interparticulate bonding by a "cold welding" mechanism (cf. Higuchi, Rao & others, 1953; Armstrong & Griffiths, 1970).

We have observed that compacts of magnesium carbonate, when placed in water, disintegrated rapidly into their component particles, presumably due to breakdown of interparticulate bonds by a liquid of high dielectric constant. We therefore considered that if particles of known size were compressed and then allowed to disintegrate, evidence of fragmentation or interparticulate bonding might be obtained.

Experimental

Material. Heavy magnesium carbonate, B.P. grade, dried at 70° to constant weight.

Particle size analyses were made using a Coulter Counter, model A Industrial, fitted with a 200 μm orifice tube. A mixture of 0·9% sodium chloride and 0·1% Dispersol T was used as electrolyte.

The compacts of magnesium carbonate, weighing 0·8 g, were prepared in a 1·27 cm stainless steel die, using an Apex model A 14 hydraulic press. The surface area of the compacts was determined by low temperature nitrogen adsorption using a Perkin–Elmer–Shell, model 212D Sorptometer, surface contamination being removed by degassing in a stream of helium (2 ml min^{-1}) for 18 h at 60°. Compacts were disintegrated by adding them to water (approximately 20 ml) and allowing the mixture to stand overnight. The resultant suspension was diluted and particle size analyses were again made; because of the low solubility of magnesium carbonate, size changes due to dissolution were ignored.

Results and discussion

The increase and subsequent decrease of surface area of magnesium carbonate with increase in compaction pressure described by earlier workers was noted, a maximum value of surface area being obtained at about 125 MNm^{-2}. A plot of the geometric mean diameter against compaction pressure indicated that size reduction takes place at low compaction pressures (i.e. up to about 140 MNm^{-2}), but further increase in pressure causes a rise in geometric mean diameter. This is emphasized by calculating the fraction of particles before and after compression which fall into two arbitrarily chosen particle size ranges, namely 20–30 μm and 90–100 μm. The percent weight fraction of the powder falling into each of these size ranges plotted against compaction pressure is shown in Fig. 1. This indicates that at pressures up to approximately 125 MNm^{-2}, the number of large particles shows a gradual reduction, while the

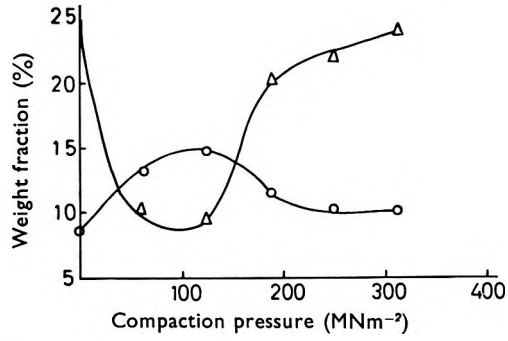

FIG. 1. Percent weight fraction—compaction pressure profile of two size fractions of magnesium carbonate; ○, 20–30; △, 90–100 μm.

number of small particles shows an increase, indicative of fragmentation. Above 125 MNm^{-2} a further increase in compression pressure reverses these trends, giving strong evidence that at such pressures, particle aggregation is the predominant process. The maxima and minima of the mean diameter–compression pressure curves were found to occur at approximately the same compression pressure as the maximum value of the surface area–compression pressure curve.

In an attempt to obtain further correlation between compaction pressure, surface area and particle diameter, magnesium carbonate was sifted on an Alpine Airjet sieve, laboratory model into the following fractions: 33–45, 53–63, 75–89, 104–124 μm. The particle size distribution of each fraction was determined by Coulter counter and the geometric mean diameter calculated. Each fraction was then compressed at 62·5 MN m^{-2} and the surface area and mean particle size of the resultant compact measured. The mean particle diameter of all fractions is reduced after compression at 62·5 MNm^{-2}.

Mean particle diameter before compression (μm) ..	39·5	61·5	87·0	121·8
Mean particle diameter after compression (μm) ..	32·2	52·0	64·5	89
Surface area (m^2g^{-1})	10·35	9·97	9·73	9·34

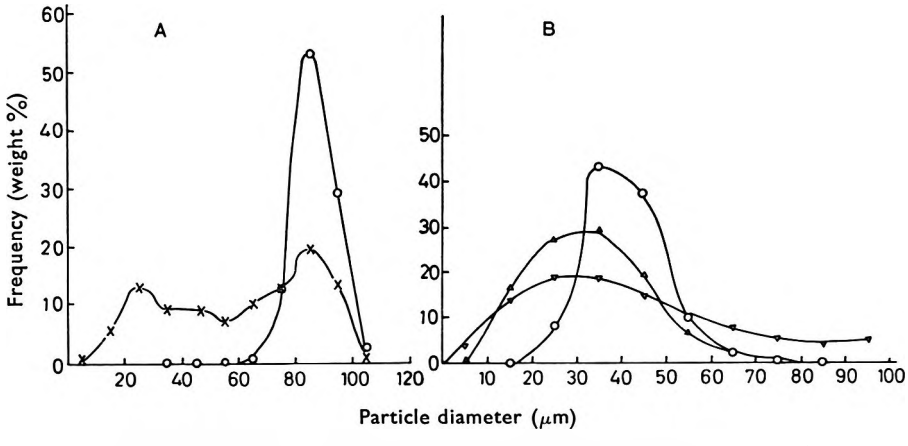

FIG. 2. Particle size distribution of (A) a nominal 75–89 μm fraction (B) a nominal 33–45 μm fraction of magnesium carbonate; ○, before compression; ×, ▲ after compression at 62·5 MNm^{-2}; ▼, after compression at 250MNm^{-2}.

As at low pressures, surface area increases with compression pressure, fragmentation is probably the only significant factor affecting particle size. Particle size reduction is especially notable with the larger particle sizes, this being emphasized by Fig. 2A which shows the particle size distribution within a nominal 75–89 μm fraction before and after compression at 62·5 MNm^{-2}.

Samples of the 33–45 μm fraction were also compressed at 250 MNm^{-2} and the mean particle diameter after compression determined. Fig. 2B demonstrates that in this case, as with the 75–89 μm fraction, fragmentation occurs at low compression pressures, the geometric mean diameter decreasing from 39·5 to 32 μm. At higher compression pressures, both fragmentation and aggregation probably occur, thereby rendering meaningful results more difficult to obtain. Nevertheless, Fig. 2B shows a significant increase in the number of large particles, the geometric mean diameter rising to 38·5 μm.

One of us (R. F. H.-N) thanks the Science Research Council for the award of a research studentship.

REFERENCES

ARMSTRONG, N. A. & GRIFFITHS, R. V. (1970). *Pharm. Acta Helv.* In the press.

HIGUCHI, T., RAO, A. N., BUSSE, L. W., SWINTOSKY, J. V. (1953). *J. Am. pharm. Ass. (Sci. Edn)*, **42**, 194–200.

J. Pharm. Pharmac., 1970, **22**, *Suppl.*, 11 S–16 S *Received March* 9, 1970

Temperature changes occurring during the compression and recompression of solids

D. N. TRAVERS AND M. P. H. MERRIMAN

School of Pharmacy, City of Leicester Polytechnic, The Newarke, Leicester, U.K.

Measurements of the temperature rise occuring on compression, recompression and relaxation of compacts formed from Asagran, sodium chloride and boric acid have been made by means of thermocouples inserted into the compressed materials. There are marked differences in temperature rise for the different compacts when compressed to a final force of 50 kN (5 tons). With all compacts there was a rise in temperature on initial compression and a fall in temperature on relaxation. The rise could be separated into two components —that due to compact formation plus a further rise due to its elastic compression. The fall in temperature is thought to result on release of the strain energy stored in the compact. The rise in temperature on recompression followed by the fall of relaxation could be repeated many times on the same compact. Both rise and fall were directly proportional to the final compression force used. The fall on relaxation appeared to be numerically less than the rise on recompression for compacts of boric acid and Asagran. Lubrication of Asagran with magnesium stearate had little effect on the temperature rises.

Compressed tablets examined immediately after manufacture are often warm especially if produced on a high speed rotary machine. This thermal effect seems to have attracted little attention.

Nelson, Busse & Higuchi (1955) predicted a temperature rise of about 5° C during the formation of a sulphathiazole tablet. Hanus & King (1968), using thermochromic indicators, suggested that the rise in temperature on hard compression of sodium chloride could be as much as 30° C; however, thermometric measurements on ejected tablets showed the rise to be far less.

No attempts have been made to measure temperature rise by means of thermocouples placed within the tablet, although Juslin (1969) has made use of them to measure temperature rise on the upper and lateral surfaces of tablets during compression. Some preliminary results obtained by using thermocouples within compacts are now described.

EXPERIMENTAL

The equipment used is shown diagrammatically in Fig. 1. A commercial flat-faced punch and die assembly (1·59 cm d) was used with the die annealed so that a hole (1 mm d) could be drilled through the wall. It was then rehardened and tempered. Thermocouples were constructed of two 30 cm lengths of enamelled copper wire (0·101 mm d) bridged by one 8 cm length of insulated Eureka wire (0·127 mm d). The junctions were formed using a capacitance discharge welder (Spembly Technical Products Ltd.).

Exactly half of a weighed quantity of the substance to be compressed was then poured into the die with the lower punch in position. One junction was pushed through the hole so that the junction was centrally placed and the remainder of the

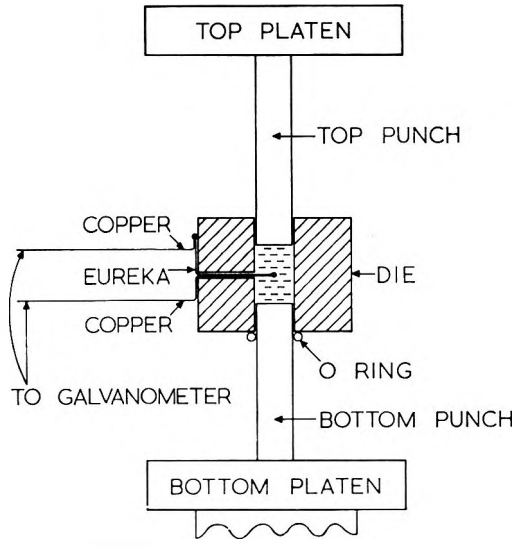

FIG. 1. The punch and die assembly.

material poured into the die. After placing the top punch into position, the assembly was placed between the platens of a C.30 manually operated hydraulic press (Research and Industrial Instruments Co. Ltd.). The remaining junction was fixed in contact with the die wall using a small piece of plasticine. The two copper wires were connected to a BB 40 galvanometer forming part of a direct recording oscillograph (Honeywell 1706 Visicorder). This symmetrical arrangement avoided the use of soldered connections or terminal blocks which can often give rise to troublesome thermal e.m.f.s. There was no detectable net e.m.f. when the copper wires were connected to a sensitive valve voltmeter of full-scale deflection 100 μV.

Thermocouples were calibrated before use by placing the junctions in separate beakers of water at room temperature. The galvanometer spot was then made coincident with a "marker" spot provided from a mirror within the recorder. A calibration curve was constructed by raising the temperature of one beaker of water by 1° C intervals and plotting the galvanometer deflection against the temperature difference of the two junctions up to a final difference of 20° C. The calibration curve was nearly linear and had a slope of 2·4 mm/°C. No differences were apparent when three such assemblies were calibrated and when thermocouples were constructed in the same way from identical lengths of wire, it was assumed that they had the same characteristics.

Measurement of temperature rise on compression

This was made when the compact was formed by compression with the recorder chart speed of 6 mm s^{-1}; the heating and cooling curves obtained are like those in Fig. 2, temperature axes being added using the calibration graph. The undulating form of the temperature rise is due to the several strokes of the ram required to reach the ultimate compression force—usually 50 kN (5 tons). When the compact was removed on completion of the measurements, the thermocouple had usually retained its central position and it did not appear to interfere with the formation of a good sound compact.

Thermal diffusivity of the compacts

A preliminary estimate of the relative thermal diffusivities of compacts formed from the materials used was obtained in the following way. Compacts of the same thickness were prepared by compression to 50 kN. These were taken in turn and one junction of the thermocouple assembly glued to one face while the other junction was immersed in water at room temperature. The opposite face of the compact was pressed in contact with a hotplate at approximately 70° ± 5° C using a thin glass rod to maintain light pressure. A trace of the rise in temperature of the far face could thus be obtained, its slope being taken as a measure of the thermal diffusivity (Table 1).

Table 1. *Rise in temperature of compacts*

	Thickness of compact mm	Rise in temperature of compact face °C s^{-1}
Asagran	4·56	0·052
Boric acid	4·69	0·176
Sodium chloride	4·76	0·41

Materials

The substances chosen for investigation were Asagran, a proprietary form of acetylsalicylic acid, Monsanto Chemicals Ltd., sodium chloride and boric acid both as crystalline B.P. material. These were not treated further except that some samples were prepared by shaking the materials with 2% w/w of magnesium stearate for use as a lubricant.

RESULTS AND DISCUSSION

Interpretation of the traces

Asagran (Fig. 2A) shows an initial temperature rise on compression (a-c) followed by a slow fall (c, d) as heat leaks out into the punch and die. To keep the trace within a reasonable length, the Visicorder was stopped at intervals until the spot returned to the base line. The true temperature rise was found by graphical extrapolation of the cooling curve to cut a perpendicular erected midway through the period of observation.

Release of the compression force after the compact had returned to room temperature led to in every case a rapid fall in temperature (e.g. d, e in fig. 2A) followed by a slow rise as heat leaked back into the compact. On recompression to a force of 50 kN, a rise in temperature again occurred but to a value lower than the initial rise. On relaxation a fall to a value similar to that of the first relaxation was noted. The temperature rise and fall on recompression and relaxation could be reproduced indefinitely and the process would seem to be analogous to the adiabatic compression and expansion of a gas.

We would suggest that the temperature rise on initial compression can be separated into two components: (1) that associated with the heat of formation of the compact and probably due to granule friction, plastic deformation and bonding; (2) that associated with the storage of strain energy within the formed compact, energy which is largely recovered when the compression force is removed. If the compact has cooled to room temperature then a fall in temperature results when the compact relaxes. The slope of the heating curve on initial compression changes significantly at b (Fig. 2A)

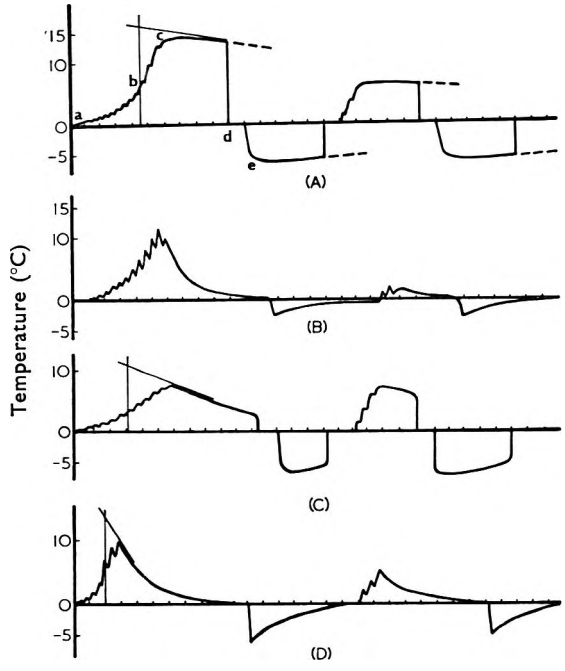

FIG. 2. Oscillograph traces resulting on compression, recompression and relaxation of unlubricated compacts (approximately half actual size). Compression force 50 kN. Time scale in s. (A) Asagran 2·0 g., (B) Sodium chloride 2·0 g., (C) Boric acid 2·0 g., (D) Asagran 0·5 g.

although pressure was applied at a constant rate. This rise can be attributed to compact formation while the further rise b—c is due to its compression.

The trace for sodium chloride (Fig. 2B) shows the same effects but because the thermal diffusivity of its compact is much greater than that of an Asagran compact (Table 1), there is a very rapid fall to room temperature. Although the slope is too steep for graphical extrapolation as used in Fig. 2A to be used here, the rise in temperature would appear to be comparable with the results obtained by Hanus & King (1968). It is likely that the temperature rise on recompression is related to the strain energy per unit weight stored in the compact, the low temperature rise on recompression of sodium chloride would then indicate a correspondingly low value for this quantity. It is known (Ridgway, Glasby & Rosser, 1969) that sodium chloride crystals have a high value of Young's modulus while that for aspirin crystals is low. Provided the compacts have similar properties, a sodium chloride compact would thus store less energy than one of aspirin when compressed with the same force.

Boric acid, sometimes used as a lubricant for soluble tablets, has crystals which are slippery. The strain energy contribution to the temperature rise on initial compression is a large part of the whole temperature rise and the rise due to compact formation is only about 2° C (Fig. 2C). The low interparticulate friction probably accounts for the low temperature of formation.

Temperature rise or fall on recompression or relaxation

These are plotted against the compression force for all three substances in Fig. 3A and B. The results support the observation of Hanus & King (1968) that temperature rise is directly proportional to compression force. Since these authors used calori-

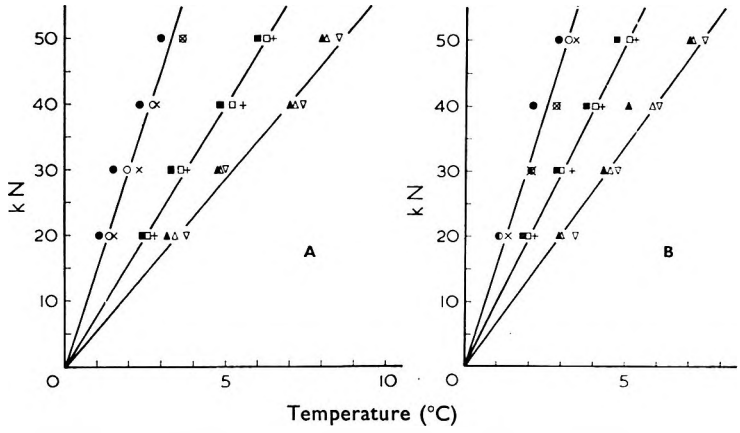

FIG. 3. A. Temperature rise attained on recompression v. compression force. B. Temperature fall on relaxation v. compression force. All compacts were unlubricated. Measurements were made on three separate compacts. Compact weight was always 2·0 g. Sodium chloride: ●○× Asagran: ■□+. Boric acid: ▲△▽

metric measurements on ejected tablets, they obtained the net temperature rise on formation and not the rises on compression or the fall on relaxation.

For boric acid and Asagran compacts the temperature fall on relaxation is always less than the rise on recompression indicating that only a proportion of the strain energy is recovered. We would predict that the compression force versus punch displacement curves for both these substances would show pronounced hysteresis loops representing the energy which is not recovered on relaxation. The high thermal diffusivity and small temperature changes of sodium chloride compacts make difficult any conclusion about the magnitude of the temperature rise and fall on its recompression and relaxation.

The effect of compact size and lubrication

The effect of varying the weight of the compacts is shown in Table 2. Although some differences in the temperatures of formation, recompression and relaxation occur, these are not pronounced and can be attributed to experimental and extrapolation

Table 2. *Temperature changes °C in Asagran compacts of varying weight compressed at* 50 kN

Compact weight (g)	Temperature rise on initial formation	Temperature fall on first relaxation	Net rise in temperature (attributed to heat of formation)	Temperature rise on recompression	Temperature fall on relaxation
0·5 (U)	15·0	6·2	8·8	7·4	5·7
1·0 (U)	15·8	5·6	10·2	7·4	5·7
1·5 (U)	14·4	5·2	9·2	6·1	5·1
2·0 (U)	*15·8	*5·6	*10·2	*6·2	*5·0
0·5 (L)	14·1	5·1	9·0	7·4	5·9
1·0 (L)	14·1	6·8	7·3	8·5	6·6
1·5 (L)	13·4	5·2	8·2	6·8	5·7
2·0 (L)	13·4	5·1	8·3	6·4	5·7

(U) Unlubricated compact
(L) Compact lubricated with 2% w/w magnesium stearate
* Mean of three results on three separate compacts.

errors. The temperatures attained are apparently independent of the compact weight and this is consistent with the idea that it is the energy supplied or given out per unit weight that determines their magnitude.

Juslin (1969) found that 1% w/w of calcium stearate greatly reduced the temperature rises on the surfaces of compressed tablets caused by die wall friction on ejection. In contrast, the addition of 2% w/w magnesium stearate to Asagran granules does not appreciably affect the internal temperature rises (Table 2). Higuchi, Rao & others (1953) and Shotton & Ganderton (1960) have shown that tablet formation is accompanied by granule fracture and rebonding. Lubricants, when present at their usual low concentrations, may have limited effect on the heat produced during these processes.

Where the material itself has lubricant properties, as with boric acid, then the much larger lubricating effect of the material could be effective during granule fracture and rebonding and may account for the low net temperature rise on formation of a compact of boric acid.

Acknowledgements

We should like to thank Mr. L. Tibbs, Chief Technician in The School of Engineering for helpful technical advice and the extended loan of the Visicorder, and Mrs. R. Faulkner for her skilful preparation of the illustrations. We are also indebted to Dr. B. G. Knowles for valuable discussion during the course of the work.

REFERENCES

HANUS, J. H. & KING, L. D. (1968). *J. pharm. Sci.*, **57**, 677–684.

HIGUCHI, T., RAO, A. N., BUSSE, L. W. & SWINTOWSKY, J. V. (1953). *J. Am. pharm. Ass. (Sci. Edn)*, **42**, 194–200.

JUSLIN, M. J. (1969). *Farmaceutiskt Notisbl.*, **78**, 201–210.

NELSON, E., BUSSE, L. W. & HIGUCHI, T. (1955). *J. Am. pharm. Ass. (Sci. Edn)*, **44**, 223–225.

RIDGWAY, K., GLASBY, J. & ROSSER, P. H. (1969). *J. Pharm. Pharmac.*, **21**, *Suppl.*, 245S–295S.

SHOTTON, E. & GANDERTON, D. (1960). *Ibid.*, **12**, 93–104

J. Pharm. Pharmac., 1970, **22**, *Suppl.*, 17 S–23 S *Received January* 21, 1970

Some observations on the ageing of sodium chloride compacts*

J. E. REES† AND E. SHOTTON

*Department of Pharmaceutics, The School of Pharmacy, University of London, Brunswick Square, London, W.C.*1, *U.K.*

The diametrical crushing strength of an ideal system of compacted particulate material, and the relation between strength and mean compaction pressure depend on the time at which the strength is determined. Strength increases of over 100% during the first hour after compression are attributed to stress relief of the sodium chloride crystals and interparticulate bonds. The effects of elevated temperature, and also humidity, on the strength and physical structure of compacts are evaluated. Relaxation behaviour of compacts containing light liquid paraffin is also investigated.

Changes in the mechanical properties of compressed tablets with time after compaction may influence their subsequent behaviour. Although such changes have been observed in industry nothing has been published about the significance of these effects.

The need to include a time factor has been recognized. Higuchi, Rao & others (1953) stated that the tablets were prepared and tested on the same day. Ganderton (1962) determined the crushing strength of compacts within 5 min of their ejection, whereas Lewis (1964) recorded the crushing strength of compacts "immediately" after their preparation. A delay of 6 h was standardized by Shotton, Deer & Ganderton (1963), and one month was quoted by Nelson, Arndt & Busse (1957).

We therefore examined the effects of several variables on the changes of strength with time of an ideal system of compacted material after its ejection from the die.

EXPERIMENTAL AND RESULTS

Sodium chloride (30–40 mesh) dried at 110° was used to form compacts without the addition of excipients. Weighed samples were compressed in a 1·2 cm (diameter) die between plane-faced punches in conjunction with an instrumented eccentric tablet press as described by Rees & Shotton (1969). In all compression experiments, each sample consisted of sufficient sodium chloride (982 mg) to produce a compact of 0·4 cm theoretical length at zero porosity.

Effect of time

Compacts were prepared in a "conditioned" die (Rees & Shotton, 1969) at a mean compaction pressure of 1200 kg cm^{-2}, and stored at 25° over silica gel. At selected time intervals the strength of a random sample of five compacts was determined by diametrical compression using the instrument described by Shotton & Ganderton (1960a). During the first hour, the strength increased by approximately 100% com-

* This work forms part of a thesis by J.E.R., accepted for the degree of Ph.D. in the University of London.

† Present address: Sandoz Ltd., Basle. Switzerland.

pared with the initial value (Fig. 1). Although the mean strength was further increased by approximately 1 kg after 140 h, Student's *t*-distribution showed only 60% probability that a significant change occurred subsequent to the first hour.

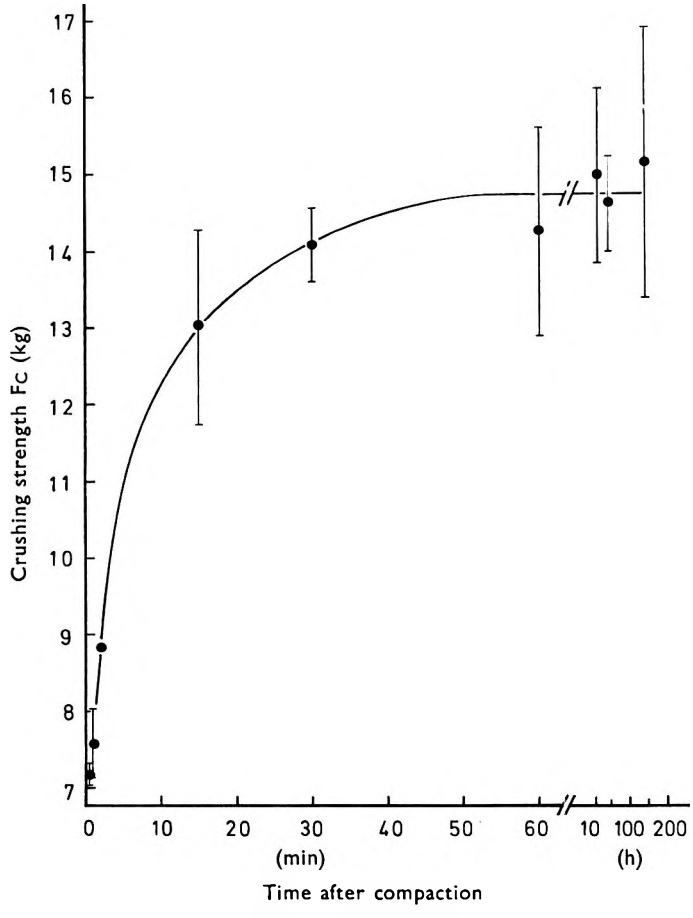

FIG. 1. Effect of time on the strength of sodium chloride compacts. Each co-ordinate represents the mean of five determinations and the standard deviation of each value is shown.

Effect of compaction pressure

The influence of compaction pressure on the changes in strength with time was evaluated, and the effects of storing compacts at 25° and at 100° were also investigated. Before preparing compacts at each pressure, the die was cleaned and conditioned.

The crushing strengths of five, randomly-selected compacts prepared at each pressure were determined less than 1 min after ejection. A linear relation was observed between the strength and mean compaction pressure, P_m, over the pressure range 0–2000 kg cm^{-2} (Fig. 2). A second group of five replicate compacts was stored over silica gel at 25° for 1 h, and five compacts prepared at each pressure were stored in an oven at 100° for 1 h. Increases in strength of up to 115% were observed. The relation between the compaction pressure and the strength was linear to 1250 kg cm^{-2} (123 MNm^{-2}), but at higher pressures a decrease in slope occurred (Fig. 2).

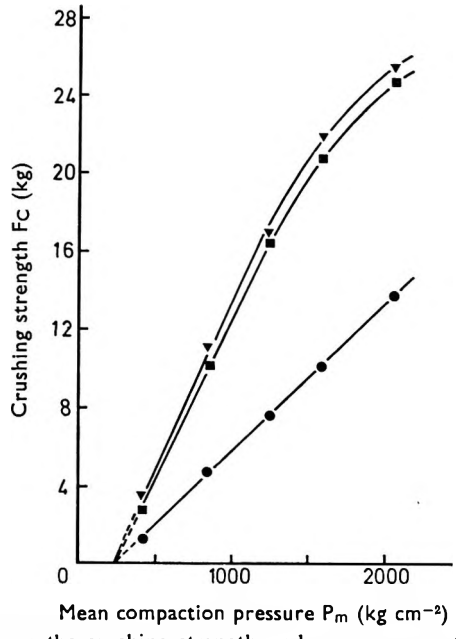

FIG. 2. Relations between the crushing strength and mean compaction pressure for compacts tested ●, immediately after ejection; ■, after 1 h at 25°; and ▼, after 1 h at 100°.

The increases in strength of compacts heated at 100° were only slightly greater than for those stored at 25°. Student's *t*-test analysis of the results for low compaction pressures indicated a significant difference between the mean strengths of compacts stored at the two temperatures. With increasing compaction pressure, there was a decrease in the statistical significance of the different values. However, in view of the apparent effect on certain compacts of heating at 100°, it was decided to dry compacts at 60° in other aspects of this investigation. Preliminary experiments had shown that this lower temperature did not affect the crushing strength of compacts prepared from dried material.

By extrapolation to zero crushing strength (Fig. 2), all three linear relations intercepted the pressure axis at 220 kg cm^{-2}, P_m (21·6 MNm^{-2}).

Effect of liquid films

The possible influence of interparticulate surface films was also studied. Owing to the problem of maintaining a constant moisture content by preventing evaporation or crystallization, experiments with compacts containing moisture were unsuccessful. For this reason, light liquid paraffin (B.P.C.) was selected as a non-volatile, non-solvent liquid and 2% by weight was added to a bulk quantity of the sodium chloride, and dispersed by standardized agitation. The weight of each sample for compression was calculated on the basis of sufficient *solid* to produce a compact of 0·4 cm length at zero porosity.

The effect of removing liquid films from the system after compaction was evaluated by solvent extraction of compacts using chloroform. Preliminary experiments with a series of compacts prepared from dried sodium chloride at a range of pressures demonstrated that this technique produced no significant changes in the weight, or crushing strength.

No direct assessment was made of the uniformity of distribution of the light liquid paraffin but the uniformity in weight of the compacts after removal of the liquid indicated that the replicate samples of compressed material were identical.

Table 1 shows the effect of time, and the influence of solvent extraction, on the crushing strength of compacts compressed with 2·0% light liquid paraffin.

Immediately after compression, the strength of compacts containing the paraffin (Table 1) was slightly less than the value of 7·6 kg, shown in Fig. 2, for compacts of dry material compressed in a conditioned die at 1220 kg cm^{-2} P_m. Compacts which were extracted with chloroform immediately after compression exhibited a final strength comparable to the value of 16·0 kg for compacts of dry material. However, the final strength of compacts containing the paraffin was approximately 3 kg below this value.

Table 1. *The effect of time of storage, and the influence of solvent extraction, on the strength of sodium chloride compacts compressed with 2·0% light liquid paraffin.* Mean compaction pressure = 1220 kg cm^{-2} (120 MN_m^{-2}).

Solvent extraction commenced at time:	Strength of compacts measured at time:	Crushing strength (kg) as mean of five replicates	Standard deviation, % of mean strength
—	<1 min	6·47	± 6·8
<1 min	8 h	16·57	±18·4
—	8 h	13·16	±12·8

Effect of humidity

The presence of moisture at the interparticulate junctions and at the die wall boundary has been shown to influence the compaction behaviour of sodium chloride and the crushing strength of the compacts produced (Shotton & Rees, 1965; Rees, 1970).

To distinguish any direct influence of moisture on the crushing strength, from the lubricant and hydrodynamic properties, compacts of dry material were exposed to 66 or 76% relative humidity for eight weeks. To minimize exchange of water vapour between the compacts and atmosphere during strength measurements, the ambient conditions were maintained in equilibrium with the samples, and the exposure time was as short as possible. Additional samples of the compacts exposed to humid conditions were dried at 60° for 1 h and cooled in a desiccator before their crushing strength was determined.

The effects of humidity on the mean strength, the strength variation and the moisture content are shown in Table 2. The moisture content of compacts was determined by a thermogravimetric technique using a Cahn Gram Electrobalance. Samples were dried at 110° and cooled in a vacuum on the balance as described previously (Shotton & Rees, 1966), to prevent errors arising from sample transfer.

Compacts stored at 76% relative humidity possessed a very low strength compared with the control samples. Subsequent drying of these compacts produced only a small increase in the mean strength, but a large standard deviation of strength values was observed. Conversely, for the compacts stored at 66% relative humidity, drying caused a large increase in strength, despite the small moisture sorption which had occurred on storage.

Table 2. *The crushing strength and moisture content of sodium chloride compacts stored at elevated humidity for eight weeks.* Mean compaction pressure = 1273 kg cm^{-2} (125 MNm^{-2}).

Storage conditions	Treatment	Crushing strength* (kg)	Standard deviation (% of mean)	Moisture content (%)
Desiccator	—	16·27	12·4	0·00
66% RH	—	17·30	2·1	0·005
66% RH	Dried	25·82	5·4	0·00
76% RH	—	1·91	7·9	0·50
76% RH	Dried	2·67	19·9	0·00

* Each value is a mean of 10 replicates.

DISCUSSION

Non-linear arithmetic relations between crushing strength and compaction pressure were reported by Higuchi & others for a sulphathiazole granulation (1953) and for aspirin and lactose (1954). Shotton & Ganderton (1960a) and Lewis (1964) also obtained non-linear relations for sodium chloride (30–40 mesh), a plot of crushing strength versus mean compaction pressure showing a continual decrease in slope. However, the present results indicate that the relation for sodium chloride is linear up to 2050 kg $cm^{-2}P_m$, provided the crushing strength of the compacts is evaluated within 1 minute of ejection from the die.

Using the Cahn Gram Electrobalance, we found no moisture in the samples for compression. Consequently, increases in strength of the magnitude observed after ejection cannot be explained in terms of interparticulate deposition of crystallized material from surface moisture films (cf. Shotton & Rees, 1966).

Baba & Nagafuji (1965) have shown for several materials, including sodium chloride, that there is a measurable strain recovery of compacts during the period immediately after compression. For compacts of sodium chloride, compressed to 15 mm length at 2230 kg cm^{-2} pressure using 20 mm diameter plane-faced punches, these authors found that 0·2% axial strain recovery occurred in the die after removing the applied pressure. After ejection, there was further strain recovery of 0·9% in the axial direction and 0·2% in the radial direction. We believe that the strength increases we observed are due to this time-dependent relaxation which provides stress relief within the compact. Increased bonding may occur if elastic or plastic flow increases the area of intimate contact between adjacent crystals. The deviation from a linear relation (Fig. 2) for compacts stored for 1 h may then be attributed to incomplete strain relief which occurs when the structure of the compact permits only partial relaxation of crystals. As the porosity of a compact is reduced, the strength will approach a maximum value corresponding to the intrinsic strength of the solid material. However, for compacts tested immediately after compression, there is no evidence of a limiting value of crushing strength at a mean compaction pressure of 2050 kg cm^{-2} (201 MNm^{-2}).

Although an elevated temperature may encourage further strain relief due to an increase in the plasticity of the crystalline material (Sperling, 1932), it is also possible that small increases in crushing strength of compacts stored at 100° are produced by an increase in surface energy. Crone & McKee (1950) stated that an increase in temperature removes adsorbed films so that surface forces are able to act to the fullest extent, although the absolute magnitude of the forces is probably decreased.

For compacts of sodium chloride it has been shown that the shear strength and crushing strength are similarly related to a parameter such as the porosity (Ganderton, 1962). It is interesting therefore, that Lewis (1964) observed a *decrease* in the shear strength of sucrose compacts with time, in contrast to the present results for crushing strength of sodium chloride.

Strain relief within a compact during ejection from the die may cause a reduction in strength and result in capping and lamination (Train, 1956; Long, 1960). The presence of lubricant confined to the die wall was shown by Shotton & Ganderton (1961) to have no effect on the strength or capping characteristics of hexamine, whereas coating the particles with a lubricant material before pressing weakened the interparticulate bond and prevented capping. Consequently, it is reasonable to assume that the effect of strain relief on the strength of a compact will depend on the rheological properties of the particulate solid material and of the interparticulate bonds that are produced by compression. For compacts containing 2% of light liquid paraffin, the strength after recovery was less than for compacts of dry material. This suggests that the liquid film does not facilitate recovery, for example by a lubricant effect or by modifying the physical properties of the crystalline material. Shotton & Rees (1966) concluded that a liquid of low viscosity could act as an interparticulate lubricant during compaction. The present results therefore suggest that, during recovery, no significant movement of the interparticulate boundary is involved and that strain recovery after ejection is predominantly an intrinsic property of the crystalline material and of interparticulate bonds. However, additional increases in strength occurred when the compacts were extracted during recovery. This result indicates that the removal of liquid films permits increased bonding, when areas of contact within a compact are increased by subsequent plastic or elastic recovery of the material.

The large decrease in standard deviation of replicate values of crushing strength on storage at 66% relative humidity (Table 2) is in agreement with the observation of Smothers, Kreglo & Moscker (1964) who tested the modulus of rupture of refractory brick, before and after immersion in water. They attributed the effects of water to a decrease in surface energy which reduces the strength distribution of flaws.

A reduction in surface energy will also reduce the overall strength of a compact. Since it is not certain that atmospheric conditions in the humidity chamber were uniform at all times, periodic dissolution and crystallization may have occurred. The slight increase in strength of compacts stored at 66% relative humidity may therefore have been caused by dissolution and removal of surface cracks and flaws in the crystals; these are known to act as centres of stress concentration.

Despite the large increases in the crushing strength on drying, of compacts stored at 66% relative humidity, the percentage standard deviation of replicate values was less than for the control samples. This is attributed to interparticulate crystallization of saturated solution within the compact causing a reduction in the incidence of crack propagation. The results suggest that small quantities of residual solvent may produce marked changes in the physical properties of a compact during storage.

No difference in microscopical appearance could be detected between the fractured surfaces of the control samples and the wet compacts stored at 66% relative humidity. However, the dried compacts exhibited a more planar fracture due to cross-grain failure (Shotton & Ganderton, 1960b, 1961) in the presence of strong bonds produced by interparticulate crystallization.

Examination of the compacts stored at 76% relative humidity showed that the original crystals (approximately 500 μm) had been almost entirely replaced by smaller crystals, and owing to the low strength of the interparticulate bonds, it was possible to detach a sufficient number of the crystals to estimate their mean size, which was approximately 70 μm. Deliquescence of sodium chloride occurs when the relative humidity exceeds 76%. The observed structure may therefore be attributed to extensive dissolution and subsequent recrystallization which could occur repeatedly following small fluctuations in the storage conditions. Consequently, the compact may no longer represent the original compacted system, since to a large extent, the interparticulate bonds formed during compaction will be removed by dissolution. New bonds will then form by recrystallization of dissolved solid material within the compact. The increased number of discontinuities which can propagate failure of the compact will contribute appreciably to the pronounced decrease in strength.

The large standard deviation in the strength of compacts which were dried after storage at 76% relative humidity, may be explained by a large variation in the strength of the bonds formed by further crystallization between the small crystals.

Acknowledgements

The authors wish to thank Dr. J. A. Hersey for helpful comment and criticism. One of us (J.E.R.) thanks the Science Research Council for the award of a Research Studentship.

REFERENCES

BABA, M. & NAGAFUJI, N. (1965). *Annual Report of Shionogi Research Laboratory*, No. 15, 147–151.

CRONE, H. G. & MCKEE, J. H. (1950). *Br. Coal Util. Res. Ass.*, **14**, No. 9.

GANDERTON, D. (1962). Ph.D. Thesis, University of London.

HIGUCHI, T., RAO, A. N., BUSSE, L. W., & SWINTOSKY, J. V. (1953). *J. Am. pharm. Ass. (Sci. Edn)*, **42**, 194–200.

HIGUCHI, T., ELOWE, L. N. & BUSSE, L. W. (1954). *Ibid.*, **43**, 685–689.

LEWIS, C. J. (1964). Ph.D. Thesis, University of London.

LONG, W. M. (1960). *Powder Metall.*, **6**, 73–86.

NELSON, E., ARNDT, J. R. & BUSSE, L. W. (1957). *J. Am. pharm. Ass.*, **46**, 257–262.

REES, J. E. & SHOTTON, E. (1969). *J. Pharm. Pharmac.*, **21**, 731–743.

REES, J. E. (1970). *Ibid.*, **22**, 245–246.

SHOTTON, E. & GANDERTON, D. (1960a). *Ibid., Suppl.*, **12**, 87T–92T.

SHOTTON, E. & GANDERTON, D. (1960b). *Ibid., Suppl.*, **12**, 93T–96T.

SHOTTON, E. & GANDERTON, D. (1961). *Ibid., Suppl.*, **13**, 144T–151T.

SHOTTON, E., DEER, J. J. & GANDERTON, D. (1963). *Ibid., Suppl.*, **15**, 106T–114T.

SHOTTON, E. & REES, J. E. (1966). *Ibid., Suppl.*, **18**, 160S–167S.

SMOTHERS, W. J., KREGLO, J. R. & MOSCKER, E. (1964). *J. Am. Ceram. Soc.*, **47**, 414–415.

SPERLING, G. F. (1932). *Z. Phys.*, **74**, 476–502.

TRAIN, D. (1956). *J. Pharm. Pharmac.*, **8**, 745–760.

J. Pharm. Pharmac., 1970, **22**, *Suppl.*, 24 S–28 S *Received February* 12, 1970

The effect of particle shape on the variation of fill of a tabletting die

K. RIDGWAY AND JANET B. SCOTTON

*Department of Pharmaceutics, School of Pharmacy, Brunswick Square, London W.C.*1, *U.K.*

A 12 mm die cavity has been repeatedly filled from batches of granular material of a range of particle shape and size distributions. The variance in the weight contained by the die was determined from the replicates. The variance, expressed as a coefficient of variation to allow for differences in the means of groups of replicates, increased from 0·2635 to 0·7222 as the particle shape, expressed as the Heywood shape coefficient, increased in irregularity from a value of 8 to 13. The mean contained weight was greater for regular than for irregular particles, and a maximum die fill occurred where the ratio of die diameter to particle diameter was about 20 for all particle shapes.

Powders are normally granulated to give a free-flowing material suitable for feeding to the dies of a tabletting machine. The aim is to obtain granules of a uniform size and of a shape not too far removed from the spherical, and it is generally accepted that the ease and accuracy of filling the die will be greater if this aim is achieved. So far as we are aware, no quantitative measurements have been made relating the variability of fill of a die to the degree of departure from the ideal aim of a uniform spherical granulation.

Hersey (1965) reported that the weight uniformity of the contents of a die in a tablet machine simulation apparatus was a function of the method adopted to fill the die, but no quantitative results were given. The die was filled (*a*) as a blind hole with one pass of the feed shoe; (*b*) by lowering the bottom punch whilst ample heaped powder was present at the die mouth; and (*c*) by allowing the lower punch to drop below its required setting as the die filled, then subsequently raising it and levelling off the powder rising above the die mouth with a knife blade. The reproducibility, and the mean weight of powder contained, both increased in the order (*a*) to (*b*) to (*c*).

In the experiments reported here, sand of particle size 60–85, 44–60, 30–36, 18–20 mesh, in batches sorted according to particle shape by the method of Ridgway & Rupp (1969), has been fed into a simple die simulator: the weight of sand contained was then measured. Repetition of the experiment allowed the variance as a function of particle shape to be assessed.

EXPERIMENTAL

The apparatus (Fig. 1) consists of a circular brass disc bored at its centre with an accurate parallel-sided hole. The disc was faced-off and a similar, thinner disc was attached to it by three screws. This assembly formed the die. A flanged cylinder formed the feed shoe.

The sand used was supplied by British Industrial Sand Limited, Reigate and by George Garside (Sand) Limited, Leighton Buzzard. It was divided into size fractions

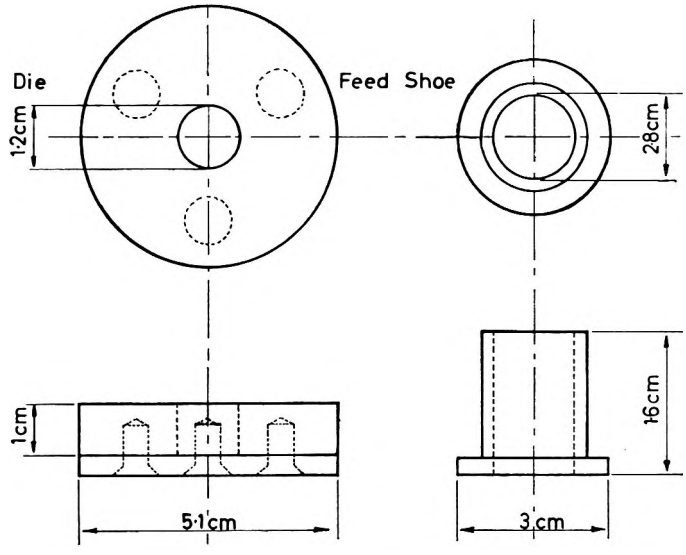

FIG. 1. The die simulator. The feed shoe cylinder is filled with the powder under test and moved manually across the face of the die.

by sieving, and the following size fractions were obtained: 60–85, 44–60, 30–36, 18–20 mesh. Each sieve cut was subdivided into four fractions of different shape by being passed over the deck of a shape-sorting machine (Jeffrey-Galion Ltd., Johannesburg).

Shape coefficients (Heywood, 1969) were determined as described previously (Ridgway & Rupp, 1969).

Sand was loaded into the feed shoe, which was passed over the die manually three times. Any sand grains on top of the die disc were removed, and the sand in the die was tipped out and weighed. Ten replicate determinations were made for each particle size and shape.

At the extremes of shape coefficient for each particle size fraction a further hundred replicate determinations of the weight of die fill for each sample of sand were made; the variance was thus determined. To allow for the change in mean weight of die fill in each group of measurements the variance was represented as the coefficient of variation.

RESULTS AND DISCUSSION

The values of particle size, shape coefficient, mean weight of die fill and variance about the mean are given in Table 1. The variance was estimated for all samples by examining the distribution of the weights of fill about the mean. But ten measurements is not a sufficiently large number from which to obtain a variance estimate of any precision. Accordingly the two samples at each size which were the most and the least spherical respectively were made the subject of 100 replications, and much more reliance can be placed upon the variance estimates derived from these measurements.

As expected the mean weight of die fill is reduced as the shape coefficient increases (Fig. 2). Irregular particles flow less freely from the feed shoe, and are less ready to rearrange into a closer packed random arrangement when they drop into the die.

Table 1. *Variation in die-fill with particle size and shape*

Mesh size mean size and sample no.	Projected diameters (μ)	Shape coeff. f/k	Mean weight g	Variance $\times 10^{-6}$ with degrees of freedom: 9	99	Coefficient of variation with degrees of freedom: 9	99
60/85 213 μm							
1	214	7·87	1·9579	28	35	0·2702	0·3012
2	218	9·15	1·8989	53		0·3833	
3	220	9·87	1·8726	44		0·3542	
4	228	11·92	1·7843	47	38	0·3841	0·3434
44/60 302 μm							
5	343	8·78	1·9289	127	34	0·5842	0·2964
6	357	10·47	1·8651	46		0·3636	
7	358	11·03	1·8272	17		0·2256	
8	378	13·03	1·7347	72	33	0·4891	0·3248
30/36 461 μm							
9	559	7·66	2·0801	132	31	0·5523	0·2635
10	609	8·70	2·0237	40		0·3125	
11	661	9·81	1·9397	115		0·5528	
12	694	11·54	1·8529	80	75	0·4827	0·4544
18/20 805 μm							
13	909	8·17	2·0668	187	94	0·6616	0·4662
14	967	9·21	2·0038	176		0·6620	
15	1024	9·87	1·9721	291		0·8649	
16	1051	11·04	1·9041	229	151	0·7947	0·7222

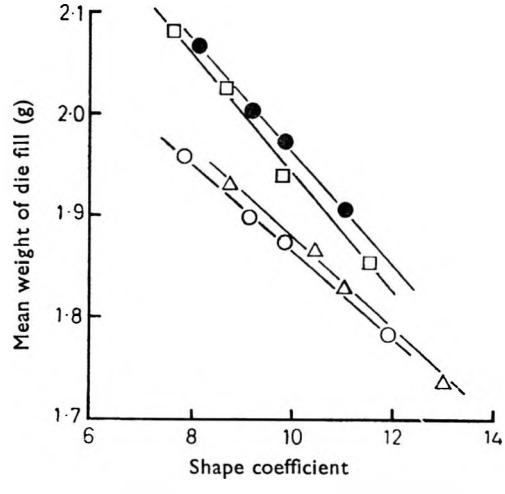

FIG. 2. The effect of shape coefficient on the mean weight of die fill for various particle sizes. ● 18–20 mesh, mean size 805 μm. □ 30–36 mesh, mean size 461 μm. △ 44–60 mesh, mean size 302 μm. ○ 60–85 mesh, mean size 213 μm.

Beyond a shape coefficient of 15, departure from linearity would be anticipated; extrapolation would otherwise predict zero weight in the die for very irregular particles.

The coefficient of variation of the die fill increases with particle size when shape is discounted: particles of mean diameter 805 μm have a coefficient of variation of 0·76, for those of 461 μm it is 0·48, for 302 μm it is 0·42 and for 213 μm it is 0·34. These mean sizes are from the sieve cuts 18–20, 30–36, 44–60 and 60–85 mesh respectively. For larger particles, where the mean diameter is 800 μm, there is only room for about 15 particles to fit across the width of the die. Thus the effect of the die wall, which is to introduce a region of variable, usually larger, voidage (Ridgway & Tarbuck, 1966) becomes paramount so that the variance is increased.

The effect of changing particle shape on the reproducibility of the weight fill of the die is shown in Fig. 3. Each line has but two points because of the large number of determinations which are needed to characterize a variance with any degree of precision. The trend is clear, however. Irregularity of particle shape at constant size causes the random variations of weight to become larger.

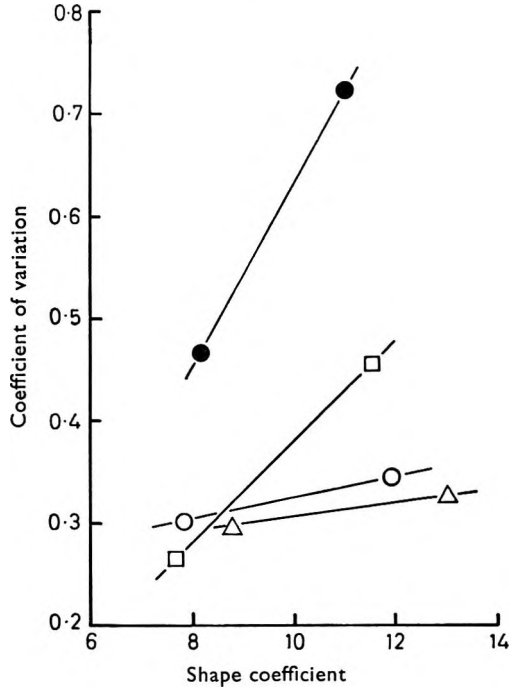

FIG. 3. The effect of shape coefficient on the coefficient of variation of the die fill. For key to points, see Fig. 2.

Finally, Fig. 4 shows how the mean weight of the die fill changes with increasing particle size, at constant shape factor. Here the points on the curves are interpolated to obtain values at rounded-off shape coefficients. At all shape coefficients, there is a maximum density which is achieved at a die diameter to particle size ratio of about 20. This is in accordance with the accepted practice of granulating to about 20 mesh for normal tablets. The maximum is flat so that no great change in mean weight will occur if the granule size is changed within reasonable limits. On the other hand, the

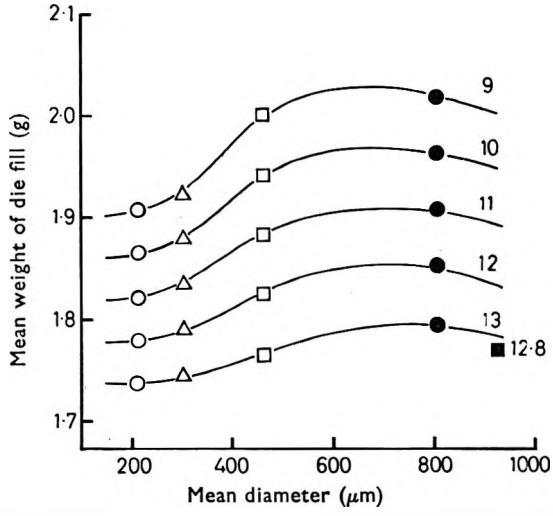

FIG. 4. The effect of particle size on the mean weight of material in the die for various shape coefficients. Key as for Fig. 2. The single point ■ represents restricted measurements made at a particle size of 925 μm (see text for details). Numbers represent values of the shape coefficient.

present work indicates that, other things being equal, a smaller granule will be better since the variation of weight will be less.

The reason for the maximum in the curves is not difficult to see. At small particle sizes, below about 200 μm, if the material will flow sufficiently well to enter the die it will have a constant bulk density. As the particle size increases, the energy or momentum obtained by each particle as it falls from the feed shoe into the die will increase. Macrae & Gray (1960) have shown that increasing the intensity of deposition of particles during pouring gives greater energy to each particle and allows rearrangement to occur in the surface layers of the bed as it builds up. The rearrangement allows increased packing density. This effect increases the bulk density of material in the die until a point is reached at which the particle size becomes appreciable compared with the size of the die cavity. This leads to restriction on the amount of rearrangement which can occur, and the restriction begins to be felt at a point where less than 10 or 12 particles can be fitted along the die diameter. The bulk density of the die fill then decreases.

The isolated point at the lower right side of Fig. 4 was obtained by making some measurements with 16/18 mesh sand, mean diameter 925 μm, with a shape coefficient of 12·84, the mean die fill being 1·77 g. This material was fine gravel rather than sand; some of the particles in it were agglomerates and were certainly not pure silica. However, the measurement does give some additional evidence for the general correctness of the trend of the lines in the graph.

REFERENCES

HERSEY, J. A. (1965). *Rheol. Acta*, **3**, 235–239.

HEYWOOD, H. (1969). Paper delivered at Inst. Chem. Engrs. Symposium "Powder Research," London, March 5th, 1969.

MACRAE, J. C. & GRAY, W. A. (1960). *Br. J. appl. Phys.*, **12**, 164.

RIDGWAY, K. & RUPP, R. (1969). *J. Pharm. Pharmac.*, **21**, *Suppl.*, 30S–39S.

RIDGWAY, K. & TARBUCK, K. J. (1966). *Ibid.*, **18**, *Suppl.*, 168S–175S.

J. Pharm. Pharmac., 1970, **22**, *Suppl.*, 29 S–33 S *Received February* 16, 1970

Preparation and characterization of the tropic acid esters of tropan-3β-ol, granatan-3α-ol and granatan-3β-ol

R. J. HUNT* AND J. B. ROBINSON†

Department of Pharmacy, University of Manchester, Manchester 13, *U.K.*

The preparation and characterization of the tropic acid esters of tropan-3β-ol and granatan-3α and 3β-ol are reported. A rapid synthesis of pseudopelletierine is described.

Reports of the mydriatic and spasmolytic activity of the tropate and mandelate esters of tropan-3β-ol, granatan-3α- and granatan-3β-ol are sparse and conflicting.

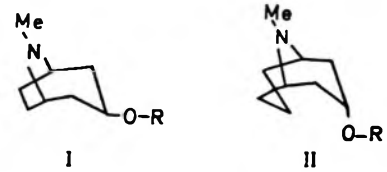

I II III

(a) R = CO·CH(CH$_2$OH)·Ph (tropate) (b) R = CO·CH(OH)·Ph (mandalate)

Although (±)-tropoyltropan-3β-ol (Ia) was initially reported to be devoid of mydriatic activity (Lieberman & Limpach, 1892), more recently Zipf, Dittman & Marquardt (1963) suggest a slight activity. [The report of mydriatic activity in (−)-Ia from *Dubiosia myoporoides* (Merck, 1892; Buanarotti, 1895) has been questioned (Carr & Reynolds, 1912), it being suggested that the compound isolated and tested was (−)-norhyoscyamine].

Early studies using the tropate and mandelate esters of the isomeric granatanols (IIa and b; IIIa and b) suggest that mydriatic activity resides in the β-isomers (IIIa and b) (Werner, 1918); the opposite conclusion has been drawn by Hartung & Gadekar (1953) employing only the mandelate esters.

In few of the above studies have the compounds been characterized: the present communication reports the preparation and characterization of (±)-tropoyl-tropan-3β-ol (Ia), (±)-tropoylgranatan-3α-ol (IIa) and (±)-tropoylgranatan-3β-ol (IIIa).

The preparation of pseudopelletierine by a Robinson-Schopf type of condensation under 'non-physiological' conditions has been carried out using the method of Elming (1960), Elming and Nedenskov (1958), Kay, Robinson & Thomas (1965).

Reduction of pseudopelletierine with (*a*) lithium aluminium hydride and (*b*) sodium in isobutanol gave granatan-3α-ol and granatan-3β-ol respectively (Chen & Le Fèvre, 1966).

The hydrochloride of the requisite amino-alcohol [tropan-3β-ol (I, R=H);

* Present address: Thomas Kerfoot & Co. Ltd., Bardsley Vale, Ashton-under-Lyne, Lancashire, U.K.

† To whom correspondence should be addressed. Present address: Faculty of Pharmacy, University of Toronto, Toronto 5, Ontario, Canada.

granatan-3α-ol (II, R=H) and granatan-3β-ol (III, R=H)] was esterified with acetoxytropoyl chloride. Mild acid hydrolysis (5 min), followed by column chromatography of the basic material yielded the required product with the expected by products (I, II, III where R=H and R=CO·CH(CH_2OAc)·Ph). A third by-product was identified as the phenylacrylyl ester (I, II, III, R=CO·C(CH_2)·Ph). Such elimination of acetic acid is in line with earlier work (Garrett, 1957) and is supported by the solvent dependant nature of such reactions (Caldwell, Finkelstein & others, 1969).

EXPERIMENTAL

All melting points were recorded on a Kofler Hot-stage apparatus and are uncorrected. Infrared spectra were recorded on a Perkin-Elmer model 237 spectrophotometer and nmr spectra on a Varian HA-100 spectrometer using $CDCl_3$ solution and tetramethylsilane as standard. Mass spectra were recorded on an A.E.I. model MS9 spectrometer.

Pseudopelletierine (Elming, 1960). Acetonedicarboxylic acid (44·1 g; 0·3 mol), methylamine hydrochloride (20·25 g; 0·3 mol) and sodium acetate (92·5 g) in water (200 ml) was heated (90 min, 55–60°) with an aqueous solution of glutaraldehyde (28 ml; 25% w/v; 0·07 mol). After it had cooled, potassium carbonate (45 g) and sodium chloride (62·5 g) were added and the solution extracted with chloroform (10 × 200 ml). The combined chloroform extracts were dried ($MgSO_4$), filtered and the solvent removed. Distillation of the brown viscous residue gave pseudopelletierine (5·5 g) $b.p._{13}$ 129–130° as a colourless liquid which rapidly solidified m.p. 47–48° (Lit m.p. 48° [Putney & Soine, 1955]). ν_{max} (Nujol) 1720 cm^{-1} (C=O), τ($CDCl_3$) 6·8 (2H, m, C–1H, C–5H), 7·45 (3H, s, N–CH_3), 7·15–8·7 (10H, m, methylene groups).

Granatan-3β-ol. Reduction of pseudopelletierine (6 g) using the method of Nickon & Fieser (1952) gave granatan-3β-ol (3·8 g) $b.p._{18}$ 141–142° crystallizing from benzene–light petroleum (b.p. 40–60°) m.p. 100° (Lit m.p. 96° [Hartung & Gadekar, 1953]), ν_{max} (Nujol) 3400 cm^{-1} (broad) (bonded-OH), τ($CDCl_3$) 5·6 broad (1H, m, C–3H; $W_{1/2}$ = 16 Hz), 7·05 (2H, m, C–1H, C–5H), 7·5 (3H, s, N–CH_3), 7·8–8·7 (10H, m, methylene groups) 7·3 (1H, s, disappears on deuteration).

Granatan-3α-ol synthesized by the method of Chen & Le Fevre (1966) had the following characteristics: $b.p._{13}$ = 138–140°, m.p. 63–64°. ν_{max} (Nujol) 3400 cm^{-1} (broad) (–OH), τ($CDCl_3$) 5·8 (1H, m, C–3H; $W_{1/2}$ = 12·5 Hz), 6·8–7·2 (3H, m, C–1H, C–5H, and OH) (collapses to 2H multiplet on adding D_2O), 7·54 (3H, s, N–CH_3), 7·4–9·0 (10H, m, methylene groups).

Tropoyltropan-3β-ol. Pseudotropine hydrochloride (2 g) (Nickon & Fieser, 1952) and acetyltropoyl chloride (3·5 g) (Wolfenstein & Mamlock, 1908) were heated (4 h: 100°), with occasional swirling. After cooling, water (30 ml) was added and the mixture heated (5 min, 100°) then rapidly cooled and immediately extracted with ether (3 × 50 ml) and the ether rejected. The aqueous solution was basified (K_2CO_3) and extracted with ether (6 × 50 ml) then with chloroform (3 × 50 ml). The combined extracts were dried ($MgSO_4$), filtered and the solvents removed to leave an oily residue which was dissolved in the minimum quantity of chloroform–ether (3:7 parts v/v) and added to a column of alumina (2·5 × 50 cm; Laporte Type H; 100–200 mesh). The column was eluted with chloroform–ether (3:7 parts by volume) (700 ml) then with chloroform–ether (3:7 parts by volume) containing (*a*) 2% ethanol

(300 ml); (*b*) 4% ethanol (300 ml); (*c*) 6% ethanol (300 ml); (*d*) 8% ethanol (300 ml); (*e*) 10% ethanol (300 ml). Fractions each of 25 ml were collected and monitored via the infrared spectrum of the residue after removal of the solvent. Four components (A–D) were isolated and identified in the eluate.

Component A (fractions 3–4): a colourless oil identified as 2-phenylacrylyltropan-3β-ol (atropoyltropan-3β-ol). ν_{max} (liquid film), 1730 cm^{-1} (C=O), 1630 cm^{-1} (C=C stretch), 1605, 1580, 1500 cm^{-1} (aromatic C=C in plane vibrations). $\tau(CDCl_3)$ 2·8 (5H, m, aromatic), 3·75, 4·15 (2H, d, [J = 2 Hz] olefinic protons), 4·85 (1H, m, C–3H), 6·8 (2H, m, C–1H, C–5H), 7·7 (3H, s, N–CH_3), 7·8–8·45 (8H, m, methylene groups). Molecular weight (mass spectrum) m/e = 271; $C_{17}H_{21}NO_2$ requires mol. wt = 271.

Component B (fractions 6–16): a colourless oil, identified as acetyltropoyltropan-3β-ol ν_{max} (liquid film), 1730, 1750 cm^{-1} (C=O), 1605, 1580, 1500 cm^{-1} (aromatic). $\tau(CDCl_3)$ 2·7 (5H, m, aromatic), 5·0 (1H, m, C–3H), 6·0–6·3 (3H, m, –CH·CH_2O), 6·8 (2H, m, C–1H, C–5H), 7·7 (3H, s, N–CH_3), 8·0 (3H, s, O·$COCH_3$), 8·1–8·5 (8H, m, methylene groups).

Component C (fractions 29–62): tropoyltropan-3β-ol (190 mg) was obtained as an oil which slowly crystallized on standing. ν_{max} (liquid film), 1740 cm^{-1} (C=O), 1605, 1580, 1500 (aromatic), 3400 cm^{-1} (broad) (bonded –OH). $\tau(CDCl_3)$ 2·75 (5H, s, aromatic), 4·95 (1H, m, C–3H) ($W_{1/2}$ = 17 Hz), 5·9–6·2 (3H, m, –CH–CH_2–O), 6·8 (2H, m, C–1H, C–5H), 7·7 (3H, s, N–CH_3), 7·9–8·5 (8H, m, methylene groups), 7·8 (1H, s, –OH) (disappears on deuteration). Molecular weight (mass spectrum) m/e = 289: $C_{17}H_{23}NO_3$ requires mol. wt = 289.

Hydrobromide, m.p. 168–169°. Found: C, 55·0; H, 6·7; N, 3·8. $C_{17}H_{24}Br.NO_3$ requires C, 55·1; H, 6·5; N, 3·8%.

Component D (fractions 65–74): colourless needles of pseudotropine m.p. 103–105°.

Fractions 5–16 were combined, and acidified to pH 3 with N/100 HCl. The solution was heated on a steam bath for 30 min, cooled and the basic products extracted. Column chromatography of the material under the same conditions as previously described gave a further quantity of tropoyltropan-3β-ol (130 mg) in fractions 29–54.

Tropoylgranatan-3β-ol was prepared as above by heating (2 h) granatan-3β-ol hydrochloride (2·5 g) and acetyltropoyl chloride (4 g). The basic product of the reaction in chloroform–ether (1 : 1 parts by volume) was added to an alumina column (2·5 × 50 cm; Type H, 100–200 mesh). Elution with chloroform–ether (1 : 1 parts by volume, 700 ml) followed by chloroform–ether (1 : 1) (300 ml) containing (*a*) 2% ethanol; (*b*) 4% ethanol; (*c*) 6% ethanol; (*d*) 8% ethanol; (*e*) 10% ethanol. Fractions each of 25 ml were collected and examined as before when the four components below, resulted.

Component A (fractions 4–6): a colourless oil (0·8 g) identified as atropoylgranatan-3β-ol. ν_{max} (liquid film), 1730 cm^{-1} (C=O), 1630 cm^{-1} (C=C stretch), 1610, 1590, 1505 (aromatic in plane vibrations). $\tau(CDCl_3)$ 2·075 (5H, m, aromatic), 3·7, 4·15 (2H, d, [J = 2 Hz], =CH_2), 4·25 (1H, m, C–3H), 7·05 (2H, m, C–1H, C–5H), 7·5 (3H, s, N–CH_3), 7·9–8·6 (10H, m, methylene groups); molecular weight (mass spectrum) m/e = 285; $C_{18}H_{23}NO_2$ requires mol. wt = 285.

Component B (fractions 7–20): a colourless oil, identified as acetyltropoylgranatan-3β-ol. ν_{max} (liquid film), 1745, 1720 cm^{-1} (C=O), 1600, 1580, 1500 cm^{-1} (aromatic).

$\tau(CDCl_3)$ 2·7 (5H, s, aromatic H), 4·4 (1H, m, C–3H), 6·0 (3H, m, $-CH{\cdot}CH_2$), 7·05 (2H, m, C–1H, C–5H), 7·5 (3H, s, $N-CH_3$), 7·95 (3H, s, $-O, CO{\cdot}CH_3$), 8·0–8·6 (10H, m, methylene groups).

Component C (fractions 29–36): a colourless oil (460 mg) identified as tropoylgranatan-3β-ol. ν_{max} (liquid film), 3420 cm^{-1} (broad, bonded –OH), 1720 cm^{-1} (C=O), 1600, 1580, 1500 cm^{-1} (aromatic in plane vibrations). $\tau(CDCl_3)$ 2·5 (5H, s, aromatic), 4·45 (1H, m, C–3H), 5·9–6·2 (3H, m, $-CH{\cdot}CH_2$), 7·1 (2H, m, C–1H, C–5H), 7·5 (1H, s, disappears on deuteration, –OH), 7·6 (3H, s, $N-CH_3$), 8·0–8·8 (10H, m, methylene groups). Molecular weight (mass spectrum) m/e = 303; $C_{18}H_{25}NO_3$ requires mol. wt = 303.

Hydrobromide, m.p. 168–169°. Found C, 56·3; H, 6·6; N, 3·4. $C_{18}H_{26}Br.NO_3$ requires C, 56·3; H, 6·8; N, 3·6%.

Component D (fractions 39–46): a colourless crystalline produce identified as granatan-3β-ol, m.p. 97–98°.

Tropoylgranatan-3α-ol was prepared as above by heating (3 h, 100°) granatan-3α-ol hydrochloride (2·6 g) and acetyltropoyl chloride (3·75 g). The basic reaction product in chloroform–ether (2 : 1 parts by volume) was added to the alumina column and eluted with chloroform–ether (2 : 1 parts by volume, 700 ml) followed by chloroform–ether (2 : 1) (300 ml) containing (*a*) 2% ethanol; (*b*) 4% ethanol; (*c*) 6% ethanol; (*d*) 8% ethanol; (*e*) 10% ethanol.

Fractions each of 25 ml were collected and examined as before when four components were isolated.

Component A (fractions 16–19): a colourless oil (0·9 g) identified as atropoylgranatan-3α-ol. ν_{max} (liquid film), 1725 cm^{-1} (C=O), 1630 cm^{-1} (C=C stretch), 1610, 1590, 1505 cm^{-1} (aromatic C=C in plane vibrations). $\tau(CDCl_3)$ 2·5 (5H, m, aromatic), 3·8–4·15 (2H, d, [J = 1 Hz], $=CH_2$), 4·7 (1H, m, C–3H), 7·15 (2H, m, C–1H, C–5H), 7·55 (3H, s, $N-CH_3$), 7·9–8·9 (10H, m, methylene groups). Molecular weight (mass spectrum) m/e = 283.

Component B (fractions 21–29): a colourless oil, identified as acetyltropoylgranatan-3α-ol. ν_{max} (liquid film), 1730, 1750 cm^{-1} (C=O), 1600, 1590, 1500 cm^{-1} (aromatic).

Component C (fractions 40–44) contained two components, but was predominantly granatan-3α-ol.

Component D (fractions 45–70): a colourless oil (0·3 g), tropoylgranatan-3α-ol, ν_{max} (liquid film), 3400 cm^{-1} (broad, bonded –OH), 1740 cm^{-1} (C=O), 1610, 1600, 1505 cm^{-1} (aromatic). $\tau(CDCl_3)$ 2·75 (5H, s, aromatic), 4·85 (1H, m, C–3H), 5·85–6·2 (3H, m, $-CH{\cdot}CH_2$), 7·1 (2H, m, C–1H, C–5H), 7·6 (3H, s, $N-CH_3$), 7·9 (1H, s, disappears on deuteration), 7·7–9 (10H, m, methylene groups). Molecular weight (mass spectrum), m/e = 303.

Hydrobromide, m.p. 183–184°. Found C, 56·2; H, 6·6; N, 3·1%.

A further quantity of tropoylgranatan-3α-ol (0·16 g) was obtained by repeating the selective hydrolysis, and purification on component B.

Hydrobromide salts of tropate esters. The isolated tropate esters were dissolved in dry ether and dry HBr gas bubbled through the solution. The precipitate was collected, dried and recrystallized to constant m.p. from ethanol ether mixture.

Acknowledgement

Thanks are due to the P.S.G.B. for financial support to one of us (R.J.H.) during the course of this work.

REFERENCES

BUANAROTTI, E. (1895). *Arch. ital. Biol.*, **23**, 211–216.

CALDWELL, H. C., FINKELSTEIN, J. A., ARBAKOV, D., PELIKAN, C. & GROVES, W. C. (1969). *J. mednl Chem.*, **12**, 477–480.

CARR, F. H. & REYNOLDS, W. C. (1912). *J. chem. Soc.*, **101**, 946–958.

CHEN, C-Y. & LE FÈVRE, R. J. W. (1966). *Ibid.*, (B), 539–544.

ELMING, N. (1960). *Adv. org. Chem.*, **2**, 67–115.

ELMING, N. & NEDENSKOV, P. (1958). Brit. Pat. No. 791,770.

GARRETT, E. R. (1957). *J. Am. chem. Soc.*, **79**, 1071–1076.

HARTUNG, W. H. & GADEKER, S. M. (1953). *J. Am. Pharm. Ass.* (*Sci. Edn*), **42**, 715–717.

KAY, J. B., ROBINSON, J. B. & THOMAS, J. (1965). *J. chem. Soc.*, 5112–5115.

LIEBERMAN, C. & LIMPACH, L. (1892). *Ber.*, **25**, 927–939 quoting unpublished report of Liebrich, O.

MERCK, E. (1893). *Arch. Pharm.*, **231**, 117–123.

NICKON, A. & FIESER, L. F. (1952). *J. Am. chem. Soc.*, **74**, 5566–5570.

PUTNEY, B. F. & SOINE, T. O. (1955). *J. Am. Pharm. Ass.* (*Sci. Edn*), **44**, 17–22.

WERNER, L. E. (1918). *J. Am. chem. Soc.*, **40**, 669–674.

WOLFFENSTEIN, R. & MAMLOCK, L. (1908). *Ber.*, **41**, 723–732.

ZIPF, von H. F., DITTMANN, E. C. & MARQUARDT, H. (1963). *Arzneimittel-Forsch.*, **13**, 1097–1100.

J. Pharm. Pharmac., 1970, **22**, *Suppl.*, 34 S–39 S *Received March* 31, 1970

The alkaloidal pattern in the leaves, stem-bark and root-bark of *Mitragyna* species from Ghana

E. J. SHELLARD AND K. SARPONG

Department of Pharmacy, Chelsea College (University of London), Manresa Road, London, S.W.3, U.K.

The leaves, stem-bark and root-bark of *Mitragyna ciliata*, *M. inermis* and *M. stipulosa* have been examined quantitatively and qualitatively for alkaloids. In addition, the plant parts of *M. stipulosa* collected at 12 regular monthly intervals have been similarly examined. The presence of mitraphylline in the leaves of this plant and the absence of indole alkaloids was confirmed. The predominant leaf alkaloids are oxindoles of the A series, those of the stem- and root-bark, oxindoles of the B series. Whereas the general alkaloidal pattern of *M. ciliata* appears similar to that of *M. inermis* rather than *M. stipulosa*, a more detailed study suggests that *M. ciliata* and *M. inermis* have a distinctly different metabolic pattern in relation to the C(9)-OMe alkaloids.

The nature of the alkaloids present in the leaves of *Mitragyna stipulosa* (D.C.) O. Kuntze, *Mitragyna ciliata* Aubr. et Pellegr. (Beckett, Shellard & Tackie, 1963) and *Mitragyna inermis* (Willd.) O. Kuntze (Shellard & Sarpong, 1969), has already been reported. Whereas *M. ciliata* and *M. stipulosa* are almost identical botanically yet have a different alkaloidal pattern, *M. inermis* which differs very markedly in its botanical character from *M. ciliata* is very similar to it in alkaloidal pattern.

A comparative study has, therefore, been made of the alkaloids present in the leaves, stem-bark and root-bark of these three species using specimens collected from the same plants on the same occasion. In addition an investigation has been made of the alkaloids present in the leaves, stem-bark and root-bark of *M. stipulosa* collected from the same tree at regular monthly intervals during the course of one year.

EXPERIMENTAL

Materials

The leaves, stem-bark and roots were collected from localities in Ghana as follows: *M. ciliata*—Tarkwa district, West Region. *M. inermis*—Sogakofe district, Volta Region. *M. stipulosa*—The University Campus, Kumasi, Ashanti Region.

The materials for the comparative study of the three species were collected in September 1966. The leaves, stem-bark and roots of *M. stipulosa* was collected from December 1968 to November 1969.

The root-bark was cut away from the xylem; leaves, stem-bark and root-bark were separately coarsely powdered.

Thin-layer plates. Silica gel (G). Merck 0·25 mm thick.

Solvent systems. Chloroform–acetone (5:4), chloroform–methanol (95:5) (for separation of rotundifoline and isorhynchophylline).

Spray reagents. 0·2M $FeCl_3$ in 35% $HClO_4$ (Shellard & Alam, 1968).

Colour intensities were determined by reflectance scanning using a Chromoscan Densitometer (Joyce Loebl) with TLC attachment (Filter 465, aperture 1003).

Method

The powdered materials (leaves and root-bark—10 g, stem-bark—25 g) were extracted with 96% ethanol. After removal of the solvent under reduced pressure, glacial acetic acid (5 ml) was added and the mixture poured into distilled water (50 ml). After 12 h the mixture was filtered, the residue being washed with 5% acetic acid. The filtrate was made alkaline with ammonia and the alkaloids extracted with chloroform. After removal of solvent the crude alkaloids were dissolved in 5% sulphuric acid and non-alkaloidal material extracted with ether, the aqueous solution was again made alkaline with ammonia and re-extracted with chloroform. The purified alkaloids were dissolved in chloroform (5 ml) and added to the top of an alumina column (5 × 1 cm) containing chloroform. The total alkaloids were eluted with chloroform and after removal of the solvent were dissolved in methanol (5 ml). Two, 5 and 10 μl quantities were applied to the thin-layer plates, five plates being used for each determination, known quantities of the individual authentic alkaloids being chromatographed on the same plates at the same time.

For the estimation of an alkaloid present only in traces, the plate was loaded sufficiently to give a spot which yielded a reasonably sized peak with the densitometer. The results are given in Table 1 and in Fig. 1A–D.

Table 1. *Percentage of alkaloids* ($\times 10^{-2}$) *present in the leaves, stem-bark and root-bark of Ghanaian species of mitragyna collected in September* 1966

	Leaves	Stem-bark	Root-bark
Mitragyna ciliata			
Isorhynchophylline . .	3·1	1·2	4·8
Rhynchophylline . .	5·7	2·4	7·2
Rotundifoline . .	9·1	0·7	0·9
Isorotundifoline . .	3·5	0·2	0·05
Rhynchociline . .	4·2	1·6	6·6
Ciliaphylline . .	1·8	0·5	6·0
Mitraciliatine . .	2·1	0·0	0·0
Mitragyna inermis			
Isorhynchophylline . .	13·8	1·5	10·8
Rhynchophylline . .	6·4	4·6	19·6
Rotundifoline . .	9·4	0·01	0·8
Isorotundifoline . .	0·4	1·8	4·4
Rhynchociline . .	2·6	0·05	6·0
Ciliaphylline . .	1·0	0·01	2·4
Speciophylline . .	2·1	0·01	0·05
Uncarine F	0·3	0·01	3·5
Mitraciliatine . .	0·05	0·0	0·0
Speciogynine . .	0·01	0·0	0·0
Mitragyna stipulosa			
Isorhynchophylline . .	2·2	2·5	6·4
Rhynchophylline . .	3·3	6·4	11·2
Rotundifoline . .	5·8	0·25	0·5
Isorotundifoline . .	1·8	0·10	0·05
Mitraphylline . .	0·0	0·0	0·0

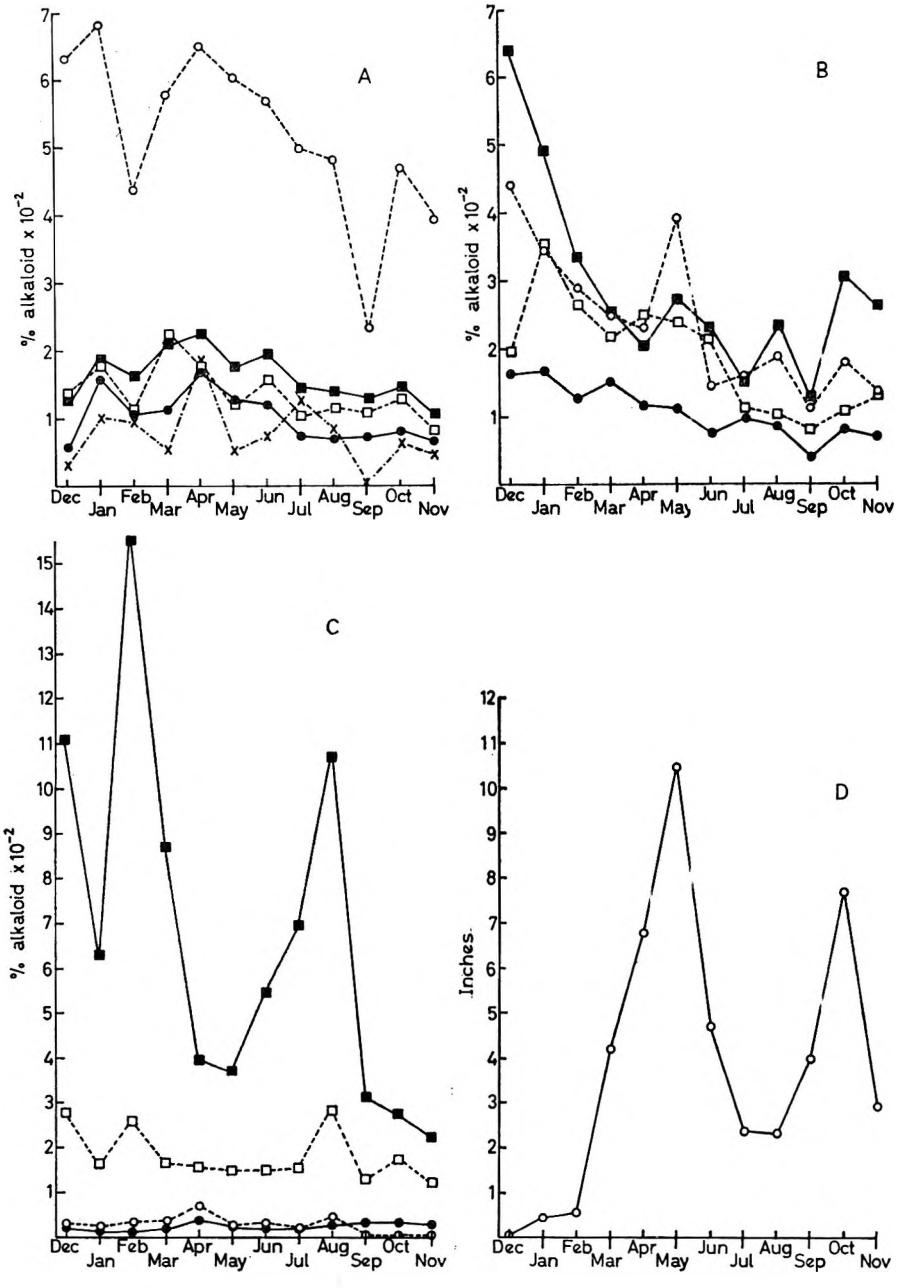

FIG. 1. Variation in the alkaloidal content of the leaves (A), root-bark (B), stem-bark (C) of *M. stipulosa* collected at monthly intervals from December 1968 to November 1969. D Rainfall of the collecting area (Kumasi) over the same period. - - ○ - - Rotundifoline. —●— Isorotundifoline. - - □ - - Isorhynchophylline. —■— Rhynchophylline. —X— Mitraphylline.

DISCUSSION

The percentage of total alkaloids in the stem-bark is lower than that in the leaves or root-bark (Table 1) which indicates that the alkaloids in the stem-bark are in the translocation stream and that no biogenesis, or storage occurs there. In *M. inermis* and *M. stipulosa* there is a higher alkaloidal content in the root-bark than in the leaves but the opposite obtains in the sample of *M. ciliata* examined. Thus there is some doubt as to whether the site of biogenesis is the leaf or the root although the fact that indole alkaloids occur in the leaf but not in the stem-bark or root-bark suggests that the alkaloids are synthesized in the leaves.

The dominant alkaloid is the same for stem and root-bark and differs from that found in the leaf. In all three species the dominant bark alkaloid is rhynchophylline (E *seco*, normal, B series, C(9)–H); for *M. ciliata* and *M. stipulosa* the main leaf alkaloid is rotundifoline (E *seco*, normal, A series, C(9)–OH); for *M. inermis* it is isorhynchophylline (E *seco*, normal, A series C(9)–H). Whereas the conversion of isorhynchophylline to rhynchophylline in *M. inermis* involves only a change in configuration from the A to the B series of oxindole alkaloids, the conversion of rotundifoline to rhynchophylline involves, in addition, the removal of the C(9)–OH.

In the leaves the dominant alkaloids are the A series oxindoles whereas in the root-bark they are the B series. With the dominant alkaloids the same for stem and root-bark it would appear that conversion takes place in the leaf before translocation to the root. Such dominance of the B series of alkaloids in the stem and root-bark is only true, however, if the total alkaloid is considered (Table 2) since with the C(9)–OMe substituted alkaloids the A series alkaloid (rhynchociline) is found in larger quantities than the B series alkaloid (ciliaphylline) in the barks as well as in the leaves (Table 1).

Table 2. *Percentage of A and B series E seco oxindole alkaloids* ($\times 10^{-2}$) *present in the leaves, stem-bark and root-bark of Ghanaian species of mitragyna collected in September* 1966

	Leaves		Stem-bark		Root-bark	
	A	B	A	B	A	B
M. ciliata	16·4	11·0	3·5	3·1	11·5	13·2
M. inermis	25·8	7·8	1·55	6·41	17·6	26·7
M. stipulosa	8·0	5·1	2·5	6·4	8·4	11·2

Table 3 shows that in *M. ciliata* the percentage of C(9)–OH alkaloid being translocated and stored in the root-bark falls considerably from the 46% present in the leaves but at the same time there are marked increases in the percentages of C(9)–H and C(9)–OMe alkaloids in the translocation stream and in the root-bark. In *M. inermis*, however, the percentage of C(9)–OMe alkaloids in the stem-bark is lower than in the leaves while the percentage of C(9)–OH alkaloid is not markedly different from that in the leaves. Thus it appears that in *M. ciliata* the C(9)–OH alkaloid is converted into the C(9)–OMe alkaloid and possibly the C(9)–H alkaloid, while in *M. inermis* the C(9)–OMe alkaloid is converted into the C(9)–OH alkaloid before translocation. The absence of C(9)–OMe alkaloids from *M. stipulosa* makes it impossible to compare this plant in the same way but it is clear that for translocation

Table 3. *Percentage of total alkaloid present as C(9)–H, C(9)–OH and C(9)–OCH_3 alkaloids in the leaves, stem-bark and root-bark of Ghanaian species of mitragyna collected in September* 1966

	Leaves	Stem-bark	Root-bark
Mitragyna ciliata			
C(9)–H	32	54·5	47
C(9)–OH	46	13·0	4·0
C(9)–OMe	22	32·5	44
Mitragyna inermis			
C(9)–H	60	76	70
C(9)–OH	29	26·5	11·8
C(9)–OMe	11	7·5	18·2
Mitragyna stipulosa			
C(9)–H	42	98·7	90
C(9)–OH	58	1·3	10
C(9)–OMe	0	0	0

the C(9)–OH alkaloids are converted to the C(9)–H series. Whereas the initial work suggested that the alkaloidal pattern of *M. ciliata* and *M. inermis* are similar, this more detailed study suggests a different metabolic pattern for the C(9)–OMe alkaloids. In *M. stipulosa* the enzyme system controlling the methylation of the C(9)–OH alkaloids appears to have been lost. This plant also differs from the others by the absence of even traces of recognizable indole alkaloids which throws some doubt upon the validity of the hypothesis for oxindole biogenesis suggested by Shellard, Phillipson & Gupta (1969) and supported by the alkaloids present in *M. inermis* and *M. ciliata* for which the suggested pathway would be:

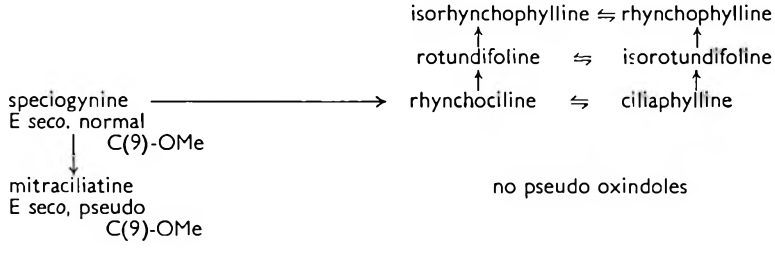

In *M. stipulosa* the pathway would have to be:

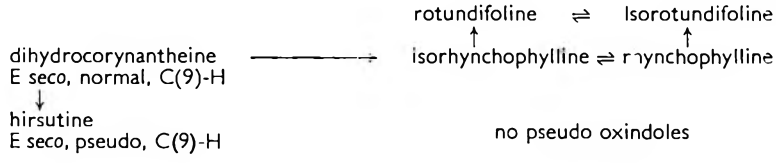

The close affinity of *M. stipulosa* to *M. ciliata* would not support this reversal in the mode of formation of the C(9)–OH although it does represent one of the pathways in *M. parvifolia* (Roxb.) Korth (Shellard & others, 1969).

The presence of the *epiallo* closed E ring oxindole alkaloids, speciophylline and uncarine F in the leaves, stem and root bark of *M. inermis* with no trace of the related

indole or oxindole alkaloids needs explanation though it is possible that an investigation similar to that made on *M. stipulosa* might reveal them at some times during the year. The absence of mitraphylline in the leaves of *M. stipulosa* collected in September might also be for this reason but no corresponding indole alkaloids, ajmalicine and 3-isoajmalicine, nor isomitraphylline, were detected at any time.

There appears to be some relation between the amount of rotundifoline in the leaf of *M. stipulosa* and the heavy rainfall while the movement of the rhynchophylline and isorhynchophylline corresponds to the dry seasons which follow the heavy rains. There must be some metabolism of the rhynchophylline and isorhynchophylline in the root bark since there is no accumulation of these alkaloids in the root-bark after the considerable translocation through the stem-bark, until the dry period at the turn of the year (Dec.–Jan.). The isorotundifoline content in the root-bark is also high at this time of the year but it also increases during the rainy period of May. The periods of minimum content of rotundifoline in the leaf correspond roughly to the periods of maximum content of rhynchophylline in the stem-bark and this supports the contention that rotundifoline is dehydroxylated to rhynchophylline for purposes of translocation.

It is possible that the isolation of immediate precursors of the indole alkaloids could lead to a modification of the hypothesis since it depends upon the identity of the D/E rings and the stereochemistry about C(3) in the indole and oxindole alkaloids. In this respect the root bark does contain indolic polar substances.

Acknowledgements

We would like to express our sincere thanks to Professor A. N. Tackie for arranging the collection, drying and transport of all the plant materials from Ghana. One of us (K.S.) would like to thank the Ghanaian Government and the University of Science and Technology, Kumasi, for a scholarship enabling him to undertake research work in the Pharmacognosy Research Laboratories at the Chelsea College of Science and Technology, University of London.

REFERENCES

Beckett, A. H., Shellard, E. J. & Tackie, A. N. (1963.) *J. Pharm. Pharmac.*, **15**, *Suppl.*, 158T–165T; 166T–169T.

Shellard, E. J. & Alam, M. Z. (1968). *J. Chromat.*, **33**, 347–369.

Shellard, E. J. & Sarpong, K. (1969). *J. Pharm. Pharmac.*, **21**, *Suppl.*, 113S–117S.

Shellard, E. J., Phillipson, J. D. & Gupta, D. (1969). *Planta Medica*, **17**, 51–58.

J. Pharm. Pharmac., 1970, **22**, *Suppl.*, 40 S–42 S

Received March 10, 1970

SHORT COMMUNICATION

Pharmacognostical examination of the roots and stems of *Rauwolfia mannii* Stapf

WILLIAM E. COURT

Pharmacognosy Laboratories, School of Pharmacy, University of Bradford, Yorks, U.K.

In previous communications the occurrence, indigenous usage, anatomy and chromatographic investigation of *R. rosea* K. Schum. have been described (Khalil, Court & Stewart, 1967; Court, Khalil & Stewart, 1967). Brief reference was made to the closely related species *R. mannii* Stapf and it was apparent that a detailed investigation was necessary to establish any differences between the species.

R. mannii was described by Stapf in 1894 and recorded with *R. cardiocarpa* K. Schum., *R. preussii* K. Schum. and *R. rosea* in Supplement I of the Kew Index (1886–1895). *R. cardiocarpa* and *R. preussii* are now considered synonymous with *R. mannii* (Feuell, 1955; Bisset, 1958). Confusion over the separate identities of *R. mannii* and *R. rosea* is related to the original morphological basis of differentiation, which depends on variations in the form of branches and peduncles (Stapf in Thiselton-Dyer, 1904). Pichon (1947) grouped both species in the section Afrovolfia of his classification of the genus. Boutique & Monseur (1955) observed close similarity between *R. mannii* growing in the Eastern Congo and *R. rosea* from the Usambaras, Tanzania, although synonymy has not been established (Bisset, 1958). Whereas Poisson (1965) does record the species as synonymous, East African botanists and the Royal Botanic Gardens, Kew (private correspondence) accept the species as distinct.

The presence of reserpine (0·04%), δ-yohimbine (ajmalicine), reserpiline, ajmaline and serpentine has been reported in the roots of *R. rosea* (Korzun, St. André & Ulshafer, 1957; Court & others, 1967) whilst reserpine, rescinnamine, reserpiline, ajmaline and serpentine have been observed in *R. mannii* (Court & others, 1967). Other authors (Kaiser & Popelak, 1959) claim serpentine and its isomer alstonine to be absent.

Habitat

R. mannii is a shrub attaining a height of 1–3 m at altitudes up to 2,300 m in forest and scrubland in Southern Nigeria, Cameroun, Gabon, Ruanda-Urundi and the Congo (Thiselton-Dyer, 1904; Dubois, 1955). *R. preussii* was reported indigenous to Southern Nigeria and French Cameroun, but no authentic specimens are available.

Indigenous usage

R. mannii is known in West Africa as Mbara and may be occasionally used as an arrow poison supplement (Lewin, 1923). The powdered bark may be applied to wounds (de Wildemann, 1939).

Plant material

The material used in this investigation was:

R. mannii roots and stems, herbarium specimens from Nigeria, obtained by the Tropical Products Institute, London, 1964; *R. mannii* roots and stems collected in Yaounde, Cameroun, 1968; *R. rosea* roots and stems collected in Tanzania in 1962 and verified by the East African Herbarium, Nairobi, Kenya; *R. rosea* roots and stems collected in Lushoto, Tanzania in 1964 and verified by the East African Herbarium.

Microscopical examination

Measurements of cells in radial, tangential and longitudinal planes and of cell inclusions and cells isolated by maceration, were obtained as described for *R. rosea* (Khalil & others, 1967). Methods for the determination of vessel diameter index values and vessel element length were as described earlier (Court, 1967).

Results and discussion

The tissue arrangement and distribution in the axis of *R. mannii* is similar to that described for *R. rosea* (Khalil & others, 1967) although sclereid development is more pronounced in *R. mannii* and can be related to the greater height of this species.

Comparison of cell dimensions corresponding to those reported for *R. rosea* indicates fair agreement except for the root vessel measurements. For *R. mannii*, R = 21 to **30** to **42** to 63 μm and T = 21 to **30** to **42** to 68 μm and for *R. rosea*, R = 25 to **34** to **55** to 84 μm and T = 21 to **29** to **50** to 67 μm where R and T refer to measurements made in the radial and tangential planes respectively.

Quantitative microscopy confirmed that the root vessel diameters are smaller for *R. mannii*, although the vessel element lengths are similar (Table 1). The laborious technique of vessel diameter index differentiates the two species. For *R. mannii* the 60 μm index is less than 10% and for *R. rosea* greater than 30%.

Stapf (1894) has recorded that young branches of *R. mannii* are quadrangular with more or less conspicuous decurrent raised lines; Schumann (Engler, 1895) describes

Table 1. *Vessel index determinations* (Vessel index = percentage of elements exceeding critical diameter) *and vessel element length.*

Vessel index determinations

Species	Critical diameter 30 μm	60 μm	90 μm	Number of specimens
R. mannii (Cameroun)	94·7 ± 0·4	1·5 ± 0·4	0	10
R. mannii (Nigeria)	94·7 ± 0·3	5·9 ± 0·8	0	10
R. rosea (Tanzania, 1962)	99·8 ± 0·1	44·4 ± 2·3	2·4 ± 0·2	9
R. rosea (Tanzania, 1964)	99·8 ± 0·2	41·0 ± 2·5	2·2 ± 0·6	9

(Arithmetic mean ± Standard error)

Vessel element length

Species	Range	Mean	Standard deviation	Number of samples	Number of observations
R. mannii (Cameroun)	58–**274**–**618**– 840 μm	446 μm	172 μm	6	900
R. mannii (Nigeria)	116–**341**–**661**– 971 μm	501 μm	160 μm	6	900
R. rosea (Tanzania, 1962)	50–**296**–**566**– 994 μm	421 μm	145μ m	6	300
R. rosea (Tanzania, 1964)	85–**355**–**709**–1,022 μm	532 μm	177 μm	6	300

the young branches of *R. rosea* as terete without decurrent lines. Examination of the available specimens confirms this differentiation.

Thin layer chromatographic examination of the specimens available using the methods described earlier (Court & others, 1967) again indicated the presence of rescinnamine in *R. mannii* but not *R. rosea*.

Khalil & others (1967) commented on the similarity between *R. rosea* and *R. volkensii* Stapf (now known to be *R. oreogiton* Mgf.) and *R. obscura* K. Schum. roots. These species exhibit small vessels and limited sclereid development and *R. mannii* must be considered in this group. The main features are compared in Table 2.

Table 2. *Comparison of the main features of four species of rauwolfia.*

Species	Normal height	Vessel diameter	Sclereid development	Reference
R. mannii	2–3 m	R 21–**30**–**42**–59 μm T 21–**30**–**42**–68 μm	Isolated or groups of up to 12	This work
R. rosea	0·5–2 m	R 25–**34**–**55**–84 μm T 21–**29**–**50**–67 μm	Isolated or small groups. Rare in roots below 1 cm diameter	Khalil & others, 1967
R. obscura	1–1·5 m	R 52–56 μm T 35–50 μm	Absent	Paris & Dillemann, 1956
R. oreogiton	2 m	R 26–**44**–**56**–96 μm T 26–**37**–**48**–78 μm	Isolated or small groups of up to 10. Rare except in specimens exceeding 4 cm diameter	Court, 1961

It is concluded that although similar in structure, the roots of *R. mannii* and *R. rosea* may be identified by careful investigation of sclereid development, vessel diameter index and by thin layer chromatography.

REFERENCES

Bisset, N. G. (1958). *Ann. Bogor.*, **3**, Part 1, 233.

Boutique, R. & Monseur, X. (1955). *Bull. agric. Congo belge*, **46**, 271–280.

Court, W. E. (1961). *J. Pharm. Pharmac.*, **13**, 422–434.

Court, W. E. (1967). *Can. J. pharm. Sci.*, **2**, 68–71.

Court, W. E., Khalil, A. A. & Stewart, A. F. (1967). *Planta Med.*, **15**, 173–178.

Dubois, L. (1955). *Bull agric. Congo Belge*, **46**, 567–595.

Engler, A. (1895). *Pflanzenw. Ost. Afr. C.*, 317.

Feuell, A. J. (1955). *Colon. Pl. Anim. Prod.*, **5**, 1–33.

Kaiser, F. & Popelak, A. (1959). *Chem. Ber.*, **92**, 278–287.

Khalil, A. A., Court, W. E. & Stewart, A. F. (1967). *Planta Med.*, **15**, 104–117.

Korzun, B. P., St. André, A. F. & Ulshafer, P. R. (1957). *J. Am. pharm. Ass.* (*Sci. Edn.*), **46**, 720–723.

Lewin, L. (1923). *Die Pfeilgifte* (Leipzig: J. A. Barth), 259.

Paris, R. & Dillemann, G. (1956). *Ann. pharm. fr.*, **14**, 505–518.

Pichon, M. (1947). *Bull. Soc. bot. Fr.*, **94**, 31–39.

Poisson, J. (1965). *Ibid.*, **112**, 162–174.

Stapf, O. (1894). *Kew Bull.*, 21.

Thiselton-Dyer, W. T. (1904). *Flora of Tropical Africa* Vol. IV, i, 113–114. London: Lovell Reeve and Co., Ltd.

de Wildeman, E. (1939). *Mém. Inst. r. colon. belge, Sect. Sci. nat. méd.*, **9**, 330.

J. Pharm. Pharmac., 1970, **22**, *Suppl.*, 43 S–52 S *Received March* 31, 1970

The effect of antioxidants on the hydrolytic and oxidative degradation of sulphacetamide in aqueous solutions

D. J. G. DAVIES, B. J. MEAKIN, AND S. H. MOSS

Pharmaceutics Group, School of Pharmacy, Bath University of Technology, Bath, U.K.

The effect of heat and light stresses on the degradation of sulphacetamide solutions at pH 7, in the presence and absence of the antioxidants sodium metabisulphite and sodium edetate, have been investigated. Sodium metabisulphite accelerates the hydrolytic degradation of sulphacetamide to sulphanilamide, whereas sodium edetate does not change the rate. The absorption peak causing colour development due to heat stress is shown to differ from that due to light stress. The development due to both stimuli has been measured quantitatively with time. Sulphanilamide present in heat-degraded solutions is shown to be insignificant in the development of colour due to heat stress, but to have a major role in colour formation under light stress.

The rate of oxidation of solutions of pharmaceuticals is generally dependent on the presence of oxygen, and the process is accelerated by heat, light and the presence of some metal ions. Stabilization relies either on the complexing of catalytic metal ions by chelating agents such as ethylenediamine tetra acetic acid (EDTA) or sodium edetate, or on the inclusion of a substance more readily oxidized than the drug, e.g. sodium metabisulphite.

Where drugs are also subject to degradation by other routes such as hydrolysis, the addition of antioxidants may produce adverse effects (Kokoski, 1958, Higuchi & Schroeter, 1959).

An example of a drug which degrades in aqueous solution by hydrolysis and oxidation is sulphacetamide sodium. Eye drops of this drug (B.P.C.) contain sodium metabisulphite which has been reported to decrease the rate of development of a yellow colour which normally forms on storage (Whittet, 1949, Anderson & Maudson, 1963 a, b), although the latter workers found a concommitant increase in rate of disappearance of sulphacetamide.

This work was initiated to investigate quantitatively the effect of sodium edetate and sodium metabisulphite on the degradation of sulphacetamide sodium solutions.

EXPERIMENTAL

Materials. Sulphacetamide sodium B.P. (mp. 183°) was recrystallized twice from ethanol, sulphanilamide B.P.C. (mp. 163·5°) was recrystallized twice from water. Sodium metabisulphite, B.P. (B.D.H.) and sodium edetate (May and Baker) were used without further purification. Oxygen and oxygen free nitrogen (white spot grade) were obtained from British Oxygen Company. All other chemicals and reagent solutions were as described elsewhere (Tansey, 1969).

Buffer solutions. In all experiments solutions were adjusted to pH 7 ± 0·05 with McIlvaine's citric acid, disodium hydrogen phosphate buffer.

pH Measurement. A Radiometer type 27 meter fitted with a Radiometer type C glass-calomel electrode system, standardized with 0·25M potassium dihydrogen phosphate and 0·25M disodium hydrogen phosphate (Bates, 1957), was used.

Oxygen tension measurement. Oxygen tensions were measured using a Radiometer type PHA 927b gas monitor fitted with a Clark type oxygen electrode, standardized with 0·1M borax containing 1% w/v sodium metabisulphite.

Heating procedure. Solutions, buffered at pH 7·0, were equilibrated with oxygen or nitrogen as required and sealed under the appropriate gaseous atmosphere, by fusion in glass ampoules (Tansey 1969). These were maintained at the required temperature ±0·5° for different graded periods of time. On removal the ampoules were chilled in crushed ice and stored at 2° until required.

Exposure to light. Solutions of sulphonamide were aspirated with oxygen to a maximum oxygen tension and transferred to stoppered 1 cm quartz cuvettes and the air space above the solutions filled with oxygen. Five of these cells were placed between two fluorescent tubes (Atlas 15W Northlight) at a distance of 5 cm from each tube to the optical surface of the cell. No precautions were taken to control the temperature in the cells as this remained constant at 27° ± 1·5°. The dose rate was determined using a thermopile (Hilger Watts No. FT.17.1) in combination with a millivoltammeter (Keithley Inst. 150B) which had been calibrated by reference to a potassium ferrioxalate actinometer (Hatchard & Parker, 1956). The dose rate was $2{\cdot}69 \times 10^{-5}$ J mm^{-2} s^{-1} (coefficient of variation of ± 1·3%). In one series of experiments the Northlight tubes were replaced by Phillips T.U. 15W low pressure tubes, emitting chiefly at 254 nm.

Assay procedures

Assay for sodium metabisulphite. Sulphacetamide was separated from its degradation products by a thin-layer chromatographic technique using silica gel G as adsorbent and a running solvent consisting of acetone–methanol–diethylamine (9 : 1 : 1). The areas of silica gel containing the sulphacetamide sodium were removed and extracted with methanolic hydrochloric acid, and the sulphacetamide assayed colorimetrically at 536 nm following a modified Bratton-Marshall reaction (Tansey, 1969). Experiments with formulated mixtures of sulphacetamide and sulphanilamide in different ratios showed that adequate separation was obtained and that all the sulphacetamide could be recovered with a coefficient of variation on ten replicate samples of 1·4%.)

Assay for sodium metabisulphite. As sodium metabisulphite is readily oxidized in aqueous solution all batches prepared were assayed. When an ampoule was opened, an aliquot (1 ml) was immediately transferred to iodine solution (25 ml) contained in a stoppered conical flask and assayed in the standard manner (coefficient of variation < 2%).

Determination of coloured degradation products. An absorption spectrum of sulphonamide solutions, exposed to heat, light, or both sequentially, was obtained in 1 cm quartz cuvettes using a Perkin-Elmer recording ultraviolet and visible spectrophotometer. Quantitative values of absorbance at specific wavelengths were subsequently measured using a Unicam SP500 ultraviolet and visible spectrophotometer.

Loss of sulphacetamide in solution on heating

Treatment of results. In the presence or absence of antioxidants, the thermal degradation of 1% solutions of sulphacetamide sodium followed apparent first order kinetics. Heated solutions were assayed for both sulphacetamide and sulphanilamide under all conditions of test, and in each case the results suggested that sulphacetamide loss can be accounted for by formation of sulphanilamide. The percentage residual concentration of sulphacetamide was calculated, with respect to an unheated sample, for each period of heating. Values for the apparent first order rate constant (k) were obtained from log % concentration—time data by means of a least squares regression analysis, which gave values of k, its associated standard error and the correlation coefficient.

The effect of 1% sodium metabisulphite. Two anoxic solutions of sulphacetamide sodium were prepared, 1% sodium metabisulphite was added to one of them and both were sealed under nitrogen into ampoules (Tansey 1969). Both were heated at 120° for varying times, removed and assayed. The appropriate log % residual concentration-time plots are shown in Fig. 1, the calculated values for the rate constants being $10{\cdot}05 \times 10^{-2}$ and $2{\cdot}79 \times 10^{-2}\,h^{-1}$ for solutions in the presence and absence respectively of sodium metabisulphite.

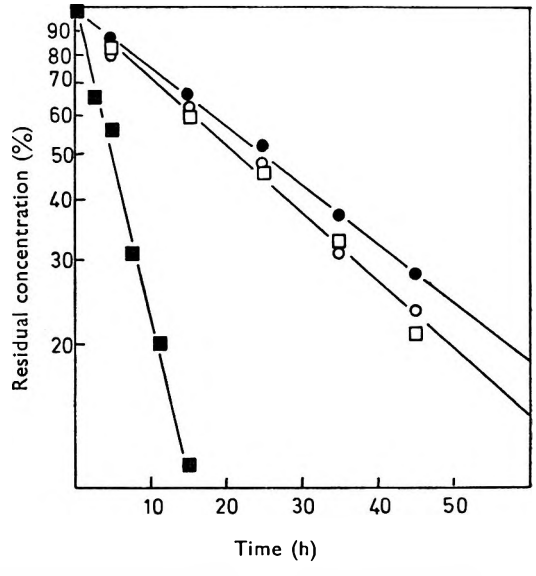

FIG. 1. Plots of percentage residual concentration against time of heating at 120° (h) for 1% solutions of sulphacetamide sodium at pH 7·0. ● Heated anoxically. ■ Heated anoxically in the presence of 1% sodium metabisulphite. ○ Heated after saturation with oxygen. □ Heated after saturation with oxygen in the presence of 1% sodium metabisulphite.

The effect of oxidized sodium metabisulphite was determined by heating solutions that had been equilibrated with and sealed under oxygen. The residual concentration of unoxidized sodium metabisulphite was less than 0·02% w/v. These results are also shown in Fig. 1, the calculated values for the rate constant are $3{\cdot}46 \times 10^{-2}$ and $3{\cdot}23 \times 10^{-2}\,h^{-1}$ for solutions in the presence and absence of oxidized sodium metabisulphite respectively.

It is evident that sodium metabisulphite has an accelerating effect on the rate of degradation of sulphacetamide in the absence of oxygen. The rate increase, due to a nominal 1% concentration (0·65% by assay) can be represented by $k_1/k_2 = 10{\cdot}05/2{\cdot}79$ a factor of 3·6. This effect is dependent on the retention of the integrity of the antioxidant molecule as, after oxidation by atmospheric oxygen, the rate of degradation is not significantly different from the rate in the absence of antioxidant (t calc. = 1·41, at $P = 0{\cdot}05$, t tabulated = 2·31). The presence of oxygen increases the rate of degradation of sulphacetamide, this effect is independent of the presence of oxidized sodium metabisulphite, the values of t being 4·12 and 3·16 respectively, for heating in the presence and absence of antioxidant (t tabulated at $P = 0{\cdot}05$ is 2·31). This increase, though significant, is small and may be due to oxidative degradation which does not occur in deoxygenated solutions.

The effect of different concentrations of sodium metabisulphite. Oxygen free solutions of sulphacetamide sodium were prepared containing different concentrations of sodium metabisulphite, the effective concentrations being determined by assay. Over the range examined an increase in the concentration of antioxidant increased the rate of degradation of sulphacetamide sodium. A plot of log k against concentration was linear with a correlation coefficient of 0·9983.

A direct relation between the rate constant and concentration of sodium metabisulphite would indicate that the accelerating effect is due to specific ion catalysis and that this was not observed may indicate a more complex accelerating mechanism. Although it has been reported that metabisulphite accelerates ephedrine degradation by chemical interaction (Schroeter, Higuchi & Schuler, 1958), this was not the mechanism responsible in the present case since no fall in the sodium metabisulphite concentration was observed during the course of the reaction (Schroeter, 1961).

The effect of sodium metabisulphite at different temperatures. Samples of sulphacetamide were heated in the presence of a nominal 0·5% w/v of sodium metabisulphite (0·46% by assay). On different occasions samples were heated at 100, 110 120 and 140° and the results used to obtain rate constants (k). These were then fitted by a least squares analysis according to the Arrhenius equation: $k = Ae^{-Ea/RT}$ to obtain values for the activation energy (Ea) and frequency factor (A) of 19·54 k cal mol^{-1} ($8{\cdot}181 \times 10^4$J mol^{-1}) and $6{\cdot}029 \times 10^9$ h^{-1} respectively. These compare with values of 22·90 k cal mol^{-1} ($9{\cdot}588 \times 10^4$J mol^{-1}) and $1{\cdot}76 \times 10^{11}$ h^{-1} obtained for sulphacetamide in McIlvaine buffer at pH 7·4 in the absence of sodium metabisulphite (unpublished observations). These also show that the rate of degradation of sulphacetamide is independent of pH over the range of 5 to 9, and so the two sets of results may be compared directly. These findings are not inconsistent with the action of metabisulphite being that of a specific ion catalyst, although as is clear from the concentration data the mechanisms involved do not appear to be open to a simple description.

The accelerating effect of sodium metabisulphite on hydrolysis rates has been reported by Fletcher & Norton (1963) and Anderson & Maudson (1963a) who observed that crystals of sulphanilamide were deposited, after exposure to high temperatures, from concentrated solutions of the drug that contained antioxidant. An unsuccessful attempt was made by Clarke (1967a) to relate the effect quantitatively to the concentration of sodium metabisulphite. Forse (1967) suggests that the effect of metabisulphite is temperature dependent, the hydrolysis being accelerated

at 116° but not at lower temperatures. In all those studies sulphanilamide had to be formed in sufficient concentration to precipitate at room temperature before an effect could be noted and this is probably the reason for the lack of correlation and difficulty of interpretation of the published work.

This report shows that the action of metabisulphite at all concentrations and temperatures studied is an accelerating one, and that this effect can be described by simple kinetic expressions. The results obtained should enable accurate predictions to be made of the stability of solutions of the drug in the presence or absence of antioxidant under normal storage conditions.

Effect of sodium edetate. Solutions of sulphacetamide sodium and 0·5% sodium edetate were heated, on separate occasions, in oxygen-free and in oxygenated solutions; the values of the first order rate constants obtained were $2{\cdot}98 \times 10^{-2}$ and $2{\cdot}99 \times 10^{-2}\ h^{-1}$ respectively. These compare with a value of $2{\cdot}79 \times 10^{-2}$ and $3{\cdot}23 \times 10^{-2}\ h^{-1}$ obtained for degradation in the absence of edetate in oxygen-free and oxygenated solutions. The value of the rate constants obtained with edetate is independent of the presence of oxygen ($t = 0{\cdot}06$, t at $P = 0{\cdot}05 = 2{\cdot}31$) and the value for oxygen-free solutions is indistinguishable from the anoxic value of $2{\cdot}79 \times 10^{-2}\ h^{-1}$ obtained in the absence of edetate ($t = 1{\cdot}70$, t tabulated $= 2{\cdot}31$). The presence of edetate however does serve to protect sulphacetamide sodium against the accelerating effect of oxygen the value of k being reduced from 3·23 to $2{\cdot}99 \times 10^{-2}\ h^{-1}$, and the value of t being 2·40 compared to the tabulated value of 2·31.

Thus it appears that the oxygen acceleration is dependent on the presence of metal ions which the sodium edetate neutralizes, probably by chelation. As its protective action will not be abolished by oxidation, and as it has no significant accelerating effect on the rate of degradation, it would appear that solutions of sulphacetamide sodium would be better preserved by sodium edetate than by sodium metabisulphite.

Colour development in sulphacetamide solutions

The development of colour in sulphacetamide solutions when exposed to a variety of stresses has been assumed to be due to oxidative breakdown. Various workers have attempted to assess the role of oxidation by absorbance measurements (Anderson & Maudson, 1963a; Clark, 1967b; Mital & Gupta, 1968; Pandula, Racz & Pajor, 1969). With the exception of Pandula & others, who used 336 nm corresponding to the wavelength of maximum absorption of their reported oxidation breakdown products, viz. azobenzene 4,4′-disulphonamide and azoxybenzene 4,4′-disulphonamide at alkaline pH, no rationale is given for the choice of the specific wavelengths used which include 370, 420 and 520 nm.

Initial experiments were made to qualitatively assess the effect of heat (120°), ultraviolet, natural, and artificial daylight on the degradation of sulphacetamide. All solutions were equilibrated with oxygen, and after degradation the absorption spectra of the solutions were obtained. These are shown in Figs 2 and 4 and indicate that the main breakdown products are different for each stress. With the ultraviolet source, colour development (brownish yellow) is quickest and this is accompanied by a general shift in the absorption curve to the visible region, with non-specific absorption extending beyond 500 nm (curve a, Fig. 4). The effect of the daylight tubes is quite different (curve c, Fig. 4), since a clearly defined maximum occurs at 450 nm in addition to a general increased absorption below 400 nm. For compara-

tive purposes samples were also stored in natural daylight (curve b, Fig. 4) which gave a similar result to the artificial daylight tubes. Thus in all subsequent experiments the light source was the Northlight tubes as these produce conditions closest to natural storage. Under the influence of heat alone a pale yellow colour was produced. This is due to an absorption peak at 365 nm (curve a, Fig. 2), there being no peak at 450 nm. as was produced by visible light. However there appears to be a shoulder in the region of 336 nm which is interesting in view of the work of Pandula & others (1969). Thus it is apparent that the coloured breakdown products produced under the influence of heat and light are different.

On the basis of these results the wavelengths chosen for quantitative measurements were 336, 365 and 450 nm.

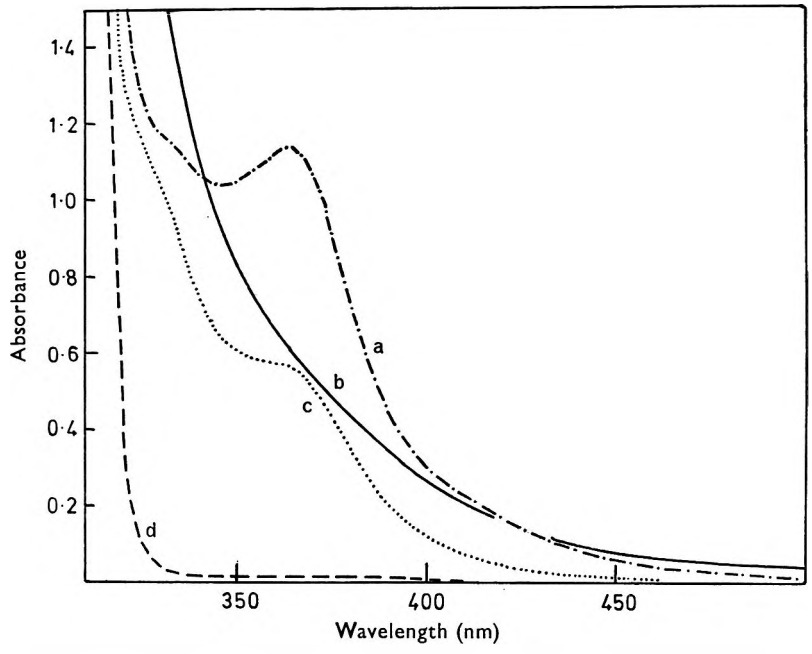

FIG. 2. Visible absorption spectra for sulphacetamide sodium and sulphanilamide solutions at pH 7·0 after heating at 120° for 36 h. (a) 0·5% sulphacetamide sodium, saturated with oxygen. (b) 0·5% sulphacetamide sodium, saturated with oxygen and with the addition of 1% sodium edetate. (c) 0·5% sulphacetamide sodium saturated with oxygen and the addition of 1% sodium metabisulphite. (d) Common spectrum for (i) 0·5% sulphacetamide sodium heated anoxically; (ii) 0·338% sulphanilamide heated either anoxically or after saturation with oxygen.

Colour development due to heat at 120°. Sulphacetamide solutions show no colour development when heated in the absence of oxygen, the absorption spectrum remaining close to curve d, Fig. 2. When heated under oxygen, however, sulphacetamide solutions soon develop a pale yellow colour and give the absorption spectrum shown in curve a, Fig. 2. The changes in absorbance with time at 120° for the three wavelengths chosen are given in Fig. 3, the increase at 450 nm is non-specific and is not due to the development of an absorbance peak. Heated solutions containing an equivalent amount of sulphanilamide, show no colour development upon heating in either oxygen or nitrogen, and no peaks in the absorption spectrum (curve d, Fig. 2), merely a slight general shift towards the visible. This indicates that the sulphanilamide, present as a result of hydrolytic degradation, plays no part in the formation of

colour in heated sulphacetamide solutions that have not been exposed to light. Indeed, the increasing amount of sulphanilamide being formed may be the reason for the apparent decreasing rate of absorbance increase at 336 and 365 nm (Fig. 3).

The effect of sodium metabisulphite and sodium edetate on colour development is also shown in Fig. 2, curves c and b respectively. Sodium metabisulphite reduces the magnitude of the absorption peaks without altering the general shape of the absorption spectrum. The action of the antioxidant in this instance is probably an indirect

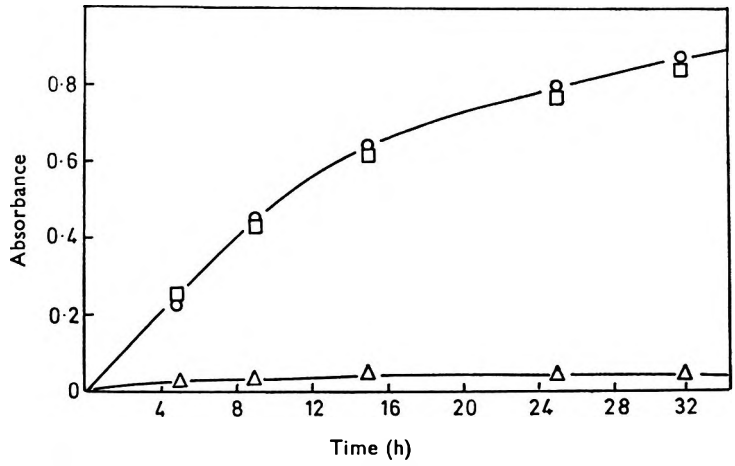

FIG. 3. Plots of absorbance against heating time at 120° (h) for 1% sulphacetamide sodium solutions at pH 7·0 measured at 336 nm (○), 365 nm (□), 450 nm (△).

one, as it acts by reducing the concentration of oxygen in the system. Sodium edetate exerts a profound effect on the general shape of the absorption curves obtained under these conditions. The removal of the 365 nm peak, and the marked reduction in general absorbance at 336 and 450 nm suggests that reactions catalysed by metal ions are largely responsible for the oxidative degradation of sulphacetamide. With the fact that edetate does not accelerate the degradation rate of sulphacetamide this would suggest that sodium edetate and not sodium metabisulphite should be added to solutions of sulphacetamide that are heat sterilized.

Colour development due to artificial daylight. After exposure to artificial daylight, unheated solutions of both sulphacetamide and sulphanilamide gave similar absorption spectra with a definite peak at 450 nm (curve c, Fig. 4). The peak height was achieved with sulphanilamide in 17 h compared with 30 h for sulphacetamide (Fig. 6).

The better to simulate normal storage conditions, 0·5% solutions of sulphacetamide were heated in the absence of oxygen at 120° for different periods before exposure to light under oxygen. These heated solutions remained colourless even on prolonged storage in natural daylight until opened, when a brown colour rapidly developed. The rate of absorbance increase at 450 nm of these heated solutions is shown in Fig. 5. The rate of colour development is dependent on time of heating up to 15 h, which is the time necessary to form 33% sulphanilamide, calculated as total sulphonamide. Longer periods of heating result in colour development data indistinguishable from sulphanilamide (0·338% w/v, equivalent to 0·5% sulphacetamide). Figs 5 and 6 show that a relation between rate of colour development and sulphanilamide concentration exists, although this is clearer in formulated

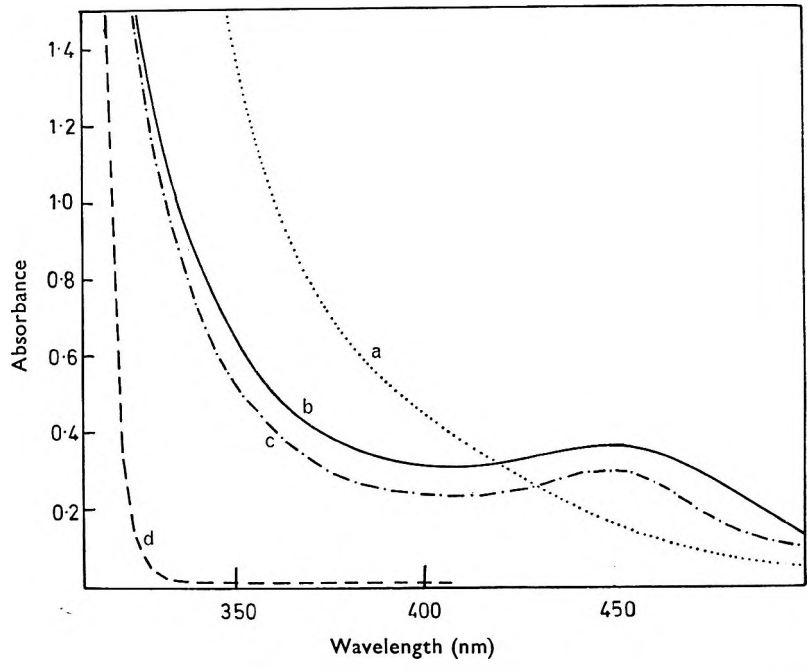

FIG. 4. Visible absorption spectra for 0·5% sulphacetamide sodium solutions at pH 7·0 after saturation with oxygen and exposure to light (unheated). (a) Ultraviolet light (4 h). (b) Diffuse natural daylight (40 days). *(c) Artificial daylight (30 h). (d) No light exposure.
* Curve "c" is also the spectrum of 0·338% sulphanilamide under the same conditions after 17 h.

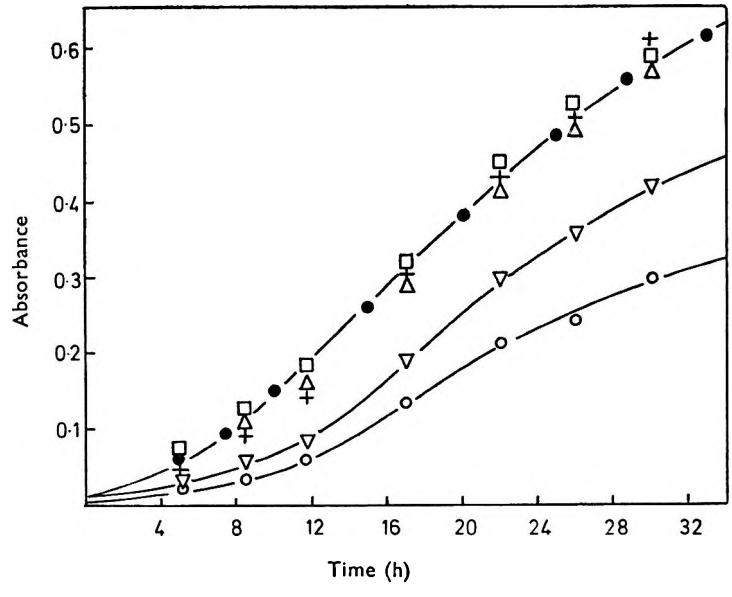

FIG. 5. Plot of absorbance, measured at 450 nm against time of exposure to artificial daylight (h) for 0·338% solutions of sulphanilamide and 0·5% sulphacetamide sodium at pH 7·0 heated anoxically at 120° for varying periods, and then saturated with oxygen. Sulphacetamide: Time of heating (h); zero (○), 5 (▽), 15 (+), 25 (□), 35 (△). Sulphanilamide: Times of heating as above, (●) represents mean values.

mixtures (Fig. 6) than in heated solutions (Fig. 5). The lag periods as illustrated in Figs 5 and 6 vary widely and such batch to batch variation has been noticed on a number of occasions; the explanation is as yet unknown. Clarke (1967b) measuring colour development at 420 nm ascribed the effect to a variation in metal ion content although this has been disputed by Forse (1967) with sulphanilamide.

Two general conclusions can be drawn; first, that colour development in sulphacetamide solutions proceeds by two distinct pathways dependent upon the degradation stimulus—heat giving a clear lemon colour, and an absorption peak at 365 nm, light in presence of oxygen giving a brown colour with an absorption peak at 450 nm.

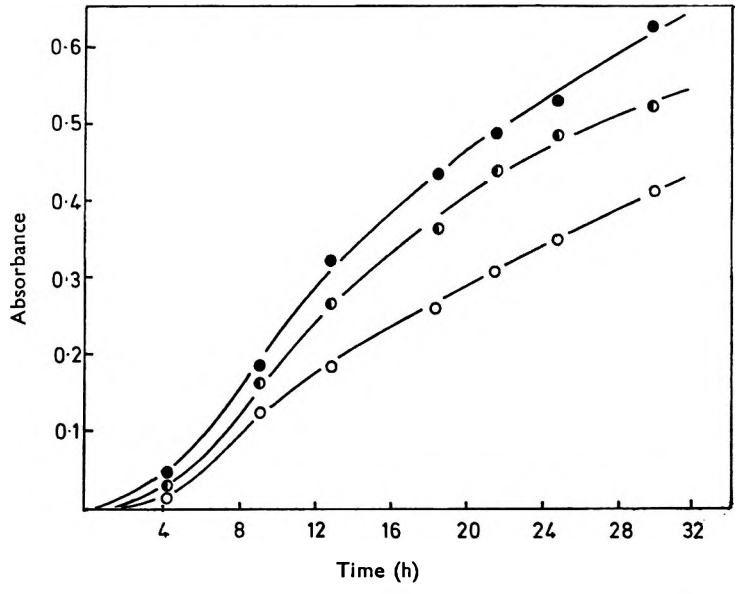

FIG. 6. Plot of absorbance, measured at 450 nm against time of exposure to artificial daylight (h) for unheated solutions of sulphacetamide and sulphanilamide at pH 7·0. ○ 0·5% sulphacetamide sodium. ● 0·33% sulphanilamide. ◐ 0·25% sulphacetamide sodium, 0·169% sulphanilamide.

Second, the sulphanilamide present as a result of hydrolysis in heated solutions plays no part in colour formation due to heat, but is significant in increasing the rate of colour development due to light.

As yet the oxidative breakdown products produced by heat and light have not been identified. We do not, however, believe that they are azobenzene 4,4′-disulphonamide (I) and azoxybenzene-4,4′-disulphonamide (II) which have been postulated both by Clarke (1965) and Pandula & others (1969) to be responsible, at least in part for the colour development. We prepared I (orange crystals) and II (yellow crystals) by the method of Seikel (1940) and authenticated their structure by nmr, infrared and mass spectroscopy. Ultraviolet spectra in aqueous 0·1N sodium hydroxide showed peaks at 232, 335, 437 nm for I and 220, 336 nm for II. However, after shaking I and II for several days in buffer solution at pH 7·0, at room temperature, followed by filtration through a millipore membrane, no detectable absorbance was recorded in either the visible or ultraviolet regions of the spectrum, indicating virtual insolubility in water at this pH. These compounds were found to be soluble only in strongly alkaline solution.

REFERENCES

ANDERSON, R. A. & MAUDSON, J. W. (1963a). *Aust. J. Pharm.*, **44**, 518, S.24.
ANDERSON, R. A. & MAUDSON, J. W. (1963b). *Ibid.*, **44**, 528, S.138.
BATES, R. G. (1957). *J. Res. Natn. Bur. Stand.*, **59**, 261.
CLARKE, P. A. (1965). *Pharm. J.*, **194**, 275–376.
CLARKE, P. A. (1967a). *Ibid.*, **198**, 374–375.
CLARKE, P. A. (1967b). *Ibid.*, **199**, 414.
D'SOUZA, L. & DAY, R. A. (1968). *Science, N.Y.*, **160**, 882.
FLETCHER, G. & NORTON, D. A. (1963). *Pharm. J.*, **191**, 145–147.
FORSE, S. F. (1967). *Ibid.*, **199**, 355–356.
GUPTA, J. L. & MITAL, H. C. (1968). *Ind. J. Pharm.*, **30**, 94–95.
HATCHARD, C. G. & PARKER, C. A. (1956). *Proc. Roy. Soc.* (*Lond.*), **A.235**, 518–536.
HIGUCHI, T. & SCHROETER, L. C. (1959). *J. Am. pharm. Ass.*, **43**, 535–540.
KOKOSKI, C. J. (1958). *Dissertation Abstr.*, 17; *through Bull. Am. Soc. Hosp. Pharm.* (1957), **14**, 6969.
MITAL, H. C. & GUPTA, J. L. (1968). *Ind. J. Pharm.*, **30**, 94–95.
PANDULA, E., RACZ, I & PAJOR, Z. (1969) *Die Pharmazie*, **24**, 155–157.
SCHROETER, L. C. (1961). *J. pharm. Sci.*, **50**, 891–901.
SCHROETER, L. C., HIGUCHI, T. & SCHULER, E. E. (1958). *J. Am. Pharm. Ass.*, **47**, 723–728.
SEIKEL, M. K. (1940). *J. Am. chem. Soc.*, **62**, 1214.
TANSEY, I. (1969). M.Sc. Thesis. University of Bath.
WHITTET, T. D. (1949). *Pharm. J.*, **1963**, 177–179.

J. Pharm. Pharmac., 1970, **22**, *Suppl.*, 53 S–59 S *Received March* 31, 1970

Physico-chemical studies of analgesics. The protein-binding of some *p*-substituted acetanilides

J. C. DEARDEN AND ERIC TOMLINSON

School of Pharmacy, Liverpool Polytechnic, Byrom Street, Liverpool L3 3AF, U.K.

The binding of fifteen *p*-substituted acetanilides to bovine serum albumin is examined at pH 7·2. An excellent correlation is obtained between the binding enthalpy and Hammett's substituent constant, σ. This is interpreted to mean that the binding is non-specific in nature. A very good correlation is also obtained between the entropy of binding and σ, which suggests that the extent of hydration of unbound drug is a function of the charge separation within the drug molecule. Of the compounds examined, those that have been used clinically as analgesics possess the best thermodynamic properties, being neither so fully bound as to give low free drug concentrations in the blood-stream, nor so little bound that there is no sustained action.

Although the significance of protein-binding in relation to the activity of drugs is well-known, there has been no intensive investigation of the protein-binding of mild analgesics such as the acetanilides. The present study is concerned with the binding on bovine serum albumin (BSA) of some *p*-substituted acetanilides, including paracetamol and phenacetin.

EXPERIMENTAL AND RESULTS

Materials

The protein used was crystallized BSA obtained from Pentex Inc., with a moisture content of 3·2%. The acetanilides, obtained commercially or prepared by standard methods, were recrystallized to constant melting point.

Method

A dynamic dialysis method, similar to that described by Meyer & Guttman (1968) was used to determine the association constants of the binding of the acetanilides to BSA. The method has advantages over equilibrium dialysis in that it is much more rapid, and less subject to error, since a single run over a wide drug concentration range can yield the association constant.

A small bag was made from 3 cm flat width Visking dialysis tubing previously treated by heating (1 h: 90°) in deionized water and washing for one week. Into this was placed 10 ml of the solution of drug and BSA in Clark and Lubs 0·2 M phosphate buffer (pH 7·2). The bag was immersed in 200 ml of the same buffer, and the whole thermostatted; runs were made at 19°, 27° and 40°, provision being made for both solutions to be stirred. The concentrations of acetanilides used were 0·4 to 4·0 $\times 10^{-3}$ M, and those of BSA, 0·35 to 3·5 $\times 10^{-4}$ M.

Because of the large volume of the external solution, the concentration of drug in this exerts only a negligible effect on the dialysis, provided it is not allowed to rise

above about 1% of that in the dialysis bag. In this work, this was achieved by withdrawing, every 30 min, a 100 ml sample from the external solution and replenishing by the same volume of fresh buffer.

Each sample withdrawn was analysed spectrophotometrically at 19°, a temperature correction being applied for samples taken at 27° and 40°. The total amount of drug dialysed at any sampling time was thus determined, and by difference the total concentration (S_T) remaining in the dialysis bag obtained.

A dialysis run in the absence of protein showed that the diffusion was first-order with respect to the drug, and that adsorption by the dialysis bag was negligible (Meyer & Guttman, 1970). In the presence of BSA, a plot of log S_T against time was curvilinear, owing to the fraction of bound drug increasing as the total concentration in the internal solution decreased.

A computer program was written to obtain instantaneous rates of diffusion (slopes) at various times from this curvilinear plot. From a knowledge of the instantaneous rates, and of the rate constant obtained from the dialysis of drug in the absence of BSA, the concentration of unbound drug (S_F), and hence of bound drug, was calculated for various times. The number of moles of drug bound per mol of BSA ($\bar{v}$) was then calculated for these times, taking a value of 69 000 as the molecular weight of BSA. In a plot of $\bar{v}/S_F$ against $\bar{v}$ (Scatchard plot), the initial slope represents the association constant for the binding of drug to primary binding sites on the BSA molecule. Extrapolation to the abscissa gives the number of primary binding sites per BSA molecule. Fig. 1 illustrates Scatchard plots for three of the acetanilides at 19°. The second, lower slope represents binding to secondary sites, and was not

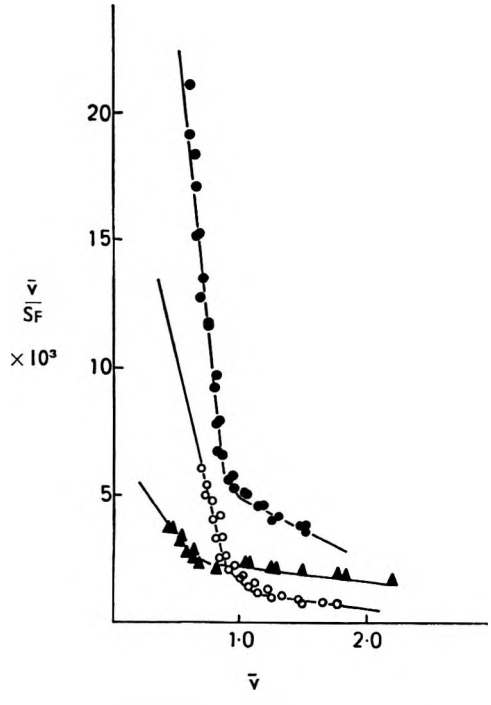

FIG. 1. Scatchard plots of the binding to BSA of acetanilide (—○—), *p*-aminoacetanilide (—▲—) and *p*-nitroacetanilide (—●—). The initial slopes for all 15 compounds intersect the abscissa at $\bar{v} = 1$, indicating a single primary binding site per BSA molecule.

considered in this work, since such binding does not generally occur until drug concentrations well above those used clinically are reached.

Association constants obtained in duplicate runs at the three temperatures gave the thermodynamic parameters of association shown in Table 1.

That no serum albumin leaked from the dialysis bag was shown by the absence of colour development when the external solution was treated with 3% sulphosalicylic acid. The possibility of disturbance of the dialysis by a Donnan effect was examined by carrying out several runs at one tenth the normal buffer concentration; identical association constants were obtained at both buffer concentrations. Finally, solutions were checked regularly for pH changes during dialysis; none were found.

Table 1. *Thermodynamic constants of the association of* p-*substituted acetanilides with bovine serum albumin, and the Hammett constants of the substituents.*

p-Substituent	Association constant at 19° (litre mol^{-1})	$\triangle G$ at 19° (kJ mol^{-1})	$\triangle H$ (kJ mol^{-1})	$\triangle S$ (J mol^{-1} deg^{-1})	Hammett's *p*-substituent constant, σ
-H	21 500	—24·2	—15·2	+30·8	0
$-CH_3$	29 800	—25·0	—18·7	+21·7	—0·170
-OH	17 000	—23·6	—20·7	+10·0	—0·370
$-OCH_3$	16 100	—23·5	—19·8	+12·7	—0·268
$-OC_2H_5$	20 200	—24·0	—17·7	+21·4	—0·240
$-NH_2$	7 000	—21·5	—24·0	— 8·7	—0·660
-F	29 900	—25·0	—14·2	+36·8	+0·062
-Cl	62 500	—26·8	—12·5	+48·8	+0·227
-Br	105 500	—28·1	—11·4	+56·9	+0·232
-I	142 000	—28·8	—12·1	+57·3	+0·180
-CHO	26 000	—24·7	—10·8	+47·4	+0·265
-COOH	13 400	—23·1	— 9·0	+48·0	+0·450
$-NO_2$	48 600	—26·2	— 2·4	+81·2	+0·778
$=N-CH_3$,-H	18 800	—23·9	—14·9	+30·9	0
$=N-CH_3$,-OH	16 000	—23·5	—19·7	+13·0	—0·370

DISCUSSION

Fig. 2 shows a good rectilinear relation between the enthalpy of binding (ΔH) and Hammett's substituent constant, σ. A high enthalpy of interaction is thus associated with ability of a substituent to donate electrons, suggesting that the drug-BSA binding is a function of the electron density within the acetanilido moiety.

The close correlation of Fig. 2 also implies that the binding enthalpy is governed almost entirely by the electron-directing properties of the substituent, and not by any specific substituent property such as the ability to form hydrogen bonds. Hansch, Kiehs & Lawrence (1965) have also shown, in the case of phenol-BSA binding, that the size of the substituent similarly appears to play no significant part in the interaction.

The compounds examined include two *N*-methylated acetanilides, and although these lack an amino-hydrogen atom, they behave in a similar fashion to the simple *p*-substituted acetanilides. Since there is but a slight decrease of the binding enthalpy on *N*-methylation, this also suggests that hydrogen bonding of the acetanilide =N–H group contributes little, if anything, to the drug-BSA interaction.

At the pH used (7·2) the carboxyl group of *p*-acetamidobenzoic acid ($pK_a = 4{\cdot}2$) is 99·9% ionized. This has, however, no appreciable effect on the binding to BSA, so that ionic forces probably play no part in the binding.

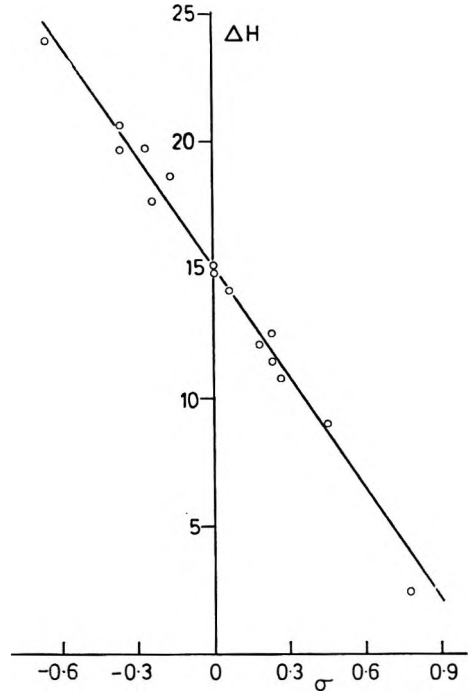

FIG. 2. Correlation of the enthalpy of substituted acetanilide-BSA binding, $\triangle H$, and Hammetts substituent constant, σ. The regression equation is $\triangle H = 14{\cdot}50\,\sigma + 15{\cdot}1$ kJ mol^{-1}, and the correlation coefficient is 0·992.

Interaction between acetanilides and BSA is thus non-specific, involving only van der Waals forces. Binding probably occurs to a hydrophobic region of the BSA molecule, as has previously been postulated for penicillins (Bird & Marshall, 1967), dyes (Weber & Young, 1964) and hydrocarbons (Wetlaufer & Lovrien, 1964); such behaviour is consistent with the role of albumins as transport proteins.

Table 1 shows that whereas the free energy of binding (ΔG) is negative in all cases, indicating spontaneous interaction, there is but little variation of ΔG amongst the different drug-BSA complexes. Variation of ΔH is therefore counteracted by opposing changes in the entropy of association, ΔS, and a good correlation in fact obtains between ΔS and σ (Fig. 3).

With the exception of *p*-aminoacetanilide, all the entropy changes on binding are positive. Although this would appear anomalous, since the association of drug and protein should result in an increase in the order of the system, a number of other factors must be considered. It has been suggested (e.g. O'Reilly, 1969) that hydration of both drug and BSA in the free state will reduce the entropy of the system. When drug-BSA association occurs, some at least of the bound water is released, thereby increasing the disorder, and thus the entropy, of the system. If this is correct, drug-protein binding should increase the total volume of the solution, and Lundgren (1945) has observed such an increase on the binding of alkylsulphonate anion by egg albumin. Using a value of $\Delta S = 20$ J mol^{-1} deg^{-1} to represent the loss of one water molecule (McMenamy & Seder, 1963) and assuming 'dehydration' to account for the bulk of the entropy gain on binding, then the binding of, for example, paracetamol involves half a water molecule, that of phenacetin involves one, and that of *p*-nitroacetanilide involves four water molecules.

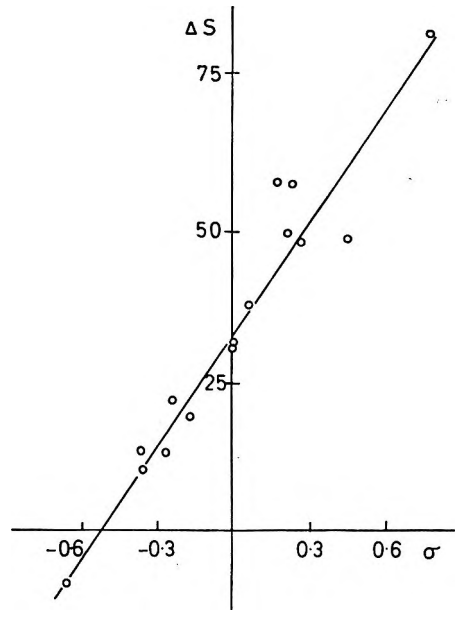

FIG. 3. Correlation of the entropy of substituted acetanilide-BSA binding, $\triangle S$, and Hammett's substituent constant, σ. The regression equation is $\triangle S = 61{\cdot}4\,\sigma + 31{\cdot}8$ J mol^{-1} deg^{-1}, and the correlation coefficient is 0·966.

Increased rotational and translational freedom in the protein, consequent upon association, could result from, for example, the transfer of interactive ability from an intramolecular to an intermolecular situation, or from the release of solvated water. Steinberg & Scheraga (1963) have shown that such an increase in intrinsic entropy can make a significant contribution to the overall positive ΔS of association.

Increased rotational freedom may also arise in the drug molecule. In the case of the acetanilides, rotational mobility around the aryl-N bond could increase on association owing to the release of solvated water (Aranow & Witten, 1960). Such an increase in entropy could probably occur only with a fairly non-specific type of binding, and might well be precluded by a more directional interaction such as hydrogen bonding. McMenamy & Seder (1963) consider that in such a case the opposite effect takes place, and that there is a decrease in intramolecular rotational (disorientational) freedom on binding. That this is not significant in the present case is shown by the fact that, using the equation of Flory (1953), the disorientation entropy per molecular segment (e.g. $-CH_2-$) is about 8 J mol^{-1} deg^{-1}. Thus if loss of disorientation occurs on binding, then the binding entropy of phenacetin should, other things being equal, be about 8 J mol^{-1} deg^{-1} more negative than that of *p*-methoxyacetanilide, whereas in fact it is some 9 J mol^{-1} deg^{-1} more positive.

Conformational changes in either drug or protein on association could also give rise to entropy changes. Discussing the binding of warfarin to human serum albumin, O'Reilly (1969) argued that such changes were unlikely since, for example, they would involve the breaking of hydrogen bonds within the albumin molecule, and hence would give rise to a positive ΔH; experimentally, however, he found ΔH to be negative. Any new conformation, however, could also permit hydrogen bond formation; thus the net ΔH of the conformational change alone might be close to

zero. Helmer, Kiehs & Hansch (1968) have reported changes in the optical activity of proteins on association with small organic molecules, indicating that conformational changes do indeed occur. It may be that these changes are associated with binding to secondary sites, for there is some evidence that such sites are generated by the initial binding to primary sites (Klotz & Ayers, 1953).

Drug-protein interactions will thus in general be accompanied by a net increase in entropy; of particular interest in this work is the good correlation between ΔS and σ for the interaction of acetanilides with BSA. The slope of the regression line is positive, entropy change becoming more positive as the electron-withdrawing ability of the substituent increases. There appear to be three possible explanations for this. Firstly, a compound tightly bound to BSA (high negative ΔH of association) will have a lower entropy when bound than will a compound that is loosely bound, because the freedom of movement of the former will be less. Secondly, the greater the electron-withdrawing ability of the substituent, the lower is the aryl-N bond order, and hence the greater is the rotational mobility around that bond upon association, i.e. when water of solvation, which restricts such mobility, is released.

Thirdly, since the acetamido-group itself is electron-donating, an electron-withdrawing substituent (positive σ) in the *para*-position will increase the charge separation in the molecule, whilst an electron-donating substituent (negative σ) will decrease it. It is suggested that the extent of solvation depends on the magnitude of the charge separation—that is, on the dipole moment. Thus *p*-nitroacetanilide, with the highest dipole moment of all the compounds examined, is solvated to the greatest extent, and hence yields the greatest positive entropy change on binding to BSA.

It is probable that all three factors mentioned above contribute towards the observed relation between ΔS and σ. We believe, following McMenamy & Seder (1963), that dehydration on binding makes the greatest contribution to the entropy of binding; hence the variation of extent of solvation with σ probably makes the greatest contribution to the relation between ΔS and σ.

Of the compounds examined, acetanilide, *p*-methoxyacetanilide, *p*-ethoxyacetanilide (phenacetin) and *p*-hydroxyacetanilide (paracetamol) have been or are at present used in medicinal preparations. The last three named all possess electron-donating substituents and have fairly high binding enthalpies which lie in the same region as those of other classes of drugs. Thus, for binding to serum albumin, values for a series of indole derivatives lie between -8 and -40 kJ mol^{-1} (McMenamy & Seder, 1963), for warfarin sodium $-14{\cdot}5$ kJ mol^{-1} (O'Reilly, 1967) and for a series of *p*-hydroxybenzoic acid esters $-0{\cdot}8$ to -16 kJ mol^{-1} (Patel, Sheen & Taylor, 1968). Binding enthalpies within the range found in this work are sufficiently low for ready dissociation of the drug-BSA complex at body temperature.

The association constants found for the four "commercial" acetanilides are sufficiently low to give fairly high free drug concentrations in the bloodstream over relatively long times. An association constant as low as that found for *p*-aminoacetanilide would give very high initial free drug concentrations, and would be suitable for the relief of acute, transient pain, assuming that formation of active metabolite was sufficiently rapid not to be the prime factor governing relief. There would, however, be a rapid decrease in the free drug concentration, as the relatively high binding enthalpy would mean a slow release of bound drug.

On the other hand, an association constant as high as that found for, say, *p*-bromoacetanilide would give rise to very low free drug concentrations. Although this would

give prolonged action, the free drug concentration could well be below the therapeutic minimum. A related factor here is that a compound with high affinity for a hydrophobic surface generally has low aqueous solubility. Thus, with a compound like *p*-bromoacetanilide, a low solubility would further decrease the concentration in the bloodstream. For comparison, the molar aqueous solubilities at 25° of the six *p*-substituted acetanilides discussed immediately above are: –H, 0·0416; –OH, 0·0771; $-OCH_3$, 0·0709; $-OC_2H_5$, 0·0430; $-NH_2$, 0·1061; –Br, 0·00074.

In conclusion, it may be said that thermodynamically the four "commercial" acetanilides are among the best of the simple *p*-substituted acetanilides for the relief of pain.

Acknowledgements

One of us (E. T.) gratefully acknowledges the receipt of a research assistantship from Liverpool Corporation. We thank Mr. R. D. Thomas for preparing the computer program.

REFERENCES

ARANOW, R. H. & WITTEN, L. (1960). *J. phys. Chem., Ithaca*, **64**, 1643–1648.
BIRD, A. E. & MARSHALL, A. C. (1967). *Biochem. Pharmac.*, **16**, 2275–2290.
FLORY, P. J. (1953). *Principles of polymer chemistry*, pp. 502, 574, Ithaca, New York: Cornell University Press.
HANSCH, C., KIEHS, K. & LAWRENCE, G. L. (1965). *J. Am. chem. Soc.*, **87**, 5770–5773.
HELMER, F., KIEHS, K. & HANSCH, C. (1968). *Biochemistry*, **7**, 2858–2863.
KLOTZ, I. M. & AYERS, J. (1953). *Discuss. Faraday Soc.*, **13**, 189–196.
LUNDGREN, H. P. (1945). *Textile Res. J.*, **15**, 335–341.
MCMENAMY, R. H. & SEDER, R. H. (1963). *J. biol. Chem.*, **238**, 3241–3248.
MEYER, M. C. & GUTTMAN, D. (1968). *J. pharm. Sci.*, **57**, 1627–1629.
MEYER, M. C. & GUTTMAN, D. (1970). *Ibid.*, **59**, 33–39.
O'REILLY, R. A. (1967). *J. clin. Invest.*, **46**, 829–837.
O'REILLY, R. A. (1969). *Ibid.*, **48**, 193–202.
PATEL, N. K., SHEEN, P.-C. & TAYLOR, K. E. (1968). *J. pharm. Sci.*, **57**, 1370–1374.
STEINBERG, I. Z. & SCHERAGA, H. A. (1963). *J. biol. Chem.*, **238**, 172–181.
WEBER, G. & YOUNG, L. B. (1964). *Ibid.*, **239**, 1415–1423.
WETLAUFER, D. B. & LOVRIEN, R. (1964). *Ibid.*, **239**, 596–603.

J. Pharm. Pharmac., 1970, **22**, *Suppl.*, 60 S–63 S

Received February 26, 1970

SHORT COMMUNICATION

Effects of dietary protein deficiency on the conjugation of foreign compounds in rat liver

G. C. WOOD AND B. G. WOODCOCK

Drug Metabolism Research Unit, Department of Pharmaceutical Chemistry, University of Strathclyde, Glasgow, U.K.

Although it is well known that the rate of metabolism of drugs may be altered by changes in various physiological and dietary conditions (see, for example, Kato, Takayanagi & Oshima, 1969), the specific effect of dietary protein level on drug metabolism has received relatively little attention.

It has recently been shown that the activities of microsomal enzyme systems responsible for some drug oxidations are markedly reduced in protein-deficient rats: these effects have been observed both *in vivo* (Kato, Oshima & Tomizawa, 1968) and with liver homogenate and microsomal preparations *in vitro* (McLean & McLean, 1966; Kato & others, 1968). Unpublished work by Dr. C. Furst, in this laboratory, is in agreement with a number of these findings.

The effect of protein deficiency on conjugation, another important pathway of drug metabolism, has not hitherto been investigated although a recent study of the effect of dietary protein on the glucuronidation of bilirubin in rat liver slices (Adlard, Lester & Lathe, 1969) suggests that this reaction is not affected by dietary protein level in the same way as is drug oxidation.

Preliminary results are now presented of the effects of protein-deficient diets on the rates of conjugation, as glucuronides or sulphates, of foreign compounds by liver transferases.

Method

Immature male Wistar rats (65–75 g), kept at 22–24°, were fed freely on a protein-free synthetic diet while control animals received an 18% casein synthetic diet (McLean & McLean, 1966). The control diet was restricted so that the calorie intake of both groups was approximately the same (experimental animals, 32 kcal (134 kJ)/100 g rat daily; control animals 36 kcal (150 kJ)/100 g daily). After seven days the rats were killed and their livers homogenized in 9 volumes of ice-cold 0·15M KCl. Each homogenate was then centrifuged (12 000 *g*, 10 min, 4°) and a microsomal fraction prepared from the resulting "low-speed" supernatant by centrifuging (105 000 *g*, 1 h, 4°). The "high-speed" supernatant was retained and the sedimented microsomes were resuspended in 0·15M KCl. They were recentrifuged (105 000 *g*, 1 h, 4°) and finally resuspended in sufficient 0·15M KCl so that 1 ml suspension was equivalent to 500 mg of liver.

Activities of conjugating enzymes were then assayed in the "low-speed" supernatant, "high-speed" supernatant and microsomal suspension. Glucuronyltransferase was assayed by measuring the rate of conjugation of *p*-nitrophenol (PNP), (Isselbacher, 1956) and *o*-aminophenol (OAP), (Dutton & Storey, 1962). Sulphotransferase was assayed by measuring the conjugation of PNP and dehydroepiandro-

sterone, DHEA, by a method based on that described for these substrates by Nose & Lipmann (1958) in which the sulphate conjugate was estimated as a complex with methylene blue.

Uridine diphosphoglucuronic acid (UDPGA) pyrophosphatase was assayed by the method of Ogawa, Sawada & Kawada (1966), the released glucuronic acid being determined according to Nir (1964). Protein was determined by the method of Miller (1959), using bovine serum albumin as a standard, liver fractions being diluted with 1% sodium deoxycholate (Juchau & Fouts, 1965).

Results

Animals fed the protein-free diet lost weight and showed other symptoms of protein deficiency including loss of hair and increased irritability when being handled. Their average calorie-intake per day was greater than maintenance requirements (Njaa, 1965); they are thus unlikely to have been calorie deficient. The control animals, on the other hand, increased steadily in weight and appeared to develop normally. The final body weights of the two groups of rats are given in Table 1. The liver weights of the two groups were the same but the protein contents (per g wet liver), of the whole liver homogenates and fractions from the protein-deficient rats, were lower than those of the control animals (Table 1).

Table 1. *Final body-weight, liver weight and protein content* (mean ± s.e.) *of liver fractions of rats fed either* 18% *protein diet or protein-free diet for* 7 *days*

	Final body weight (g)	Liver weight (g)	Protein content (mg/g wet liver)		
			Whole liver homogenate	Microsomal fraction	"High-speed" supernatant fraction
18% protein diet	90 ± 2 (10)	3·4 ± 0·3 (10)	204 ± 12 (5)	10·5 ± 1·0 (5)	73 ± 5·2 (5)
Protein-free diet	65 ± 2 (10)	3·0 ± 0·2 (10)	141 ± 7 (5)	8·0 ± 0·4 (3)	56 ± 4·5 (5)
% change with protein-free diet	−28*	−13	−31*	−26	−23*

* $P < 0·05$ at least.

Figures in parentheses are numbers of observations; with protein determinations pairs of livers were pooled.

The activities of glucuronyltransferase in "low-speed" supernatant or microsomal fractions, were markedly elevated in the protein-deficient animals (Table 2). When the results are expressed as "n mol conjugated/g wet liver h^{-1}" the rate of conjugation of PNP in the "low-speed" supernatant was 59% higher. In the microsomal fraction, the conjugation of PNP was 64% higher, and of OAP, 71% higher than in the corresponding controls. The differences are even more marked when the results are expressed "per liver from 100 g body weight" (Fig. 1, Table 2) or "per mg microsomal protein" (Table 2).

Sulphotransferase activity in the "high-speed" supernatant fraction was not affected in the same manner (Table 2, Fig. 1). With DHEA as substrate the activity in protein-deficient rats was lower than in controls but with PNP as substrate it was not significantly affected.

Table 2. *Glucuronyltransferase and sulphotransferase activities in liver fractions of rats fed either* 18% *protein diet or protein-free diet for* 7 *days. Values in nmol compound conjugated per hour* (mean ± s.e. of 5 observations each on 2 pooled livers)

		Glucuronyltransferase			Sulphotransferase	
		"Low-speed" supernatant fraction	Microsomal fraction		"high-speed" supernatant fraction	
		PNP	PNP	OAP	PNP	DHEA
Activity per g wet liver	18% protein diet	3990 ± 330	894 ± 70	70 ± 10	2440 ± 170	750 ± 110
	Protein-free diet	6360 ± 380	1465 ± 72	120 ± 19	2000 ± 200	440 ± 60
	% change	+59†	+64†	+71*	−18	−42*
Activity per liver from 100 g body weight	18% protein diet	15 000 ± 1900	3380 ± 410	264 ± 33	9200 ± 1200	2810 ± 330
	Protein-free diet	29 400 ± 2800	6760 ± 590	554 ± 59	9200 ± 1200	2010 ± 270
	% change	+95†	+100†	+110†	0	−28
Activity per mg protein in fraction	18% protein diet	—	85 ± 10	6·7 ± 1·[illegible]	34 ± 3	10·2 ± 1·6
	Protein-free diet		183 ± 13	15·0 ± 2·5	36 ± 5	7·8 ± 1·2
	% change		+115†	+124†	+6	−31

PNP, *p*-nitrophenol; OAP, *o*-aminophenol; DHEA, dehydroepiandrosterone.
* $P < 0.05$. † $P < 0.01$, at least.

The most remarkable result of these experiments is the elevated glucuronyltransferase activity observed with the protein-deficient rats. This enzyme is microsomal, like the oxido-reductases involved in drug metabolism, yet the activity is affected by protein deficiency in a radically different way (Fig. 1).

This effect cannot be accounted for by differences in activity of microsomal UDPGA pyrophosphatase. Activities of this enzyme were not significantly different in the experimental and control animals, when assayed either at pH 3·9, the optimum pH for the pyrophosphatase, or at pH 7·4, the pH used for assay of glucuronyltransferase (at pH 8·9 controls showed 27·2 ± 4·9, experimental animals 24·8 ± 4·2 μ mol/g

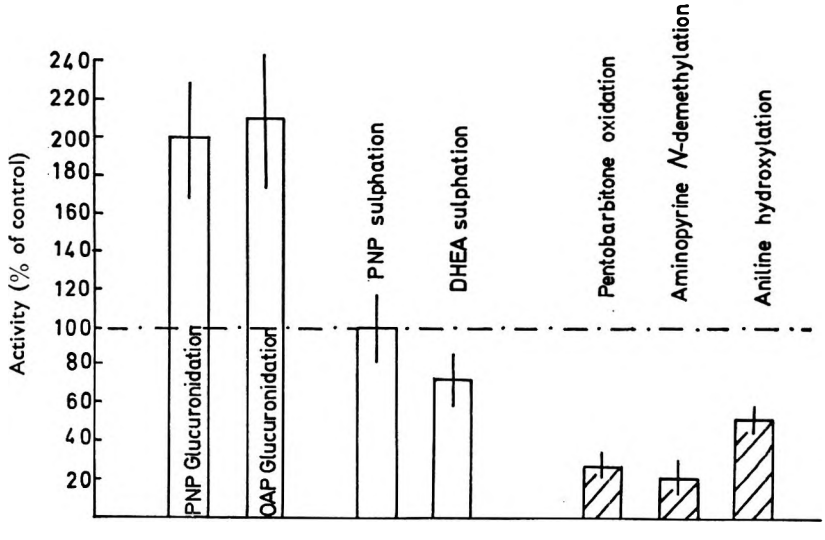

FIG. 1. Effects of protein-free diet on liver glucuronyltransferase and sulphotransferase activities (per liver from 100 g body weight, Table 2). Hatched columns are oxidoreductase activities of animals fed a protein-free diet (Kato, Oshima & Tomizawa, 1968). Control animals fed 18% protein diet. Vertical bars on top of columns indicate standard error.

wet liver h^{-1}). Furthermore, it is unlikely that the differences in glucuronyltransferase activity can be due to differences in activity of β-glucuronidase in the microsomal fractions from the two groups of animals. β-Glucuronidase is only weakly active at pH 7·4 and when a boiled solution of potassium hydrogen saccharate was added to assays of glucuronyltransferase in amounts sufficient to inhibit β-glucuronidase (Levvy, 1952), the differences between protein-deficient and control animals were unchanged.

Thus the results indicate that protein-deficiency induces a real increase in glucuronyltransferase activity. It is unlikely that this increase is due to synthesis of new enzyme protein, since the general level of protein synthesis is low in these animals. It is more likely to result from an increase in catalytic activity arising from alterations in the composition or structure of the endoplasmic reticulum, or both. Recent studies (Graham & Wood, 1969) have shown that the activity of guinea-pig liver microsomal UDP-glucuronyltransferase depends on the structural integrity of the microsomal membrane, particularly its phospholipid composition.

We are grateful to the Nuffield Foundation for financial support, to Mrs. M. Stewart and Mr. A. Millar for technical assistance, and to Dr. I. H. Stevenson of the University of Dundee, Scotland, for a gift of *o*-aminophenol glucuronide.

REFERENCES

ADLARD, B. P. F., LESTER, R. G. & LATHE, G. H. (1969). *Biochem. Pharmac.*, **18**, 59–63.

DUTTON, G. J. & STOREY, I. D. E. (1962). *Methods in Enzymology*, Vol. 5, p. 159. Editors: Colowick, S. P. & Kaplan, N. O. New York: Academic Press.

GRAHAM, A. & WOOD, G. C. (1969). *Biochem. Biophys. Res. Commun.*, **37**, 567–575.

ISSELBACHER, K. J. (1956). *Recent Prog. Horm. Res.*, **12**, 134–151.

JUCHAU, M. R. & FOUTS, J. R. (1965). *Biochem. Pharmac.*, **16**, 155–161

KATO, R., OSHIMA, T. & TOMIZAWA, S. (1968). *Jap. J. Pharmac.*, **18**, 356–366.

KATO, R., TAKAYANAGI, M. & OSHIMA, T. (1969). *Ibid.*, **19**, 53–62.

LEVVY, G. A. (1952). *Biochem. J.*, **52**, 464–472.

MCLEAN, A. E. M. & MCLEAN, E. K. (1966). *Ibid.*, **100**, 564–571.

MILLER, G. L. (1959). *Analyt. Chem.*, **31**, 964.

NIR, I. (1964). *Analyt. Biochem.*, **8**, 20–23.

NJAA, L. R. (1965). *Br. J. Nutr.*, **19**, 443–457.

NOSE, Y. & LIPMANN, F. (1958). *J. biol. Chem.*, **233**, 1348–1351.

OGAWA, H., SAWADA, M. & KAWADA, M. (1966). *J. Biochem., Tokyo*, **59**, 126–134

J. Pharm. Pharmac., 1970, **22**, *Suppl.*, 64 S–69 S *Received March* 17, 1970

The effect of rate of loading on the strength of tablets

J. E. REES, J. A. HERSEY AND E. T. COLE

Pharmaceutical Research & Development, Sandoz A.G., CH-4002 Basel, Switzerland

The breaking strength of tablets containing lactose and microcrystalline cellulose has been determined using an Instron Universal Testing Instrument at loading rates corresponding to cross-head movements of 0·05 to 5·0 cm min^{-1}. For tablets of 2 to 30 kg, nominal strength, an increase in the loading rate produced a significant increase in the breaking strength, although the absolute increase in the mean strength value was only 2 kg for the strongest tablets. The standard deviation of replicate values was apparently unaffected by loading rate. Results obtained using the motorized Heberlein and Erweka instruments to determine the strength of compressed tablets, indicated that discrepancies in the strength values may be partially attributed to differences in the rates of loading.

Several authors have compared the methods used to determine the mechanical strength of compressed tablets. However, few attempts have been made to isolate selected operational variables to rationalize discrepancies in the strength values obtained in these comparisons, although Brook & Marshall (1968) obtained accurate calibration figures for several instruments by using a load transducer in place of the tablet.

The strength of pharmaceutical tablets is usually determined by failure in diametrical compression. Rudnick, Hunter & Holden (1963) have shown that the tensile strength of a compact can be computed from the results of this test, provided shear failure is prevented by correct load distribution.

Smith (1949) and McCallum, Buchter & Albrecht (1955) concluded that variations between operators influence the reproducibility of results obtained in diametrical compression tests using the Monsanto (or "Stokes") and Strong Cobb instruments. Variability in the rate of loading may be a critical factor in the discrepancies observed.

A simple attempt to compare the effect of high and low rates of loading, using the Monsanto tester was described by Fairchild & Michel (1961). Neither the mean strengths nor the coefficients of variation differed appreciably.

Ritschel, Skinner & Schlumpf (1969), using eight different instruments found no significant differences in the reproducibility of strength values due to variation in the rate of loading but, for most instruments, there were significant differences between the results of operators.

Mahler & Mitchem (1964), using dental amalgam, found the rate of loading to have no effect on the tensile strength measured in an elongation test, or the transverse strength determined in a three-point loading, cross-breaking test. However, the axial crushing strength of cylindrical specimens increased with the rate of loading as reported by Taylor, Sweeney & others (1949). These results may explain the conclusions of Endicott, Lowenthal & Gross (1961) and Delonca, Puech & others (1967),

Table 1. *Particle size analysis of constituent powders*

Sieve size μm	Avicel % oversize	Lactose % oversize
250	—	18·0
177	0	35·2
149	1·3	49·3
125	3·9	58·2
105	7·4	65·0
74	22·1	78·5
53	34·7	84·5
37	53·0	—

Sifting time 5 min. Sift amplitude 8. Pulse amplitude 10.

that a three-point-loading, cross-breaking test provides a more reproducible measurement of tablet strength than a diametrical compression test.

We set out to determine whether the load required to fracture a compact in diametrical compression depends on the rate at which the load is applied. By the isolation of this operating variable, a more fundamental comparison can be made between the results of strength tests using different instruments, or between such tests made by different operators using the same instrument.

EXPERIMENTAL

Compacts of uniform strength were required to reduce the number of replicates examined, whilst maintaining the necessary statistical significance for interpretation of the results. A suitable tablet was made from: lactose, anhydrous (Sheffield Chemical) 49·5, microcrystalline cellulose (Avicel) 49·5, colloidal silica (Aerosil) 0·5, magnesium stearate 0·5. The particle size distribution of the two major constituents was determined using an Allen-Bradley Sonic Sifter (Table 1). The maximum particle size of the colloidal silica was 160 μm and of the magnesium stearate, 96 μm (determined by microscopic examination). This composition was dry mixed, and sufficient material (410 mg) was compressed to form a compact of approximately 4 mm thickness at zero porosity. An eccentric tablet press (Oerlikon), with plane-faced, bevel-edged punches of 10 mm diameter, was operated continuously at approximately 50 cycles/min with automatic die filling.

Tablets were prepared at five different pressures corresponding to nominal strengths of 2, 5, 10, 20 and 30 kg. The weight uniformity of tablets prepared at each pressure is shown in Table 2.

The strength of each series of tablets was measured on the same day, after 3 months storage to eliminate ageing effects (Rees & Shotton, 1970). The compacts were subjected to a conventional diametrical compression test, using an Instron Universal Testing Instrument, Model TTDM. A range of crosshead speeds was selected between 0·05 and 5·0 cm min^{-1}, and the force applied was measured using a type

Table 2. *Weight variation between tablets*

Nominal tablet strength kg	Mean tablet weight (g)	No. of determinations	Standard deviation of weight	Coefficient of variation
2	0·406	10	0·006	1·3
5	0·403	20	0·002	0·546
10	0·402	20	0·003	0·648
20	0·404	20	0·003	0·655
30	0·405	20	0·002	0·568

CCM load cell (maximum load 50 kg). It was necessary to replace the pen recorder by a recording ultraviolet oscillograph (SE Laboratories 3006) to achieve acceptable rates of response at high loading rates. At a cross head speed of 5·0 cm min^{-1} a 400 Hz galvanometer was needed to ensure adequate frequency response. The galvanometer was fitted with a pre-amplifier and a double-T filter which were enclosed in a Faraday cage to eliminate noise effects, whilst maintaining sufficiently high sensitivity. The sensitivity response, expressed as galvanometer trace deflection for 10 kg was 36·5, 18·1, 9·1, 3·7, 3·7 cm for the nominal tablet strengths of 2, 5, 10, 20, 30 kg respectively.

To relate our results to conventional tablet strength tests, and to compare them with those of Ritschel & others (1969), some measurements were made using an Erweka instrument and a motorized Heberlein testing instrument, under standard conditions of use.

RESULTS

The mean values of strength and the standard deviations were determined for each group of tablets at five rates of loading as shown in Table 3. For tablets of each nominal strength, the load required to cause fracture in diametrical compression increased with the rate of loading. This effect was more pronounced with tablets of high strength (Fig. 1).

For the tablets of 2 kg nominal strength, small differences in the mean strength values were observed at high and low rates of loading. Consequently, the statistical significance of the effect of loading rate was determined using the Student *t*-test (Table 4). For each group of tablets, the strength at a rate corresponding to 0·05 cm

Table 3. *The effect of loading rate on the diametrical crushing strength of tablets*

Nominal strength	Cross-head movement	Loading rate	Diametrical breaking strength		
			Mean†	Standard deviation	Coefficient of variation
kg	cm min^{-1}	kg s^{-1}	kg	kg	%
2	0·05	0·096	1·92	0·07	3·6
	0·2	0·42	1·97	0·12	6·1
	0·5	1·09	2·09	0·16	7·7
	2·0	4·3	2·09	0·08	3·8
	5·0	10·1	2·13	0·09	4·2
5	0·05	0·33	5·66	0·28	4·9
	0·2	1·31	5·71	0·33	5·8
	0·5	3·34	5·98	0·41	6·9
	2·0	13·5	5·99	0·31	5·2
	5·0	28·5	6·33	0·34	5·4
10	0·05	0·59	10·3	0·7	6·8
	0·2	2·35	10·6	0·6	5·7
	0·5	6·38	11·3	0·6	5·3
	2·0	23·2	11·3	0·4	3·5
	5·0	57·8	11·8	1·0	8·5
20	0·05	1·1*	21·9	0·9	4·1
	0·2	4·29	22·5	0·9	4·0
	0·5	11·7	22·9	0·9	3·9
	2·0	39·6	23·5	1·2	5·1
	5·0	113·2	24·0	1·3	5·4
30	0·05	1·29	28·6	1·0	3·5
	0·2	5·16	29·6	1·3	4·4
	0·5	12·9	29·7	1·0	3·4
	2·0	52·4	30·8	1·1	3·6
	5·0	128·3	30·8	0·9	2·9

* No experimental data available—value determined by extrapolation.
† Mean of 10 replicate samples.

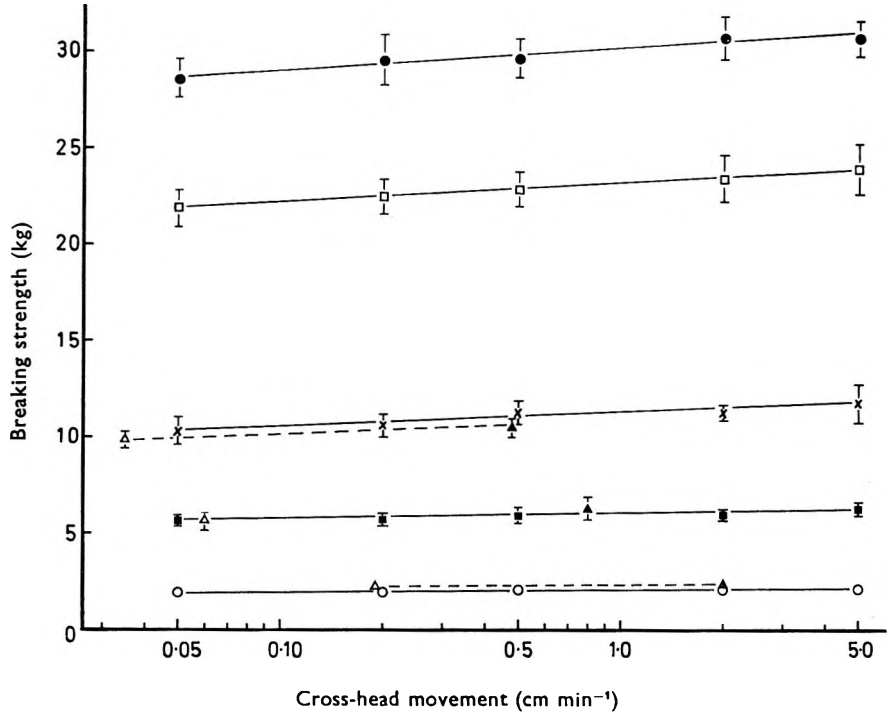

FIG. 1. The effect of rate of loading on the breaking strength of tablets. The range for each co-ordinate represents the standard deviation. Nominal strength: ○, 2 kg; ■, 5 kg; ×, 10 kg; □, 20 kg; ●, 30 kg; ▲, motorized Heberlein; △ Erweka.

min^{-1} cross-head movement was compared with the strength at the higher rates of loading. In most cases, there was 95% probability of a significant difference between the breaking strength at 0·05 cm min^{-1} and at 0·5 cm min^{-1}. In all cases, the value at 2·0 cm min^{-1} was significantly greater than at 0·05 cm min^{-1}.

A change in the rate of loading had no apparent effect on the standard deviation of replicate values of strength (Table 3).

Results from the Erweka instrument and the motorized Heberlein tester, for tablets of nominal strength 2, 5 and 10 kg, are recorded in Fig. 1 along with the results obtained using the Instron machine.

Table 4. *Comparison of the mean strength values at different loading rates, using the Student* t*-distribution*

	Comparison of mean strengths at different loading rates							
Nominal strength	0·05–0·2 cm min^{-1}		0·05–0·5 cm min^{-1}		0·05–2·0 cm min^{-1}		0·05–5·0 cm min^{-1}	
kg	*t*	(1–P)*	*t*	(1–P)*	*t*	(1–P)*	*t*	(1–P)*
2	1·19	70%	3·28	99·5%	5·69	99·9%	6·65	99·9%
5	0·36	20%	2·04	90%	2·48	97·5%	4·79	99·9%
10	1·02	60%	3·53	99·5%	3·84	99·5%	3·89	99.5%
20	1·72	80%	2·44	95%	3·48	99·5%	4·19	99·9%
30	1·88	90%	2·41	95%	4·60	99·9%	5·26	99·9%

* Minimum % probability of a significant difference between the mean values of strength at the two different rates of loading.

DISCUSSION

Statistical evaluation of the results for tablets of high and low strength has shown that there is a significant increase in the diametrical crushing strength as the rate of loading is increased from 0·02 to 5·0 cm min^{-1} cross-head movement.

The negative conclusions of Ritschel & others (1969) about the effect of loading rate may be attributed to the low strength of the tablets evaluated (1·8 and 4·7 kg) and also to the relatively large standard deviation of strength determinations compared with the present values for tablets of similar mean strength. The present results show that, for tablets of 2 and 5 kg nominal strength the dependency of strength on the loading rate is not large. Accordingly, only a small increase in the standard deviation of replicate strength values may be necessary to reduce to an insignificant level the differences between mean values of strength at different loading rates.

Although Ritschel & others (1969) did not quote values for the actual time between the onset of loading and the failure of a tablet, the mean times required to test ten tablets using each instrument were specified. Assuming that this arbitrary time period was related to the loading time for each tablet, it is interesting that the results of Ritschel & others show an increase in the strength values with a decrease in the time required for measurement, using those instruments for which the loading rate is approximately constant (Fig. 2). By contrast, for those instruments which do not apply the load at a regular rate, there was no apparent correlation. For the motorized Heberlein and Erweka instruments the rate of operation cannot be altered, and the data in Fig. 2 for these instruments correspond to a reliable and constant rate of loading.

Our findings have confirmed that the rate of loading, for tablets of 2, 5 and 10 kg nominal strength, is approximately ten times greater with the motorized Heberlein than with the Erweka (Table 5). There were significant differences between the strength values for the same tablets using these two instruments, and the results

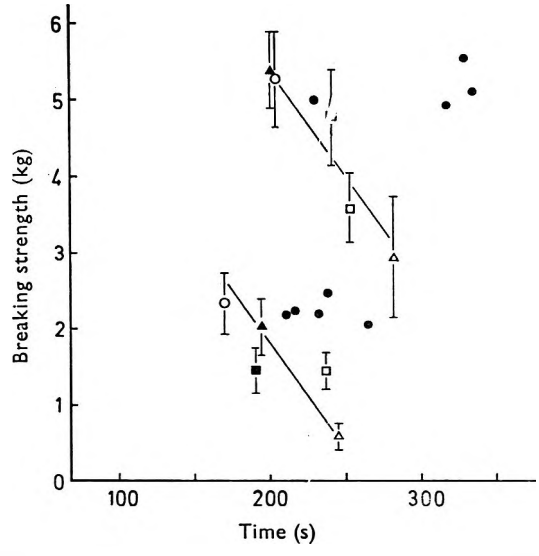

FIG. 2. The strength of tablets, and the standard deviation, determined by Ritschel & others (1969) using several instruments. The abscissa represents the time required to test the strength of ten tablets. ▲, motorized Heberlein; △, Erweka; ■, Strong-Cobb; □, DBT ("Siegfried"); ○, Pfizer; ●, other instruments.

Table 5. *Comparison of the results for diametrical crushing strength obtained using the motorized Heberlein and Erweka instruments*

	Erweka			Comparison of the mean strength values Erweka–Heberlein		Heberlein		
Nominal strength	Mean loading rate	Mean rate of platten movement	Mean strength† and standard deviation			Mean loading rate	Mean rate of platten movement	Mean strength† and standard deviation
kg	kg s^{-1}	cm min^{-1}	kg	*t*	(1–P)*	kg s^{-1}	cm min^{-1}	kg
2	0·4	0·19	2·25 ± 0·04	4·10	99·9%	4·2	2·0	2·49 ± 0·18
5	0·4	0·06	5·61 ± 0·47	3·40	99·5%	5·3	0·8	6·37 ± 0·59
10	0·4	0·035	9·84 ± 0·44	3·73	99·5%	5·7	0·48	10·56 ± 0·53

* Probability of a significant difference between the mean values of strength, using the two different instruments.
† Mean of 10 replicates.

obtained agree with the Instron data (Fig. 1) for the same rates of loading. This indicates that the calibration figure quoted by Brook & Marshall (1968), to convert the Erweka scale reading to a breaking load in kg, is not appropriate to the particular instrument we used. Thus, it is not certain that identical values for breaking strength will be obtained using different models of the Erweka instrument.

In addition, the effect of loading rate on the strength of different tablet formulations may not be identical. It is therefore interesting that the results of Ritschel & others (1969), for two appreciably different tablet compositions, show similar relations between strength and loading rate (Fig. 2), although the differences between the Heberlein and Erweka values were much greater than for the present tablet formulation. It is possible that the differences recorded by Ritschel & others may be due in part to calibration discrepancies between the two testing instruments used.

Even for the tablets of 20 kg nominal strength, studied in the present investigation, an increase in the loading rate by a factor of one hundred increased the mean strength value by only 2 kg. However, for manually-operated instruments it is possible that variation in the rate of loading at the instant of tablet failure may be sufficient to increase the deviation of replicate strength determinations, and to alter the mean value obtained.

Acknowledgements

We wish to express our gratitude to Mr. R. Best for advice and technical assistance with respect to the frequency response of recording instruments.

REFERENCES

Brook, D. B. & Marshall, K. (1968). *J. pharm. Sci.*, **57**, 481–484.
Delonca, H., Puech, A., Youakim, J., Jacob, M. (1967). *J. pharm. Belg.*, **22**, 21–30.
Endicott, C. J., Lowenthal, W. & Gross, H. M. (1961). *J. pharm. Sci.*, **50**, 343–346.
Fairchild, H. J. & Michel, F. (1961). *Ibid.*, **50**, 966–969.
Mahler, D. B. & Mitchem, J. C. (1964). *J. dent. Res.*, **43**, 121–130.
McCallum, A., Buchter, J. & Albrecht, R. (1955). *J. Am. pharm. Assoc. (Sci. Edn)*, **44**, 83–85.
Rees, J. E. & Shotton, E. (1970). *J. Pharm. Pharmac.*, **22**, *Suppl.*, 17S–23S.
Ritschel, W. A., Skinner, F. S. & Schlumpf, R. (1969). *Pharm. Acta Helv.*, **44**, 547–569.
Rudnick, A., Hunter, A. R. & Holden, F. C. (1963). *Matl. Res. Stand.*, **3**, 283–289.
Smith, A. N. (1949). *Pharm. J.*, **163**, 227–228.
Taylor, N. O., Sweeney, W. T., Mahler, D. B. & Dinger, E. J. (1949). *J. dent. Res.*, **28**, 228–241.

J. Pharm. Pharmac., 1970, **22**, *Suppl.*, 70 S–78S *Received February* 12, 1970

The surface hardness of tablets

K. RIDGWAY, M. E. AULTON AND P. H. ROSSER

*Department of Pharmaceutics, School of Pharmacy, University of London, Brunswick Square, London, W.C.*1, *U.K.*

A pneumatic micro-indentation apparatus has been used to determine the hardness of tablets of aspirin at various points on their diameter. All the tablets were 13 mm diameter; the compaction pressure and the particle size of the initial material were varied. The compression was carried out in a Perspex die so that radial pressure could also be assessed during compaction. The micro-indentation apparatus measured the total deformation at the loaded point on the tablet, and also the elastic recovery when the load was removed.

The strength, porosity, abrasion resistance and ease of disintegration of a tablet vary over its surface and through its thickness. By compacting magnesium carbonate in a 2 inch diameter die with gelatin-encapsulated manganin strain gauges buried in the powder, Train (1957) showed that a distribution of pressure existed. The pressure distribution was closely paralleled by the distribution of density as determined by machining and weighing the compact. Shear at the surface of a tablet is known to produce a denser skin, and Train & Hersey (1960) demonstrated this effect in compacts made from lead shot; good adhesion was obtained only where shear had been intense. By increasing the compaction pressure, the density of tablets is increased (Higuchi, 1954; Lewis & Train, 1965). The friability decreases, and the disintegration rate and penetrability by water or solvents also decline (Ganderton, 1969).

Aspirin on compaction can be work-hardened (Ridgway, Glasby & Rosser, 1969) and it thus seemed possible that, by making aspirin tablets and assessing their hardness at various points on their surfaces, it might be possible to show that non-uniformity persists even in comparatively small compacts in which it might not be expected.

EXPERIMENTAL

The aspirin was a crystalline product (Laporte Industries Limited). Four fractions were obtained by sieving: 20–30 mesh, 30–40, 40–44 and 44–60, mean particle sizes 670, 460, 388 and 303 μm respectively.

Weighed quantities were compacted by a hydraulic press with steel punches in a 13 mm diameter Perspex die of the type described by Ridgway (1966), which when viewed by polarized light gave an interference fringe pattern from which the radial pressure at the die wall could be estimated. Fringe patterns were photographed for subsequent examination. Tablets were ejected from the die with more difficulty than from steel dies, but were of good quality and adequate for subsequent testing.

Two series of tests were made, in each of which one parameter was held constant whilst the other was varied; the two parameters being compaction pressure and particle size. The tablet weight remained constant within each series. Five indentations were made over each test area and the average value used in the plotting of the graphs. The test areas were five concentric regions of equal width on the tablet face.

Point hardnesses were determined using a pneumatic micro-indentation apparatus [Research Equipment (London) Ltd.] that was originally developed for the testing of paint coatings. It consists of a spherical sapphire indenter, diameter 1·55 mm, which can be lowered on to the test surface under a selected load of a few grams. The depth of the indentation and the recovery when the load is removed can both be measured, the timing of the loading–unloading cycle being automatically programmed. The indenter movement is measured by a double pneumatic amplification system of the flapper and nozzle type and is displayed on a pneumatic recorder, on which the full scale deflection corresponds to 6 μm indenter movement. A typical chart record is shown in Fig. 1. ABC is the loading curve, the vertical

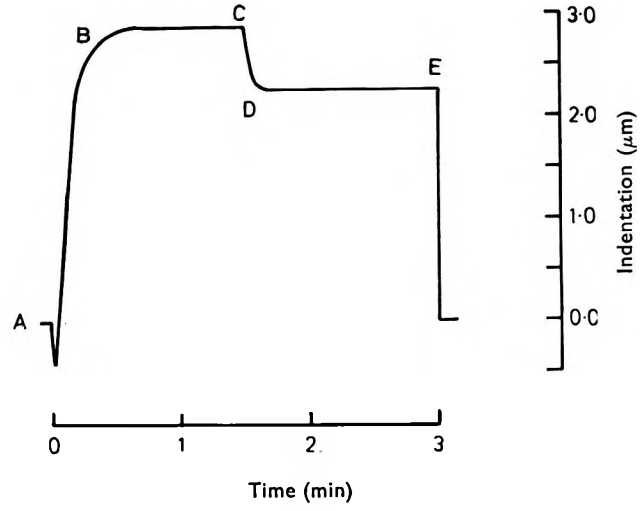

FIG. 1. The curve produced by the pneumatic recorder during the indentation of a tablet. The abscissa is time, the indentation and relaxation taking about 1½ min each. The ordinate is the depth of penetration of the indenter into the tablet, the maximum deflection representing 6 μm. ABC is the penetration under load, and CDE the recovery on removal of the load.

distance AC being the depth to which the indenter penetrates. CDE is the recovery curve followed when the load is removed at C, so that CE is the elastic recovery of the specimen from the indentation. The vertical distance AE is the plastic deformation or permanent set, being the depth of the indentation which remained in the tablet surface. This is the depth which would be measured, inferentially, in a conventional pyramidal diamond-indentation test where the diameter of the impression is measured by a microscope and graticule. The depth of the impression is usually a fifth of the length of its diagonal. As the pneumatic indentation test measures both elastic and plastic components of the deformation, the test is more useful than the normal microhardness test. A further advantage is that the indentation size is measured and displayed, so that inaccuracies due to the poor visibility of the indentation in a microscope graticule do not arise.

The thickness of each tablet was measured with a micrometer. In conjunction with the weight and the diameter, this enabled the density of the compact to be found.

At each level of compaction pressure and particle size listed in the tables of results, one tablet was made. At each radial position, five determinations of hardness were

made. For both elasticity and hardness, the standard deviation was about 20%. The measurement technique is much more precise than this: almost all the experimental scatter is caused by the intrinsic variability of the material under test.

RESULTS AND DISCUSSION

We first make some comments on the pneumatic hardness test. As the spherical sapphire indenter is lowered slowly onto the tablet surface, the following stages occur.

The tablet first deforms elastically according to the equation first deduced by Hertz (1881). The area of contact, a circle of diameter d, follows the law

$$\frac{d}{2} = \left\{ \frac{3}{4} Wr \left(\frac{1 - \sigma_1^2}{E_1} + \frac{1 - \sigma_2^2}{E_2} \right) \right\}^{\frac{1}{3}} \quad .. \quad .. \quad (1)$$

where W is the applied load, r is the indenter radius, E_1 and E_2 are the Young's moduli of the tablet and the indenter, and σ_1 and σ_2 are the corresponding Poisson's ratios. As more of the total load able to act on the indenter is progressively transferred to it by the micro-indentation apparatus, W is effectively increasing continuously during loading. The distribution of pressure and stress in and below the circular area of contact between the indenter and the tablet is not uniform. The pressure is a maximum at the centre, where the value $P_{max} = 3/2\ P_{mean}$, P_{mean} being defined as $W/\pi/_4\ d^2$. The pressure falls from the centre to the periphery of the indentation according to the equation

$$P_x = P_{max} \{1 - x^2/(d/2)^2\}^{\frac{1}{2}} \quad .. \quad .. \quad .. \quad .. \quad (2)$$

where P_X is the pressure at a distance x from the centre.

Stresses in the material beneath the indentation follow a rather complex pattern, but the maximum shear stress occurs on the centre line at a depth of about half the radius of the contact zone, and has a value of 0·47 P_{mean}, for a material having a Poisson's ratio of 0·3. Since most materials in tension yield at a shear stress of about half their yield stress, Y, plastic deformation of the material beneath the indenter will begin at a loading for which $P_{mean} = 1{\cdot}1$ Y. Plastic deformation then spreads until all the material beneath the indenter is yielding. The pressure distribution gradually changes from the parabolic so that the pressure at the edge of the indentation rises ($P_{max} \approx 3{:}5$ Y, $P_{mean} \approx 2{\cdot}8$ Y). Deviation from the parabolic distribution is small enough to ensure that, when the load is removed from the indenter, the elastic recovery reduces the depth of the impression but does not change its diameter. It is this fact which makes ordinary Brinell hardness measurements possible (see Fig. 2).

Normally, in hardness testing, the diameter of the impression is determined and, from it, the hardness is calculated by means of the formula

$$\text{Brinell hardness number} = \frac{W}{\frac{\pi D}{2}(D - \sqrt{D^2 - d^2})} \quad .. \quad .. \quad (3)$$

where D is the diameter of the spherical indenter. The diameter of the impression is unchanged by removing the load. To determine the extent of the elastic recovery it is necessary to measure the change in depth of the indentation on unloading, and this the pneumatic micro-indentation apparatus does.

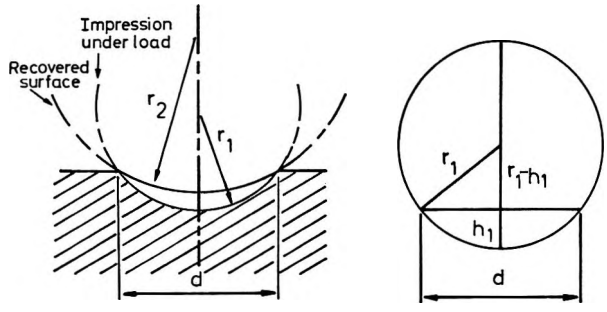

FIG. 2. The change in form of the indentation when the load is removed. Under load, the indenter, radius of curvature r_1, penetrates to a depth h_1 giving an impression of diameter d. When the load is removed, elastic recovery occurs, and the radius of curvature of the impression increases to r_2, its depth decreasing to h_2. The change, $h_1 - h_2 = \triangle h$, is a measure of the elasticity.

Referring to Fig. 2, the following equations may be obtained (Tabor, 1951):

(a) $$d = 2{\cdot}2 \left\{ \frac{W}{2} \cdot \frac{r_1 r_2}{r_2 - r_1} \left\{ \frac{1}{E_1} + \frac{1}{E_2} \right\} \right\}^{\frac{1}{3}} \quad .. \quad .. \quad (4)$$

This is the Hertz equation for the load W necessary to push the sphere, radius r_1, back into the residual spherical indentation, radius r_2, which is left when the load is removed; it is the reverse of the elastic recovery step. The Poisson's ratios σ_1 and σ_2 have been taken as 0·3.

(b) It can be seen from the geometry of Fig. 2 that $h \simeq \frac{d^2}{8r}$ provided $h \ll r$ and that

$$\Delta h = h_1 - h_2 = \frac{d^2}{8} \left\{ \frac{r_2 - r_1}{r_1 r_2} \right\}$$

where h_1 and h_2 are the depths of penetration with the load present and with the load removed. Now from the equation (4)

$$\frac{r_2 - r_1}{r_1 r_2} = \frac{2{\cdot}2^3}{d^3} \cdot \frac{W}{2} \cdot \left(\frac{1}{E_1} + \frac{1}{E_2} \right)$$

$$\therefore \quad \Delta h = \frac{2{\cdot}2^3}{8d} \cdot \frac{W}{2} \cdot \frac{1}{E_1} \quad .. \quad .. \quad .. \quad .. \quad .. \quad (5)$$

where E_1 is the Young's modulus of elasticity of the tablet. E_2, the Young's modulus of the sapphire indenter, is so large that $1/E_2$ is negligible. Since $h_1 = d^2/8r_1$, $d = \sqrt{8\, h_1 r_1}$, and $r_1 = 0{\cdot}775$ mm, thus $\Delta h = 0{\cdot}268 \frac{W}{E_1 \sqrt{h_1}}$ or, rearranging, $E_1 = 0{\cdot}268 \frac{W}{\Delta h \sqrt{h_1}}$, where W is in kg, Δh and h_1 in mm and E_1 is in kg/mm^2. Thus the Brinell hardness is obtainable from the initial depth of penetration using equation (3), and the modulus of elasticity from the recovery after removal of the load.

The results of the measurements are given in Tables 1 and 2. In all cases the applied pressure was sufficient to compress the aspirin practically to zero porosity.

Table 1. *Variation of tablet hardness and modulus of elasticity over a tablet face as a result of changing the compaction pressure.* Table weight = 0·5 g. Indentation load = 4 g. The tablets were compressed from aspirin of ungraded size.

Compaction pressure kg cm^{-2}	Position on tablet	Indentation depth h_1 (μm)	Elastic recovery $\triangle h$ (μm)	Brinell hardness number kg mm^{-2}	Modulus of elasticity kg mm^{-2}
Surface 1: adjacent to stationary punch					
1088	1	1·46	0·54	0·56	7·7
	2	2·14	0·88	0·38	3·9
	3	2·39	0·99	0·34	3·3
	4	2·39	1·04	0·34	3·2
	5	2·62	1·21	0·31	2·6
	Av.	2·20	0·93	0·39	4·1
1453	1	1·66	0·62	0·50	6·4
	2	1·89	0·62	0·44	6·0
	3	2·19	1·14	0·38	3·0
	4	2·11	1·00	0·39	3·5
	5	1·46	0·62	0·56	6·7
	Av.	1·86	0·80	0·45	5·1
1815	1	1·46	0·69	0·56	6·1
	2	1·37	0·62	0·60	7·0
	3	1·34	0·84	0·61	5·1
	4	2·02	1·13	0·41	3·2
	5	1·81	0·85	0·45	4·1
	Av.	1·60	0·83	0·53	5·1
2183	1	1·47	0·87	0·60	4·8
	2	1·48	0·81	0·56	5·1
	3	1·52	0·82	0·54	5·0
	4	1·85	1·17	0·45	3·2
	5	1·43	0·70	0·57	6·1
	Av.	1·55	0·87	0·54	4·9
Surface 2: adjacent to moving punch					
1088	1	1·59	0·58	0·58	6·9
	2	1·39	0·54	0·59	8·9
	3	1·66	0·74	0·50	5·3
	4	2·38	1·04	0·35	3·2
	5	2·46	1·36	0·33	2·4
	Av.	1·90	0·85	0·46	5·3
1453	1	1·27	0·50	0·65	8·9
	2	1·51	0·53	0·54	7·7
	3	1·49	0·63	0·55	6·6
	4	1·82	0·95	0·45	3·9
	5	2·06	0·76	0·40	4·6
	Av.	1·63	0·67	0·52	6·4
1815	1	1·48	0·78	0·56	5·3
	2	1·33	0·77	0·62	5·7
	3	1·45	0·80	0·57	5·2
	4	1·69	0·95	0·49	4·1
	5	1·52	0·92	0·54	4·5
	Av.	1·49	0·84	0·55	5·0
2183	1	1·06	0·53	0·78	9·2
	2	1·25	0·56	0·66	8·0
	3	1·75	0·77	0·47	4·9
	4	2·17	0·85	0·38	4·0
	5	1·56	0·66	0·53	6·1
	Av.	1·56	0·67	0·56	6·5

Table 2. *Variation of tablet hardness and modulus of elasticity over a tablet face as a result of changing the particle size of the compressed material.* Tablet weight = 1·0 g. Indentation load = 4 g. All tablets were compressed at 1453 kg cm^{-2} (143 MNm^{-2}).

Particle size μm	Position on tablet	Indentation depth h_1 (μm)	Elastic recovery $\triangle h$ (μm)	Brinell hardness number kg mm^{-2}	Modulus of elasticity kg mm^{-2}
Surface 2: adjacent to moving punch					
303	1	1·19	0·42	0·69	11·0
	2	1·18	0·50	0·70	9·2
	3	1·21	0·55	0·68	8·5
	4	1·07	0·49	0·77	10·0
	5	1·34	0·59	0·61	7·4
	Av.	1·20	0·51	0·69	9·2
388	1	1·35	0·59	0·61	7·4
	2	1·03	0·35	0·80	14·3
	3	1·20	0·49	0·68	9·3
	4	1·36	0·52	0·60	8·3
	5	1·49	0·51	0·55	8·1
	Av.	1·29	0·49	0·65	9·5
460	1	1·15	0·45	0·71	10·5
	2	1·47	0·59	0·56	7·1
	3	1·81	0·64	0·45	5·9
	4	1·45	0·79	0·56	5·3
	5	1·80	0·91	0·46	4·1
	Av.	1·54	0·68	0·55	6·6
670	1	1·63	0·58	0·50	6·9
	2	1·83	0·60	0·50	6·2
	3	1·86	0·55	0·44	6·8
	4	1·97	0·79	0·42	4·6
	5	2·14	0·52	0·38	6·7
	Av.	1·89	0·61	0·44	6·2

Measured tablet densities all lay between 1·284 and 1·297 g/cm^3. This 1% variation in density is not thought to be significant: compaction to zero voidage was probably achieved in all cases. Thus any variation in mechanical properties over the tablet surface cannot be ascribed to a voidage distribution since the voidage is everywhere zero. The radial pressure exerted on the die wall during each compression increased with increasing compaction pressure, but no significant difference could be found between the behaviour of the different particle size fractions.

Fig. 3(a) shows that there is an increase in the surface hardness of the tablet as the compaction pressure is increased; such behaviour is characteristic of a work-hardening substance. It has been observed previously (Ridgway, Glasby & Rosser, 1969) and was one reason for carrying out the present investigation. Provided that other factors are kept constant, increase in particle size causes the tablets to be softer; as the initial crystal size is increased from 300 to 700 μm, the Brinell hardness is linearly reduced from 0·7 to 0·4 kg/mm^2. Smaller crystals have more inter-particle contacts per unit volume of crystalline material than do larger ones, so that for a given degree of compaction there is more contact pressure and consequent work-hardening.

Fig. 3(b) shows the change of hardness across the faces of a tablet. These tablets were made by applying thrust to one punch only, the other being stationary and that

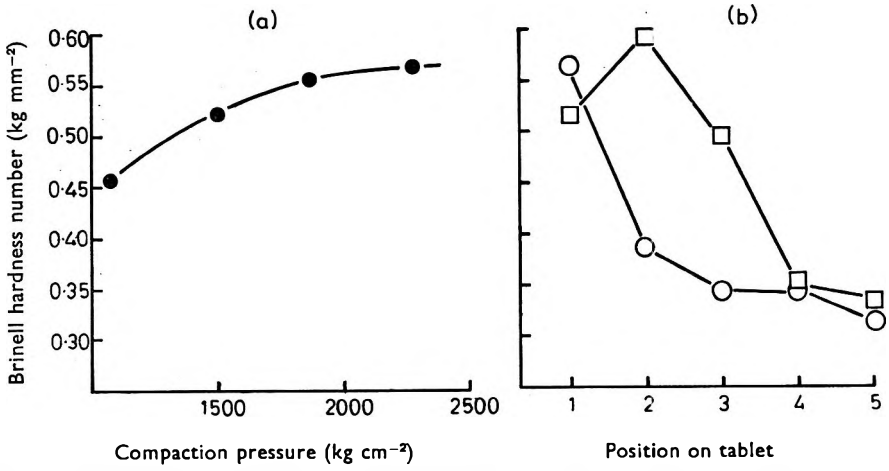

FIG. 3. (a) The average hardness of the tablet surface as the compaction pressure is increased, showing the overall work-hardening effect. (Compaction pressure range 100-250 MNm^{-2})

(b) Surface hardness of the two faces of a tablet. The centre is harder than the outer edge for both faces, and the face contacted by the moving punch is harder than that contacted by the stationary punch. —○—Stationary punch face. —□— Moving punch face. Numbers 1-5 refer to radially equally-spaced positions, 1 at the centre and 5 at the outer edge of the tablet.

side of the tablet adjacent to the moving punch is harder than the other. Also, the tablet is harder at the centre than at the edge. This conclusion is rather unexpected. In the work of Train, shearing and wedge action were thought to be greatest near the outer edge of the moving punch, as this was a region of greater pressure and resultant tablet density. Train's explanation was that the Boussinesq (1876) pressure bulb was modified by the die wall to give high pressure regions in the lower central part of the compact and in the upper edge. However, there are several differences between Train's compacts and ours. He used magnesium carbonate in much smaller particle sizes than we have used for aspirin. His compacts were large, about 2 inches across and 3 inches deep, whereas ours are much smaller overall and have a depth only about $\frac{1}{4}$ of their diameter. His applied pressures compacted his powder to about 70% of the theoretical density. Train's results were in agreement with those of Kamm, Steinberg & Wulff (1949) but not with those of Duwez & Zwell (1949).

We suggest that in small tablets the Train mechanism may be considerably modified

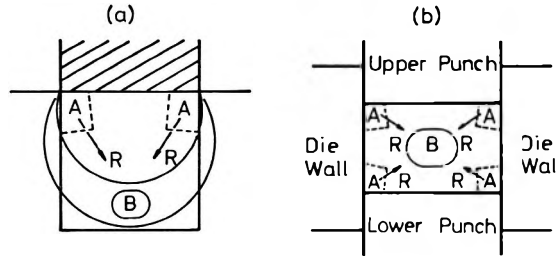

FIG. 4. (a) The Boussinesq pressure bulb, as modified by the die wall. The wedging action produces shear and a high density at A, and the forces R acting together give a high pressure and density at B.

(b) For a tablet whose depth is much less in comparison with its diameter, forces R, acting from both sides and at a greater angle to the vertical, produce a high pressure and density at the centre, with perhaps a high shear zone at the outer edge. This shear is increased if the tablet is moved relative to the die wall during compaction.

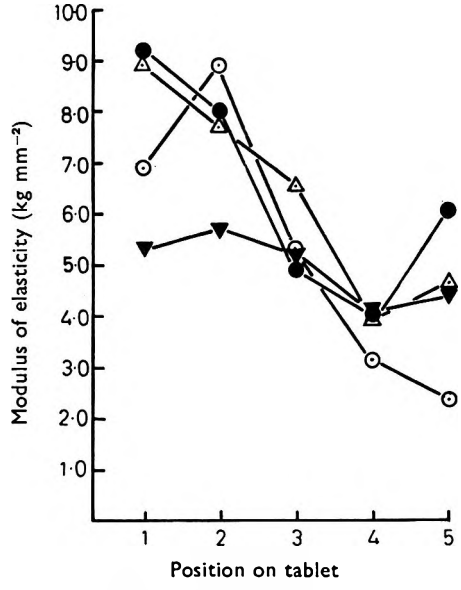

FIG. 5. Young's modulus of elasticity as a function of distance from the centre of the tablet The compaction pressures are: —⊙— 1088 kg/cm². —△— 1453 kg/cm². —▼— 1815 kg/cm². —●— 2183 kg/cm². (Range 106-216 MNm^{-2})

as shown in Fig. 4. In Fig. 4 (a), the pressure bulb modified by the die wall is shown. In Fig. 4 (b) a further stage is indicated. The resultants R of the Train mechanism are caused, by the proximity of the other punch and its reaction, to swing round at a greater angle to the vertical. The high density region found by Train near the base of his compacts will now occur at the tablet centre. In the case of aspirin there will not be a region of higher density, but a region of greater work-hardening, since

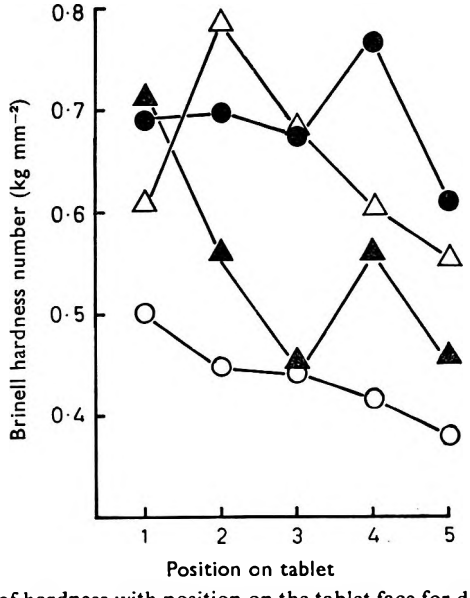

FIG. 6. The variation of hardness with position on the tablet face for different particle sizes of the initial material. —●— 44–60 mesh, mean 303 μm. —△— 40–44 mesh, mean 388 μm. —▲— 30–40 mesh, mean 460 μm. —○— 20–30 mesh, mean 670 μm.

greater applied pressure and greater hardness correlate for this substance. Using concave punch faces might well assist this process by directing pressure towards the tablet centre and enlarging the central hard region so that it formed a greater proportion of the tablet.

The elasticity for the surface adjacent to the moving punch is plotted in Fig. 5. The elasticity does not change greatly with pressure level. It is high at the centre, where the material is work-hardened and therefore able to resist further deformation and permanent set. It decreases outwardly along the radius, but shows a slight increase at the extreme outer edge. This behaviour differs from that of the Brinell hardness itself, and indicates that the effect of a hydrostatic pressure upon aspirin, such as obtains at the centre of the compact when it is made, may well be different from the effect of a shear force which occurs at points near to the edge of the punch faces. Sheared aspirin is softer, but will elastically recover better from a deformation. Compressed aspirin is physically harder, but when it deforms it does so plastically with less recovery.

Fig. 6 shows the variation of hardness with position on the tablet face for the different particle sizes used. Although the experimental scatter is large, the increase of hardness with decrease of crystal size is apparent and there is a decrease of hardness from the centre of the tablet to the outer edge.

REFERENCES

BOUSSINESQ, J. (1876). "Memoires couronnes et memoires des savants étrangers." Brussels.

DUWEZ, P. & ZWELL, L. (1949). *Trans. Am. Inst. Min. metall. Engrs.*, **185**, 137–144.

GANDERTON, D. (1969). *J. Pharm. Pharmac.*, **21**, *Suppl.*, 9S–18S.

HERTZ, H. (1881). *J. reine angew. Math.*, **92**, 156.

HIGUCHI, T., ELOWE, L. N. & BUSSE, L. W. (1954). *J. Am. pharm. Ass.*, **43**, 685–689.

KAMM, R., STEINBERG, M. & WULFF, J. (1949). *Trans. Am. Inst. Min. metall. Engrs.*, **180**, 694–704.

LEWIS, C. J. & TRAIN, D. (1965). *J. Pharm. Pharmac.*, **17**, 1–9.

RIDGWAY, K. (1966). *Ibid.*, **18**, *Suppl.*, 176S–181S.

RIDGWAY, K., GLASBY, J. & ROSSER, P. H. (1969). *Ibid.*, **21**, *Suppl.*, 24S–29S.

TABOR, D. (1951). "*The Hardness of Metals*," Oxford: University Press.

TRAIN, D. (1957). *Trans. Instn chem. Engrs.*, **35**, 258–266.

TRAIN, D. & HERSEY, J. A. (1960). *Powder Metall.*, (6), 20–35.

J. Pharm. Pharmac., 1970, **22**, *Suppl.*, 79 S–85 S *Received March* 12, 1970

An investigation of the pore structure of tablets of sucrose and lactose by mercury porosimetry

ALASTAIR B. SELKIRK* AND DAVID GANDERTON†

Department of Pharmaceutical Technology, School of Pharmacy, University of Strathclyde, Glasgow, C.1, U.K.

The pore structure of tablets has been investigated by mercury porosimetry. Tablets, when prepared from ungranulated powder, showed a narrow pore size distribution, the mode of which decreased from 9 to 1 μm over the pressure range studied. Granulation caused the size distribution of tablet pores to widen. Large robust granules, compressed at low pressures, gave tablets with a bimodal pore size distribution. Decrease in granule size and strength, promoted a more uniform tablet structure and fine, friable, granules, compressed at high pressures, gave tablets with almost the same structure as those prepared from ungranulated powder.

Some investigations of the pore structure of tablets of sucrose and lactose using permeability and liquid penetration tests were recently reported (Ganderton & Selkirk, 1970). The inferences drawn from experiments in which the properties of the granules and the degree of compression were varied were of a wide and possibly discontinuous distribution in the size of the pores. The measurement of such a distribution can be made by the intrusion of a non-wetting liquid. In the work reported below this technique is described and its application to the estimation of tablet structure assessed.

THEORETICAL CONSIDERATIONS

An external force must be applied to any non-wetting liquid, such as mercury, for its penetration into a pore. The surface tension, γ, opposing entry acts along the perimeter. If the capillary is circular in cross section, the force opposing entry normal to the plane of contact is given by

$$F_o = -2\pi r\gamma \cos\theta$$

where r is the radius of the pore and θ the contact angle the liquid makes with the pore surface.

The external force, which must be applied for penetration to occur, acts over the area of the circle of contact and is given by the equation

$$F_a = \pi r^2 p$$

where p is the applied external pressure.

At equilibrium

$$\pi r^2 p = -2\pi r\gamma \cos\theta$$

$$\therefore pr = -2\gamma \cos\theta \quad .. \quad .. \quad .. \quad .. \quad (1)$$

No pores will be penetrated by a non-wetting liquid under zero external pressure but as the pressure is increased the amount of liquid forced into the pores will increase

Present address: *School of Pharmacy, Sunderland Polytechnic, Sunderland;
†ICI Pharmaceuticals Division, Alderley Park, Cheshire.

and will be proportional to the differential pore volume, the size of which is related to the changing pressure by equation (1).

This derivation assumes the pore is circular in cross section, the assumption appearing as the ratio of perimeter to area, 2/r. While the pore network within a tablet is invariably complex and seldom are the pores circular in shape, the variation of this ratio for non-circular cross sections will not be great. The shape of the distribution curve will not be appreciably altered and the calculated radius will be changed by a consistent factor.

Pore size distribution function

If, within a tablet, the volume of the pore having a radius between r and r + dr is dV, then,

$$dV = D(r)dr \quad .. \quad .. \quad .. \quad .. \quad (2)$$

where D(r) is the pore size distribution function of that tablet, i.e. the fraction of the pore volume with a radius between r and r + dr.

If a constant surface tension and contact angle are assumed, differentiation of equation (1) with respect to r and p gives

$$pdr + rdp = 0 \quad .. \quad .. \quad .. \quad .. \quad (3)$$

Combining equations (2) and (3)

$$dV = -D(r)\, r/p \cdot dp$$

$$\text{or } D(r) = -p/r \cdot \frac{dV}{dp} \quad .. \quad .. \quad .. \quad .. \quad (4)$$

For a tablet with a given pore size distribution, an increase in pressure on the non-wetting liquid gives a unique pressure uptake volume curve; conversely a given pressure–volume curve affords a determination of the pore size distribution.

For a number of values of p the experimental pressure volume curve may be differentiated to obtain dV/dp while r may be calculated from equation (1). A plot of D(r) against r gives the pore size distribution.

EXPERIMENTAL

Granulation. The finely powdered lactose and sucrose were massed in a Z blade mixer with water for 5 min. The resultant wet mass was passed through an oscillating granulator fitted with a coarse screen. The granules were dried to a constant weight at 70° and rescreened.

Two sucrose batches were made with a massing water content of 5% in one case and 9% in the other. With lactose, the massing water content was varied in four equal steps from 13 to 25%. The granules were finely sieved and the sieve fractions −8 + 16 and −60 + 85 were collected for study.

Compression. Granules (0·5 g) were compressed in a punch and die set of diameter 12·7 mm by means of a hydraulic press. Using a predetermined pressure and thickness, tablets were prepared with a porosity of 29, 26·5, 22 or 15%.

Mercury intrusion. The relation between the mercury penetration volume and intrusion pressure was measured with a mercury penetration porosimeter (Model 905–1, Coulter Electronics Ltd., Dunstable). Five tablets were used in each deter-

mination; they were placed in the sample cell and this in turn was placed in the bomb of the porosimeter.

The cell was evacuated and mercury was allowed to enter; when full, the pressure was allowed to rise to 3·5 kNm^{-2}. This, the initial penetration pressure, is the lowest pressure readily usable since the dimensions of the sample holder are such that the hydrostatic pressure of the mercury above the tablets is of a similar magnitude. The pressure was incrementally increased to atmospheric and the volume of mercury penetrating the tablet at each pressure was measured by the apparent volume of the mercury in the sample holder. Pressure above atmospheric was applied with compressed air after filling the bomb with oil. The maximum pressure used was 350 MNm^{-2}.

In deriving the pore size distribution, the surface tension of the mercury was assumed to be 0·474 Nm^{-1} and its contact angle with lactose and sucrose 130°. From equation (1) this allows a corresponding pore radius to be calculated for any given pressure. As the volume of the void space in each tablet was known, the saturation of the tablet by mercury at each pressure level was calculated and expressed as a percentage.

RESULTS AND DISCUSSION

Sucrose. Fig. 1 shows typical porosimetric results for tablets made from ungranulated sucrose powder. These results are presented both as the percentage of voids filled for a given penetration pressure (Fig. 1a) and as the corresponding pore size distribution (Fig. 1b). The sigmoid shape of the curve shown in Fig. 1 is characteristic of this determination. Absence of intrusion at low pressure followed

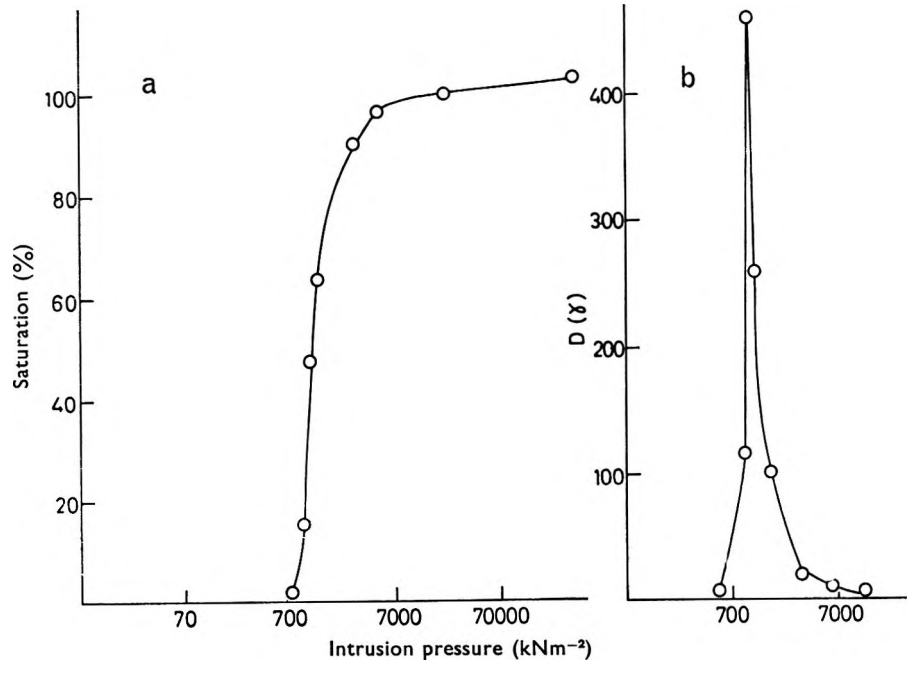

FIG. 1. Cumulative pore size distribution curve (a) and pore size distribution (b) of tablets of sucrose powder at 22% porosity.

by rapid saturation over a relatively small pressure range is indicative of a system of a narrow pore size distribution containing few coarse pores. However, as shown in Fig. 1b some tailing off at lower pore sizes does occur.

The susceptibility of the pore structure of these tablets to compression pressure is illustrated in Fig. 2. As the porosity is decreased the position of the curves moves steadily towards the lower pore sizes. This shift is relatively small, the pore radius at 50% saturation decreasing from 1·6 to 0·6 μm for a reduction of 14% in porosity. Microscopic examination of the uncompressed sucrose powder showed a narrow size distribution, 80% of the particles lying between 8 and 25 μm. Compression of this material will form a tablet of small pores and such a system will be characterized

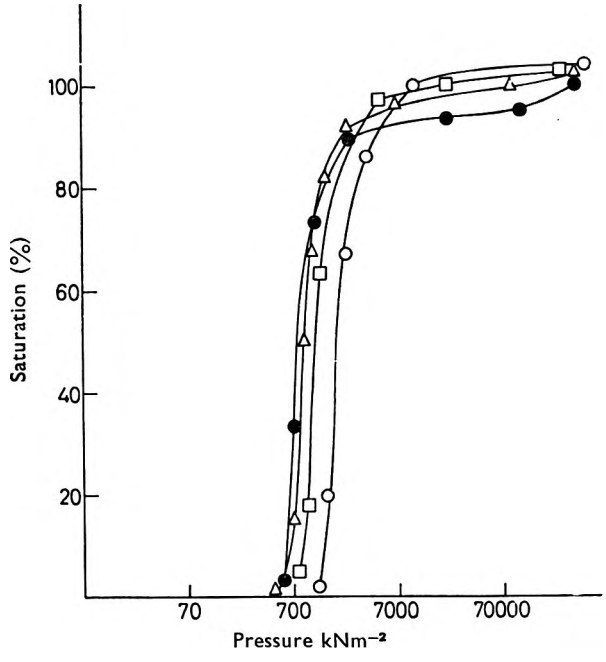

FIG. 2. The effect of compression on the pore structure of tablets of sucrose powder. ● 29% porosity. △ 26·5% porosity. □ 22% porosity. ○ 15% porosity.

by low permeability. Marshall (1958) has derived a relation between permeability and size distribution of pore in an isotropic medium. If the mean radius of the pores in each of n equal fractions of the total pore space is represented in decreasing order of size $r_1, r_2 \ldots r_n$ cm, then the permeability B_0 is given by

$$B_0 = \frac{\epsilon^2 n^{-2} (r_1^2 + 3r_2^2 + 5r_3^2 + \ldots + (2n-1)r_n^2)}{8} \quad \ldots \quad (5)$$

where ϵ = porosity.

This equation enables a calculation of the permeability of a tablet from a knowledge of its pore size distribution, and its application to a tablet prepared at 29% porosity from sucrose powder gave a permeability value of $8{\cdot}5.10^{-14}$ m². This is in close agreement with the experimental value of $7{\cdot}0.10^{-14}$ m² (Gandertɔn & Selkirk, 1970).

The structure of such a system containing only small powder particles will not

be readily susceptible to breakdown with increase in compression pressure. This is manifest in the small shift in pore distribution as the porosity is reduced.

The effect of granulation on the pore structure of sucrose tablets is shown in Fig. 3. This process leads to a very marked increase in the proportion of coarse pores present and to a considerable widening of the pore size distribution. Such marked opening of the pore structure is maintained even at relatively low porosities. Opening of pore structure will result in a more permeable tablet. Calculation of the permeability from a knowledge of the pore size distribution (eqn 5) again gave values much higher than those from tablets of the ungranulated powder. These values were in close agreement with the values found experimentally.

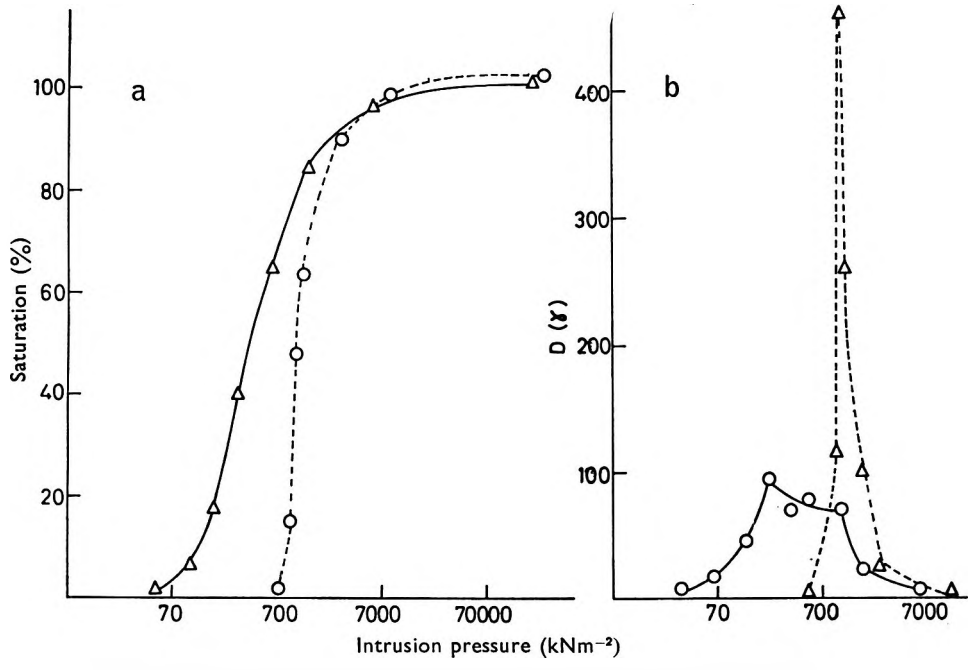

FIG. 3. (a) The effect of granulation on the cumulative pore size distribution of sucrose tablets of 22% porosity. △ Tablets prepared from −16 + 22 mesh granules massed with 5% water. ○ Tablets prepared from ungranulated powder.
(b) The effect of granulation on the pore size distribution of sucrose tablets of 22% porosity. ○ Tablets prepared from −16 + 22 mesh granules massed with 5% water. △ Tablets prepared from ungranulated powder.

Within a tablet compressed from granular material there are two types of pores. The first, intragranular pores, are formed within the granules themselves during the aggregation of the powder. The second type, intergranular pores, are formed between the granules during tabletting. While the former are invariably small the latter, especially in an uncompressed bed or a tablet of high porosity may be relatively large. Thus tablets made from these materials have a wide and perhaps discontinuous pore size distribution. On compression, however, fragmentation of the granules leads to a breakdown of the coarse intergranular pore network resulting in a tablet of more even pore size distribution. This process is described in Fig. 4. On compression, a large change in the pore structure occurs with the pore radius at 50% saturation decreasing from 9·0 to 1·0 μm for a 14% reduction in porosity.

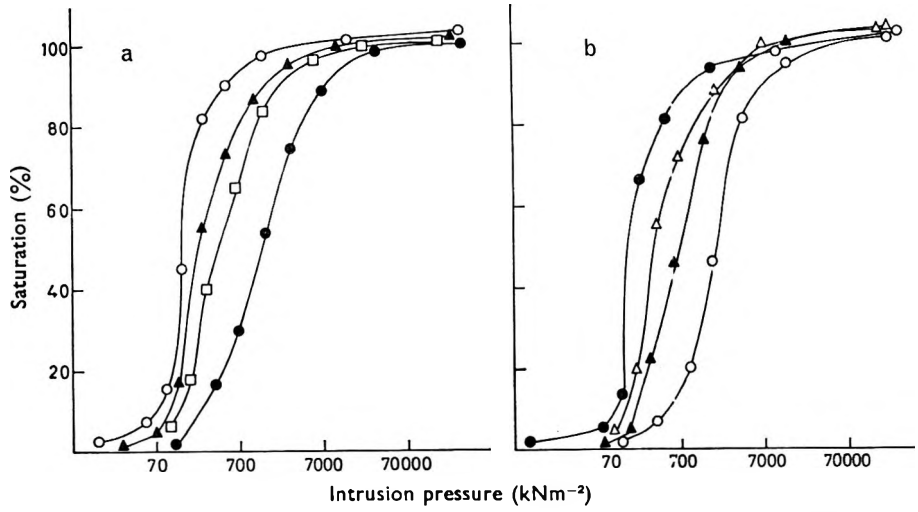

FIG. 4. The effect of compression on the pore structure of tablets prepared from —16—22 mesh sucrose (a) and —8+16 mesh lactose (b) granules. ○ 29% porosity. ▲ 26·5% porosity. □ 22% porosity. ● 15% porosity.

The photographs in Fig. 5 show that for a tablet made from granular material the coarse intergranular pores are not randomly distributed within the tablet but are closely related to the original granule configuration. As expected, tablets prepared from the ungranulated powder gave no visual evidence of any intergranular pore network.

Granule size and massing water concentration during granulation also affect the pore size distribution of the resultant tablets and a summary of such effects is given in Table 1.

An increase in granule size and massing water concentration simultaneously operates to open the pore structure of the tablet. Granule size initially defines the size of the intergranular pores with the coarser granules promoting a more open pore structure. In the early stages of compression while fragmentation is still small this

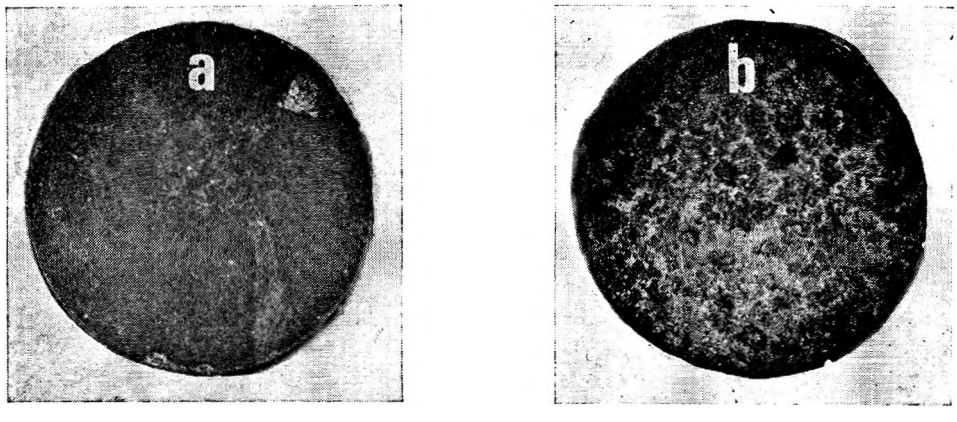

FIG. 5. Photographs of sucrose tablets on completion of a mercury intrusion determination. a. Tablets prepared from the ungranulated powder. b. Tablets prepared from —16+22 mesh granules.

Table 1. *Granule size and massing water concentration during granulation of sucrose and lactose*

Granule size	29% Porosity % Voids ⩾ 12 μm	29% Porosity % Voids ⩽ 1·2 μm	15% Porosity % Voids ⩾ 12 μm	15% Porosity % Voids ⩽ 1·2 μm	29% Porosity % Voids ⩾ 12 μm	29% Porosity % Voids ⩽ 1·2 μm	15% Porosity % Voids ⩾ 12 μm	15% Porosity % Voids ⩽ 1·2 μm
Sucrose	5% Massing water concentration				9% Massing water concentration			
—16 + 22	25·0	5·0	0	52·0	49·0	9·5	0	51·0
—60 + 55	15·0	7·0	0	49·5	16·5	4·0	0	49·0
Lactose	13% Massing water concentration				25% Massing water concentration			
—16 + 22	7·0	12·5	0	30·0	14·5	15·0	0	33·0
—60 + 85	6·5	13·0	0	31·0	8·0	14·0	0	30·0

influence is sustained. As compression is increased and as fragmentation becomes marked, these effects disappear.

Massing water concentration affects both intragranular porosity and the resistance of the granules to deformation. Since intragranular porosity is decreased by higher massing water concentrations (Ganderton & Selkirk, 1970), compaction to a given overall porosity requires less deformation. This, together with their increased robustness, results in tablets of a more open pore structure. Thus at 29% porosity, tablets prepared from coarse granules massed with 9% water had 49% of the void space as pores greater than 12 μm. The corresponding material massed with 5% water had 25% greater than 12 μm. Again this effect was eroded by an increase in compression pressure.

Lactose. The change in the pore size distribution with a decrease in porosity is similar to the changes observed with sucrose tablets with the pore radius corresponding to 50% saturation decreasing from 8 to 0·8 μm. The effect of granule size and massing water concentration is shown in Table 1 which indicates that the contribution of the coarse pores to the overall porosity is less than with the sucrose. For example, lactose massed with 13% water, compressed to 29% porosity gave a tablet with 7·0% of the voids present as pores greater than 12 μm.

Acknowledgements

The authors would like to express their sincere thanks to Dr. H. Palmer of ICI, Dyestuffs Division, for his invaluable assistance. They gratefully acknowledge the financial support of the Science Research Council.

REFERENCES

Ganderton, D. & Selkirk, A. B. (1970). *J. Pharm. Pharmac.*, **22**, 345–353.
Marshall, T. J. (1958). *J. Soil Sci.*, **9**, 1–8.

J. Pharm. Pharmac., 1970, **22**, *Suppl.*, 86 S–94 S *Received March* 3, 1970

The influence of wet and dry granulation methods on the pore structure of lactose tablets

ALASTAIR B. SELKIRK* AND DAVID GANDERTON†

Department of Pharmaceutical Technology, School of Pharmacy, University of Strathclyde, Glasgow, C.1, U.K.

The conditions of wet granulation influenced the pore structure of lactose tablets, prepared over a wide range of tabletting pressures. Dry granulation, on the other hand, only influenced pore structure when slugging pressures were high, the granules were coarse and tabletting pressures were low. Mercury porosimetry revealed intense granule fragmentation when dry granulated materials were compressed. The effect of the change of pore size distribution on liquid penetration into tablets is discussed.

Granulation exerts a considerable influence on many properties of a tablet, such as dissolution (Solvang & Finholt, 1970), compressibility (Gray, 1968), weight and dose uniformity (Hersey, 1965) and strength (Raff, Robinson & Svedres, 1961). One mechanism by which granulation may affect the properties of a tablet is by its influence on pore structure. Ganderton & Selkirk (1970) have shown that binder concentration and granule size affect pore structure.

The present study examines two fundamentally different methods of granulation: a dry method in which the granules are produced by compression causing cohesion of the particles (slugging) and a wet method in which the particles are linked by solid bridges, formed during drying of the wetted powder mix (wet massing and screening). The influence of these granulation methods on pore structure has been investigated by measuring porosity, air permeability and the penetration of wetting and non-wetting liquids into a tablet.

EXPERIMENTAL

Wet granulation

Finely powdered lactose was mixed with water in a Z-blade mixer (Duplex Model OO, Morton Machines Ltd., Wishaw, Scotland) for 5 min and forced through a coarse screen. The granules were dried to a constant weight at 70° and rescreened. Sieve fractions $-8 + 16$, $-16 + 22$, $-30 + 44$ and $-60 + 85$ were collected. The granules were made with a mass containing 13 or 25% v/w of water. The lower massing water concentration represented the minimum amount of water necessary to form coherent granules and the higher massing water concentration, the wettest conditions allowing satisfactory movement of the mass through the screen.

Dry granulation

Lactose powder was compressed, in a large punch and die set, at pressures of 50, 150 and 270 MNm^{-2} to form cylindrical slugs 38·1 mm in diameter. The slugs were removed from the die, broken down on a reciprocating granulator (Model 6, Jackson

Present address: *School of Pharmacy, Sunderland Polytechnic, Sunderland; †ICI Pharmaceuticals Division, Alderley Park, Cheshire.

and Crockatt Ltd., Glasgow) and the granules sieved. The sieve fractions $-8 + 16$, $-16 + 22$, $-30 + 44$, $-60 + 85$ were collected.

Compression

A weighed quantity of granules was placed in a lubricated die sealed at one end by a spigot. The upper punch was inserted and the assembly compressed over a pressure range of 7 to 140 MNm^{-2} between the platens of a hydraulic press. The compaction force was measured in the manner described by Shotton & Ganderton (1960) by means of strain gauges affixed to the shank of the punch.

Porosity, permeability and liquid penetration tests

The porosity of a tablet was calculated from its volume, weight and the density of the material.

The permeability was measured by the method of Lea & Nurse (1939) and the results are expressed as the permeability coefficient previously described (Ganderton & Selkirk, 1970).

The rate of penetration of cyclohexane into a tablet under the influence of capillary forces was measured by the method of Ganderton & Selkirk (1969).

Measurement of the penetration of mercury into tablets was made with a Mercury Penetration Porosimeter (Model 905-1, Coulter Electronics Ltd., Dunstable, Bedfordshire). Five tablets were placed in the sampler holder. The pressure was reduced to 2·7 Nm^{-2} and the holder completely filled with mercury. The penetration pressure was increased incrementally from 3·5 kNm^{-2} to a maximum of 350 MNm^{-2} and for each increase the volume of mercury penetrating the pores was noted.

The distribution of the size of the pores within the tablet was derived from the data by the method of Ritter & Drake (1945).

RESULTS

Dry granulation

The decrease in porosity of lactose slugs with increasing slugging pressure is given in Table 1. When these slugs are broken up to form granules, the pore space within the granules (intragranular porosity) will show similar variation.

Table 1. *The effect of compression on the porosity of lactose slugs*

Slugging pressure MNm^{-2}	Porosity %
50	22·0
150	14·4
270	10·5

When these materials were tabletted, granules of $-8 + 16$ mesh size, prepared at high slugging pressures, gave the most permeable tablets (Fig. 1A). However, the influence of slugging pressure decreased as the degree of tablet compression increased. With tablets made from $-60 + 85$ mesh granules (Fig. 1B), slugging pressure only influenced permeability when the porosity of the tablets was 20% or more.

The effect of slugging pressure on the pore size distribution of tablets, prepared from $-8 + 16$ mesh granules is shown in Fig. 2A and the corresponding results for tablets made from $-60 + 85$ mesh granules in Fig. 2B.

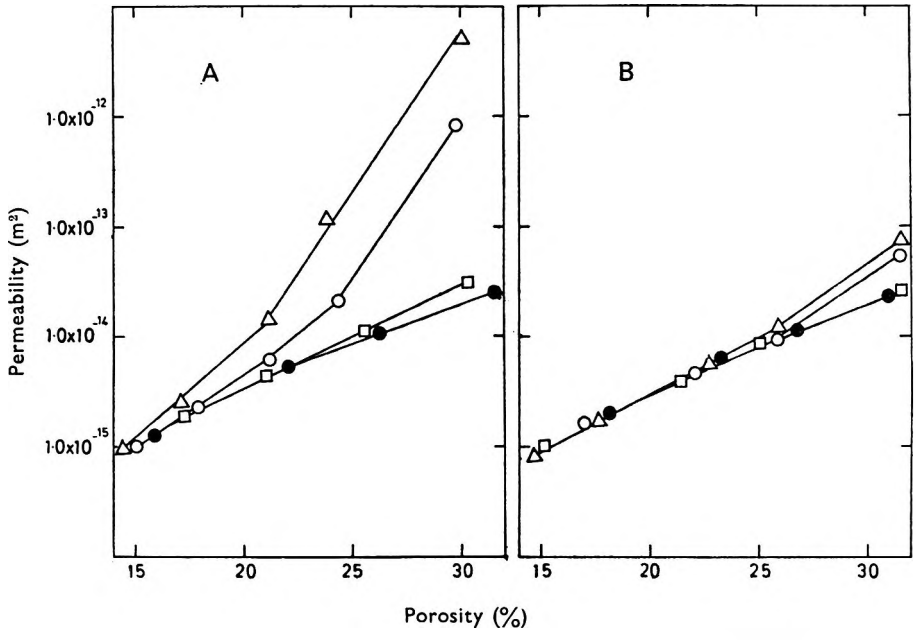

FIG. 1. The effect of slugging pressure on the permeability of lactose tablets made from (A) —8 + 16 sieve granules and from the ungranulated powder and (B) from —60 + 85 sieve granules and ungranulated powder. △ 270 MNm^{-2}. ○ 150 MNm^{-2}. □ 50 MNm^{-2}. ● Ungranulated powder.

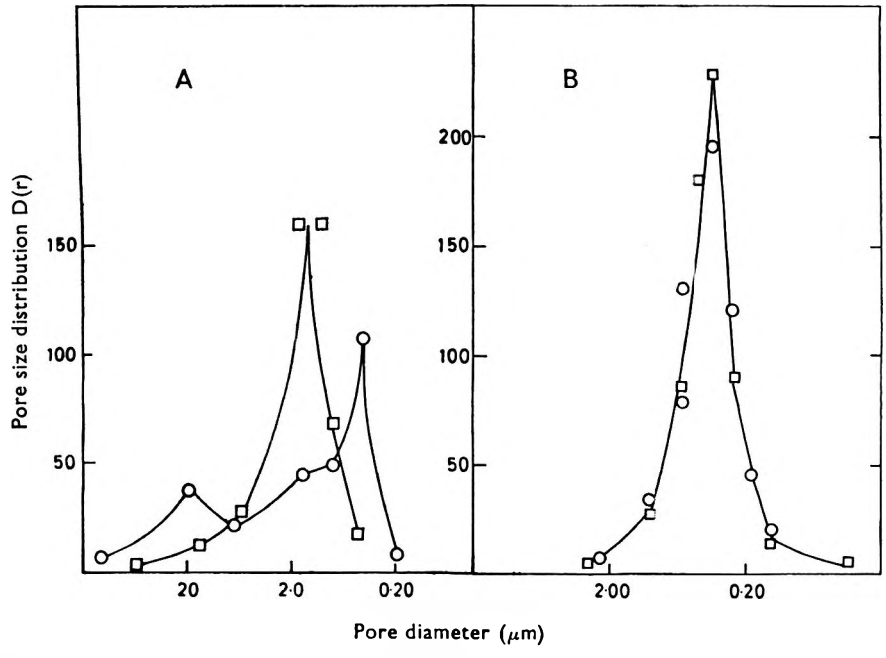

FIG. 2. The effect of slugging pressure on the pore size distribution of lactose tablets of porosity 26·5%, made from (A) —8 + 16 mesh (B) —60 + 85 mesh granules. ○ 270 MNm^{-2}. □ 50 MNm^{-2}.

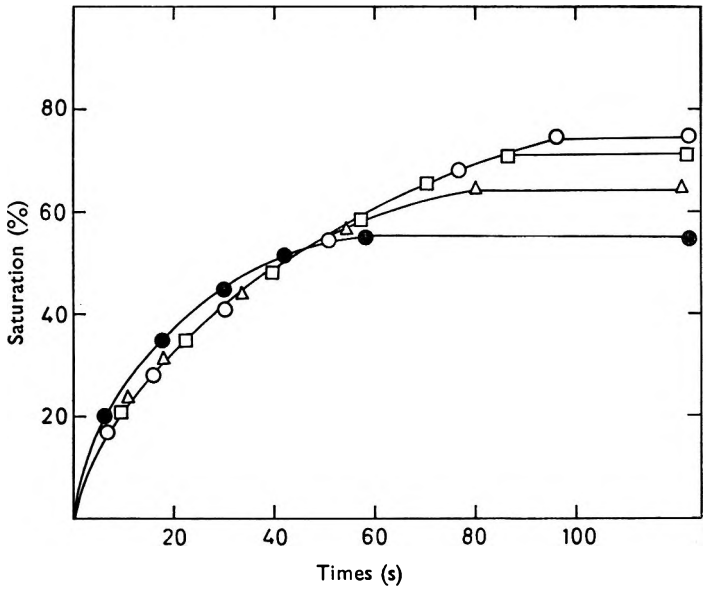

FIG. 3. The effect of granule size on the rate of cyclohexane penetration into lactose tablets made from granules slugged at 270 MNm^{-2}. ● —8 + 16 sieve fraction. △ —16 + 22 sieve fraction. □ —30 + 44 sieve fraction. ○ —60 + 85 sieve fraction.

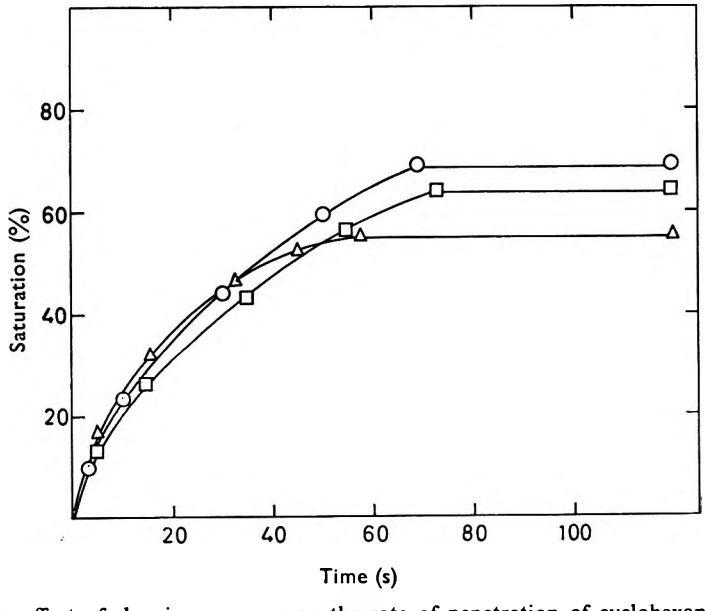

FIG. 4. The effect of slugging pressure on the rate of penetration of cyclohexane into lactose tablets prepared from —8 + 16 mesh granules. ○ 50 MNm^{-2}. □ 150 MNm^{-2}. △270 MNm^{-2}.

The influence of granule size on the penetration, by cyclohexane, into tablets made from granules prepared at a slugging pressure of 270 MNm^{-2} is shown in Fig. 3. The fraction of void space saturated, when penetration ceased, was found to decrease with an increase in the size of the granules which had been tabletted. The initial rate of penetration was however unaffected by granule size. The rate of cyclohexane penetration into tablets made from $-8 + 16$ granules was also independent of slugging pressure but the extent of saturation decreased as the slugging pressure increased (Fig. 4).

Table 2 indicates the role of tabletting pressure on the penetration of cyclohexane into tablets prepared from $-8 + 16$ mesh granules. As tabletting pressure increased, the rate of cyclohexane penetration decreased but the extent of saturation of the tablets increased. This increase in saturation with increase in tabletting pressure was most marked in those tablets prepared from granules made at a slugging pressure of 270 MNm^{-2}.

Table 2. *The effect of compression on the penetration of cyclohexane in lactose tablets made from coarse slugged granules*

	Time for 30% saturation (s) at Slugging pressures:		
Tabletting pressure	50 MNm^{-2}	150 MNm^{-2}	270 MNm^{-2}
30 MNm^{-2}	15·0 ± 1·0	18·0 ± 1·0	13·0 ± 1·0
50 MNm^{-2}	29·0 ± 2·0	23·0 ± 2·0	20·0 ± 2·0
130 MNm^{-2}	62·0 ± 2·0	58·0 ± 2·0	61·0 ± 2·0

	Final % saturation at Slugging pressures:		
Tabletting pressure	50 MNm^{-2}	150 MNm^{-2}	270 MNm^{-2}
30 MNm^{-2}	69·0 ± 2·0	64·0 ± 2·0	54·5 ± 2·0
50 MNm^{-2}	75·0 ± 1·5	73·5 ± 2·0	60·7 ± 1·5
130 MNm^{-2}	78·5 ± 1·5	80·0 ± 1·0	80·0 ± 1·5

Comparative data for wet and dry granulation

A comparison of the permeability of tablets made from wet granulated and dry granulated materials is made in Fig. 5. Changes in permeability, induced by variation in massing water concentration, are much smaller than those produced by variation in slugging pressure.

Fig. 6 shows the effect of the method of granulation on the cumulative pore size distribution of tablets. Tablets of 29% porosity, made from dry granulated material, showed a coarser pore structure than the corresponding tablets made from wet granulated material. However, for tablets of 15% porosity, the position was reversed, with a coarser pore structure being found with tablets made from the wet granulated materials.

In Table 3, values for the extent of saturation on cessation of penetration of cyclohexane into tablets prepared from wet and dry granulated material are compared with tablets made from the ungranulated powder.

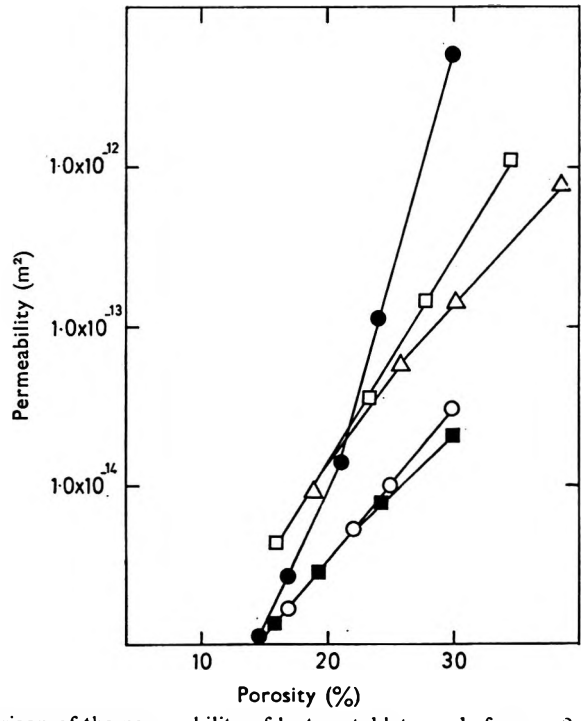

FIG. 5. A comparison of the permeability of lactose tablets made from —8 + 16 mesh granules prepared by wet and dry granulation processes. ● Granules slugged at 270 MNm^{-2}. ○ Granules slugged at 50 MNm^{-2}. □ Granules massed with 25% water. △ Granules massed with 13% water. ■ Ungranulated powder.

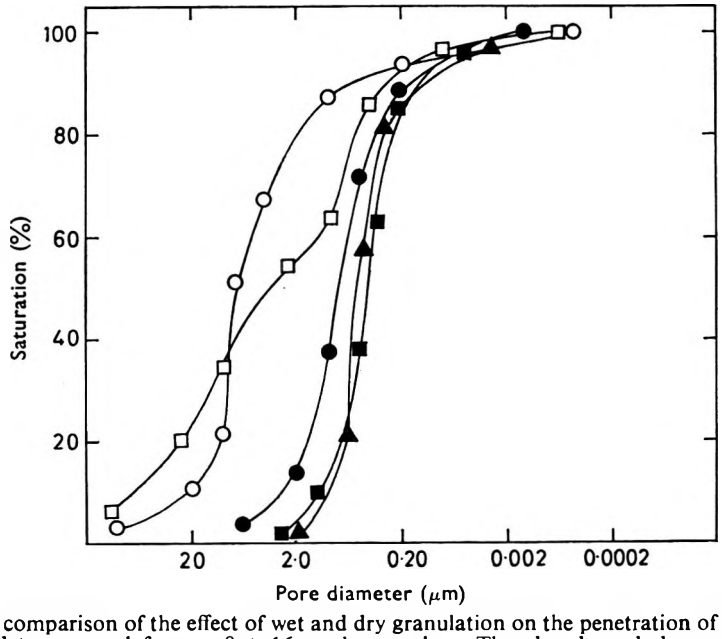

FIG. 6. A comparison of the effect of wet and dry granulation on the penetration of mercury into lactose tablets prepared from —8 + 16 mesh granules. The closed symbols represent results made at 15% porosity and the open symbols at 29% porosity. ○ Granules massed with 25% water. □ Granules slugged at 270 MNm^{-2}. ▲ Ungranulated powder.

Table 3. *A comparison of the saturation of lactose tablets of porosity* 26·5%, *made from granules prepared by wet and dry granulation methods*

Type of granulation	Granule size (mesh fraction)	Final % saturation
13% force screened	— 8 + 16	65·5
13% force screened	— 60 + 85	72·0
25% force screened	— 8 + 16	58·0
25% force screened	— 60 + 85	69·5
270 MNm^{-2} slugged	— 8 + 16	54·5
270 MNm^{-2} slugged	— 60 + 85	75·0
50 MNm^{-2} slugged	— 8 + 16	69·0
50 MNm^{-2} slugged	— 60 + 85	76·5
Ungranulated powder	<170	75·0

DISCUSSION

For a given powder, the methods and conditions of granulation interact with tabletting pressure and granule size to determine the pore structure of a tablet. An increase in tabletting pressure produces a finer pore structure for all materials, as shown by their decrease in permeability. Granule size influences that part of the pore structure of a tablet which arises during compression from the spaces between granules (intergranular porosity). The method and conditions of granulation affect both *inter*granular and *intra*granular pore structure by changing the degree of packing within the granules, and the strength of the granules.

The highest slugging pressures used produced a granule with an intragranular porosity of 10·5%. Compression of this material to form a tablet of a given porosity will require less deformation of the granules than a tablet made from dry granulated material of higher intragranular porosity. A coarse intergranular pore system will be more readily sustained, especially when tabletting pressures are low. The discontinuous pore size distribution, shown in Fig. 3, is then obtained. It has a maximum frequency of coarse pores at 17 μm and of fine pores at 0·3 μm. Such a pore size distribution will give rise to the high permeability shown in Fig. 1. This bimodal pore size distribution is absent in tablets made from granules prepared at a slugging pressure of 50 MNm^{-2}. A high intragranular porosity and low granule strength permits extensive granule fragmentation. The pore system is reorganized to give a simple size distribution with a maximum frequency at 1·3 μm. Such a tablet is only slightly more permeable than the corresponding one prepared from ungranulated powder (Fig. 1A).

If small granules are tabletted, the pores between the granules are much finer and the pore size distribution is less complex. At low tabletting pressures, the pore size distribution of tablets made from granules slugged at 50 and 270 MNm^{-2} is very similar, the mode occurring at a little under 1 μm.

In a wet granulation process, increase in massing liquid concentration has only a small effect on the intragranular porosity (Hunter, B. M., unpublished observations). The effect on the strength of the granules however, can be marked, so that a coarse structured tablet can be made if coarse, strong granules are used (Ganderton & Selkirk, 1970).

Granules prepared by wet and dry methods behave differently on compression. In the permeability comparisons made in Fig. 5 the coarsest pore structures are found

in tablets, produced at low tabletting pressures, from $-8 + 16$ mesh granules made at a slugging pressure of 270 MNm^{-2}.

There is, however, a marked reduction in the permeability of these tablets as tabletting pressure is increased so that, for tablet porosities of less than 20%, the permeability is less than that of the same materials which have been wet granulated and compressed. Thus, although a coarse intergranular network may be envisaged for tablets prepared at low tabletting pressures from dry granulated materials, a period of intense granule fragmentation must occur. This fragmentation is shown by the change in the cumulative pore size distribution given in Fig. 6. At 29% tablet porosity a much wider pore size distribution is exhibited by tablets prepared from coarse granules slugged at 270 MNm^{-2}. A fifth of the void space exists as pores greater than 27·0 μm, whereas the comparable figure for the tablets of wet granulated material is only 9·8 μm. The position is reversed at 15% porosity where the respective values are 0·63 and 1·2 μm. The pore size distribution of tablets made from dry granulated material is then only slightly different from tablets prepared from the ungranulated powder.

Decrease in granule size, or slugging pressure, reduces the influence of the dry granulation process on the pore structure of a tablet. The simultaneous operation of both factors yields tablets with permeabilities little different to compressed powder (Fig. 5). In contrast the permeability of tablets made from the wet granulated fine materials is some four times higher than tablets of ungranulated powder at the highest tabletting pressures used.

On this evidence the influence of granulation by slugging on the pore structure of tablets is destroyed by high tabletting pressures. Granules formed by wet granulation, on the other hand, seem more robust and the influence of granulation in promoting a coarser, wider pore size distribution persists to the highest tabletting pressures used. These conclusions are reached despite the wider variations possible in the conditions of dry granulation. Granulation pressures are only limited by the mechanical aspects of the compressors and, in this study, very high pressures were used. On the other hand, critical limits are placed on the conditions of wet granulation to ensure satisfactory performance during forced screening.

Pore size distribution influences the penetration of a wetting liquid into a tablet. Despite the lower suction potential of a coarse capillary, the rate of advance of a liquid is higher (Carman, 1941). The contribution of such capillaries should give a higher overall penetration rate for structures of wide pore size distributions. Uptake of cyclohexane is not, however, enhanced by formulation variables such as granule size or granule strength which widen pore size distribution (Figs 3 and 4). This may be explained by uneven penetration. A relatively coarse pore structure is produced by the interaction of high slugging pressure, coarse granules and low tabletting pressure. Rapid penetration of the largest capillaries isolates other areas of finer pore structure from which air cannot escape. These areas then make no contribution to the overall uptake of liquid. In tablets of narrower pore size distribution, although the rates of capillary penetration are lower, larger parts of the pore structure participate in liquid uptake. Such a concept is supported by the fraction of the pore space filled when penetration ceases; this falls as the pore size distribution widens. Higher final saturations are therefore found in dry granulated tablets (Table 3). Coarse granules formed at high slugging pressures give tablets of low final saturation when tabletting pressures are low. This provides an exception consistent with its

wide pore size distribution. With tablets prepared from granules made by slugging, the erosion of the coarse pore structure with increasing compression provides the high saturation values given in Table 2.

Acknowledgements

The authors would like to express their sincere thanks to Dr. H. Palmer of ICI Dyestuffs Division for his invaluable assistance. They gratefully acknowledge the financial support of the Science Research Council.

REFERENCES

CARMAN, P. C. (1941). *Soil Sci.*, **52**, 1–14.

GANDERTON, D. & SELKIRK, A. B. (1969). *Symposium on 'Powders', Society of Cosmetic Chemists of Great Britain.* Dublin, 1969.

GANDERTON, D. & SELKIRK, A. B. (1970). *J. Pharm. Pharmac.*, **22**, 345–353.

GRAY, W. A. (1968). *The Packing of Solid Particles.* London: Chapman and Hall.

HERSEY, J. A. (1965). *Rheol. Acta*, **4**, 235–239.

LEA, F. M. & NURSE, R. W. (1939). *J. Soc. chem. Ind.*, **58**, 277–283.

RAFF, A., ROBINSON, M. & SVEDRES, E. (1961). *J. pharm. Sci.*, **50**, 76–79.

RITTER, H. L. & DRAKE, L. G. (1945). *Ind. Engng Chem. analyt. Edn*, **17**, 782–786.

SHOTTON, E. & GANDERTON, D. (1960). *J. Pharm. Pharmac.*, **12** *Suppl.*, 87T–92T.

SOLVANG, S & FINHOLT, P. (1970). *J. pharm. Sci.*, **59**, 49–52.

J. Pharm. Pharmac., 1970, **22**, *Suppl.*, 95 S–103 S *Received March* 3, 1970

Some observations of the penetration and disruption of tablets by water

D. GANDERTON* AND D. R. FRASER

Department of Pharmaceutical Technology, University of Strathclyde, Glasgow, C.1, U.K.

The effect of compressibility, particle size, granulation and the addition of starch on the pore structure on tablets of aspirin, calcium carbonate, lactose, magnesium carbonate, phenindione and sucrose has been measured using air permeability and liquid penetration techniques. The addition of starch to the various materials produced no significant effect on the pore structure of the dry tablet but caused disruption and alteration of this structure when the tablet was penetrated by water. This disruptive effect produced by starch depends on the compressibility of the constituent material and the pressure used to form the tablet.

The aim of the tablet formulator is to produce a hard tablet which, when ingested, disintegrates to give a particulate system of similar size distribution to the original powder blend before processing. Such disintegration is achieved by penetration of the strong compact by gastric fluids and by the disruption of the bonds which unite it.

The rate of penetration of liquid into the tablet is determined by the balance of the capillary forces promoting movement of fluid towards the interior, and the viscous forces opposing it. Since the latter increase with penetration whereas the former remain reasonably constant, penetration rate into a tablet that retains its overall structure during penetration, will fall as saturation proceeds. When disruption of a tablet occurs, an increased rate of penetration is achieved because the viscous forces acting along the disrupted pore system are reduced while capillary forces remain unchanged. This arises since the curvature of the meniscus of the advancing liquid, on which capillary activity depends, is determined by the dry undisrupted pore system.

Although the extent to which the balance between capillary and viscous forces is influenced both by the physical properties of the liquid and the pore structure of the tablet, pore structure is the only factor which the tablet formulator can control. This paper reports a quantitative examination of some of the variables in formulation which may influence pore structure. The factors investigated here include the effect of tabletting pressure, differences in the compressibility of the materials comprising the tablet, the particle-size distribution of the powders and the granulation process.

EXPERIMENTAL

Materials and granulation

Aspirin was used in three forms: fine powder, coarse crystals, and granules prepared by massing fine powder with absolute ethanol (31·5% by weight).

Calcium phosphate was used as fine powder and as granules prepared by massing with 10% dextrose solution (50% by weight).

*Present address: ICI Pharmaceuticals Division, Alderley Park, Cheshire.

Lactose was studied in the form of coarse powder, fine powder, and granules prepared by massing the coarse powder with water (20% by weight).

Magnesium carbonate was used as coarse powder, fine powder, and as granules prepared by massing the fine powder with a 10% gum acacia solution (45% by weight).

Phenindione was studied in three forms: coarse crystals, fine powder, and as granules prepared by massing the fine powder with 10% dextrose solution (70% by weight).

Sucrose was examined as fine powder and as granules prepared by massing with water (8% by weight).

All granular materials were screened and those fractions passing a 16 mesh sieve but retained on a 22 mesh sieve were selected for study.

Granules of the above materials were also prepared including, before massing, 10% by weight of potato starch. A proportionately larger quantity of binding solution was used.

Particle-size analysis

The particle-size distributions of sucrose, fine lactose, potato starch and fine aspirin powders were measured by microscope, those of fine phenindione and fine and coarse magnesium carbonate powders by Coulter Counter and the sizing of coarse lactose, coarse aspirin and coarse phenindione powders was by sieving.

Compression

A weighed quantity of material was placed in a lubricated die, sealed at one end by a spigot. The upper punch was inserted and the assembly compressed over a pressure range of 12–300 MNm^{-2} between the platens of a hydraulic press. Compaction pressure was measured as described by Shotton & Ganderton (1960) by means of strain gauges affixed to the shank of the punch. The porosity at any given pressure was calculated from the weight and volume of the tablet whilst still in the die: the tablet was therefore under radial constraint when the measurements were taken. These conditions were reproduced in the permeability and penetration studies by testing the tablet in the die.

Permeability and penetration measurements

The permeability of the tablets to air was measured with an apparatus similar to that designed by Lea & Nurse (1939) and the permeability coefficient calculated was that defined by Ganderton & Selkirk (1970). The rate at which water penetrated the tablet was measured in an apparatus similar in design to that described by Ganderton & Selkirk (1970). The values quoted in Fig. 4 are those occurring when the liquid had penetrated 1 mm into the tablet.

RESULTS AND DISCUSSION

The pressure adopted for the manufacture of compressed tablets is usually determined by the strength of the tablet, its disintegration characteristics having been assessed during formulation. It is probable that common pressures are usually within the range 50–200 MNm^{-2}. The interaction of tabletting pressure with the other variables of formulation is therefore considered over this range.

PERMEABILITY STUDIES

Effect of compressibility

A comparison of the permeability and porosity of tablets made at the same compression is shown in Table 1. There are wide variations in both permeability and porosity factors and also in the compressibility of the powders, expressed in Fig. 1 as the relation between porosity and tabletting pressure. For example, the porosity of calcium phosphate compressed at 100 MNm^{-2} is over 42% whereas that of an aspirin tablet made at the same pressure is only 4·4%. Thus, in normal tabletting a large difference in porosity can be expected between a tablet containing a high proportion of an incompressible diluent and a tablet of a compressible drug.

Table 1. *Permeabilities and porosities of tablets compressed to* 100·0 MNm^{-2}

Material	Porosity (%)	Permeability (m^2)
Aspirin powder	4·4	$6·7 \times 10^{-15}$
Aspirin coarse powder	3·2	$6·4 \times 10^{-15}$
Aspirin granules	6·0	$6·6 \times 10^{-15}$
Calcium phosphate powder	42·0	$2·7 \times 10^{-14}$
Calcium phosphate granules	39·1	$2·4 \times 10^{-14}$
Lactose powder	15·9	$1·7 \times 10^{-13}$
Lactose coarse powder	11·6	$6·0 \times 10^{-13}$
Lactose granules	16·8	$3·3 \times 10^{-13}$
Magnesium carbonate fine powder	42·2	$1·1 \times 10^{-14}$
Magnesium carbonate coarse powder	39·6	$7·4 \times 10^{-14}$
Magnesium carbonate granules	36·4	$1·9 \times 10^{-13}$
Phenindione powder	8·2	$5·3 \times 10^{-15}$
Phenindione coarse powder	7·6	$7·4 \times 10^{-14}$
Phenindione granules	6·7	$4·2 \times 10^{-15}$
Sucrose powder	14·5	$1·6 \times 10^{-13}$
Sucrose granules	14·3	$3·1 \times 10^{-13}$

The effect of tabletting pressure on the permeability of tablets is given in Fig. 3. If tablets prepared from powders of the same particle size distribution are compressed at the same pressure, differences in permeability can be ascribed mainly to the compressibilities of the starting materials. The size distributions in Fig. 2 show that lactose can be compared with aspirin, and magnesium carbonate with phenindione. The results in Table 1 show that lactose, which is intermediate in compressibility, gives tablets 25 times more permeable than those of aspirin which is compressible. Comparison of the finer materials showed that magnesium carbonate, which is incompressible, was 13 times more permeable than phenindione.

Effect of particle size

The effect of particle size distribution on porosity and permeability was examined by comparing coarse and fine samples of the same material. Although tablets prepared from coarse powder were less porous, their permeabilities to air were greater, with the exception of aspirin. Tablets prepared from coarse phenindione powder were ten times more permeable than those compressed from the fine powder. The effect of particle size distribution on permeability was less marked with magnesium carbonate and lactose and was absent with aspirin.

Effect of granulation

Granulation of coarse magnesium carbonate powder increased the permeability coefficient of tablets prepared at 100 MNm^{-2} from $7·4 \times 10^{-14}$ to $1·84 \times 10^{-13} m^2$.

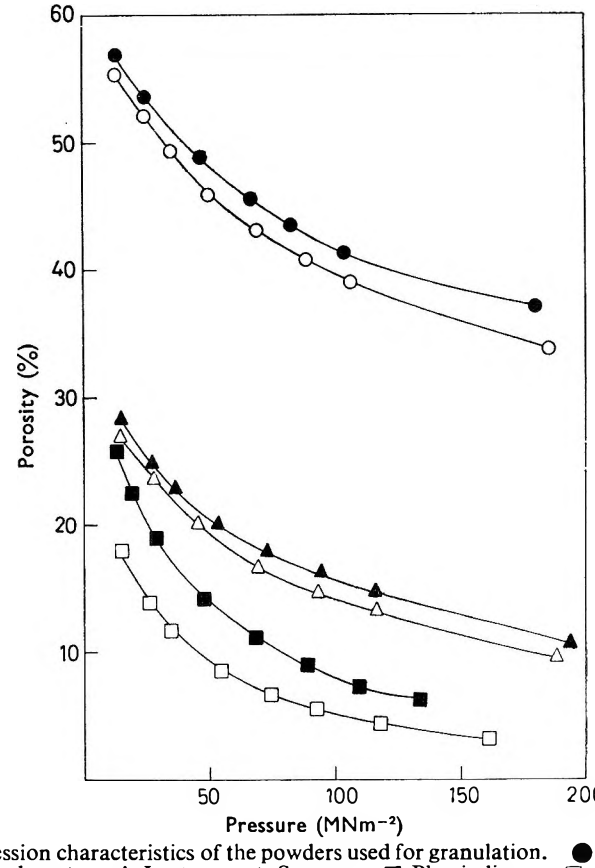

FIG. 1. Compression characteristics of the powders used for granulation. ● Calcium phosphate. ○ Magnesium carbonate. ▲ Lactose. △ Sucrose. ■ Phenindione. □ Aspirin.

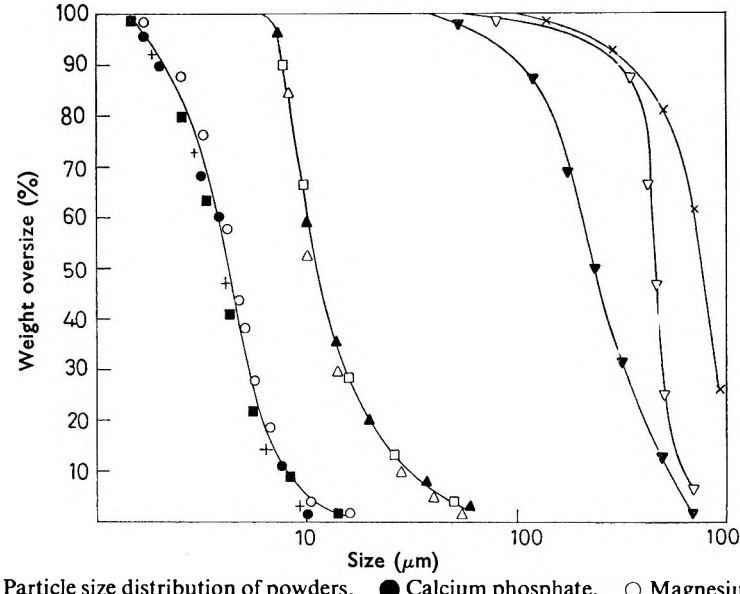

FIG. 2. Particle size distribution of powders. ● Calcium phosphate. ○ Magnesium carbonate. ▲ Lactose. △ Sucrose. ■ Phenindione. □ Aspirin. ▽ Potato starch. + Fine magnesium carbonate. × Coarse phenindione. ▼ Coarse aspirin.

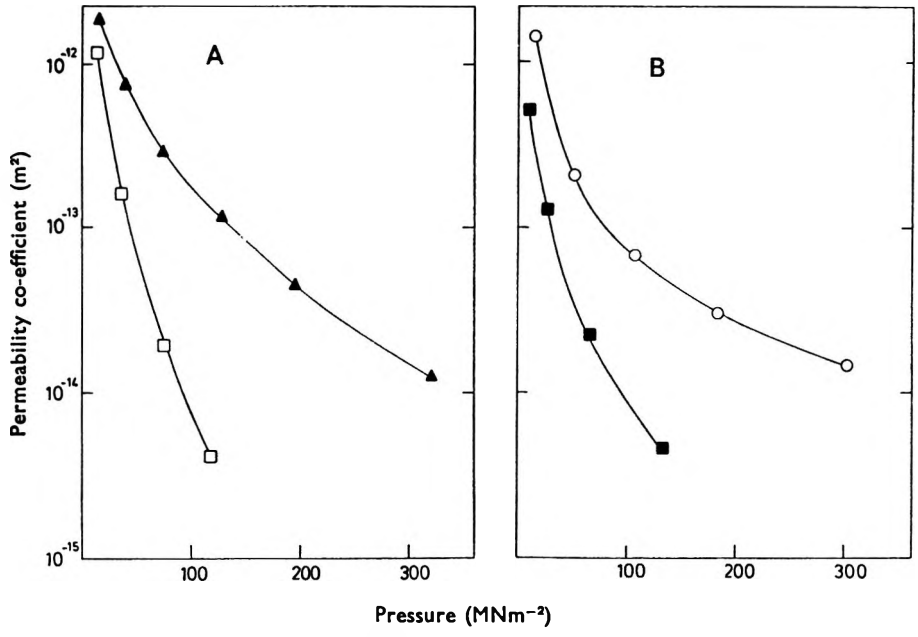

FIG. 3. The permeability-pressure relation of ungranulated powder. A. ▲ Lactose. □ Aspirin. B. ○ Magnesium carbonate. ■ Phenindione.

With sucrose and lactose, the increase in permeability with granulation was small. Granulation produced no effect with calcium phosphate, aspirin and phenindione. These differences are probably explained by the fact that the granulation techniques used produced hard gritty granules of magnesium carbonate, whereas granules of aspirin, phenindione and calcium phosphate were soft, reverting to powder when pressed with a spatula. Lactose and sucrose granules were of intermediate strength.

Effect of starch

Comparison of Tables 1 and 2 indicates that the effect of potato starch on the porosity and permeability of tablets is largely additive. Starch has the same compressibility as lactose and sucrose and when added to these materials its effect on the porosity of tablets compressed at 100 MNm^{-2} was negligible. The presence of starch in phenindione and aspirin tablets increased the porosity of tablets prepared at 100 MNm^{-2}. When mixed with the relatively incompressible calcium phosphate or magnesium carbonate the porosity of these tablets decreased.

Table 2. *Permeabilities and porosities of granules containing* 10% *potato starch compressed to* 100 MNm^{-2}

Material	Porosity (%)	Permeability (m^2)
Aspirin	6·6	$1·1 \times 10^{-14}$
Calcium phosphate	36·0	$2·9 \times 10^{-14}$
Lactose	16·3	$3·3 \times 10^{-13}$
Magnesium carbonate	33·4	$2·8 \times 10^{-13}$
Phenindione	8·1	$7·6 \times 10^{-15}$
Sucrose	14·7	$3·0 \times 10^{-13}$

The permeability of lactose and sucrose tablets containing starch was unaffected whereas tablets of all other materials showed a small increase in permeability consistent with the introduction of a component of much larger particle size.

Conclusions

The interaction of compressibility and particle size distribution has given permeability differences of over one hundred fold in tablets compressed at 100 MNm^{-2}. This indicates marked variation in the capillary network within the tablet. Compressible materials in fine particle form produced impermeable structures. The effect of granulation on pore structure is smaller and appears to be restricted to granules which strongly resist deformation. The introduction of up to 10% by weight of potato starch has only a small effect on the pore structure of a tablet.

THE EXTENT OF PENETRATION BY WATER

Compressibility and particle size distribution, which largely dominate gross variations in permeability have the same influence on rate of liquid penetration.

When comparative liquid penetration studies are made, factors in addition to those which determine pore structure of a dry tablet must be considered. Most important are the wettability of the tablet ingredients, and the varying degrees of disruption caused by the penetrating liquid. Nevertheless, the general form of the relation between penetration rate and tabletting pressure is similar to the permeability-pressure relation described by Fig. 3. The results, presented in Fig. 4, show that the rates of penetration for aspirin and phenindione, both of which give impermeable

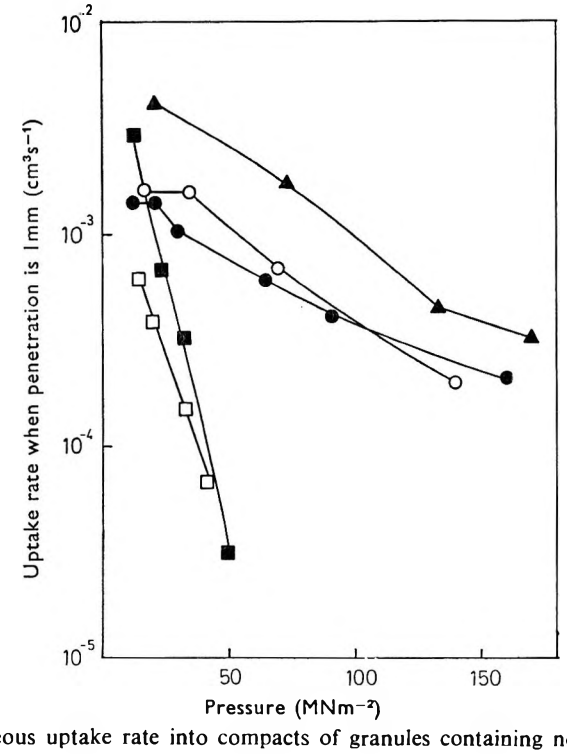

FIG. 4. The aqueous uptake rate into compacts of granules containing no starch when penetration is 1 mm.

tablets, declined rapidly becoming immeasurably slow for tablets compressed at 50 MNm^{-2}. Lactose which gave the most permeable tablets also had the highest penetration rate.

Differing wettability appears to play a subordinate role in liquid penetrability and this role cannot be precisely identified from these experiments. Contamination of the powders by granulation fluids would probably reduce differences in the wettability of the powders used in this study.

Disruption by an aqueous penetrant occurs only with calcium phosphate and magnesium carbonate tablets produced at low pressure. Increase of tabletting pressure had a small effect on the penetration rate of tablets of all materials even though the marked reduction in permeability, shown in Fig. 3, indicated large changes in pore structure. Tablets prepared at pressures up to 50 MNm^{-2} showed softening of the wetted portion so that viscous resistance to penetration was never fully developed.

At pressures above 50 MNm^{-2}, tablets of calcium phosphate and magnesium carbonate retained their shape during liquid penetration and further increase in pressure gave a commensurate decrease in penetrability. All tablets prepared from granules of lactose, aspirin and phenindione retained their shape after penetration by water. A decrease in penetrability was therefore observed over the entire pressure range studied.

Effect of starch

Starch, which produces only small effects on pore structures, profoundly affected penetration rate. For example, addition of starch to lactose affected neither porosity nor permeability of the tablet produced at 100 MNm^{-2}. The effect on aqueous penetration is, however, dramatic. As shown in Fig. 5, the initial phase of penetration is similar in form to that of lactose without starch—although somewhat faster. This is followed by a period in which wetting of the starch–lactose tablet is almost instantaneous. Viscous resistance to penetration disappeared as the result of tablet collapse. Severe and sometimes explosive disintegration occurred with all materials to give the increased penetration rates reported in Table 3.

The actual mechanism by which starch acts as a disintegrant has long been the subject of dispute. Two theories, disruption by swelling (Patel & Hopponen, 1966), and the formation of a capillary network (Curlin, 1955) that accelerates the wetting of a tablet, have been proposed. The rate of penetration of water into lightly compressed tablets of phenindione (Fig. 6), is only slightly increased by the inclusion of starch. This is commensurate with the small increase in the permeability coefficient which starch produces. Thus, evidence of a significant change due to the formation of a capillary network of different wettability is lacking. In the absence of starch, further compression only decreased the rate of saturation of the pore network by water (Fig. 6A). When the phenindione tablets contained starch (Fig. 6B), the changing form of the saturation curve indicated that disruption became more pronounced as tabletting pressure increased. After a period of slow penetration, relatively high rates of saturation were observed even in tablets produced at a pressure of 75 MNm^{-2}, but at 100 MNm^{-2}, saturation rates became slow again and the degree of tablet disruption decreased.

The failure of starch to disrupt tablets that had been lightly compressed (15 MNm^{-2}) was also observed with lactose and aspirin during the penetration test. Magnesium

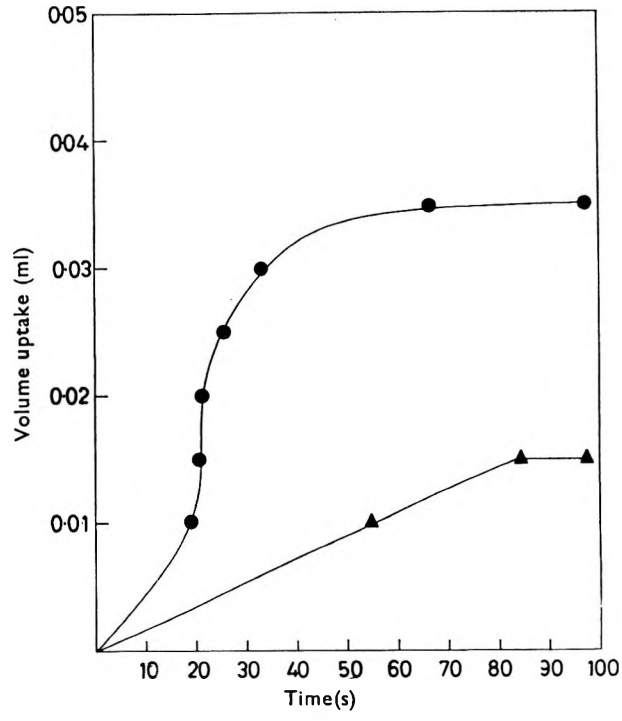

FIG. 5. Aqueous penetration of lactose tablets prepared from granules compressed to a porosity of 10%. ● 10% potato starch. ▲ No starch.

carbonate and calcium phosphate, on the other hand, slowly collapsed. At higher pressures, i.e. 75 MNm^{-2}, the pattern of aqueous penetration of all tablets showed the same dependence on tabletting pressure as that of phenindione. The observation that starch does not fully exert its disruptive capacity in tablets produced at low pressure is in accordance with the explanation of its effect by a swelling mechanism since swelling would be more effective in rigid tablets of low porosity. However the penetration rates given in Table 3 show that the effect of starch is much modified by the structure of the tablet. Phenindione which, in the absence of starch, was the least permeable and most slowly penetrated tablet, retained these characteristics when starch was added. Lactose, in the absence of starch, was most permeable and the most rapidly penetrated tablet on addition of starch. Of the other materials, starch was more disruptive in aspirin tablets than in tablets of calcium phosphate.

Table 3. *Times for 30% saturation of tablets prepared from granules compressed to* 100 MNm^{-2}

Material	Time (s)	
	Without starch	With starch
Aspirin	300	14
Calcium phosphate ..	52	20
Lactose..	26	10
Magnesium carbonate	80	30
Phenindione	600	215

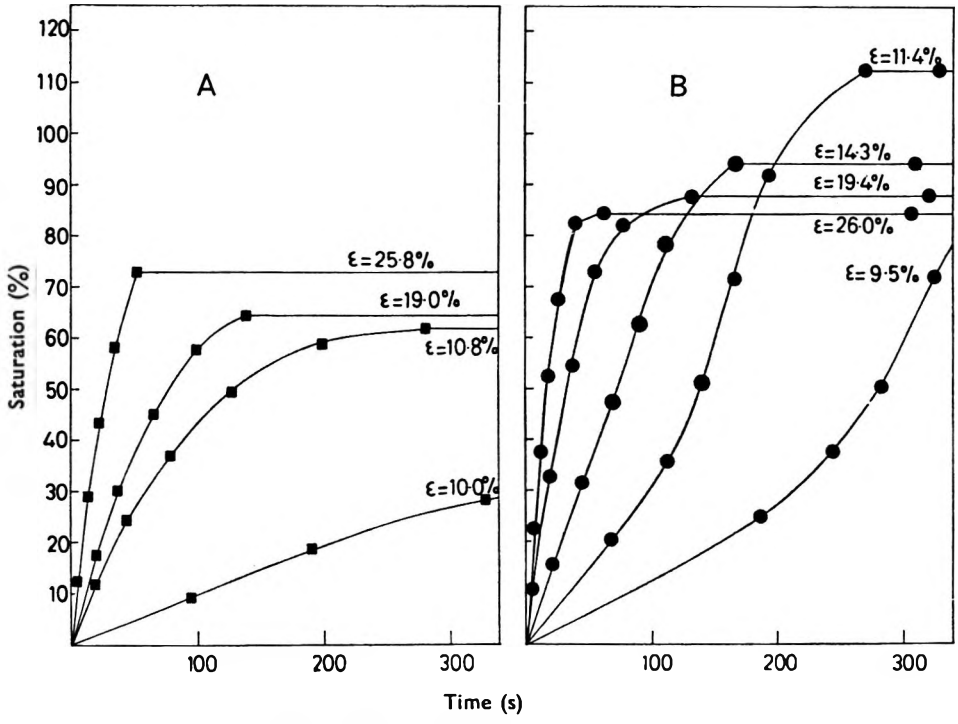

FIG. 6. Saturation of phenindione tablets prepared from granules. A. ■ No starch. B. ● 10% potato starch. (ε = tablet porosity)

The factors that determine tablet structure do not therefore entirely determine the aqueous penetration of a porous system which is being disrupted. It is probable that when starch is present the extent of bonding will also influence the susceptibility of the tablet to break-up when water causes the starch grains to swell.

Acknowledgements

The authors gratefully acknowledge the financial assistance of the Science Research Council.

REFERENCES

CURLIN, L. C. (1955). *J. Am. pharm. Ass.* (*Sci. Edn*), **44**, 16.
GANDERTON, D. & SELKIRK, A. B. (1970). *J. Pharm. Pharmac.*, **22**, 345–353.
LEA, F. M. & NURSE, R. W. (1939). *J. Soc. chem. Ind. Lond.*, **58**, 277–283.
PATEL, N. R. & HOPPONEN, R. E. (1966). *J. pharm. Sci.*, **55**, 1065–1068.
SHOTTON, E. & GANDERTON, D. (1960). *J. Pharm. Pharmac.*, **12**, *Suppl.*, 87T–92T.

J. Pharm. Pharmac., 1970, **22**, *Suppl.*, 104 S–108 S *Received February* 2, 1970

The effect of temperature on the solubilities of testosterone propionate in low polarity solvents

D. B. BOWEN* AND K. C. JAMES

Welsh School of Pharmacy, University of Wales Institute of Science and Technology, Cathays Park, Cardiff, U.K.

The solubilities of testosterone propionate have been determined between 25 and 100° in 15 solvents and compared with theoretical values obtained from regular solution theory. Entropy considerations show that solvent-solute interactions occur in some solvents, increasing the solubility and resulting in deviations from regular solution behaviour. "Regular solutions" are obtained only in saturated hydrocarbon solvents, and the solubility is more accurately predicted as the temperature approaches the melting point, and as the molar volumes of solvent approach that of the solute.

It is seldom possible to predict the extent to which a particular solute will dissolve in a particular solvent. Regular solutions (Hildebrand & Scott, 1962) are an exception. In these, the mol fraction solubility (x_2) of a solid solute can be calculated from the equation,

$$-\ln x_2 = \frac{\Delta H^F}{R}\left[\frac{T_M - T}{T_M T}\right] + \frac{V_2 \phi_1^2}{RT}(\delta_1 - \delta_2)^2 \quad \ldots \quad \ldots \quad (1)$$

The first term represents ideal solubility, and is derived from a consideration of the energy required to liquify the solid at temperature T. ΔH^F is the heat of fusion and T_M the melting point; V_2 the molar volume of the solute and ϕ_1 the volume fraction of the solvent. The second term represents the heat of mixing which is assessed in terms of the solubility parameters, δ_1 and δ_2, the square roots of the cohesive energy densities of solvent and solute respectively. Expansion of the squared term thus gives the sum of the cohesive energy densities of solvent and solute minus twice their geometric mean, which is placed equal to the energy gained in bringing the unlike molecules into contact.

The use of equation (1), in an attempt to predict the solubilities of the lower testosterone esters (James & Roberts, 1968), led to poor agreement between experimental and predicted results and it was suggested that this was due either to the method of obtaining ΔH^F, or to the large difference between molar volumes of solute and solvent preventing random distribution. It has already been shown (Bowen & James, 1968) that the former was not the cause of the discrepancy and the second hypothesis is tested in this paper by measuring solubilities in a larger number of solvents and over a range of temperatures.

* Present address, Imperial Chemical Industries Ltd., Hurdsfield Industrial Estate, Macclesfield, Cheshire, SK10 2NA, U.K.

EXPERIMENTAL

Testosterone propionate, a gift from Organon Laboratories Ltd, was used without further purification. Organic solvents were fractionally distilled and their purities checked by refractive index and density determinations.

Determination of solubilities. Solubilities below 60° were determined by the U tube method (James & Roberts, 1968) and at higher temperatures by the capillary tube method (Bowen & James, 1968).

At the lower end of the temperature range 40–70° many solubilities could not be determined by the capillary tube method because of slow rates of solution and the U-tube method was unsuitable at the higher end of the range because of the volatility of the solvents. Extrapolation of results from one method formed a continuous line with the others.

DISCUSSION

Provided the solution is dilute, or the solubility parameters of solute and solvent are similar, the entropy change of a solid forming a regular solution in a liquid is given by

$$\bar{S} - S^s = \frac{R.\, d\ln x_2}{d\ln T} \qquad (2)$$

(Hildebrand, 1952), where x_2 represents mol fraction solubility at temperature T. S^s is the entropy of the solid solute and $\bar{S}$ the partial entropy of the solute in solution. $\bar{S} - S^s$ is therefore the sum of the entropies of fusion and dilution. Entropies of solution of testosterone propionate were investigated by plotting log mol fraction solubility against log temperature. Two types of behaviour were observed; entropies of solution were independent of temperature with the aliphatic hydrocarbons, but increased with increasing temperature with the other solvents. Typical plots are shown in Fig. 1. Entropies of solution were obtained from the slopes of the straight lines, or from the tangents to the curves at the temperatures of interest.

The theoretical entropy change on dispersing a liquid solute in a solvent is given by

$$\bar{S} - S^\circ = -R \ln x_2 \qquad (3)$$

derived from a consideration of the number of possible configurations in a random distribution. S° is the entropy of the liquid solute, so that $\bar{S} - S^\circ$ represents the entropy of dilution.

The effects of molar volumes on entropies of solution were tested by plotting entropies obtained from equation (2) against those calculated from equation (3). A typical result is shown in Fig. 2, the points were widely scattered and regression analysis gave low correlation coefficients and negative intercepts on the $d\log x_2/d\log T$ axis, indicating negative entropies of fusion. In contrast, the points for the saturated aliphatic hydrocarbons gave good straight line plots, extrapolating to positive entropies of fusion, which agreed reasonably well with those obtained calorimetrically.

A similar situation has been observed by Hildebrand & Glew (1956), who determined the entropies of solution of iodine in a series of solvents. Their line, corresponding to that of the saturated hydrocarbon solvents in Fig. 2, was followed by the violet iodine solutions, which are known to be regular. All their other points lay below this line, and represented brown solutions, in which iodine is known to be

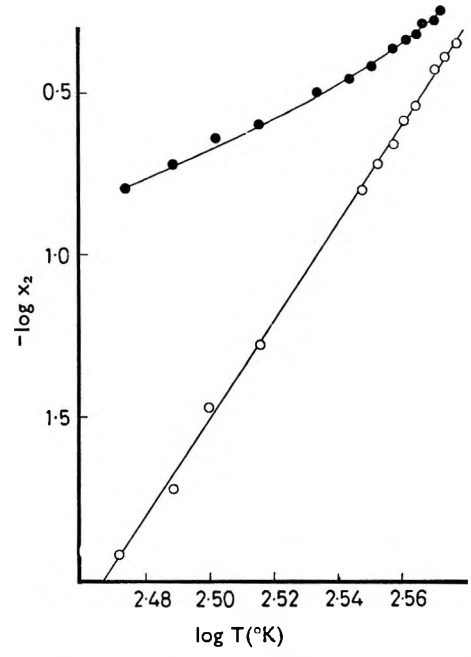

FIG. 1. Determination of entropies of solution: ○ cyclohexane; ● carbon tetrachloride.

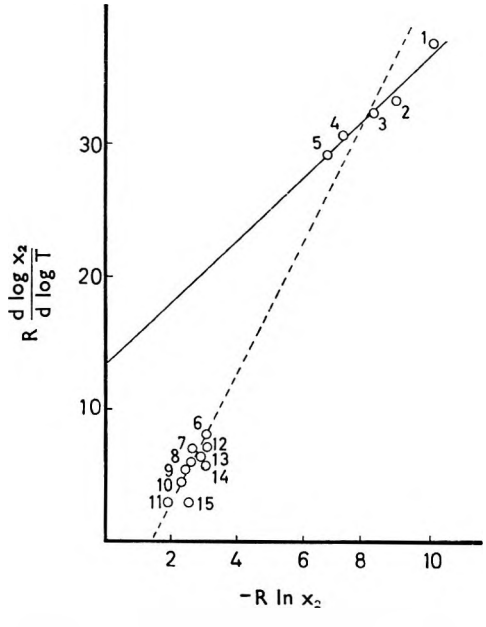

FIG. 2. Entropies of soln of testosterone propionate at 40°; 1, n-pentane (116); 2, n-hexane (132); 3, cyclopentane (95); 4, cyclohexane (109); 5, decalin (153); 6, carbon tetrachloride; 7, nitrobenzene; 8, benzene; 9, 1,2-dichloroethane; 10, *cis*- and *trans*-1,2-dichloroethylene; 11, chloroform; 12, carbon disulphide; 13, tetralin; 14, toluene; 15, chlorobenzene. - - - Regression on all points. — Regression on saturated hydrocarbons only. Figures in brackets are molar volumes.

complexed. Analogy suggests that the saturated hydrocarbon solutions of testosterone propionate are regular and that the diminished entropy in the other solvents may be due to complex formation.

The order in which the saturated aliphatic hydrocarbon solvents occur on their regression line was independent of molar volume, indicating that entropy of solution is not related to the relative molar volumes of solute and solvent and that random distribution is not prevented when the steroid molecules are much larger than those of the solvent.

The variation in observed solubility, as a function of calculated regular solubility, with temperature is shown in Fig. 3. Calculated solubilities were obtained using the integrated heat of fusion. This method appeared to be the better method for calculating regular solubilities since it gave straight lines or smooth curves, whereas the plots using mean heats of fusion were irregular. In all the solvents examined the experimental values approached the calculated values as the temperature increased. The solvents could be divided into the same two groups, in one group the ratio of experimental solubility to calculated solubility increased linearly with temperature, and in the other the ratio decreased uniformly, but not linearly with increasing temperature.

Although the entropy results indicate that the solvents in the first of the above groups form regular solutions of testosterone propionate, this appears to be contradicted by the fact that the observed solubilities are lower than those anticipated for regular solutions. Hiraoko & Hildebrand (1963) demonstrated that solvents containing substituted methyl groups did not obey the normal linear relation when mol fraction solubilities of iodine were plotted against the square of solubility parameter differences. Shinoda & Hildebrand (1965) showed that the solutions gave regular entropy plots and concluded that the solubility parameter did not give a correct measure of attractive forces between the iodine and the methyl groups, the geometric mean being too high an estimate of the intermolecular attraction between solute molecules and solvent molecules. It is probable that, in solutions which otherwise behave regularly, the solubilities of testosterone propionate are low for the same reason. When the molar volume of the solvent is significantly less than that of testosterone propionate, solvent molecules will be unable to approach solute molecules as closely as their own kind. The result will be a lower cohesive energy between solute and solvent than predicted by the geometric mean assumption, and a lower solubility than anticipated. This difference will diminish as the molar volume of the solvent approaches that of the solute, the geometric mean will become a better estimate of cohesive energy between solvent and solute and the observed solubility will approach the calculated value. Fig. 3 illustrates this because the straight lines occur in order of solvent molar volume. A similar argument can be advanced for the effect of temperature on the regular solutions, shown in Fig. 3. Translational molecular motion increases with temperature and opposes close molecular packing. Steric effects therefore become less important as the temperature increases, with a resulting increase in the reliability of the geometric mean and in the observed solubility.

It has been suggested that the entropy results indicate complexation between the solvents of the second group and testosterone propionate. Complexation affects the geometric mean in the opposite way to that outlined above. Attractive forces between unlike molecules are now greater than those between like molecules, and the cohesive energy is greater than that given by the geometric mean. The result is

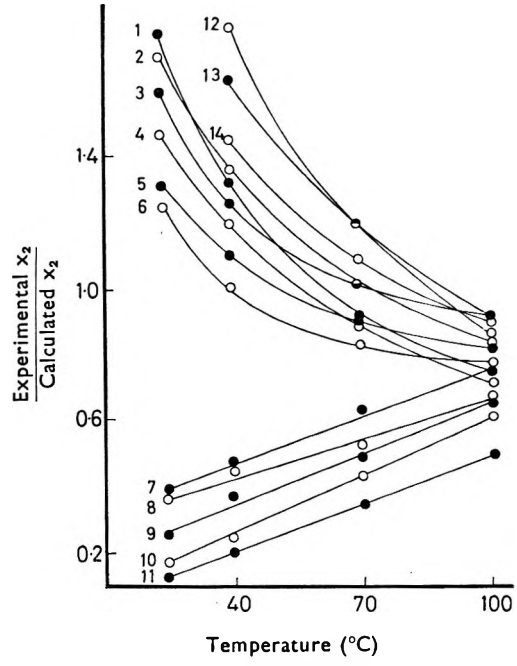

FIG. 3. Variation of experimental/calculated solubilities of testosterone propionate with temperature; 1, chlorobenzene; 2, benzene; 3, nitrobenzene; 4, tetralin; 5, carbon tetrachloride; 6, carbon disulphide; 7, decalin (153); 8, n-hexane (132); 9, n-pentane (116); 10, cyclohexane (109); 11, cyclopentane (95); 12, chloroform; 13, *cis*- and *trans*-1,2-dichloroethylene; 14, 1,2-dichloroethane. Figures in brackets are molar volumes.

that the solubilities are higher than those calculated for regular solutions, as is shown in Fig. 3. Complexation would be expected to decrease with increasing temperature, accounting for the fall in solubility observed in Fig. 3.

Acknowledgements

We are grateful to the Science Research Council for a grant to D.B.B. and to Organon Laboratories Ltd., for the gift of testosterone propionate.

REFERENCES

BOWEN, D. B. & JAMES, K. C. (1968). *J. Pharm. Pharmac.*, **20**, 104S–107S.
HILDEBRAND, J. H. (1952). *J. chem. Phys.*, **20**, 190–191.
HILDEBRAND, J. H. & SCOTT, R. L. (1962). *Regular Solutions*, New Jersey: Prentice-Hall Inc.
HILDEBRAND, J. H. & GLEW, D. N. (1952). *J. chem. Phys.*, **20**, 1522–1524.
HIRAOKO, H. & HILDEBRAND, J. H. (1963). *J. phys. Chem.*, **67**, 916–918.
JAMES, K. C. & ROBERTS, M. (1968). *J. Pharm. Pharmac.*, **20**, 709–714.
SHINODA, K. & HILDEBRAND, J. H. (1965). *J. phys. Chem.*, **69**, 605–608.

J. Pharm. Pharmac., 1970, **22**, *Suppl.*, 109 S–113 S *Received March* 11, 1970

An infrared study of solute-solvent interactions of testosterone propionate

K. C. JAMES AND P. R. NOYCE

Welsh School of Pharmacy, University of Wales Institute of Science and Technology, Cathays Park, Cardiff, U.K.

Interactions between testosterone propionate and 10 different organic solvents have been investigated by observing the shifts of the stretching frequencies of the ketone and ester carbonyl groups. The shifts are shown to be approximately proportional to the degree of deviation from regular solution behaviour. The solvents are classified into three groups and the possible interactions in each discussed.

In a study of the solubilities of testosterone propionate in various solvents (Bowen & James, 1970), a plot of the ratios of experimental to calculated solubilities against temperature indicated that the solvents fell into two different groups. The difference between these groups was accounted for in terms of entropy, from which a postulate was made that specific solute-solvent interactions occurred in one of the groups. We have used infrared spectroscopy to investigate these interactions since the shifts in frequency of a particular group vibration are indicative of the energy changes occurring when that group interacts with another (Badger & Bauer, 1937; Searles, Tamres & Barrow, 1953). In testosterone propionate the reactive groups are the Δ^4-3-ketone and the ester carbonyl on the 17β-side chain; the stretching bands ($\nu_{C:O}$) of these dipoles have been examined by scanning in the 1770–1650 cm^{-1} region.

EXPERIMENTAL

Testosterone propionate was a gift from Organon Laboratories Ltd. *cis*- and *trans*-1,2-Dichloroethylenes were Eastman Kodak solvents, other substances were obtained from British Drug Houses Ltd. Solvents were dried over either sodium or anhydrous calcium chloride and those below 99·0% purity were fractionally distilled. Spectra were run on a Perkin-Elmer 521 grating spectrophotometer, using a linear scale expanded by a factor of 10. On over 80 preliminary measurements made to test reproducibility not one determination varied from the mean by more than $\pm 0{\cdot}5$ cm^{-1}. Sodium chloride cells (0·1 mm) were used with cyclohexane placed in the reference beam.

Binary solvent systems were selected to give a complete concentration range of each component solvent from pure cyclohexane to the pure solvent under investigation. Each sample was 0·12M with respect to testosterone propionate and was prepared by weighing into a 5 ml ampoule, which was sealed immediately to prevent evaporation of volatile components.

RESULTS AND DISCUSSION

The shift in frequency of a particular vibration upon a change of environment has led to various theories, for example, Kirkwood (see West & Edwards, 1937), Bauer & Magat (1938) and Buckingham (1958). As a measure of the shift these workers

used the difference between the frequency of the vibration in the vapour state and that in a solution of the solvent being examined. It has been suggested by Horak & Plíva (1965) that to compare the frequency of a particular group in a non-polar solvent with that in a polar one is of doubtful validity, since the interactions involved are different. Having studied the solvent effect of some saturated hydrocarbons on the respective carbonyl stretching bands of testosterone propionate under high resolution and found no observable shift, we decided to adopt cyclohexane as an arbitrary standard; the shift $\Delta\nu_{C:O}$ then represents the parameter ($\nu_{cyclohexane} - \nu_{solvent}$). The frequencies of both the conjugated ketone and the ester groups in various solvents, together with the respective shifts are in Tables 1 and 2.

Table 1. *Effect of solvents on* Δ^4*-3-ketone group stretching frequency*

Solvent	Frequency of peak in pure solvent (cm^{-1})	Shift (cm^{-1})	Number of complexes	Isosbestic points (cm^{-1})
Chloroform	1662·1	21·8	2	1682·0 1676·5
trans-1,2-Dichloroethylene ..	1667·0	16·9	1	1682·5
cis-1,2-Dichloroethylene ..	1668·0	15·9	1	1681·7
1,2-Dichloroethane	1668·5	15·4	2	1681·9 1676·6
Nitrobenzene	1673·5	10·4	1	1681·8
Chlorobenzene	1677·0	6·9	1	1681·8
Benzene	1678·6	5·3	1	1682·2
Toluene	1679·4	4·5	1	1682·0
Carbon disulphide	1678·9	5·0	—	—
Carbon tetrachloride	1679·8	4·1	—	—

Table 2. *Effect of solvents on* 17β*-ester group stretching frequency*

Solvent	Frequency of peak in pure solvent (cm^{-1})	Shift (cm^{-1})	Number of complexes	Isosbestic points (cm^{-1})
Chloroform	1727·8	17·8	1	1739·8
cis-1,2-Dichloroethylene ..	1729·8	15·8	1	1741·4
1,2-Dichloroethane	1730·2	15·4	1	1741·4
trans-1,2-Dichloroethylene ..	1732·2	13·4	1	1741·4
Nitrobenzene	1731·7	13·9	1	1742·4
Chlorobenzene	1733·5	12·1	1	1742·0
Benzene	1737·6	8·0	1	1742·0
Toluene	1738·7	6·9	1	1742·7
Carbon disulphide	1738·7	6·9	—	—
Carbon tetrachloride	1738·8	6·8	—	—

Earlier work on ketones (Whetsel & Kagarise, 1962) had demonstrated that proton-donating solvents, such as chloroform, may form hydrogen bonds with a carbonyl group. We investigated chloroform, using a similar technique of ternary systems in which the polar solvent progressively replaces cyclohexane (James & Noyce, 1970). We have now extended the study to other solvents. The position of the isosbestic points and the number of specific complexes proposed are in Tables 1 and 2.

The solubility of a substance depends largely on the type and magnitude of its interactions with the solvent. These interactions affect the bond strength within the dipolar moiety involved, which is expressed as a decrease in the force constant

characterized by a spectral shift of the group vibration under consideration. We have inferred from our results that the intermolecular forces acting on both the ester group and the Δ^4-3-ketone are similar in type and magnitude. Since the relative contributions of the groups to the total interacting potential of the steroid molecule could not be ascertained, the shifts of the two groups were added together and plotted against the ratio of the experimental to the calculated solubility for each solvent in an attempt to correlate spectral data with solubility (Fig. 1). The graph suggests a correlation and shows that three distinct groups of solvents are discernible: partially chlorinated hydrocarbons, aromatics and completely substituted derivatives of methane.

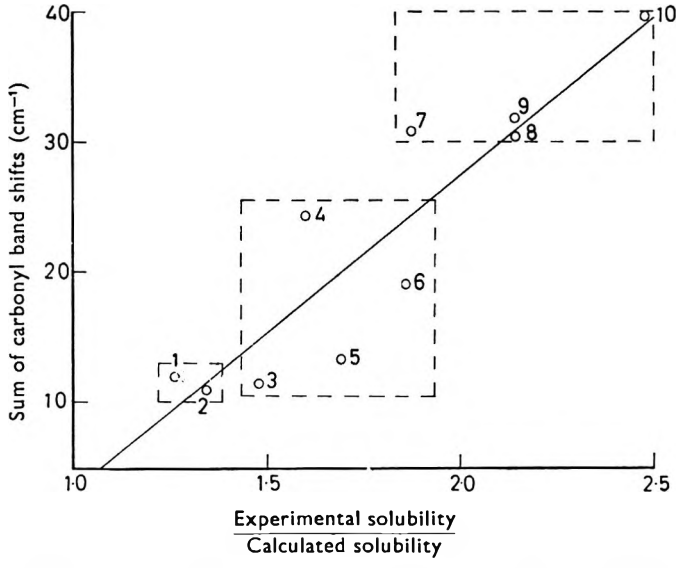

FIG. 1. Correlation between solubility and spectral shift. 1. Carbon disulphide. 2. Carbon tetrachloride. 3. Toluene. 4. Nitrobenzene. 5. Benzene. 6. Chlorobenzene. 7. 1,2-Dichloroethane. 8. *trans*-1,2-Dichloroethylene. 9. *cis*-1,2-Dichloroethylene. 10. Chloroform. All shifts are the mean of three results. Solubility data are from Bowen (1969).

The chlorinated hydrocarbons as a group are responsible for the largest spectral shifts. The formation of hydrogen bonds between chloroform and testosterone propionate has already been demonstrated (James & Noyce, 1970) and we consider that the enhanced solubility in these solvents is due to association in this way. This idea is supported by the formation of isosbestic points (Cohen & Fischer, 1962) in both ester and conjugated ketone bands when the environments of the groups are changed stepwise from completely non-polar to the pure solvent. The simultaneous increase in the breadth of the bands further corroborates the postulate; this is a characteristic of associated species. These spectral modifications are shown in Fig. 2.

With aromatic solvents, specific interactions again occur between solute and solvent since isosbestic points are formed. The carbonyl vibrational bands are modified slightly (Fig. 3) with a smaller increase in bandwidth and a lower value of $\Delta\nu_{C:O}$ than in the halogenated aliphatic solvents, thus indicating that the interaction is weaker. It therefore follows that the solubilities of testosterone propionate in these solvents should be lower than in the first group, and this is borne out by the experimental results.

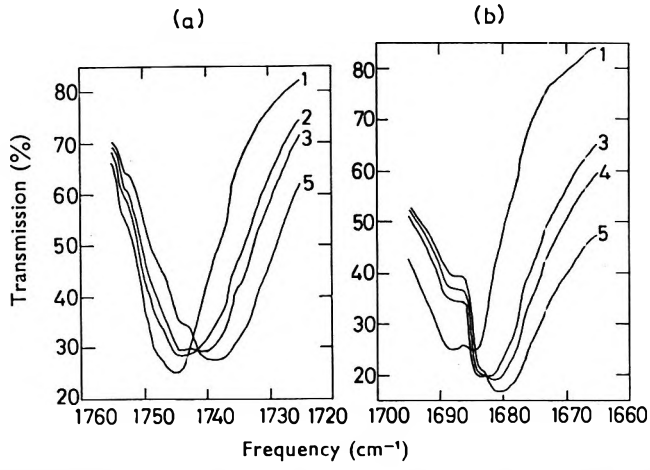

FIG. 2. Carbonyl stretching bands of (a) 17β-ester group, and (b) Δ^4-3-ketone group in *trans*-1,2-dichloroethylene-cyclohexane solvent systems. Molar ratio *trans*-1,2-dichloroethylene–testosterone propionate. 1. 0 (pure cyclohexane solvent). 2. 10·3. 3. 15·5. 4. 20·6. 5. 30·9.

Since the π-electron cloud of an aromatic compound is the probable area of interaction, hydrogen bonding is unlikely as both the π-cloud and the carbonyl oxygen are proton accepting. Laszlo & Williams (1966) and Williams & Wilson (1966), in their nuclear magnetic resonance studies of steroids in benzene and toluene, calculated that a collision complex in which the plane of the aromatic solvent was at right angles to that of the steroid, could account for their observed shifts. This mode of interaction has recently been questioned (Baker & Wilson, 1970). Our results indicate that interaction between the π-electrons and a positive centre in the steroid is unlikely because the shifts are in inverse order to the electron densities on the aromatic nuclei.

By the measurement of band widths it has previously been established that weak,

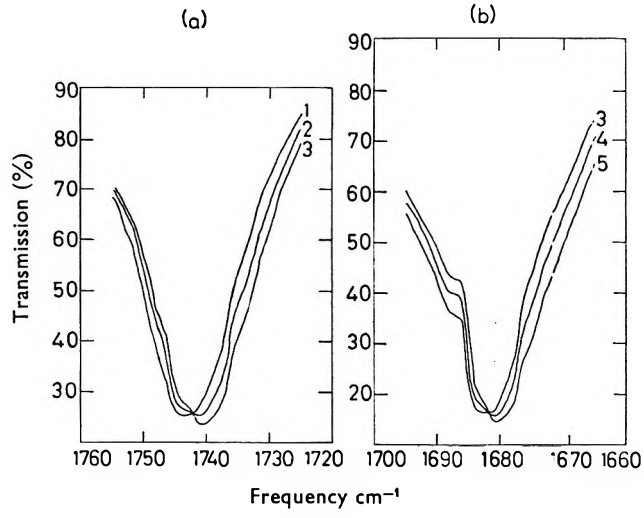

FIG. 3. Carbonyl stretching bands of (a) 17β-ester group and (b) Δ^4-3-ketone group in benzene-cyclohexane solvent systems. Molar ratio benzene–testosterone propionate. 1. 25·6. 2. 38·4. 3. 51·2. 4. 63·9. 5. 76·7.

but specific, interactions occur between carbonyl groups and carbon tetrachloride (Whetsel & Kagarise, 1962). The weak nature is further emphasized by the absence of isosbestic points (Fig. 4). In considering the characteristics of the carbonyl

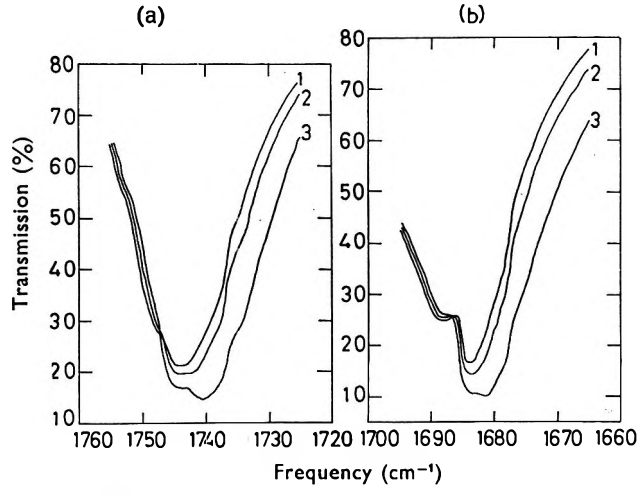

FIG. 4. Carbonyl stretching bands of (a) 17β-ester group and (b) Δ^4-3-ketone group in carbon tetrachloride–cyclohexane solvent systems. Molar ratio carbon tetrachloride–testosterone propionate. 1. 19·5. 2. 26·0. 3. 39·0.

vibrations in carbon disulphide, we assume that similar forces are involved to those in carbon tetrachloride, although in accordance with the suggestions of Caldow & Thomson (1960) bulk dielectric effects may contribute to the change in $\nu_{C:O}$ in moving from carbon disulphide to carbon tetrachloride.

Acknowledgements

We thank Mr. A. Henson, Head of the Department of Applied Chemistry for the use of the spectrophotometer and his technical staff for assistance in its operation. One of us (P.R.N.) also acknowledges an award of a research studentship of the University of Wales.

REFERENCES

BADGER, R. M. & BAUER, S. M. (1937). *J. chem. Phys.*, **5**, 839–851.
BAKER, K. M. & WILSON, R. G. (1970). *J. chem. Soc.* (B), 236–239.
BAUER, E. & MAGAT, M. (1938). *J. Phys. Radium*, **9**, 319–330.
BOWEN, D. B. (1969). Ph.D. Thesis, University of Wales.
BOWEN, D. B. & JAMES, K. C. (1970). *J. Pharm. Pharmac.*, **22**, *Suppl.*, 104S–108S.
BUCKINGHAM, A. D. (1958). *Proc. Roy. Soc.*, A, **248**, 169–181.
CALDOW, G. L. & THOMPSON, H. W. (1960). *Ibid.*, A, **254**, 1–16.
COHEN, M. D. & FISCHER, E. (1962). *J. chem. Soc.*, 3044–3052.
HORAK, M. & PLÍVA, J. (1965). *Spectrochimica Acta*, **21**, 911–917.
JAMES, K. C. & NOYCE, P. R. (1971). *Ibid.*, In the press.
LASZLO, P. & WILLIAMS, D. H. (1966). *J. Am. chem. Soc.*, **88**, 2799–2802.
SEARLES, S., TAMRES, M. & BARROW, G. M. (1953). *Ibid.*, **75**, 71–73.
WEST, W. & EDWARDS, R. T. (1937). *J. chem. Phys.*, **5**, 14–22.
WHETSEL, K. B. & KAGARISE, R. E. (1962). *Spectrochimica Acta*, **18**, 329–339.
WILLIAMS, D. H. & WILSON, D. A. (1966). *J. chem. Soc.* (B), 144–148.

J. Pharm. Pharmac., 1970, **22**, *Suppl.*, 114 S–120 S *Received January* 29, 1970

Adsorption of non-ionic surfactants at the griseofulvin–solution interface

P. H. ELWORTHY AND W. G. GUTHRIE

Department of Pharmaceutical Technology, University of Strathclyde, Glasgow, C.1, U.K.

The adsorption from solution onto griseofulvin powder of a series of non-ionic detergents of the polyoxyethylene glycol mono alkyl ether type is described. Results are also given for polyethylene glycol 400 and a new detergent, pentaerythritol mono-n-octyl ether, whose synthesis and purification is reported. The effect of temperature on the adsorption is studied and possible explanations of the variation of adsorption with temperature are based on the orientation of the molecules at the interface; this is deduced from measured molecular areas.

Surfactants are of use in controlling the properties of powders to be formulated as suspensions. As well as affecting wetting of the powder, the adsorbed film of surfactant can control the physical stability of the suspension. Ionized surfactants can affect control by charge effects while non-ionic surfactants act through electrostatic and entropic factors. The contribution of electrostatic and entropic factors to the stabilization of emulsions by non-ionic surfactants has been investigated (Elworthy & Florence, 1969), but little work has been done on the mechanism of stabilization of pharmaceutical suspensions by non-ionic surfactants.

Few studies of adsorption of non-ionic surfactants from solution have been made: Corkill, Goodman & Tate (1966) used graphitized carbon black as adsorbent and short chain polyoxyethylene glycol ethers as adsorbates whilst Abe & Kuno (1961, 1962) studied the adsorption of octyl phenol non-ionics on carbon and calcium carbonate. Other authors have examined the adsorption of polyoxyethylene ethers on paraffin wax (Lange, 1960) and silver iodide particles (Mathai & Ottewill, 1962, 1966). In their 1966 paper, Mathai & Ottewill related the stability of the dispersion to the adsorption results.

Griseofulvin is virtually insoluble in water, and can be formulated as a suspension. In this paper the adsorption of seven non-ionic surfactants and a polyoxyethylene glycol from aqueous solution onto griseofulvin is reported.

EXPERIMENTAL

Materials

Griseofulvin was recrystallized from absolute ethanol, dried, and ground in a glass mortar. Coarse particles were removed on a mesh 120 sieve, and the fraction retained by the 170 mesh sieve was used. M.p. 497° K (British Pharmacopoeia gives m.p. 491°–497° K). Two batches were prepared, the particle size distribution being determined with a Model A Coulter Counter using 0·9% sodium chloride solution

with the addition of 0·05% cetomacrogol 1000 as the suspension medium, the suspension being irradiated ultrasonically just before sizing. The mean particle diameters were 4·3 and 5·2 μm respectively from which the mean volume surface diameters were calculated from the Hatch-Choate relation. Values of 1550 and 1310 m^2/kg were found for the specific surface areas.

Six of the surfactants used were polyoxyethylene glycol monohexadecyl ethers, i.e. $C_{16}E_x$. Texofor A10, A45 and A60 (Glovers Chemicals Ltd.) were characterized with x = 10, 47 and 62 ethylene oxide units respectively. Cetomacrogol 1000 B.P.C. (Macarthys Ltd.) contained 23 units. The ethylene oxide content was determined by nmr spectroscopy, according to Humphreys (1968). The synthetic surfactants were prepared according to Elworthy & Macfarlane (1962). $C_{16}E_7$ had m.p. 311° K (311·5° K), ethylene oxide content, by the method of Siggia, Stark & others (1958) 55·6%); $C_{16}E_9$ had m.p. 317° K (318° K), ethylene oxide content 62·07% (62·05%). Literature, or "required" analytical figures are given in brackets.

The remaining surfactant pentaerythritol mono-n-octyl ether (C_8P) was synthesized as follows (Barth, 1953).

A solution of 1 mol of paraformaldehyde in 0·925 mol n-octyl alcohol (10% by volume) was added to a solution of sodium hydroxide (0·35 mol) of n-octyl alcohol (1·625 mol) at 296° K. The remainder of the paraformaldehyde solution plus acetaldehyde (0·2 mol) was mixed and added slowly to the caustic solution.

The mixture was allowed to stand for 24 h, heated to 328° K, and stirred for 12 h. It was then neutralized with dilute hydrochloric acid, filtered and the excess octyl alcohol removed by vacuum distillation (13·3 Nm^{-2}). Methanol (5×10^{-4} m^3; 500 ml) and concentrated hydrochloric acid (2×10^{-6} m^3; 2 ml) were added to the residue and the resulting solution distilled slowly at 323° K to remove any formaldehyde as methylal.

Acetylation was accomplished by refluxing for 3 h with a slight excess of acetic anhydride (0·5 mol). Excess acetic acid was removed by distillation and any precipitated pentaerythritol tetra acetate filtered off.

The crude esters were distilled (6·66 Nm^{-2}) to yield four fractions with boiling ranges 333–358° K; 393–403° K; 403–421° K; and 441–445° K respectively. Infrared examination showed the second, third and fourth fractions to have ether linkages. Fraction four was assumed to be the di-ether due to the magnitude of the 11·20 m^{-1} adsorption peak (ether peak) and also its higher boiling point. The spectra of fractions two and three were almost identical and those two fractions were combined as the crude tri-acetyl mono-ether. Saponification of the ester was effected by refluxing with sodium ethoxide in absolute ethanol (Wawzonek & Issidorides, 1953). The reactants were neutralized, filtered and distilled leaving a viscous residue which solidified on standing.

The impure material (2·5 g) was chromatographed on a mixed silicic acid/Celite column (27 g + 7 g) using benzene–acetone as solvent. The pure compound eluted by 5% acetone in benzene was dried and recrystallized from anhydrous ether to give a white solid m.p. 311° K, mol. wt. 247·8 (theoretical 248·3). $C_{13}H_{28}O_4$ requires C, 62·9; H, 11·4%. Found, C, 62·7 (62·9); H, 12·4 (11·4). The C_8P compound has been described in detail as it has not been previously prepared pure enough for surface chemical work. No minimum was observed in a surface tension-log concentration curve.

Polyoxyethylene glycol 400 (B.D.H.) was used as supplied.

Adsorption measurements

Griseofulvin (0·5 g) and surfactant solution (1×10^{-5} m^3; 10 ml) of known concentration were placed in a screw-capped bottle, which was shaken until the powder was dispersed. The suspension was irradiated for 15 s using an M.S.E. Ultrasonic generator, and allowed to equilibrate in a thermostat ($\pm 0{\cdot}01°$) for 16 h. The supernatant liquid was decanted, centrifuged and analysed by one of the methods listed below. Neither degassing the suspension before placing in the thermostat, nor varying the irradiation time had any effect on the amount adsorbed. Measurements made over 3 days indicated that adsorption was complete at 16 h.

Analytical methods

The presence of dissolved griseofulvin interfered with concentration measurements by interference refractometry. For analysis of $C_{16}E_x$ compounds the iodine method of Ross & Olivier (1959) was adapted. A sample (2×10^{-6} m^3; 2 ml) of the surfactant solution was mixed with an aqueous iodine solution containing 200 mg dm^{-3} (1×10^{-6} m^3; 1 ml), and the extinction measured in 10 mm cells at 390 nm. Calibration graphs using known surfactant concentrations were linear in the concentration region of interest. The method is very sensitive, and concentrations of the order of 4×10^{-7} mol dm^{-3} can be determined.

For polyoxyethylene glycol 400 Milwidsky's (1969) method was used, the blue water-insoluble complex formed between the glycol and ammonium cobaltothiocyanate being estimated in 20 mm cells at 628 nm.

C_8P was estimated by Reid & Salmon's (1955) method.

RESULTS AND DISCUSSION

Representative isotherms for the $C_{16}E_x$ series of surfactants (Figs 1 and 2) are of the Langmuirian type over the concentration range studied. The maximum amount of surfactant adsorbed was obtained from the plateau region of the isotherms. The region of maximum adsorption occurs in most cases at or close to the critical micelle concentration (shown by arrows on the Figures).

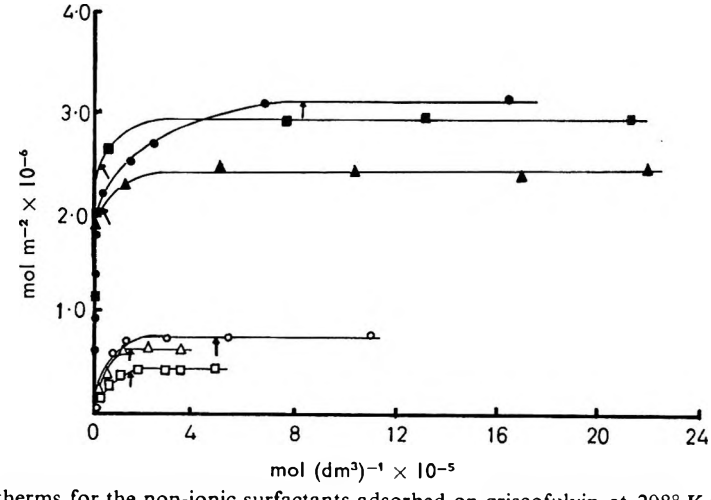

FIG. 1. Isotherms for the non-ionic surfactants adsorbed on griseofulvin at 298° K: ●, A10; ■ $C_{16}E_7$; ▲, $C_{16}E_9$; ○, Cetomacrogol; △, A45; □, A60. Arrows mark CMC.

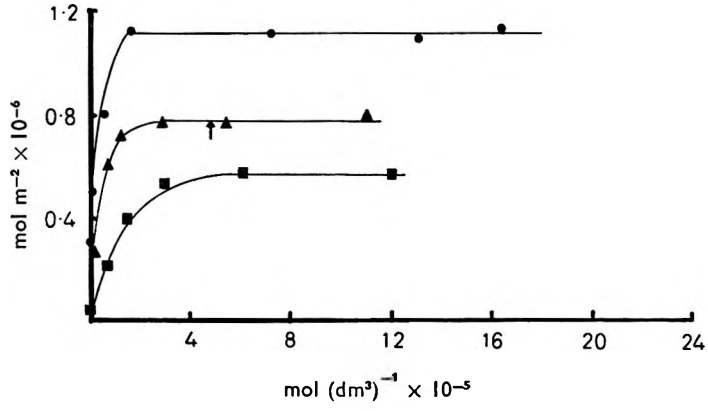

FIG. 2. Effect of temperature on the adsorption of cetomacrogol on griseofulvin: ●, 288° K; ▲, 298° K; ■, 308° K.

The isotherms for C_8P (Fig. 3) show a small and roughly constant adsorption at low concentrations, followed by a greatly increased adsorption, which is possibly due to multilayer formation. PEG 400 (Fig. 4) shows a similar behaviour, but with no secondary increase in adsorption over the concentration range used.

Temperature has a considerable effect on adsorption. For cetomacrogol (Fig. 2) an increase in temperature decreases adsorption and causes monolayer coverage to occur at higher equilibrium concentrations. This decrease in adsorption with rise of temperature is also shown by C_8P, $C_{16}E_{45}$, and $C_{16}E_7$. PEG 400 behaves differently —adsorption increasing with a rise in temperature (Fig. 4), and monolayer coverage shifting to lower equilibrium concentrations.

The PEG 400 results indicate that this head group (of the surfactants) has a tendency to adsorb on the griseofulvin surface. The area occupied by a Catalin model corresponding to PEG 400 is 1·50 nm², while the observed area/molecule at monolayer coverage is 2·96 nm², indicating that the glycol is likely to be adsorbed flat on the

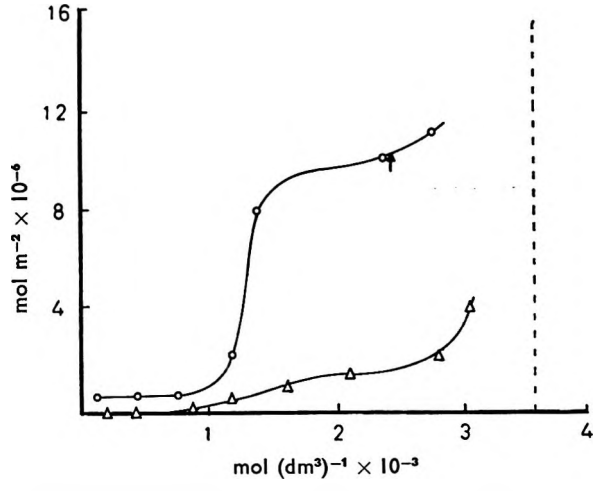

FIG. 3. Adsorption isotherms for C_8P at two temperatures: ○, 298° K; △, 308° K. The dotted line represents the phase boundary.

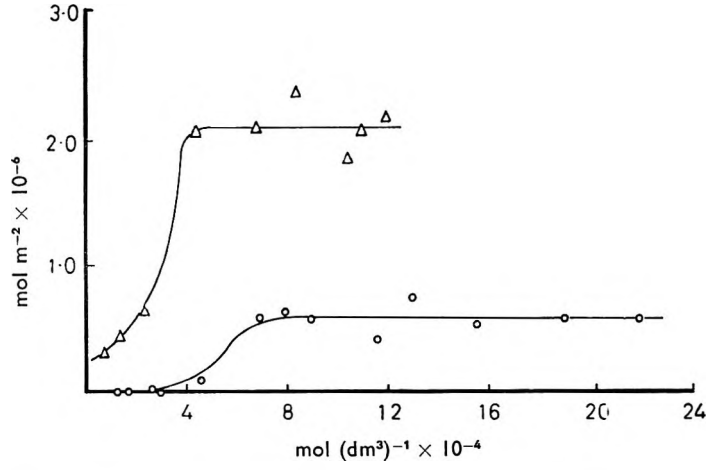

FIG. 4. Effect of temperature on the adsorption of polyethylene glycol 400: ○, 298° K; △, 308° K.

surface. When the hexadecyl chain is attached to one end of the PEG 400 chain (i.e. $C_{16}E_9$ or Texofor A10), the number of moles adsorbed at monolayer coverage increases, and the area/molecule decreases by factors of 4 to 5. This indicates that the hydrocarbon chain is adsorbed at the surface; if it were not, the area/molecule would not change significantly. Increasing the polyoxyethylene chain length of the surfactant has the effect of decreasing the maximum amount adsorbed and increasing the area/molecule (Table 1). It seems possible that the hydrocarbon chain is adsorbed end on to the surface, and that the polyoxyethylene chain bends towards the surface and is also attached to it.

The values calculated for the areas/molecule at the griseofulvin–solution interface are greater than those published for the closest packing at the air–water interface, e.g. cetomacrogol 2·13 nm² (1·20 nm²), $C_{16}E_7$ 0·57 nm² (0·45 nm²), and $C_{16}E_9$ 0·69 nm² (0·53 nm²), the values in brackets being those for the air–water interface. This comparison indicates that the polyoxyethylene chain is contributing more to the area/molecule at the solution–solid than at the air–water interface, and also that the surfactants containing the shortest PEG chains are most closely packed; this is in accordance with the work of Corkill & others (1966). The increase of area/molecule

Table 1. *Values of the maximum adsorbed and the areas/molecule for the compounds examined.*

Compound	Maximum adsorbed (mol m⁻² × 10⁶)			nm² Area/molecule at the griseofulvin–solution interface		
	288° K	298° K	308° K	288° K	298° K	308° K
Texofor A10	—	3·12	—	—	0·52	—
Cetomacrogol 1000 ..	1·12	0·78	0·57	1·48	2·13	3·43
Texofor A45	—	0·65	0·25	—	2·55	6·64
Texofor A60	—	0·44	—	—	3·77	—
$C_{16}E_7$	—	2·92	2·43	—	0·57	0·68
$C_{16}E_9$	—	2·39	—	—	0·69	—
PEG 400	—	0·56	2·11	—	2·96	1·27
C_8P	—	10·11	1·81	—	0·16	0·92

with polyoxyethylene chain length has also been shown by Abe & Kuno (1962) for nonyl phenols on carbon.

Fig. 5 shows the variation in maximum amount adsorbed with ethylene oxide chain length. Within experimental error, the synthetic surfactants $C_{16}E_7$ and $C_{16}E_9$ and the commercial surfactants $C_{16}E_{10}$, $C_{16}E_{45}$ and $C_{16}E_{60}$ fall on the same line which represents the change in adsorption with increasing length of ethylene oxide chain. This indicates that the width of the chain length distributions in the commercial surfactants does not have a marked effect on the adsorption. A similar conclusion has already been reached for adsorption of non-ionics on quartz (Dunning, 1957).

The shape of the isotherm for the pentaerythrityl ether C_8P (Fig. 3) differs considerably from those given by the other surfactants. The area/molecule at the griseofulvin–solution interface is 0·16 nm² compared with a value of 0·47 nm² at

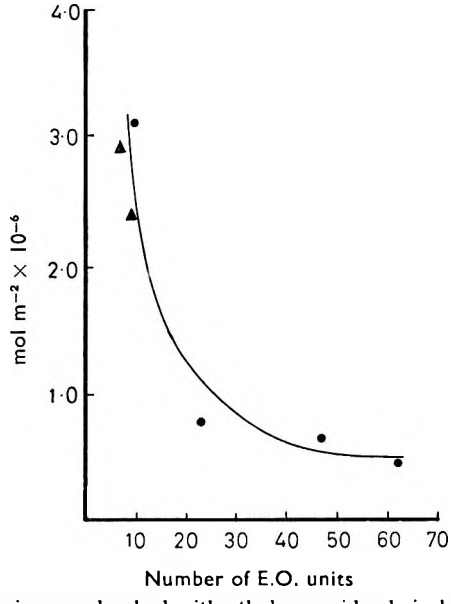

FIG. 5. Variation in maximum adsorbed with ethylene oxide chain length: ▲, Synthetic detergents; ●, Commercial detergents.

the air–water interface (Elworthy & Guthrie, unpublished), which suggests multilayer adsorption at the former interface. Sigmoid isotherms, similar to those given by C_8P have been found by Corkill & others (1966) and Kuno & Abe (1961) when adsorption was studied at concentrations close to a phase boundary. The phase boundary is shown in Fig. 3, and it is possible that surface nucleation leading to multilayer formation occurs. The decrease in adsorption with increased temperature may be due to thermal agitation opposing the tendency to multilayer formation.

Factors affecting the change of adsorption with temperature are likely to be complex, involving alterations of water structure around hydrocarbon chains, and the alteration of chain conformation. PEG 400 shows an increased adsorption as the temperature rises. This may be due to desolvation, or to increased thermal agitations causing one end of the molecule (which appears to be flat on the surface at 298° K) to become desorbed, and provide additional sites for adsorption of other molecules.

The polyoxyethylene-containing surfactants are adsorbed to a lesser extent at higher temperatures than at lower ones. This may be due to an altered conformation of the PEG chain, or to an alteration of hydration.

Acknowledgements

We thank Glaxo Laboratories Limited for the gift of griseofulvin and Dr. D. Attwood for the $C_{16}E_7$ detergent.

REFERENCES

ABE, R. & KUNO, H. (1962). *Kolloid-Z. u. Z. Polymere*, **181**, 70.
BARTH, R. H. (1953). U.S. Patent 2,644,013.
CORKILL, J. M., GOODMAN, J. F. & TATE, J. R. (1966). *Trans. Faraday Soc.*, **62**, 979–986.
DUNNING, H. N. (1957). *Ind. Engng Chem., Chem. Engng Data Series*, **2**, 88–91.
ELWORTHY, P. H. & FLORENCE, A. T. (1969). *J. Pharm. Pharmac.*, **21**, *Suppl.*, 79S–90S.
ELWORTHY, P. H. & MACFARLANE, C. B. (1962). *J. chem. Soc.*, 537–541.
HUMPHREYS, K. J. (1968). M.Sc. Thesis, London.
KUNO, H. & ABE, R. (1961). *Kolloid-Z. u. Z. Polymere*, **177**, 40–44.
LANGE, H. (1960). *J. phys. Chem.*, **64**, 538–541.
MATHAI, K. G. & OTTEWILL, R. H. (1962). *Kolloid-Z. u. Z. Polymere*, **185**, 55–62.
MATHAI, K. G. & OTTEWILL, R. H. (1966). *Trans. Faraday Soc.*, **62**, 750–758.
MILWIDSKY, B. M. (1969). *Analyst*, **94**, 377–386.
REID, V. W. & SALMON, D. G. (155). *Ibid.*, **80**, 704–705.
ROSS, S. & OLIVIER, J. P. (1959). *J. phys. Chem.*, **63**, 1671–1673.
SIGGIA, S., STARK, A. C., GARRIS, J. J. & STAHL, C. R. (1958). *Analyt. Chem.*, **30**, 115–116.
WAWZONEK, S. & ISSIDORIDES, C. (1953). *J. Am. chem. Soc.*, **75**, 2373–2375.

J. Pharm. Pharmac., 1970, **22**, *Suppl.*, 121 S–125 S *Received February*, 11 1970

Nuclear magnetic resonance studies on micelle formation by promethazine hydrochloride

A. T. FLORENCE AND R. T. PARFITT*

School of Pharmaceutical Sciences, University of Strathclyde, Glasgow, C.1, U.K.

The pmr spectra of solutions of promethazine hydrochloride in D_2O have been obtained as a function of concentration above and below the critical micellar concentration of the drug. Chemical shifts were obtained relative to an external standard of a 20% promethazine solution (micellar). The shifts of the spectrum of the hydrophilic $\overset{+}{N}H(CH_3)_2$ group to higher fields on increasing concentration were explained by the increased dissociation of the group at the micelle surface, an effect illustrated by the decrease in bulk pH at the critical micelle concentration. Diamagnetic shifts of the aromatic ring protons are compatible with the non-polar environment and a parallel stacking of the phenothiazine rings in the interior of the micelle.

Micelle formation by drugs in solutions is a widespread phenomenon (Florence, 1968). With ionic compounds in aqueous solution micellization results in the removal of hydrophobic portions of the monomer from contact with water and concentration of the hydrophilic head groups at the surface of the micelle. The changes in the environment of these groups leads to changes in their proton magnetic resonance absorption. Nuclear magnetic resonance investigations on surfactant solutions have, since Eriksson's (1963) study, led to a more detailed understanding of the process of micelle formation and of the structure of micelles at the molecular level (Inoue & Nakagawa, 1966; Müller & Birkhahn, 1967; Clifford & Pethica, 1964).

The low critical micellar concentration (CMC) of the cetyl pyridinium bromide with which he worked prevented Eriksson (1963) from making measurements on the monomeric state before micellization. To obviate this difficulty we have chosen a phenothiazine derivative, promethazine hydrochloride (I),

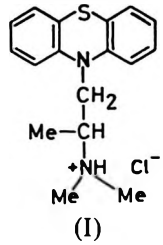

(I)

which has a CMC of approximately 4×10^{-2}M (1·33%). This compound has the additional advantage that the proton resonance of *three* portions of the molecule,

* Present address: Chemical Research Department, Pfizer Ltd., Sandwich, Kent.

namely the aromatic, the CH–$C\underline{H}_3$ and $N(C\underline{H}_3)_2$ groups, can be examined in monomeric and micellar form. Promethazine HCl forms micelles containing 27 monomers in 0·9% sodium chloride (Scholtan, 1955).

The purpose of the present paper is to discuss the chemical shifts which occur on micellization, in particular those caused by the proximity of the groups at the micellar surface.

EXPERIMENTAL

Promethazine hydrochloride, used without further purification, was obtained from May & Baker Ltd. Solutions of the compound in deuterium oxide (D_2O) were prepared immediately before use to minimize breakdown of the promethazine.

Proton magnetic resonance spectra (60 MHz) were obtained at 34° on a Perkin-Elmer R-12 spectrometer with a 20% solution of promethazine hydrochloride in D_2O as external reference. Chemical shifts of the proton absorptions of $\overset{+}{N}H(CH_3)_2$ (singlet), CH–$C\underline{H}_3$ (doublet) and the aromatic ring (multiplet) were measured relative to the corresponding reference resonance line at a sweep width of 100 Hz. Results were not corrected for bulk magnetic susceptibility effects which are expected to be small (cf. Bailey & Cady, 1969; Arrington, Clouse & others, 1970).

Coaxial sample tubes were prepared by the accurate concentric drilling of nylon bushes and the insertion of a sealed capillary containing the external reference into the drill holes: this unit was then fitted into a standard 5 mm pmr sample tube.

pH measurements were made with a Pye Model 78 pH meter by titration of the drug solution into distilled water at room temperature (about 22°).

RESULTS AND DISCUSSION

The pmr spectrum of a 20% solution of promethazine HCl in D_2O with sodium 2,2-dimethyl-2-silapentane-5-sulphonate (DSS) as internal reference, is not well resolved. At this solution strength the environment of most promethazine hydrochloride molecules is micellar and the broadening of the signal may, therefore, be attributed to the more facile spin-lattice relaxation of the micellar species.

Pmr data on promethazine hydrochloride in D_2O and of the base in deuterochloroform and benzene-D_6 are summarized in Table 1. Fig. 1 shows the scale-expanded $\overset{+}{N}H(CH_3)_2$ resonance signal of solutions of promethazine hydrochloride. The $\overset{+}{N}H(CH_3)_2$ signal of a 5·2% solution is almost indistinguishable in shift from the 20% reference solution line and can be detected only in the form of line broadening at the base of the absorption band. As solution concentration is lowered, two

Table 1. *Pmr data on promethazine*

Compound	Solvent	$\overset{+}{N}(C\underline{H}_3)_2$	CH–$C\underline{H}_3$	Aromatic
Promethazine HCl 20% solution ..	D_2O	7·17 s	8·71 d *J* 6Hz	2·8 m
Promethazine HCl 5% solution ..	D_2O	7·17 s	8·66 d	2·85 m
Promethazine base	$CDCl_3$	7·68 s	8·97 d	2·97 m
Promethazine base	Benzene-D6	7·87 s	9·10 d	3·07 m

s = singlet d = doublet m = multiplet

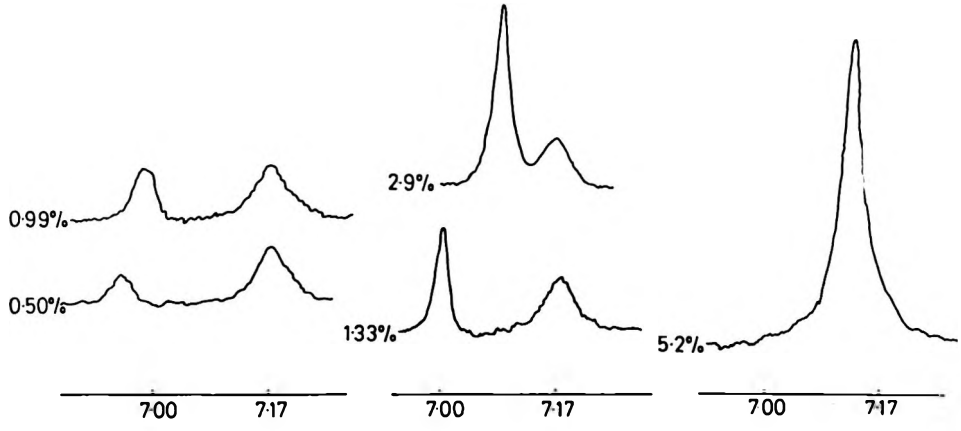

FIG. 1. Pmr signal of the $\overset{+}{N}(CH_3)_2$ protons of promethazine hydrochloride in D_2O. The high-field line of constant intensity is due to the external reference signal of 20% promethazine HCl in D_2O. The concentrations of the solution are marked.

distinct lines appear, the separation increasing with decrease in concentration. The broad high-field line in Fig. 1 does not change in intensity whereas the sharper low-field signal decreases in intensity as the solution concentration decreases. We therefore assign the broad high-field line to the reference (micellar) form and the low-field signal to the solution containing an increasing concentration of monomer.

The diamagnetic shift (13·1 Hz maximum) observed on changing from a solution composed mainly of promethazine HCl monomers (0·51%) to the solution consisting largely of micellized drug may be attributed to an increased dissociation of the polar head groups at the micelle surface. Koch & Doyle (1967) have shown that the chemical shift of the NCH_3 group in a number of amines was linearly dependent on the fractional number of free base and salt molecules present. That increased dissociation is occurring above the CMC is confirmed by the dramatic fall in pH which

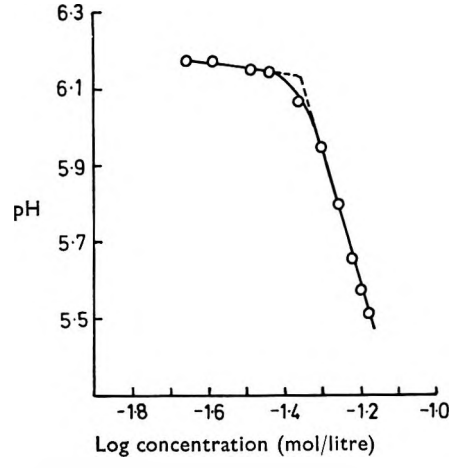

FIG. 2. The variation of pH of promethazine hydrochloride, at room temperature, in H_2O as a function of the concentration of drug.

occurs at the CMC (Fig. 2). Titration of promethazine HCl solutions with NaOH above and below the CMC shows that the change in apparent pK_a on micellization is −0·48. Similar pK_a changes on micellization of decylamine and dodecylamine hydrochlorides have been reported (−1·1 and −1·63 units respectively) (Veis & Hoerr, 1960). Since $\Delta pK_a = \Delta G_e/2{\cdot}303kT$ (Veis & Hoerr, 1960) this allows the calculation of the electrostatic free energy of micellization ($\Delta G\hat{e}$) for promethazine hydrochloride as +1·1 kT. This is much lower than the 3·75 kT obtained for dodecylamine hydrochloride probably because the packing of the phenothiazine molecules into a micelle is more difficult than with n-aliphatic amines and, as a result, the polar head groups do not approach each other as closely in the smaller micelle.

The $CH–C\underline{H}_3$ doublet which is proximate to the polar head group also experiences a change in magnetic environment (23·4 Hz maximum to high-field values) (Table 2) being more shielded in the micelle. This shift, greater than that observed for the $N(CH_3)_2$ signals, may be explained by the alkyl chains of adjacent molecules in the micelle providing extra shielding.

Table 2. *Chemical shifts* of promethazine HCl as function of concentration in D_2O at 34°*

Concentration† (%)	Shifts (Hz) $\overset{+}{N}(CH_3)_2$	$-CH-CH_3$	Aromatics
5·23	—	5·8	5·9
4·161	2·4	7·5	7·0
2·89	4·6	9·9	9·4
1·585	9·4	18·0	11·7
1·355	10·3	19·9	13·0
1·027	11·1	21·1	15·0
0·986	11·4	21·6	15·8
0·724	12·1	22·1	18·2
0·509	13·1	23·4	19·6

* Shifts measured relative to the corresponding resonance lines of the external standard (20% promethazine HCl in D_2O).

† % w/w.

A diamagnetic shift also occurs in the major peak of the phenothiazine ring protons. This is compatible with the aromatic groups residing in a non-polar environment and being influenced by the diamagnetic anisotropy of adjacent aromatic moieties. The shift to a lower field on dilution suggests that the rings are stacked parallel to each other in the micelle. Rings packed in a coplanar configuration would produce a high-field shift on being removed from the micelle, according to Blears & Danyluk (1966).

Fig. 3 shows the observed shifts of the three parts of the molecule as a function of concentration. All plots show breaks of varying abruptness at the CMC. The mean CMC value obtained at 34° in D_2O is 1·3% w/w ($4{\cdot}06 \times 10^{-2}$M). The changes in proton magnetic absorption below the CMC might be explained for the $\overset{+}{N}(CH_3)_2$ peak by the changes in bulk pH (see Fig. 2), but the changes in the $CH–CH_3$ and aromatic absorptions cannot. It is surprising that the aromatic protons show such large shifts below the CMC. This contrasts with the behaviour of ω-phenylalkyltrimethylammonium bromides (Inoue & Nakagawa, 1966), in which the signal of the

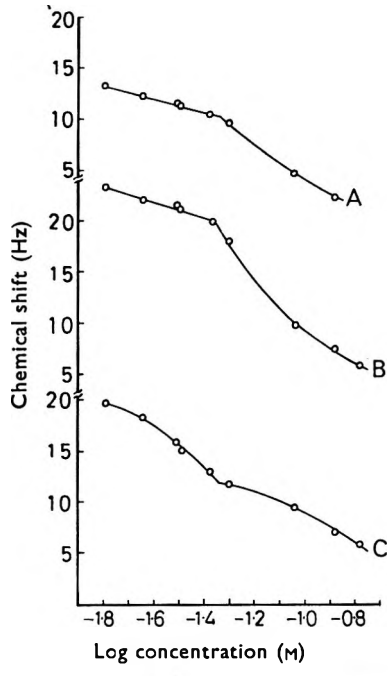

FIG. 3. Chemical shifts (Hz) of signal of A: $\overset{+}{N}(CH_3)_2$, B: $CH-CH_3$ and C: aromatic ring protons, as a function of the concentration of solution, relative to position of 20% promethazine HCl signals from the respective groups.

phenyl protons remained at the same position at concentrations below the CMC. It is possible that dimers of promethazine are forming below the critical micellar concentration constituted in such a way that the $-\overset{+}{N}(CH_3)_2$ groups are unaffected.

Acknowledgements

We thank May & Baker Ltd. for the gifts of drug.

REFERENCES

ARRINGTON, P. A., CLOUSE, A., DODDRELL, D., DUNLOP, R. B. & CORDES, E. H. (1970). *J. phys. Chem., Ithaca*, **74**, 665–668.

BAILEY, R. E. & CADY, G. H. (1969). *Ibid.*, **73**, 1612–1614.

BLEARS, D. G. & DANYLUK, S. S. (1966). *J. Am. chem. Soc.*, **88**, 1084–1085.

CLIFFORD, J. & PETHICA, B. A. (1964). *Trans. Faraday Soc.*, **60**, 1483–1490.

ERIKSSON, J. C. (1963). *Acta chem. scand.*, **17**, 1478–1481.

FLORENCE, A. T. (1968). *Adv. Colloid Inter. Sci.*, **2**, 115–149.

INOUE, H. & NAKAGAWA, T. (1966). *J. phys. Chem., Ithaca*, **70**, 1108–1113.

KOCH, S. A. & DOYLE, T. D. (1967). *Analyt. Chem.*, **39**, 1273–1276.

MÜLLER, N. & BIRKHAHN, R. H. (1967). *J. phys. Chem., Ithaca*, **71**, 957–962.

SCHOLTAN, W. (1955). *Kolloid-Z.*, **142**, 84–104.

VEIS, A. & HOERR, C. W. (1960). *J. Colloid Sci.*, **15**, 427–436.

J. Pharm. Pharmac., 1970, **22**, *Suppl.*, 126 S–130 S *Received March* 26, 1970

The use of a bromide ion selective electrode for the measurement of counter-ion activity in cationic surfactant solutions

J. T. PEARSON AND K. J. HUMPHREYS

School of Pharmacy, The Polytechnic, Sunderland, Co. Durham, U.K.

A bromide ion selective electrode has been used in conjunction with a saturated calomel reference electrode to measure bromide ion activity in solutions of n-decyl, n-dodecyl, n-tetradecyl and n-hexadecyl 1-trimethylammonium bromides at 30°; the critical micelle concentrations of the surfactants were measured by electrical conductance. Calibration of the electrode pair in potassium bromide solutions produced a linear response over the range 0·5 to 5·0p Br_a^- with a slope of 59·1 mV for a 10-fold change in activity. Results for the surfactants were treated to give values for the degree of micellar dissociation; literature values for this quantity reveal wide variation depending on the technique used.

The degree of dissociation (α) of ionic micelles required for an adequate description of surfactant solutions may be expressed as the ratio p/n, where p represents the number of effective charges per micelle and n the aggregation number. A variety of experimental techniques have been used for the measurement of α. Values obtained from electrode systems employing solid ion exchange membranes (Botré, Crescenzi & Mele, 1959; Ingram & Jones, 1969) and ion selective glass electrodes (Shedlovsky, Jakob & Epstein, 1963; Lawrence & Pearson, 1967; Feinstein & Rosano, 1967) have been reported on a wide range of surfactants. Covington (1969) has reviewed the complete range of ion selective electrodes.

The behaviour of ion selective electrodes in cationic surfactant solutions has not previously been reported and the present work was undertaken to assess the feasibility of using a heterogeneous bromide ion selective electrode in conjunction with a saturated calomel reference electrode for the direct measurement of counter-ion activity in a series of quaternary ammonium surfactant solutions. Electrodes of this type have membranes consisting of finely divided insoluble silver salts dispersed in an inert binder of silicone rubber to give a composition which possesses suitable electrical and mechanical properties and have been developed largely as a result of work by Pungor (1967); further details are given by Moody, Oke & Thomas (1969).

EXPERIMENTAL

Apparatus and materials

The bromide ion selective electrode (Pungor-Radelkis, Type OP–Br–711; Protech Advisory Services, Rickmansworth) was used in conjunction with a calomel reference electrode employing a saturated potassium chloride salt bridge (E.I.L., Type RJ23). The output potential produced by the electrode pair was measured with an E.I.L. Vibret Model 46A pH meter and all solutions were equilibrated in a thermostat maintained at 30° ± 0·1°. This temperature was chosen since it is several degrees

higher than the Krafft point of n-hexadecyl 1-trimethylammonium bromide, the compound of greatest n-alkyl chain length in the homologous series of surfactants used. Electrical conductance measurements for the determination of critical micelle concentration (CMC) were made with a Philips Type PR9500 conductance bridge operating at 1000 Hz using Pye Type 7407 conductance cells with blackened platinum electrodes.

Quaternary ammonium surfactants used were n-decyl, n-dodecyl, n-tetradecyl and n-hexadecyl 1-trimethylammonium bromides ($C_{10,12,14,16}$ TAB's respectively). These were synthesized by direct quaternization of the purest grades of 1-bromo n-alkanes available (Fluka) using anhydrous trimethylamine (B.D.H.). Crude quaternary salts were continuously extracted with ether to remove unchanged alkyl bromide then recrystallized from diethylketone. All physical measurements were made in aqueous solution using triple distilled water.

Calibration and procedure

The electrode pair was calibrated by measuring the e.m.f. response in solutions of potassium bromide (AR). A graph of potential (mV) against pBr_a^- ($-\log_{10}$ bromide ion activity) is linear in the region pBr_a^- 0·5–5·0 with a slope of 59·1 mV for a 10-fold change in activity, in good agreement with the theoretical Nernst slope, 2·303RT/F of 60·16 mV at 30°. Activity coefficients used are those given by Scatchard & Prentiss (1933). Bromide ion activity of the cationic surfactants was measured by direct reference to this calibration graph which has a range of e.m.f. values from −160 to +120 mV.

Equilibration times were rapid in potassium bromide solutions, about 30 s for more concentrated solutions, several minutes for dilute solutions. In cationic surfactant solutions equilibration times were somewhat longer (*c* 1–4 min). Since long-chain surfactant ions probably adsorb on to the membrane of the ion selective electrode, frequent checks were made to confirm that the electrode pair produced a satisfactory calibration response in potassium bromide. Particularly after immersion of the electrodes in concentrated solutions of C_{16} TAB response was sluggish but in all cases satisfactory reproduction of the calibration graph was observed.

Reactivity of the electrode to potassium bromide after use in cationic surfactant solutions may be achieved by pre-soaking in concentrated solutions of potassium bromide. The performance can be improved further if the electrodes are lightly wiped with tissue on passing from one solution to the next in order of increasing concentration, rather than rinsing with water which greatly increases the response time.

RESULTS

Fig. 1 shows a plot of pBr_a^- values against pBr_c^- (i.e. $-\log_{10}$ surfactant concentration) for the various surfactants. For reasons of clarity the curves for the homologues are separated by an interval, and the results for potassium bromide are as for C_{10} TAB including the extrapolated portion at high concentrations, shown as the broken line of the figure. Behaviour as conventional 1 : 1 electrolytes is apparent up to the CMC's of the surfactants (denoted by arrows), when marked positive deviation of pBr_a^- is observed, an effect attributable to the strong binding of counter-ions to the micelles. Such counter-ions do not contribute therefore to the development of electrode potential and may be regarded as kinetic entities with the micelles. Since

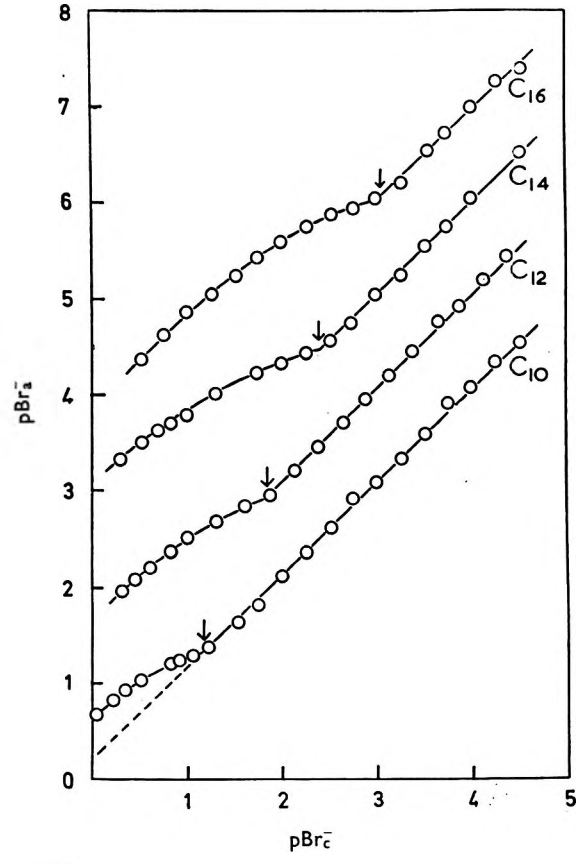

FIG. 1. Graph of pBr_a^- against pBr_c^- for the $C_{10,12,14,16}$ TAB surfactants. pBr_a^- points for the $C_{12,14,16}$ compounds are increased by +1, +2 and +3 units respectively to prevent the curves overlapping. Data for KBr is the same as for the pre-CMC line for C_{10} TAB plus the extrapolated portion (broken line). The arrows denote the CMC's of the surfactants which occur at pBr_c^- values of 1·17, 1·84, 2·39 and 3·05 for the $C_{10,12,14,16}$ TAB's respectively.

$a_s/C = \gamma_{expt}$, where a_s = activity of counter-ions, C = concentration of surfactant and γ_{expt} = apparent experimental activity coefficient, the data shown in Fig. 1 may readily be used to give a series of values of γ_{expt} as a function of concentration. It is necessary to assume throughout that the mean ionic activity coefficient at any given concentration is identical with the single ion activity coefficient (Guggenheim, 1930), and that with sufficient accuracy, 0° data can be used at 30°. A further assumption is implicit, namely that the liquid junction potential between saturated KCl and surfactant solution is zero.

Using the theoretical treatments of Botré & others (1959) and Ingram & Jones (1969), the counter-ion activity may be written as:

$$a_s = C\gamma_{expt} = \gamma_s [C_o + \alpha (C - C_o)]$$

where γ_s is the activity coefficient and C_o the CMC.

Therefore:

$$\gamma_{expt} = \gamma_s (C_o/C) (1 - \alpha) + \alpha\gamma_s$$

from which α may be found using the relation $\alpha = C_o/(S/I + C_o)$, where S and I are

the slope and intercept respectively of a plot of γ_{expt} against C^{-1} using values above the CMC (below the CMC the plot is not linear).

Values of α obtained in this manner are given in Table 1 together with literature values. Also shown are the CMC's of the surfactants obtained from plots of specific conductance against concentration; this method gives values which are more precise than those obtainable from the logarithmic data of Fig. 1. Slopes and intercepts involved in the calculation of α were computed using the method of least squares.

DISCUSSION

Since no definitive values for α are available, Table 1 serves only to show the range of values observed using a variety of different techniques. The degree of dissociation of ionic micelles decreases with increasing chain length of the surfactant. This may be attributed to increased inter-chain attraction leading to closer packing of the ionic head groups in the micelle, whence more counter-ions become strongly bound to reduce the increased ionic repulsion. The degree of dissociation (α) is also

Table 1. *Derived values of α, and values of critical micelle concentrations obtained from plots of specific conductance against concentration*

		C_{10} TAB	C_{12} TAB	C_{14} TAB	C_{16} TAB
CMC (molar)		0·0670	0·0145	0·0041	0·0009
α (this work)		0·27	0·24	0·13	0·12
α (lit.)	Ref. 1	0·224	0·193	0·131	0·091*
	Ref. 2	—	0·256	—	—
	Ref. 3	—	0·22	0·15	—
	Ref. 4 (*a*)	—	—	0·249	—
	Ref. 4 (*b*)	—	—	0·321	—
	Ref. 5	—	—	—	0·11

* In the presence of 0·013 M KBr.

Notes on references and techniques

1. Mysels (1955). Refined calculations based on the light scattering measurements of Debye (1949).
2. Ingram & Jones (1969). Membrane potential measurements employing BDH Permaplex A-20 anion exchange membranes.
3. Padday (1967). Potentiometric method using a calomel/Ag-AgBr cell.
4. Cushman, Brady & McBain (1948). Values obtained from (*a*) osmotic and (*b*) conductance data.
5. Vold (1950). Application of the Law of Mass Action to osmotic data.

affected by the presence of additives (or impurities) which become solubilized in the surfactant micelles or by the presence of inorganic salts (Lawrence & Pearson, 1967). In the present work, measurements of potential were recorded in quiescent solutions since stirring caused the readings to drift to higher values. The high value for C_{12} TAB reported by Ingram & Jones (1969) may be due to the fact that their solutions were vigorously stirred until the e.m.f. of the cell had reached a maximum. Because various techniques may respond to a different extent to the counter-ions present in the "free" or "bound" state, it is not yet possible to define the proportion of counter-ions in the electrical double layer that are responsible for the observed e.m.f. produced by the electrode pair.

The data in Fig. 1 do not provide information about the possible formation of pre-CMC aggregates which have been previously reported for certain *N*-alkylpyridinium

halides containing a non-ionic polar group in the pyridinium ring (Butler, Stead & Taylor, 1969) and for C_{16}TAB (Bair & Krauss, 1951; McDowell & Krauss 1951). In spite of the limitations of the method we consider it of potential value in surfactant systems, in problems of solubilization and for the analysis of quaternary ammonium surfactants.

Acknowledgements

The authors wish to thank the Sunderland Polytechnic Computer Centre and Mr. I. Boyd for helpful di cussions during the course of the work.

REFERENCES

BAIR, E. J. & KRAUSS, C. A. (1951). *J. Am. chem. Soc.*, **73**, 1129–1131.
BOTRÉ, C., CRESCENZI, V. L. & MELE, A. (1959). *J. phys. Chem., Ithaca*, **63**, 650–653.
BUTLER, C. G., STEAD, J. A. & TAYLOR, H. (1969). *J. Colloid Inter. Sci.*, **30**, 489–499.
COVINGTON, A. K. (1969). *Chem. Br.*, **5**, 388–394.
CUSHMAN, A., BRADY, A. P. & MCBAIN, J. W. (1948). *J. Colloid Sci.*, **3**, 425–436.
DEBYE, P. (1949). *J. phys. Colloid Chem., Ithaca*, **53**, 1–8.
FEINSTEIN, M. E. & ROSANO, H. L. (1967). *J. Colloid Inter. Sci.*, **24**, 73–79.
GUGGENHEIM, E. A. (1930). *J. phys. Chem.*, **34**, 1758–1766.
INGRAM, T. & JONES, M. N. (1969). *Trans. Faraday Soc.*, **65**, 297–304.
LAWRENCE, A. S. C. & PEARSON, J. T. (1967). *Ibid.*, **63**, 495–504.
MCDOWELL, M. J. & KRAUSS, C. A. (1951). *J. Am. chem. Soc.*, **73**, 2170–2173.
MOODY, G. J., OKE, R. B. & THOMAS, J. D. R. (1969). *Lab. Practice*, **18**, 1056–1062.
MYSELS, K. J. (1955). *J. Colloid Sci.*, **10**, 507–522.
PADDAY, J. F. (1967). *J. phys. Chem., Ithaca*, **71**, 3488–3493.
PUNGOR E. (1967). *Analyt. Chem.*, **39**, No. 13, 28A–45A.
SCATCHARD, G. & PRENTISS, S. S. (1933). *J. Am. chem. Soc.*, **55**, 4355–4362.
SHEDLOVSKY, L., JAKOB, C. W. & EPSTEIN, M. B. (1963). *J. phys. Chem., Ithaca*, **67**, 2075–2079.
VOLD, M. J. (1950). *J. Colloid Sci.*, **5**, 506–513.

J. Pharm. Pharmac., 1970, **22**, *Suppl.*, 131 S–138 S *Received February* 19, 1970

The correlation of unsteady-state heat transfer data from a sterilizing oven

D. G. PEACOCK AND K. RIDGWAY

*The School of Pharmacy, University of London, Brunswick Square, London, W.C.*1, *U.K.*

Data, showing the pattern of temperature rise in articles undergoing sterilization in an oven under normal working conditions, have been studied. Simple mathematical models, each expressed in terms of a set of differential equations rather than in an explicit analytical form, have been fitted to these data, and the quality of fit and possible applications are here discussed.

To achieve satisfactory sterilization by dry heat it is necessary to heat all parts of an article up to a required (minimum) temperature and to maintain this temperature for a specified period (for example 160°C for 1 hour: British Pharmacopoeia, 1968). Articles to be sterilized are usually stacked in containers in an oven, which is then brought to a temperature above the required minimum. The temperature of the articles themselves rises more slowly, and it is essential to allow sufficient time for the innermost parts to reach the requisite temperature. The heating time may be long, especially if the maximum oven temperature must be severely restricted, due for example to thermal instability of the materials undergoing treatment.

In principle the heating time may be predicted if one has a knowledge of the heat-transfer coefficients at all surfaces under the prevailing conditions, of the system geometry, and of the thermal conductivity and specific heat of the materials involved. Heat transfer coefficients are classically measured by setting up a steady-state experiment, in which the quantity of heat passing through a surface is determined under a constant temperature difference. The apparatus and technique for these measurements can be complex, and the results are dependent on conditions including the fluid flow pattern prevailing. In a sense, too, these measurements are intrinsically artificial, in that the experimental apparatus may differ substantially from the practical configuration, and the relation between the two may be open to debate.

Given the heat transfer coefficients and other requisite data, the problem of predicting the temperature-time profile for an article may be solved analytically only for relatively simple geometrical shapes and for a simple pattern of change in the environmental temperature. Even with substantial simplifying assumptions analytical solutions for particular cases can be extremely complicated (Jaeger, 1945; Carslaw & Jaeger, 1959), and in most cases a numerical solution is required.

In the work outlined here, an attempt has been made to explore an alternative approach to the unsteady-state heat transfer problem. Temperature-time records from an actual sterilization have been examined and mathematical models fitted to them. The models so fitted contain implicitly the heat transfer coefficients and other system properties, although it may not be possible to separate the various quantities contributing to the overall behaviour of the system.

EXPERIMENTAL

The hot-air oven was an electrically-heated, fan-circulated Barlow-Whitney type E3/232S with internal dimensions 96 cm high, 61 cm wide, and 56 cm deep. This was packed with a typical load of articles for sterilization, as shown in Fig. 1. The lower shelf carried tubes and pipettes; the two upper shelves each carried four tin-plate boxes packed with glass Petri dishes. The temperature recordings used were taken at 1 min intervals from each of three thermocouples, respectively (*a*) midway between the four tins on the top shelf, (*b*) in the air space at the centre of one of these tins, and (*c*) in the middle of a Petri dish in the same tin.

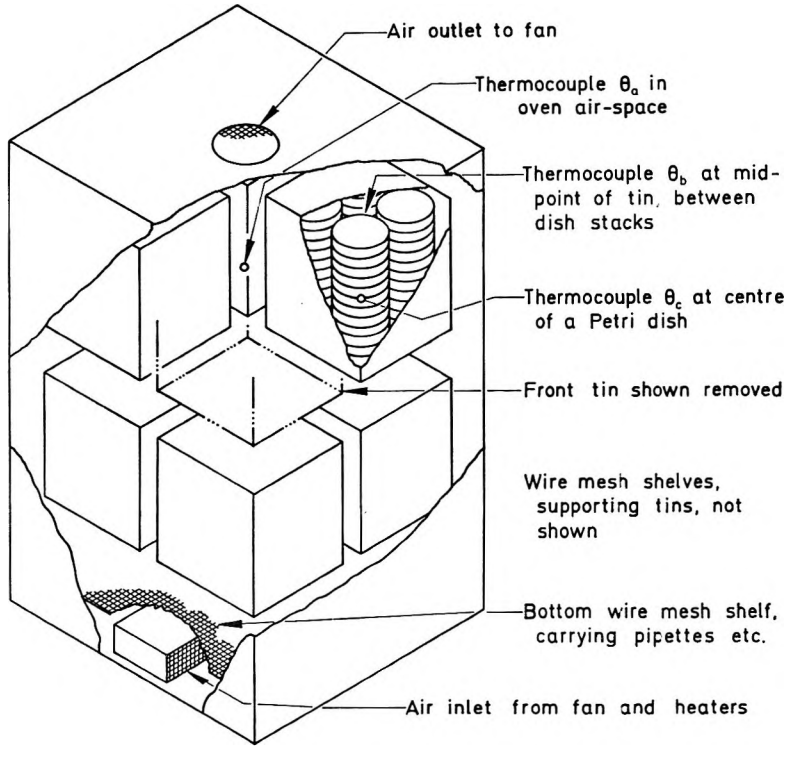

FIG 1. Diagram of the oven and its load, showing the positions of thermocouples.

Mathematical treatment

Let θ_0, θ_1, θ_2 be respectively the temperatures of the air surrounding a tin, of the metal wall of the tin itself, and of the air inside the tin, each assumed to be approximately uniform over the surface. From the definition of a heat transfer coefficient:

$$\text{Heat transfer to tin} = h_{01} A_{01} (\theta_0 - \theta_1)$$

and

$$\text{Heat transfer from tin} = h_{12} A_{12} (\theta_1 - \theta_2)$$

where h_{01}, h_{12} are the local heat transfer coefficients at the inner and outer surfaces and A_{01}, A_{12} are the external and internal surface areas of the tin, respectively.

A net heat gain by the tin will result in a rise in its temperature θ_1, thus:

$$\frac{d\theta_1}{dt} = \frac{1}{C_1}\{h_{01}A_{01}(\theta_0-\theta_1)-h_{12}A_{12}(\theta_1-\theta_2)\} \quad .. \quad .. \quad (1)$$

or

$$\frac{d\theta_1}{dt} = \frac{1}{C_1}\{p_{01}(\theta_0-\theta_1)-p_{12}(\theta_1-\theta_2)\} \quad .. \quad .. \quad .. \quad (2)$$

where C_1 is the heat capacity of the tin, and

p_{01}, p_{12} are respectively the products $h_{01}A_{01}$,$h_{12}A_{12}$.

The heat transfer to the payload of Petri dishes presents a more complicated problem, since this is thick in the direction of heat flow. A reasonably rigorous treatment would require a stack of dishes to be regarded as a distributed heat-transfer stage, considering it as an infinite set of isothermal, coaxial laminae, each receiving heat from the lamina without, passing heat to that within, and increasing in temperature as a result of the difference; such a treatment would present difficulties due to the relatively complicated shape of the dishes, and would itself disregard asymmetry due to the way the stacks were packed.

A simpler approach is to treat the stack of dishes as a finite number of discrete, notionally-coaxial elements, which behave as the laminae referred to above, and are each supposedly at a uniform temperature at any instant. Such a model has characteristics which approach those of the distributed stage as the number of elements is increased. In the present exercise, only the two simplest forms from this set of possible models have been used.

Model A. This is the grossest possible simplification; the stack of Petri dishes is treated as a single element, at a uniform temperature at any instant. If this has heat capacity C_3 and the temperature is θ_3 an equation analogous to (2) may be obtained

$$\frac{d\theta_3}{dt} = \frac{1}{C_3}p_{23}(\theta_2-\theta_3) \quad .. \quad .. \quad .. \quad .. \quad (3)$$

Since the air contained in the tin is of negligible heat capacity the rate at which heat leaves the inner surface of the tin must equal that at which it enters the Petri dishes, thus:

$$p_{12}(\theta_1-\theta_2) = p_{23}(\theta_2-\theta_3) \quad .. \quad .. \quad .. \quad .. \quad (4)$$

or

$$\theta_2 = \frac{p_{12}\theta_1 + p_{23}\theta_3}{p_{12}+p_{23}} \quad .. \quad .. \quad .. \quad .. \quad (5)$$

Model B. The stack of dishes is treated as composed of two elements, an outer (denoted by subscript 3′) and an inner (subscript 4). The heat transfer equations are:

$$\frac{d\theta_{3'}}{dt} = \frac{1}{C_{3'}}\{p_{23'}(\theta_2-\theta_{3'})-p_{3'4}(\theta_{3'}-\theta_4)\} \quad .. \quad .. \quad .. \quad (6)$$

$$\frac{d\theta_4}{dt} = \frac{1}{C_4}p_{3'4}(\theta_{3'}-\theta_4) \quad .. \quad .. \quad .. \quad .. \quad (7)$$

$$\theta_2 = \frac{p_{12}\theta_1 + p_{23'}\theta_{3'}}{p_{12}+p_{23'}} \quad .. \quad .. \quad .. \quad .. \quad (8)$$

These two models are represented in block diagram form in Figs 2 and 3.

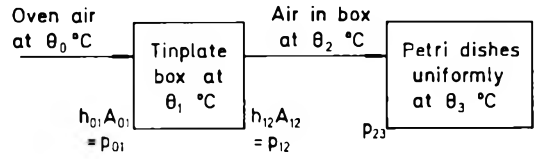

FIG. 2. Block diagram of model A. The temperatures θ_2, θ_3 were compared with the observed values θ_b, θ_c.

Considering the problem in terms of model A, it is possible to solve numerically the set of equations (2), (3) and (5) which represents this model, provided that the initial temperatures and the coefficients **C**,**p** are available and the oven air temperature θ_0 is known as a function of time. The solution may be presented in the form of graphs of θ_1, θ_2, θ_3 against time. The profiles of θ_2, θ_3 will resemble the observed pattern of change of θ_b, θ_c to a greater or lesser degree according to the values of **p** used.

Both model A and model B have been simulated in this way, using smoothed values of the observed air temperatures θ_a as θ_0 and optimizing the vectors **p** to give a best fit, in the least-squares sense, of the models to the observed results. The optimization consisted of minimizing the function

$$\sum\left\{(\theta_2-\theta_b)^2\right\}+\sum\left\{(\theta_3-\theta_c)^2\right\}$$

for model A, or the corresponding function with θ_3 replaced by θ_4 in the case of model B.

The optimization algorithm used was that due to Coggan (1967), based on work by Davidon (1959) and by Fletcher & Powell (1963). The differential equations were solved by Gill's modification of the Runge-Kutta method. The choice of these methods was made primarily on grounds of availability; a general discussion of the treatment of problems of this type has been presented by Rosenbrock and Storey (1966).

In the fitting of model A the parameters p_{01}, p_{12}, and p_{23} were optimized without constraint. To simplify the fitting of model B, the ratio p_{12}/p_{01} was arbitrarily fixed at 1·6 (the ratio optimal for model A); the payload of Petri dishes was treated as 70% outer element, 30% inner element, corresponding roughly to the outer flanged portions and the inner flat portions respectively (Fig. 4). Thus $C_{3'} = 0{\cdot}7\ C_3$ and $C_4 = 0{\cdot}3\ C_3$. With these arbitrary simplifications p_{01}, $p_{23'}$ and $p_{3'4}$ were optimized without constraint.

RESULTS AND DISCUSSION

The time: temperature profiles for the two fitted models A and B are shown in Figs 5 and 6. The observed temperatures θ_b and θ_c are shown for comparison, represented by broken lines.

The simpler model (A) represents the observed behaviour within about 5°C over

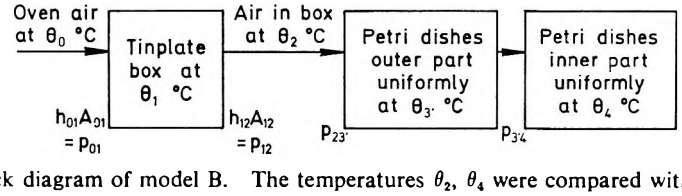

FIG. 3. Block diagram of model B. The temperatures θ_2, θ_4 were compared with the observed values θ_b, θ_c.

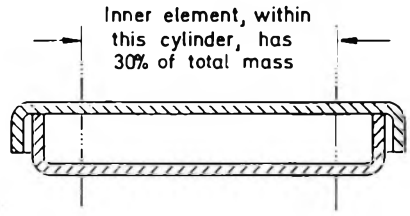

FIG. 4. The two-element model B visualized in terms of a partitioned Petri dish.

the entire range. The observed innermost temperature θ_c rises later and more rapidly than the fitted model; this is the difference to be expected from an attempt to represent a distributed stage by a single exponential transfer stage. The two-element model (B) represents the observed behaviour much more closely—within about 2°C over the entire range. The systematic differences between observations and model still take the same form but are less marked.

The principal numerical data and results are presented in Table 1. It may be noted that the heat capacity of the tinplate container is very much less than that of

Table 1. *Numerical data and results*

Tinplate box: dimensions, cm.	22·0 × 23·3 × 25·4 high	
surface area, cm^2	3220	
weight, g	923	
estimated heat capacity C_1 cal $°C^{-1}$	102	
Petri dishes: dimensions, cm.	10·2 dia. × 1·8 high	
weight, g	153	
number in box	48	
estimated heat capacity per box, C_3 cal $°C^{-1}$	1490	
	Model A	Model B
Heat capacity coefficients for elements of dish stacks:		
outer, C_3' cal $°C^{-1}$	—	1043
inner, C_4 cal $°C^{-1}$	—	447
Values of fitted heat transfer parameters, cal min^{-1} $°C^{-1}$		
p_{01}	31·5	32·5
p_{12}	50·5	52·0
p_{23} or p_{23}'	71·1	137·0
$p_{3'4}$	—	33·7
Heat transfer coefficients at surface of box, cal min^{-1} cm^{-2} $°C^{-1}$		
outside h_{01}	0·0098	(0·010)
inside h_{12}	0·016	(0·016)
$\left\{\frac{1}{h_{01}}+\frac{1}{h_{12}}\right\}^{-1}$	0·0060	0·0062
Overall coefficient, Chu h^{-1} ft^{-2} $°C^{-1}$	7·4	7·6
Residual variance of inner air temperature about fitted θ_2, $°C^2$	0·40	1·81
Corresponding standard deviation, °C	0·63	1·34
Residual variance of dish centre temperature about fitted θ_3 or θ_4, $°C^2$	9·91	2·14
Corresponding standard deviation, °C	3·15	1·46

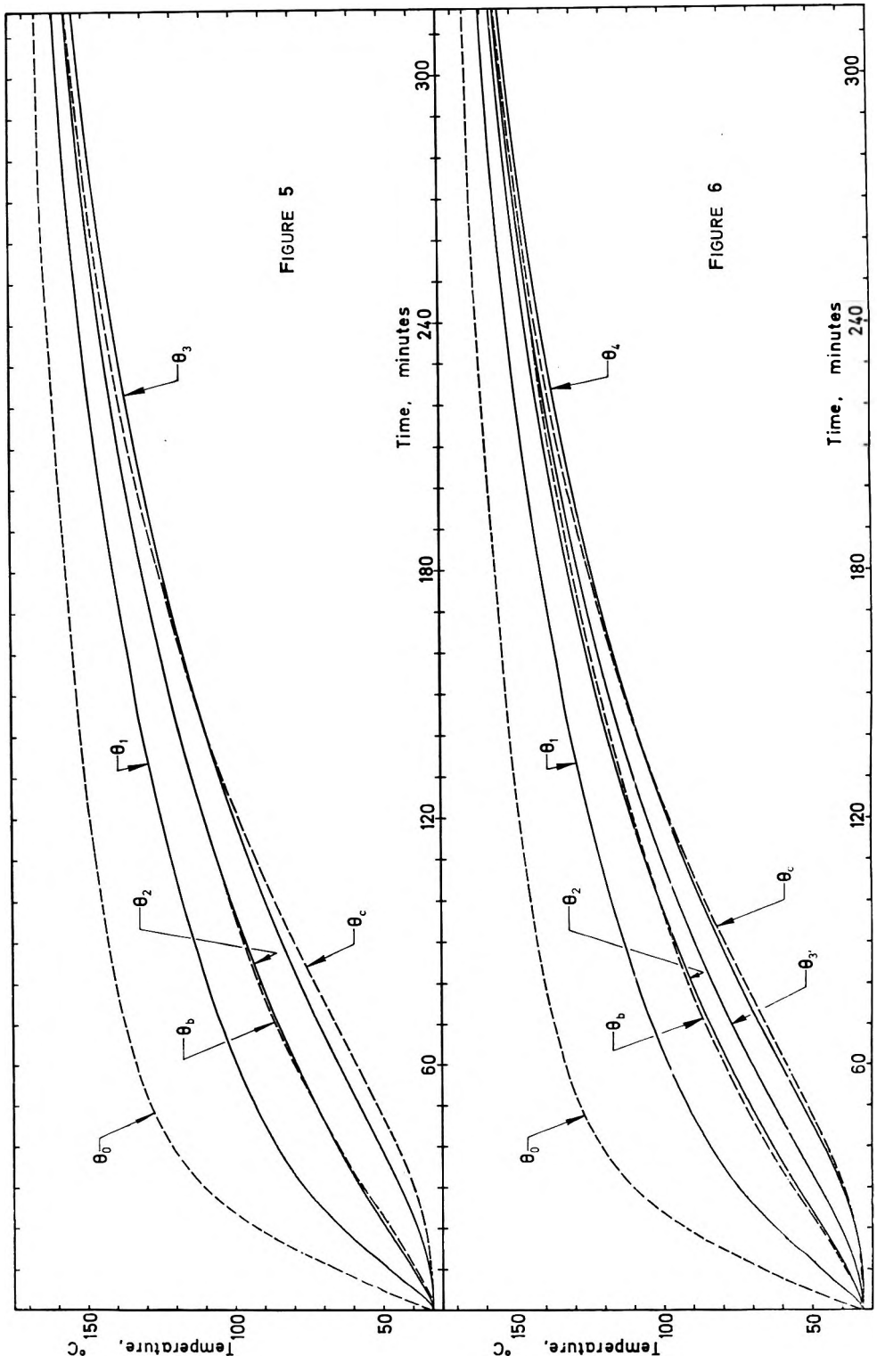
FIGURE 5
Temperature, °C
Time, minutes
50
100
150
60
120
180
240
300
θ0
θb
θ2
θ1
θc
θ3
FIGURE 6
Temperature, °C
Time, minutes
50
100
150
60
120
180
240
300
θ0
θb
θ2
θ1
θc
θ3'
θ4

the payload of Petri dishes inside it, and a consequence of this was apparent in the process of fitting model A. The values of the individual parameters p_{01}, p_{12}, containing the heat transfer coefficients h_{01}, h_{12} for the outer and inner surfaces of the tin, were clearly much less important than the overall resistance to heat transfer from the outside to the inside of the tin, represented by the overall coefficient in the table. This observation led to the arbitrary decision to fix the ratio p_{01}/p_{12} when fitting model B.

A surprising and as yet unexplained result is that the inner air temperature θ_b was less well represented by model B than by model A. This may be the result of an imperfection of the fitting process rather than of more fundamental origin. As was noted earlier the fitting process used was selected for availability and convenience rather than for fundamental suitability for this purpose. The minimization procedure used had proved highly reliable in previous applications and converged well in initial tests with artificial data. Model A was fitted without excessive difficulty, but with model B convergence was less satisfactory and some attempts with models of this type failed. For this reason more complicated models have not yet been tried.

Conclusions

The practicability has been demonstrated of fitting relatively simple mathematical models to experimental data for a system undergoing sterilization under practical conditions. The models obtained, expressed as a set of simultaneous linear differential equations which contain the heat transfer coefficients in their parameters, yield estimates of these heat-transfer coefficients as a by-product.

The applicability of this approach to design is a matter of conjecture, but it seems probable that correlations obtained in this way, from data for various combinations of sterilizing oven, packing or payload, could be used to predict the behaviour of further, different combinations. Such a treatment might offer practical advantages over either more conventional methods of prediction or a purely empirical approach.

Acknowledgements

Our thanks are due to Dr. K. Wibberley of this School for his helpful comments on the draft of this paper, to Dr. G. C. Coggan for full details of his Multifit programme, and to the University of London Institute of Computer Science for the provision of computing facilities.

FIG. 5. Time-temperature profiles for model A.

Broken lines:

θ_0 Oven air temperatures—smoothed observed values from thermocouple θ_a.

θ_b Observed inner air temperature.

θ_c Observed dish-centre temperature.

Continuous lines:

θ_1 Temperature of tinplate container, from model.

θ_2 Inner air temperature, from model (comparable with θ_b).

θ_3 Dish temperature from model (comparable with θ_c).

FIG. 6. Time-temperature profiles for model B.

Continuous lines:

θ_3' Temperature of dish outer element, from model.

θ_4 Temperature of dish inner element, from model (comparable with θ_c).

All other details are as for FIG. 5, above.

REFERENCES

CARSLAW, H. S. & JAEGER, J. C. (1959). *The conduction of heat in solids*, 2nd edn., Oxford: Clarendon Press.

COGGAN, G. C. (1967). In *Symposium on efficient computer methods for the practising chemical engineer*, Nottingham, April, 1967. Editor: Pirie, J. M. London: The Institution of Chemical Engineers.

DAVIDON, W. C. (1959). *A.E.C. Research and development report ANL*-5990/1959. New York: Argonne National Laboratory.

FLETCHER, R. & POWELL, M. J. D. (1963). *Computer J.*, **6**, 163–168.

JAEGER, J. C. (1945). *Proc. Camb. phil. Soc. math. phys. Sci.*, **41**, 43–49.

ROSENBROCK, H. H. & STOREY, C. (1966). *Computational techniques for chemical engineers*, 1st edn., Oxford: Pergamon Press.

J. Pharm. Pharmac., 1970, **22**, *Suppl.*, 139 S–146 S *Received March* 25, 1970

Rheology of systems containing cetrimide–cetostearyl alcohol: variation with temperature

B. W. BARRY AND G. M. SAUNDERS

School of Pharmacy, Portsmouth Polytechnic, Portsmouth, U.K.

The viscoelastic gel in the continuous phase of a liquid paraffin in water emulsion (stabilized by the mixed emulsifier cetrimide–cetostearyl alcohol) is similar to that formed by dispersing cetrimide and cetostearyl alcohol in water. The effect of temperature changes on the rheological properties of the emulsion and ternary system have been examined in continuous shear and in creep, and variations in the viscosities and compliances have been correlated with thermal phase transitions determined microscopically. The emulsion and ternary system were of maximum consistency at approximately 38° and 43° respectively; these temperatures respresent the transition from frozen smectic to liquid crystalline phase. At higher temperatures, the compliances rose and the viscosities fell as the network weakened and finally dissolved to form an isotropic solution.

The "self bodying" action of a mixed emulsifier is its ability to form mobile emulsions when present in low concentrations, and semisolid emulsions when present in moderate amounts (Barry, 1969). In the pharmaceutical and cosmetic industry, combinations of anionic, cationic or non-ionic surfactants with a fatty alcohol are widely used to control the rheological behaviour of emulsions by varying the concentration of mixed emulsifier.

The self bodying action of the mixed emulsifiers sodium dodecyl sulphate–cetyl alcohol and of cetrimide–cetostearyl alcohol has been studied (Barry, 1968; Barry & Saunders, 1970). In these emulsions the gel structure responsible for the self bodying phenomenon consists of frozen smectic phase with similar properties to an oil-free ternary system formed by dispersing cetrimide and cetostearyl alcohol in water.

In the present paper, the rheological stability of this gel network to temperature changes is investigated in an emulsion, and when formulated as a comparable ternary system.

EXPERIMENTAL AND RESULTS

Materials

Water, liquid paraffin B.P., cetrimide B.P. and cetostearyl alcohol B.P. were as used by Barry & Saunders (1970).

Penetration temperature

The penetration temperature (Tpen) of aqueous cetrimide solution into cetostearyl alcohol was determined by the method described by Lawrence (1959, 1961) and Barry & Shotton (1968). Because of confusion in the literature about the effects of surfactant concentration on the penetration temperature (Barry & Shotton, 1968),

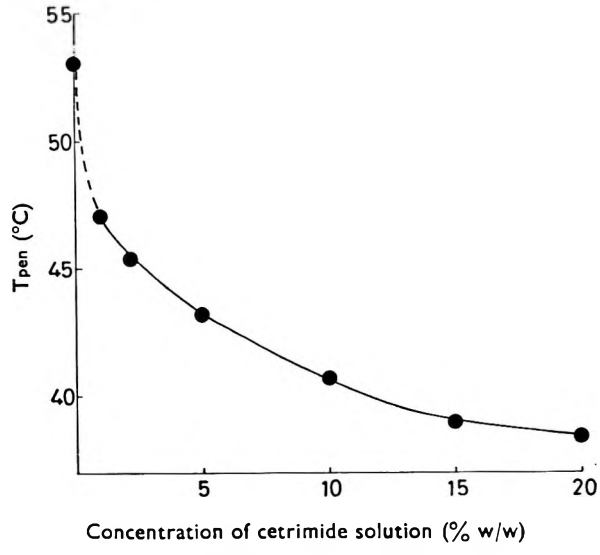

FIG. 1. Penetration temperature, Tpen, of aqueous solutions of cetrimide into cetostearyl alcohol.

measurements were made for various concentrations of cetrimide in water. The results (Fig. 1) indicated that variations in penetration temperature were most marked at low cetrimide concentrations.

Preparation and appearance of systems

The ternary system and the emulsion were made by the method of Barry & Saunders (1970) according to the formulae in Table 1. The ternary system was a white glossy semisolid which flowed only slowly under its own weight. The emulsion was a white glossy cream, of similar consistency.

Microscopy

The systems were examined microscopically using a Kofler Micro Hot Stage attached to a polarizing microscope. The ternary system contained scattered deformed globules, which often had the appearance of distorted maltese crosses when viewed between crossed polars. Most of the material became isotropic between 57–59°, and became anisotropic again on cooling.

In the emulsion, distorted oil globules often contained anisotropic crystals along the straight sides. Remnants of an ordered anisotropic filamentous matrix were visible surrounding larger globules and often enclosing aggregates of smaller globules (c.f. Barry & Saunders, 1970). Much of the anisotropic material inside or very close to the oil globules became isotropic between 38–40°. Although at about 50°,

Table 1. *Composition of ternary system and emulsion*

	Liquid paraffin	Water	Cetostearyl alcohol	Cetrimide
Ternary system	—	360	36	4·0 g
Emulsion	100	300	28·8	3·2 g

the filamentous matrix appeared unaltered in ordinary light, it was less ordered in polarized light: the matrix became completely invisible at 59°.

On cooling the emulsion, the matrix reappeared enveloping some of the larger globules. It did not regain the ordered anisotropic structure and on further cooling, acicular crystals often appeared inside the globules; these were similar to those photographed by Talman & Rowan (1968).

Continuous shear

The ternary system and the emulsion were tested at each temperature using a Ferranti Shirley Cone and Plate Viscometer (Barry & Shotton, 1967; Barry & Saunders, 1970). The apparent viscosity at 1671 s^{-1} was derived, and the approximation being made that the systems under the conditions of testing behaved as simple liquids, an apparent relative viscosity was defined as:

$$\eta'_{rel} = \frac{\text{Apparent viscosity at 1671 } s^{-1} \text{ at T°}}{\text{Viscosity of water at T°}}$$

The viscosity of water at T° was obtained from tables (Lange, 1961). This procedure eliminated the effect on the consistency of the system of a fall in the viscosity of water due solely to a rise in temperature.

Figs 2 and 3 show plots of η'_{rel} against temperature for the ternary system and the emulsion respectively.

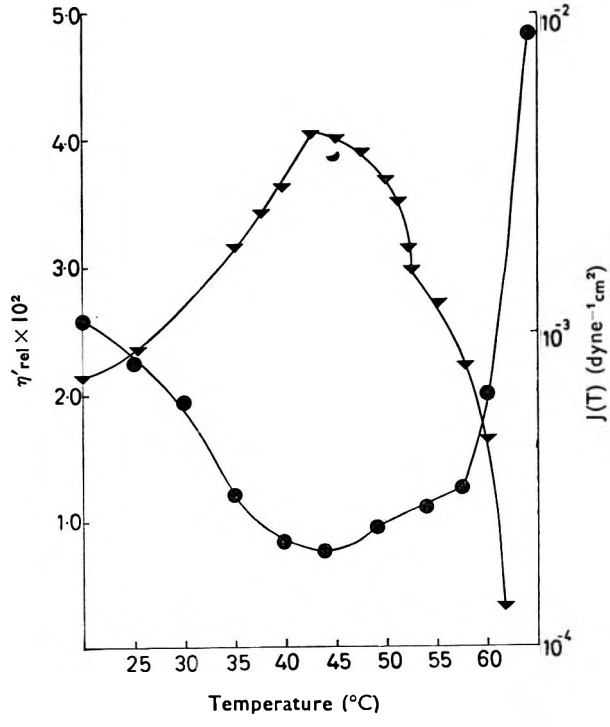

FIG. 2. Ternary system. Total compliance J (T) after 50 min creep (dyne^{-1} cm^2) —●— and apparent relative viscosity η'_{rel} —▼— versus temperature.

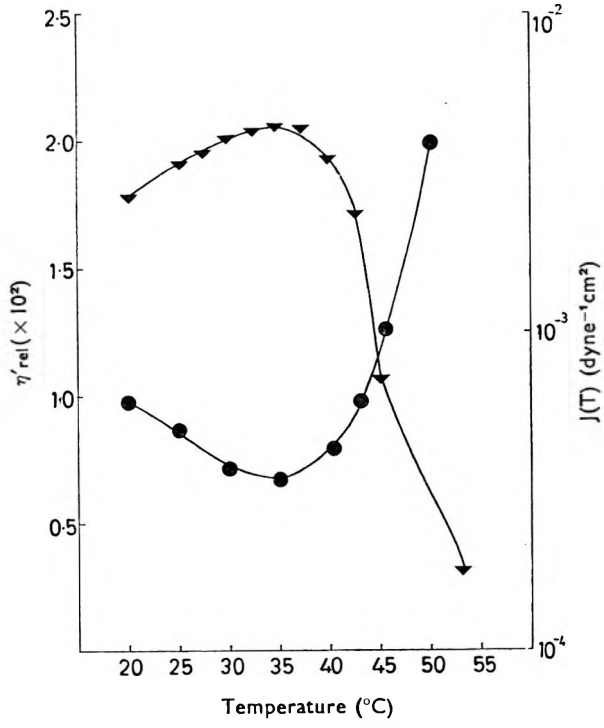

FIG. 3. Emulsion. Total compliance J (T) after 50 min (dyne^{-1} cm^2) —●— and apparent relative viscosity η'_{rel} —▼— versus temperature.

Creep compliance with time at a constant low shear stress

To apply the creep test, a concentric cylinder reaction air turbine viscometer was used, in which an air bearing centred and supported the inner cylinder, and turbine air applied a constant torque. A Kent recorder registered the development of strain with time as a continuous trace. The apparatus was calibrated in the vertical position (Barry & Saunders, 1969).

The viscometer was loaded and left overnight for stresses to relax and for temperature to equilibrate, and each test was performed in the linear region. Curves were analysed by the method of Warburton & Barry (1968), and could be represented by a mechanical model of a Maxwell Unit in series with three Voigt Units. The creep compliance was represented by the equation

$$J(t) = J_o + \sum_{n=1}^{3} J_n (1 - e^{-t/\tau_n}) + \frac{t}{\eta_o}$$

J(t) = total creep compliance at time t, where J is the ratio of shear strain to shear stress. J_o = residual shear compliance. J_1, J_2, J_3 = shear compliances of elastic parts of Voigt Units 1, 2, 3 respectively. τ_1, τ_2, τ_3 = retardation times of Voigt Units 1, 2, 3 respectively. η_o = residual shear viscosity. Figs 2 and 3 include plots of total compliance against temperature for the ternary system and the emulsion. Table 2 includes the creep parameters for the ternary system. Figs 4–7 are plots of the residual and Voigt Unit compliances and viscosities for the emulsion.

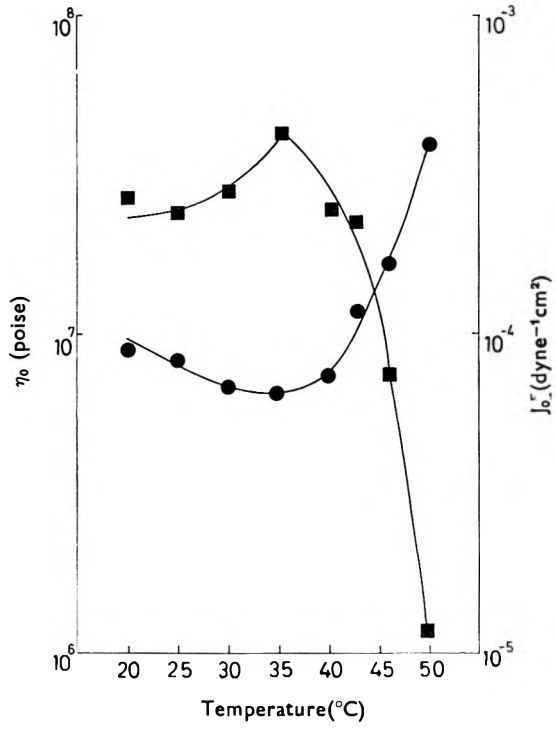

FIG. 4. Residual compliance J_0 (dyne^{-1} cm^2) —●— and residual viscosity η_0 (poise) —■— versus emulsion temperature.

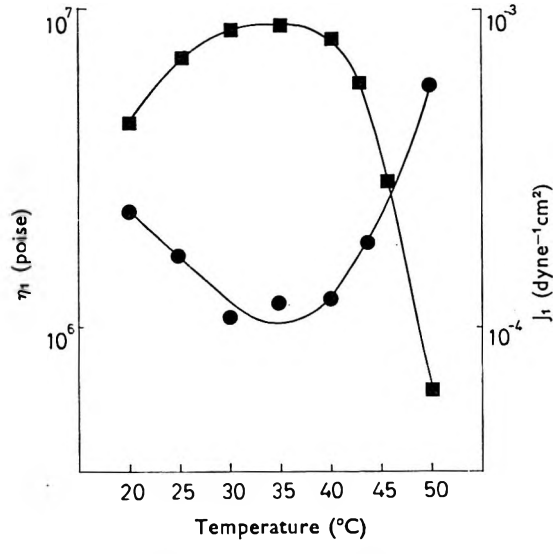

FIG. 5. Compliance J_1 (dyne^{-1} cm^2) —●— and viscosity η_1 (poise) —■— of Voigt Unit 1 versus emulsion temperature.

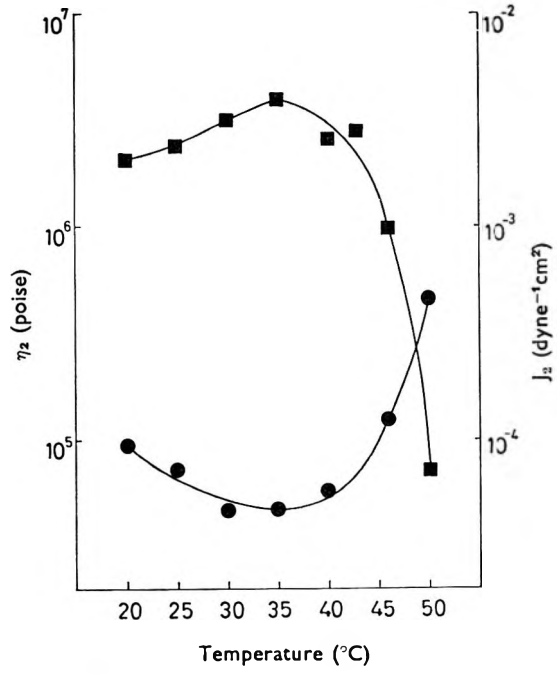

FIG. 6. Compliance J_2 (dyne^{-1} cm^2) —●— and viscosity η_2 (poise) —■— of Voigt Unit 2 versus emulsion temperature.

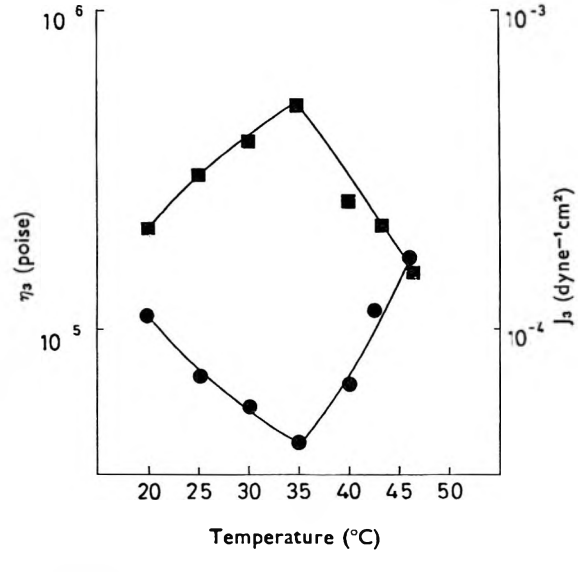

FIG. 7. Compliance J_3 (dyne^{-1} cm^2) —●— and viscosity η_3 (poise) —■— of Voigt Unit 3 versus emulsion temperature.

DISCUSSION

From the penetration temperature experiments, the minimum temperature for interaction between 1% cetrimide solution and cetostearyl alcohol to form liquid crystals is 47°. During mixing of the ternary system, molten alcohol streamed through the mixture and cetrimide solution penetrated it to form liquid crystals. As the system rapidly cooled to below the penetration temperature, interaction was greatly reduced and the system precipitated to form a three dimensional viscoelastic gel network. When viewed between crossed polars, anisotropic structures often failed to become isotropic at the melting point of the cetostearyl alcohol but did so at a higher temperature. They were thus frozen smectic phase: similar, though larger, structures have been reported in anionic ternary systems (Barry & Shotton, 1967).

During the preparation of the emulsion, as the ingredients cooled, the alcohol diffused into the continuous phase and formed liquid crystals; a small proportion of the liquid paraffin was also solubilized. Thus the cooled emulsion consisted essentially of a ternary cetrimide–cetostearyl alcohol–water gel with liquid paraffin droplets dispersed in it. When the emulsion was diluted, remnants of this gel were visible microscopically as an anisotropic filamentous matrix which surrounded large oil globules and aggregates of smaller globules. Microscopic examination showed that this gel network melted and dissolved to form an isotropic solution over a temperature range of approximately 38° to 59°.

These thermal phase transitions in the ternary system and the emulsion are important for an explanation of the rheological properties of the formulations.

Rheological examination

At all temperatures the flow curves from the continuous shear experiments were hysteresis loops, with the down curves to the left of the up curves. These loops were caused by breakdown of structure on shearing, and thus the results obtained in this work were a measure of the ability of the systems to resist structural breakdown in continuous shear; they also reflect the relation between this ability and temperature. In creep, the method of testing does not significantly alter the structure, and thus systems were examined in their rheological ground state.

Upon raising the temperature, the consistency of the ternary system increased to a maximum at 43°. This was shown in continuous shear by the maximum viscosity at 43°. In creep, similar maxima were obtained for all the viscosities and corresponding minima for all the compliances at this temperature (Table 2, Fig. 2).

Table 2. *Ternary system: analysis of creep curves*

Temperature °C	Residual Dashpot η_0 (poise × 10^7)	Residual spring J_0 (dyne^{-1} cm^2 × 10^{-6})	Voigt Unit 1 η_1 (× 10^7)	Voigt Unit 1 J_1 (× 10^{-6})	Voigt Unit 1 τ_1 (s)	Voigt Unit 2 η_2 (× 10^6)	Voigt Unit 2 J_2 (× 10^{-6})	Voigt Unit 2 τ_2 (s)	Voigt Unit 3 η_3 (× 10^6)	Voigt Unit 3 J_3 (× 10^{-6})	Voigt Unit 3 τ_3 (s)
20	0·71	9·14	0·38	26·1	1010	1·26	10·70	136	2·05	15·90	32
25	0·97	10·4	0·32	29·8	958	1·34	10·9	145	2·40	8·81	21
30	1·77	10·4	0·64	17·2	1100	2·98	8·10	241	3·77	9·4	35
35	5·29	5·6	1·03	11·4	1180	3·50	4·48	157	4·24	4·35	18·5
40	7·11	3·99	1·43	8·32	1190	6·17	2·99	185	6·53	3·54	23
44	4·89	3·63	2·11	5·44	1150	5·20	3·06	159	5·66	3·00	17
49	6·23	3·82	1·38	7·88	1090	4·59	4·24	195	7·12	4·35	31
54	4·29	5·06	1·47	10·1	1480	6·41	4·03	258	5·13	4·59	24
57·5	2·74	4·71	8·11	9·88	871	4·08	4·12	168	5·00	5·12	26
60	1·59	8·63	7·28	21·8	1580	1·57	11·1	174	2·75	8·87	24

dyne^{-1} cm^2 = N^{-1} m^2 × 10^1

Such a gradual increase in consistency up to 43° may be caused by increased Brownian movement in the system. This is believed to bring free ends of strands into contact with the main meshwork so as to form new linkages and strengthen the network. As the retardation times did not change markedly with rise in temperature (Table 2) the nature of any such secondary bonds would not alter, although their number would increase.

The temperature for maximum consistency was close to the transition temperature from frozen smectic to liquid crystalline phase, and this temperature was lower than the penetration temperature of 1% cetrimide solution into cetostearyl alcohol. As the temperature increased above 43°, the consistency decreased as the network became true smectic phase. This phase was still viscoelastic and thus there were shoulders on the continuous shear and creep curves between approximately 50° and 57°. Above 57°, significant quantities of the smectic phase dissolved to form an isotropic solution and the network disintegrated causing a steep fall in viscosity with a rise in compliance (Fig. 2).

In the emulsion, as in the ternary system, there was an initial increase in consistency as the temperature increased. This was shown in the continuous shear results, and by the viscoelastic parameters obtained in creep. From the positions of the maxima and minima in Figs 3–7 the transition temperature from frozen smectic to smectic phase in the emulsion was about 37°, i.e. several degrees lower than the transition temperature for the ternary system. Such a shift is attributed to the liquid paraffin in the emulsion, which lowers the temperature for phase transitions. Davis (1969) has obtained similar results for a commercial sample of cetrimide cream B.P.C., although the maxima and minima were not as well defined.

Further evidence that the gel network in the continuous phase of the emulsion was similar to the network in the ternary system was obtained from the plots of total compliance against temperature (Figs 2 and 3). The shapes of the curves are almost identical, although the emulsion plot is shifted along the temperature axis towards lower values, due to the lowering of phase transition temperatures by the liquid paraffin.

The similarities were less marked in the continuous shear results, which showed a very rapid reduction in viscosity above the transition temperature (Fig. 3). At high shear rates and high temperatures the rheology was complicated as oil globules coalesced.

REFERENCES

BARRY, B. W. (1968). *J. Colloid. Inter. Sci.*, **28**, 82–91.

BARRY, B. W. (1969). *J. Pharm. Pharmac.*, **21**, 533–540.

BARRY, B. W. & SAUNDERS, G. M. (1969). *Ibid.*, **21**, 607–609.

BARRY, B. W. & SAUNDERS, G. M. (1970). *J. Colloid Inter. Sci.*, in the press.

BARRY, B. W. & SHOTTON, E. (1967). *J. Pharm. Pharmac.*, **19**, *Suppl.*, 110S–120S.

BARRY, B. W. & SHOTTON, E. (1968). *Ibid.*, **20**, 242–243.

DAVIS, S. S. (1969). *J. pharm. Sci.*, **58**, 418–421.

LANGE, N. A. (1961). *Handbook of Chemistry*, 10th Edn, p. 1668. New York: McGraw-Hill.

LAWRENCE, A. S. C. (1959). *Nature, Lond.*, **183**, 1491–1494.

LAWRENCE, A. S. C. (1961). *Surface Activity and Detergency*, pp. 158–192. Editor: Durham, K. London: Macmillian.

TALMAN, F. A. J. & ROWAN, E. M. (1968). *J. Pharm. Pharmac.*, **20**, 810–811.

WARBURTON, B. & BARRY, B. W. (1968). *Ibid.*, **20**, 255–268.

J. Pharm. Pharmac., 1970, **22**, *Suppl.*, 147 S–156 S *Received March* 25, 1970

Grade variation in the rheology of white soft paraffin B.P.

B. W. BARRY AND A. J. GRACE

School of Pharmacy, Portsmouth Polytechnic, Portsmouth, Hants, U.K.

The rheology of six grades of white soft paraffin B.P. at 25° has been investigated using continuous shear viscometry and a creep viscometer. Temperature effects between 25° and 50° have been measured in continuous shear, and activation energies from 14·0 to 25·3 k cal mol^{-1} (58·6 to 105·9 k J mol^{-1}) have been determined. Working the samples on a triple roller mill at 25° was found to decrease the apparent viscosity and, initially, to increase the yield stress. Five of the grades were linear viscoelastic, one was non-linear viscoelastic. The nature of ductility and its relation to measured rheological parameters have been discussed. Creep viscometry data gave a better correlation with the manufacturer's data than did continuous shear measurements.

White soft paraffin, which consists mainly of n-paraffins, iso-paraffins, and naphthenes (Nelson & Stewart, 1949; Asinger, 1968; Meyer, 1968), forms a colloidal gel type of structure containing oil, microcrystalline waxes and discrete crystals (Franks, 1964; Longworth & French, 1969). Its physical nature is influenced by the ratios of the component fractions of the material, and the constituents within the fractions, and thus depends on the source of the crude petroleum, the type and degree of refining, and possibly on subsequent blending processes (Mutimer, Riffkin & others, 1956; Schulte & Kassem, 1963).

There is controversy about the rheological properties of white soft paraffin which may be derived using continuous shear and small strain experiments, as well as semi-empirical methods such as penetration techniques. The soft paraffins and similar paraffinic materials have been variously reported as (*a*) elastic (Davis, 1969a), (*b*) non-linear viscoelastic (Bogie, 1968) and (*c*) linear viscoelastic (Hutton & Mathews, 1953; Criddle, 1965; Barry & Grace, 1970) in small strain experiments. Continuous shear viscometry causes either irreversible shear breakdown (Weltmann & Kuhns, 1957) or thixotropic shear breakdown (Bondi, 1951; Barry & Grace, 1970).

The purpose of this work is to investigate a series of soft paraffins of pharmacopoeial standard, using continuous shear and creep viscometers, to indicate the variation in rheological properties which may occur in white soft paraffin B.P. A more detailed rheological profile of a single sample of white soft paraffin has already been made (Barry & Grace, 1970).

EXPERIMENTAL

Materials. Samples of white soft paraffin (B.P.) were obtained from two sources. One grade (sample 1) from J. M. Loveridge Ltd. (Southampton), and five grades from Dalton & Co. Ltd. (Silkolene Oil Refinery, Belper). The manufacturer's data on these grades are given below.

Grade 783/L (Sample 2), the basic paraffin from which the others in the range are derived, is resistant to shear breakdown, and is a general use petroleum jelly; Grades 892 and 910 (Samples 3 and 4 respectively) are soft paraffins with low stability to shearing stress; Grade 944 (Sample 5) has a medium stability to shearing stresses; Grade 783/L/40A (Sample 6) is highly resistant to shear breakdown, with low ductility and viscosity. Samples 5 and 6 are produced for use in ointment manufacture. Further physical data supplied by the manufacturer are given in Table 1.

Table 1. *Manufacturer's data on the physical properties of samples 2 to 6, and activation energies for viscous flow and apparent viscosity data derived from the curves in Fig. 1*

	Manufacturer's data		Experimental data	
Sample No.	Drop point* (I.P. 31/57)°C	Unworked penetration No.* at 25°	Activation energy for viscous flow k cal mol^{-1}‡	Apparent viscosity at 25° and 1754 s^{-1} poise
1	—	—	21·9	10·2
2	46–50	155–175	21·3	6·8†
3	43–49	170–190	15·1	1·2
4	46–50	150–170	22·4	4·2†
5	47–51	200–220	14·0	4·8
6	44–48	155–175	25·3	6·2†

* Standards for Petroleum and its products, 23rd Edn (1964) part 1, pp. 266–268.
† Values derived by extrapolation of the curves.
‡ 1 k cal = 4·1868 kJ.

Continuous shear experiments. A Ferranti–Shirley cone and plate viscometer, with automatic flow curve recorder unit, was employed for continuous shear investigations (Boylan, 1967; Barry & Shotton, 1968). The viscometer, with medium cone, was used in the automatic mode and 600 s sweep time for two test regimes: (1) rates of shear varied from 0·0 to 1754·0 s^{-1} and (2) rates of shear varied from 0·0 to 175·4 s^{-1}. The temperature range was 25° to 50° (±0·1°).

The test samples were melted on a water bath at 70° and cooled for 2 h at 25° (±1·2°), as a standard procedure before comparative rheological testing (Kinsel & Phillips, 1950; Weltmann, 1960; Ackroyd & Aubrey, 1964). Apparent viscosity values were determined from the apex of the continuous shear curves (Boylan, 1967); the value obtained is equivalent to that of the Newtonian fluid whose flow curve would pass through the point used in the determination. Yield stresses were derived from the spur points in the curves where the slope of the curve became infinite for the first time. The apparent viscosity and yield stress data derived in continuous shear are given in Table 2. Fig. 1 is an Arrhenius-type plot of apparent viscosity at 1754 s^{-1} for each sample. The activation energies derived are given in Table 1.

To investigate the effect of working the samples, these were worked in an arbitrary manner using a triple roller mill (Erwerka-apparatebau Gmbh) of three ceramic rollers with axes of rotation parallel. The central roller rotated in the opposite direction to the end rollers, and each roller rotated at a different speed. A sample of material was placed on one of the end rollers and was forced into a thin film and momentarily stressed at a high rate of shear as it passed between the rollers. The sample was then carried through the second gap by the central roller. The maximum

Table 2. *Apparent viscosity and yield stress data derived by continuous shear viscometry.* η' is apparent viscosity at apex of loop (poise), σ is yield stress derived from spur points (dyne cm^{-2} or $Nm^{-2} \times 10^{-1}$). Regime 1, 0·0 to 1754·0 s^{-1} in 600 s; Regime 2, 0·0 to 175·4 s^{-1} in 600 s. The asterisks indicate gross ejection of the test sample from the measuring gap of the viscometer

	25°		30°		35°		40°		45°		50°
Regime 1 Sample No.	η'	σ	η'	σ	η'	σ	η'	σ	η'	σ	η'
1	10·2	7700	5·7	5200	3·3	2100	2·2	1300	1·2	700	0·6
2	*	3550	*	2700	2·1	1300	0·9	600	0·7	200	0·4
3	1·2	2300	1·0	1600	0·7	900	0·4	400	0·3	175	0·2
4	*	4200	2·2	2300	1·2	1900	0·7	600	0·4	250	0·2
5	4·8	2100	3·4	1400	2·2	650	1·5	450	1·1	200	0·9
6	*	4500	3·3	1600	1·5	1200	0·6	400	0·4	150	0·3
Regime 2 Sample No.											
1	61·1	5100	15·8	2900	9·2	1800	5·2	770	2·5	—	—
2	12·1	2600	10·2	1500	6·4	850	3·2	200	0·5	—	—
3	6·5	2150	5·2	950	3·3	550	2·3	200	1·0	—	—
4	10·8	3200	7·6	2100	4·4	1050	2·0	950	1·9	37	—
5	12·7	1250	8·8	910	5·7	500	4·0	200	1·8	—	—
6	19·0	2800	13·8	2700	3·6	550	2·7	300	0·6	—	—

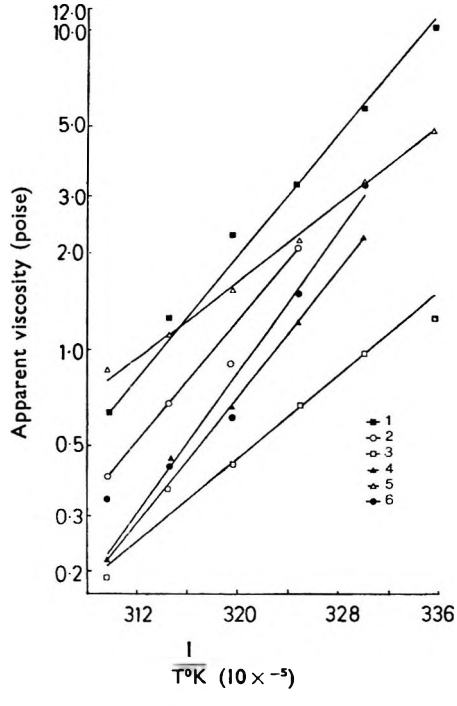

FIG. 1. Arrhenius-type plots of apparent viscosity of soft paraffin samples determined at 1754 s^{-1} using continuous shear viscometry.

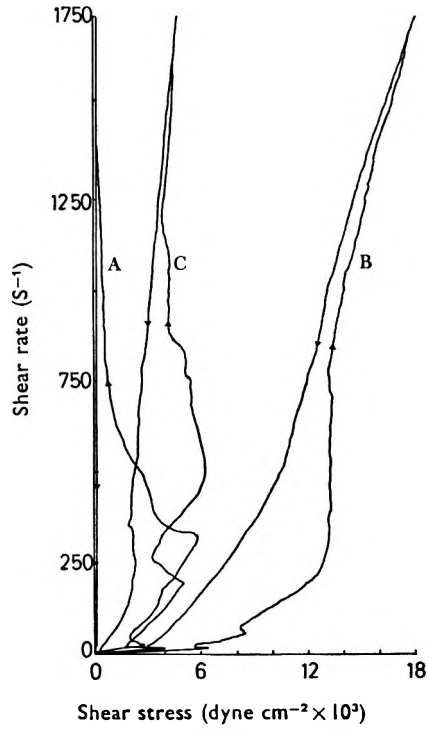

FIG. 2. Continuous shear rheograms for sample 2, obtained using Regime 1 (0·0 to 1754·0 s^{-1} n 600 s). Curve A is an unworked sample; B, worked once; C. worked four times.

shear rates in each gap were approximately 6300 s^{-1} and 10300 s^{-1}, calculated by dividing the linear velocity differences at the roller surfaces by the gap distances between them, assuming plane laminar flow in the gap.

One working thus consisted of two very short periods of shearing stress at high rates of shear.

Creep experiments. Fig. 3a is a diagram of the creep viscometer which is a modification based on a Westwind PCB III reaction air turbine (Davis, Deer & Warburton, 1968; Davis, 1969b) calibrated by the method of Barry & Saunders (1969). The inner cylinder of the viscometer was machined to the dimensions of the Haake Rotovisko MVII cylinder. The outer cylinder and water bath were adapted from those used on the Rotovisko viscometer. The water bath and enclosed cylinder were made concentric with the inner cylinder by means of a centering ring with lockable adjustable screws, and a dial gauge attached to the bearing in place of the inner cylinder. The turbine pressure, which applied the torque, was measured by mercury and water manometers at high and low pressures respectively. An air bearing pulley wheel and weights were used to supply torques in excess of those available from the compressed air supply (Barry & Saunders, 1969). The temperature was controlled by circulation of an ethylene glycol-water mixture using a Shandon Circotherm unit. A Grant CC20 cooler unit was available for temperatures below ambient.

The creep viscometer was loaded by heating the test sample to 60° in a water bath, and pouring the molten material into the outer cylinder. The inner cylinder

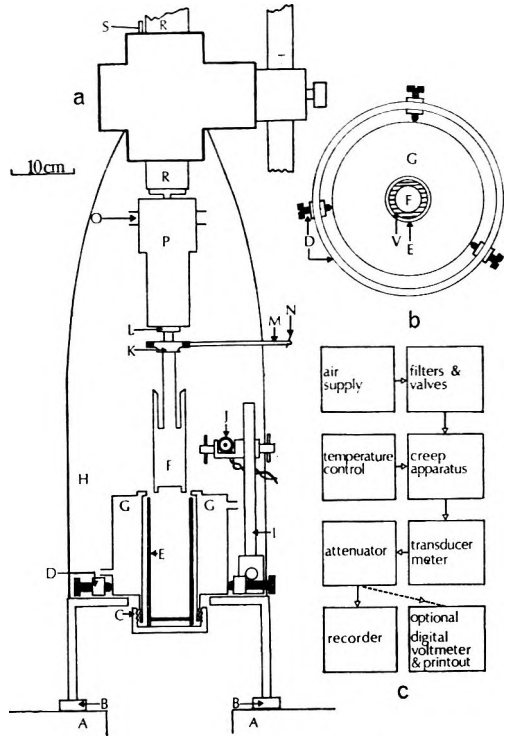

FIG. 3. (a) Sectional diagram of the creep apparatus, with transducer armature free of transducer coil, and inner cylinder in the raised position. The scale is expanded laterally to show the viscometer elements with greater clarity. A, bench; B, antivibration mounting; C, screwcap holding (E) in position; D, centering ring with adjustable lockable screws; E, outer cylinder; F, inner cylinder; G, waterbath; H, mandrell press; I, magnetic stand; J, transducer coil; K, boss; L, chuck screw; M, arm, bearing the transducer armature, N; O, ducts for air supply; P, Westwind PCB III reaction air turbine; R, operating arm; S, locating pin; T, cranking arm. (b) Plan of centering arrangement. Key as in Fig. 3a, with V as sample gap. (c) Flow chart, indicating relation between creep apparatus and ancilliary equipment.

was lowered into the liquid, and the sample left overnight at the test temperature for stresses to relax, crystallization to occur, and for temperature equilibration. As crystallization of soft paraffins has been shown to be time dependent (Kato & Saito, 1967), the samples used in creep viscometry may be considered to be one day old.

Each sample was checked for linearity and a creep test performed at 25° (±0·2°) in the linear region. The curves were analysed by the method of Warburton & Barry (1968) using the equation for a line spectrum of retardation times,

$$J(t) = J_o + \sum_{i=1}^{n} J_1 (1 - e^{-t/\tau_1}) + \frac{t}{\eta_o} \quad .. \quad .. \quad .. \quad (1)$$

where J(t) is the compliance at time t, J_o is the initial elastic compliance, J_1 is an elastic compliance associated with a viscous element, τ_1 is a retardation time, and η_o is the residual Newtonian viscosity.

A computer program was written which reconstituted the original creep curve when the derived parameters were used as input data. Analyses were accepted if the reconstituted curve lay within 2% of the experimental curve. Fig. 4 contains

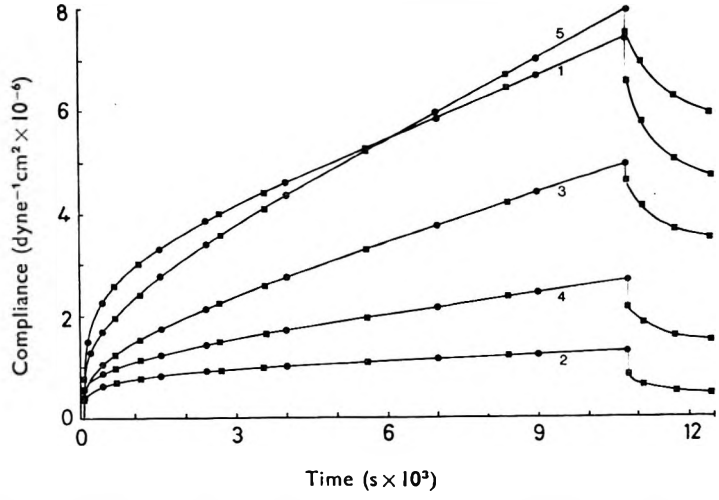

FIG. 4. Creep curves of linear viscoelastic soft paraffins. ■ Experimental data, ● reconstituted data.

creep curves for samples 1 to 5, with typical original and reconstituted coordinates, which indicate the agreement between the two sets of data.

The data derived by creep viscometry are given in Table 3. Samples 1 to 5 exhibited linear viscoelastic properties, and sample 6 was non linear (minimum stress applied 3·03 Nm^{-2}, resulting strain 4×10^{-6}). Fig. 4 indicates the differences in the flow properties at very low rates of shear. Samples 1 and 5 are similar, with

Table 3. *Rheological parameters derived for soft paraffins using creep viscometry.* The value of J_0 for sample 6 is derived from a non linear creep curve at a shear stress of 120 dyne cm^{-2}

	Sample No.					
	1	2	3	4	5	6
Compliance ($dyne^{-1}\ cm^2 \times 10^{-8}$)*						
J_0	75·7	35·5	42·6	47·3	51·0	34·9
J_1	98·0	31·5	75·0	37·0	105·0	
J_2	45·2	10·0	23·0	14·6	39·3	
J_3	38·8	6·20	2·40	12·5	34·7	
J_4	46·0	5·50	10·4	9·90	—	Exhibits non-linear visco-elastic behaviour
Retardation time (s)						
τ_1	1360	1424	1495	2059	1413	
τ_2	236	238	104	487	38	
τ_3	45	38	12	52	2	
τ_4	8	5	2	7	—	
Viscosity (poise × 10^8)						
η_1	13·9	45·2	19·9	55·7	13·5	
η_2	5·2	23·8	4·54	33·4	0·98	
η_3	1·16	6·13	5·00	4·18	0·06	
η_4	0·18	0·83	0·20	0·75	—	
η_0	24·6	278	31·5	73·5	19·0	

* $dyne^{-1}\ cm^2 = N^{-1}\ m^2 \times 10^1$.

large elastic compliance and low residual Newtonian viscosity. Sample 2 had a high residual viscosity and low elastic compliance. The total elastic compliance of sample 1 is over three times that of sample 2, and their residual viscosities differ by a factor of ten. The mechanical representation of the linear viscoelastic properties of the samples of soft paraffin used in this work consists of one Maxwell unit in series with four Voigt (Kelvin) units, except for sample 5 which has three Voigt units.

DISCUSSION

The continuous shear flow curves determined for these samples are anticlockwise hysteresis loops, each containing a spur point indicating a yield stress. At higher temperatures the extent of hysteresis, as measured by the area of the loop, was reduced, and the magnitude of the yield stresses decreased. The anticlockwise loops indicate either irreversible shear breakdown or thixotropy. It has been shown that sample 1 may undergo partial thixotropic breakdown (Barry & Grace, 1970).

The apparent viscosity of some of the soft paraffins could not be determined at low temperatures as test samples were ejected from the cone-plate gap; this may be due to elastic recovery or fracture of the material, or both (Hutton, 1963; Davis, 1969a). Application of a cone and plate instrument to routine testing procedures is severely limited when the phenomenon occurs. Sample 2 was almost completely ejected immediately after the spur point (see Fig. 2); with sample 1 there was no visible ejection of the test material, but the possibility exists that a small amount is lost, causing errors in viscosity determination.

The Arrhenius-type plots of apparent viscosity at 1754 s^{-1} versus inverse absolute temperature, Fig. 1, are approximately linear (c.f. Barry & Grace, 1970). The values of apparent viscosity derived using regime 2 also give linear plots, although the data are more scattered. Extrapolation of the curves in Fig. 1 indicates that there is not a large difference in the apparent viscosity between samples at 25°, see Table 1. The expulsion of the test samples from the measuring gap of the cone and plate viscometer is thus probably not a function of viscosity alone.

Activation energies for viscous flow of the samples were derived from Fig. 1 using equation 2, which is a viscosity modification of the Arrhenius equation (Arrhenius, 1912), and these are listed in Table 1.

$$\eta = Ke^{E/RT} \qquad (2)$$

Where η is the apparent viscosity, K is a constant, E is the activation energy for viscous flow, R is the gas constant, and T the absolute temperature. Although controversy exists about the validity of activation energies derived using this equation (Jobling, 1953; Bondi, 1956)—the data may not be of fundamental significance—they are given to indicate the differences which may occur in the flow properties of the soft paraffins. Activation energies for viscous flow derived by continuous shear viscometry are in the form of an overall average (Barry & Grace, 1970) and they are concerned with the energy necessary to cause the individual components of the paraffin to move from one equilibrium position to another in the direction of flow (Glasstone, Laidler & Eyring, 1947; Eyring, 1956). The difference between the upper and lower values is approximately 10 k cal mol^{-1} (42 kJ mol^{-1}), which indicates that the sizes of the flowing entities vary considerably. A possible cause

of such variation is the differences in the ratios of solid to liquid paraffins within the different samples. A high percentage of solid paraffins would increase the mean size of the flow units. These would have to overcome a higher potential energy barrier in order to flow, and therefore require a higher activation energy.

Arrhenius-type plots of the yield stresses determined in continuous shear were linear for each sample, as previously reported for sample 1 (Barry & Grace, 1970) and in agreement with earlier work on similar materials (Ramaya, 1944; Berneis & Münzel, 1964).

When the soft paraffins were milled, structure broke down. This was indicated rheologically by a lower value of apparent viscosity at high rates of shear, see Fig. 2. The unworked sample was ejected from the cone-plate gap at high rates of shear. After one passage through the triple roller mill the material gave a full rheogram with a *larger* yield stress than in the unworked test sample. The single working damaged the fibrous crystal matrix (Jones & Tyson, 1952; Van der Have & Verver, 1957) and ruptured secondary valence bonds within the material (Münzel, 1968). Two possible causes for the increase in yield stress are: (*a*) a thin film of soft paraffin forms on the roller mill which may cause orientation of the large acicular crystals thus superimposing further structure upon that remaining in the sample, and (*b*) it is possible that ejection of unworked sample from the measuring gap begins to occur while the spur point is forming. The reduction in the elastic modulus of the material caused by milling would tend to allow the material to remain in the measuring gap for a longer period, thus increasing the stress reading. After the test sample was milled four times, it gave a rheogram with a much lower apparent viscosity, and the yield stress was less than after one working, but still larger than in the unmilled sample. This decrease indicates a gross breakdown of the three dimensional matrix within the test sample of soft paraffin.

The continuous shear investigations indicate that sample 1 differs from samples 2 to 6. The apparent viscosity and yield stress for temperatures up to 40° are generally higher than those of samples 2 to 6, although the activation energy is comparable with those of samples 2 and 4.

Yield stresses measured in continuous shear viscometry are a function of some property of the material, and not due solely to instrumental effects, although these may contribute to the magnitude of the yield stresses (Barry & Grace, 1970). Davis (1969a) has suggested that yield phenomena are associated with crystalline materials which are susceptible to mechanical strain, and has correlated long retardation times determined in creep with high yield stresses determined in continuous shear. Comparison of the continuous shear and creep data derived for samples 2 to 5 indicates a similar correlation, especially with the second and third retardation times. Sample 6 is not considered as it is non-linear viscoelastic and the creep curve cannot be represented by the equation used in this work. Sample 1 is exceptional (c.f. continuous shear work) as it has large yield stresses, but only moderate retardation times.

Ductility, a rheological property of soft paraffins, is concerned with the capacity of the material to form filaments when subjected to a tensile stress and depends on the variation in viscosity which occurs during elongation of the filament (Bikerman, 1960). Stefan's equation (Stefan, 1874) indicates that the initial force necessary for filament elongation in a Newtonian material is directly proportional to the shear viscosity of the material. The behaviour of non-Newtonian materials cannot readily

be treated mathematically, but is quantitatively similar. The ductility, or fibre length, of soft paraffins is variable (Warth, 1956) and is usually determined subjectively, although a physical test has been proposed (Kinsel & Schindler, 1948). In our work there is no clear relation between ductility and the continuous shear data. In creep, with the exception of sample 6, which is non-linear, the total compliance at any given time is greater the more ductile the sample. For example, sample 2 has a low compliance, indicating a high residual viscosity, and the manufacturers' data indicate that it is resistant to shear breakdown. Under such conditions the force necessary to cause filament elongation exceeds the cohesive strength of the material and fracture occurs. The material is thus of low ductility, or short fibre length. Sample 5 is compliant in creep, and is less resistant to stress than is sample 2. Thus an applied tensile stress causes formation and elongation of filaments, and the material is highly ductile. The creep curve of sample 6, which has a low ductility, could not be analysed, but it indicated a large total compliance, that is, a low apparent viscosity, at 120 dyne cm^{-2} (12·0 Nm^{-2}). The manufacturer reports that this sample is highly resistant to stress. Thus, in elongational strain, fracture occurs despite the low apparent viscosity of the material.

When soft paraffins are used in cold working procedures, the apparent viscosity of the material needs to be considered, as more energy is required to manipulate a highly viscous material. The determination of apparent viscosity of the soft paraffins at 25° using continuous shear viscometry was inconclusive, due to expulsion of the material from the cone-plate gap. Creep viscometry indicated that sample 2 is highly viscous, but samples 5 and 6, which are derived from it, are both of low viscosity, which confirms their suitability for ointment manufacture with respect to low energy consumption. However, sample 5 is highly ductile, which is a disadvantage in cold working. Sample 6, which has a low ductility and a low apparent viscosity, is therefore best suited for cold working procedures.

When soft paraffins are used in ointments manufactured by fusion, the apparent viscosity and ductility have little effect on the efficiency of manufacture, whilst factors such as melting and congealing points become important.

This work has shown the rheological variation which may occur between different grades of white soft paraffin of pharmacopoeial quality. Interbatch variations have not been studied, although they may be considerable, since the blending of soft paraffins with other paraffinic petroleum derivatives to specific requirements is an empirical procedure. Subsequent grading depends on physical tests such as melting point, worked and unworked penetration tests, and complex parameters determined subjectively. The investigation indicates that rheological techniques may be utilized, and that whilst creep viscometry uses very low rates of shear, the data derived show the pattern of the grade properties (as indicated by the manufacturer) far better than do those data derived in cone and plate continuous shear viscometry at high rates of shear.

REFERENCES

ACKROYD, G. C. & AUBREY, K. V. (1954). *Proc. 2nd. Intern. Cong. Rheol.*, pp. 397–407. Editor: Harrison, V. G. W. London: Butterworths.

ARRHENIUS, S. (1912). *Medd. Rungl. Velenskapsakad. Nobel Inst.*, **2**, 8.

ASINGER, F. (1968). *Paraffins, Chemistry and Technology*, Oxford: Pergamon.

BARRY, B. W. & GRACE, A. J. (1970). Paper delivered at conference '*Rheology in Medicine and Pharmacy*,' School of Pharmacy, London. Proceedings to be published.

BARRY, B. W. & SAUNDERS, G. M. (1969). *J. Pharm. Pharmac.*, **21**, 607–609.

BARRY, B. W. & SHOTTON, E. (1968). *Ibid.*, **20**, 167–168.

BERNEIS, K. & MÜNZEL, K. (1964). *Pharm. Acta Helv.*, **39**, 88–100.

BIKERMAN, J. J. (1960). *Rheology, Theory and Applications*, vol. 3, pp. 481–482. Editor: Eirich, F. R. London: Academic Press.

BOGIE, K. D. (1968). *Paper delivered at Brit. Soc. Rheol. Conf.*, Swindon, England.

BONDI, A. (1951). *Physical Chemistry of Lubricating Oils*, p. 68. New York: Reingold.

BONDI, A. (1956). *Rheology, Theory and Applications*, vol. 1, p. 329. Editor: Eirich, F. R. London: Academic Press.

BOYLAN, J. C. (1967). *J. pharm. Sci.*, **56**, 1164–1169.

CRIDDLE, D. W. (1965). *Trans. Soc. Rheol.*, **9**, 287–297.

DAVIS, S. S. (1969a). *J. pharm. Sci.*, **58**, 412–418.

DAVIS, S. S. (1969b). *J. Scient. Instrum., series* 2, **2**, 102–103.

DAVIS, S. S., DEER, J. J. & WARBURTON, B. (1968). *Ibid.*, **1**, 933–936.

EYRING, H. (1956). *Rheology, Theory and Applications*, vol. 1, pp. 469–471. Editor: Eirich, F. R. London: Academic Press.

FRANKS, A. J. (1964). *Soap Perfum. Cosm.*, **37**, 221–230.

GLASSTONE, S., LAIDLER, K. J. & EYRING, H. (1947). *Theory of Rate Processes*, New York: McGraw-Hill.

HUTTON, J. F. (1963). *Nature, Lond.*, **200**, 646–648.

HUTTON, J. F. & MATHEWS, J. B. (1953). *Proc. 2nd Intern. Cong. Rheol.*, pp. 408–413. Editor: Harrison, V. G. W. London: Butterworths.

INSTITUTE OF PETROLEUM (1964a). *Standards for Petroleum and its Products*, 23rd edition, part 1, pp. 545–546.

INSTITUTE OF PETROLEUM (1964b). *Ibid.*, pp. 266–268.

JOBLING, A. (1953). *Proc. 2nd Intern. Cong. Rheol.*, p. 444. Editor: Harrison, V. G. W. London: Butterworths.

JONES, S. P. & TYSON, J. K. (1952). *J. colloid Sci.*, **7**, 272–283.

KATO, Y. & SAITO, T. (1967). *Arch. Pract. Pharm.*, **27**, 127–129.

KINSEL, A. & PHILLIPS, J. (1950). *Drug all. Ind.*, **36**, 25–29.

KINSEL, A. & SCHINDLER, H. (1948). *Petrol. Refiner*, **27**, 124–127.

LONGWORTH, A. R. & FRENCH, J. D. (1969). *J. Pharm. Pharmac.*, **21**, *Suppl.*, 1S–5S.

MEYER, E. (1968). *White Mineral Oil and Petrolatum and their related products*, New York: Chemical Pub. Co.

MÜNZEL, K. (1968). *J. Soc. cosmet. Chem.*, **19**, 289–343.

MUTIMER, M. N., RIFFKIN, C., HILL, J. A. & CYR, G. N. (1956). *J. Am. pharm. Soc. (Sci. Edn)*, **45**, 101–105.

NELSON, W. L. & STEWART, L. D. (1949). *Ind. Engng Chem.*, **41**, 2231–2238.

RAMAYA, K. S. (1944). *Conf. on Viscosity of Liquids and Colloidal Solutions, U.S.S.R.*, **2**, 179–187.

SCHULTE, K. E. & KASSEM, M. A. (1963). *Pharm. Acta Helv.*, **38**, 358–370.

STEFAN, M. J. (1874). *Sitzber. Akad. Wiss. Wien. Math-Naturw. Kl. Abt.*, II **69**, 713–735.

VAN DER HAVE, J. H. & VERVER, C. G. (1957). *Petroleum and its products*, pp. 334–348. London: Pitman.

WARBURTON, B. & BARRY, B. W. (1968). *J. Pharm. Pharmac.*, **20**, 255–268.

WARTH, A. H. (1956). *Chemistry and Technology of Waxes*, 2nd Edition, New York: Reingold.

WELTMANN, R. N. (1960). *Rheology, Theory and Applications*, vol. 3, pp. 208–209. Editor: Eirich, F. R. London: Academic Press.

WELTMANN, R. N. & KUHNS, P. W. (1957). *Lubric. Engng.*, **13**, 43–50.

J. Pharm. Pharmac., 1970, **22**, *Suppl.*, 157 S–162 S *Received March* 18, 1970

Application of the Ferguson principle to the antibacterial activity of mono- and multi-component solutions of quaternary ammonium surface-active agents

H. H. LAYCOCK AND B. A. MULLEY

Postgraduate School of Studies in Pharmacy, University of Bradford, Bradford 7, U.K.

Critical micelle concentrations (CMC) have been measured by the surface tension method for binary mixtures of dodecyltrimethylammonium bromide with tetradecyltrimethylammonium bromide, binary mixtures of C_{14}/C_{16} homologues, a ternary mixture of the $C_{12}/C_{14}/C_{16}$ compounds and additionally for each component individually. The antibacterial activities of the systems against *Escherichia coli* were determined by a British Standard Method (B.S. 3286: 1960). Thermodynamic activities of the solutions at two survivor levels, calculated from the physical and biological measurements, were sufficiently constant to sustain the Ferguson principle for these micelle-forming antibacterial agents. A theoretical treatment of micelle formation for multi-component solutions of surfactants gave CMC's by calculation in close agreement with the experimentally determined values. The purity and composition of the surfactants was determined by gas liquid chromatography.

Links between the surface and micellar properties of quaternary ammonium compounds and their antibacterial action have been noted in many literature reports and attempts have been made to put these relations on a more fundamental basis by suggesting that the Ferguson principle applied to the antibacterial action of cationic surfactants (Ecanow & Siegel, 1963). In a study on three quaternary ammonium chlorides, that were not members of a homologous series, Weiner, Hart & Zografi (1965) reported a clear relation between the thermodynamic and antibacterial activities could be recognized if the former were expressed as a ratio of the surface concentration produced by a solution and the surface concentration at the critical micelle concentration (CMC), rather than by using bulk solution concentrations.

In practice most quaternary ammonium compounds are mixtures of homologues and it therefore seemed of value to test whether the Ferguson principle extended to multi-component solutions. Further experimental evidence on mono-component systems using a different series of compounds from those investigated by Weiner & others also seemed desirable. This paper describes experiments on both aspects using the widely studied homologous series n-dodecyl, n-tetradecyl and n-hexadecyl trimethylammonium bromides individually, and with binary systems containing C_{12}/C_{14} or C_{14}/C_{16} mixtures over a wide range of mol fractions of each component. Cetrimide B.P., a ternary mixture containing the same three homologues, was also investigated.

EXPERIMENTAL AND RESULTS

Assessment of homologue composition and purity of the surfactants

(a) *n-Alkyltrimethylammonium bromides.* Samples of dodecyltrimethylammonium bromide (DTAB) (C_{12}), tetradecyltrimethylammonium bromide (TTAB) (C_{14}) and hexadecyltrimethylammonium bromide (HTAB) (C_{16}) were kindly provided by Dr. J. E. Adderson. Certain analytical data for TTAB has been given by Adderson & Taylor (1964). The homogeneity of the three surfactants was confirmed by the method of Laycock & Mulley (1966).

(b) *Cetrimide B.P.* This was identical with sample B, Table 1 of our earlier paper. It contained about 27, 62, and 11% respectively of the C_{12}, C_{14}, and C_{16} homologues (mol fractions 0·251, 0·628 and 0·121) and the mean molecular weight calculated from this composition is 332.

Table 1. *Bactericidal concentrations of quaternary ammonium compounds and their mixtures for two survivor levels of* E. coli, *and associated* CMC *and thermodynamic activities*

Compound or mixture (mol fraction)	Bactericidal concentration (mM) at survivor levels of 1·0%	0·01%	CMC (mM)	Thermodynamic activities at survivor levels of 1·0%	0·01%
C_{12}	0·26	0·60	14·7	0·018	0·041
C_{12}/C_{14} (0·766/0·234)	0·11	0·30	6·90	0·016	0·043
C_{12}/C_{14} (0·522/0·478)	0·076	0·175	4·3	0·018	0·041
C_{12}/C_{14} (0·267/0·733)	0·06	0·13	3·2	0·019	0·041
C_{14}	0·047	0·11	3·1	0·015	0·036
C_{14}/C_{16} (0·764/0·236)	0·026	0·068	1·57	0·017	0·043
C_{14}/C_{16} (0·520/0·480)	0·019	0·052	1·12	0·017	0·046
C_{14}/C_{16} (0·265/0·735)	0·015	0·039	0·95	0·016	0·041
C_{16}	0·014	0·036	0·90	0·016	0·040
$C_{12}/C_{14}/C_{16}$ (0·251/0·628/0·121)	0·033	0·087	2·20	0·015	0·040

CMC *measurements.* The surface tension method was adopted using the Du Nouy ring apparatus (Cambridge Instrument Co.). Solutions of the surfactants or surfactant mixtures were prepared in water which had been distilled from an all-glass apparatus, and the surface-tensions measured at 21° ± 1°. Plots of surface-tension against the logarithm of the surfactant concentration were linear, giving two straight lines the intersect of which was taken as the CMC. Surface ageing (Padday, 1960), observed at the lower concentrations, was not significant near the CMC. Although the Harkins & Jordan (1930) corrections altered the surface-tension values in the expected way, the CMC values did not change by more than 1–2% i.e. CMC obtained from corrected and uncorrected surface-tension values for DTAB, TTAB and HTAB were 14·7 and 15·0, 3·10 and 3·15, and 0·9 and 0·9 mmol litre^{-1} respectively. These agree well with the more reliable published results (for a detailed discussion see Laycock, 1969). Results for binary mixtures of the three surfactants and the ternary cetrimide sample were obtained, therefore, using uncorrected surface-tension data and are shown in Fig. 1.

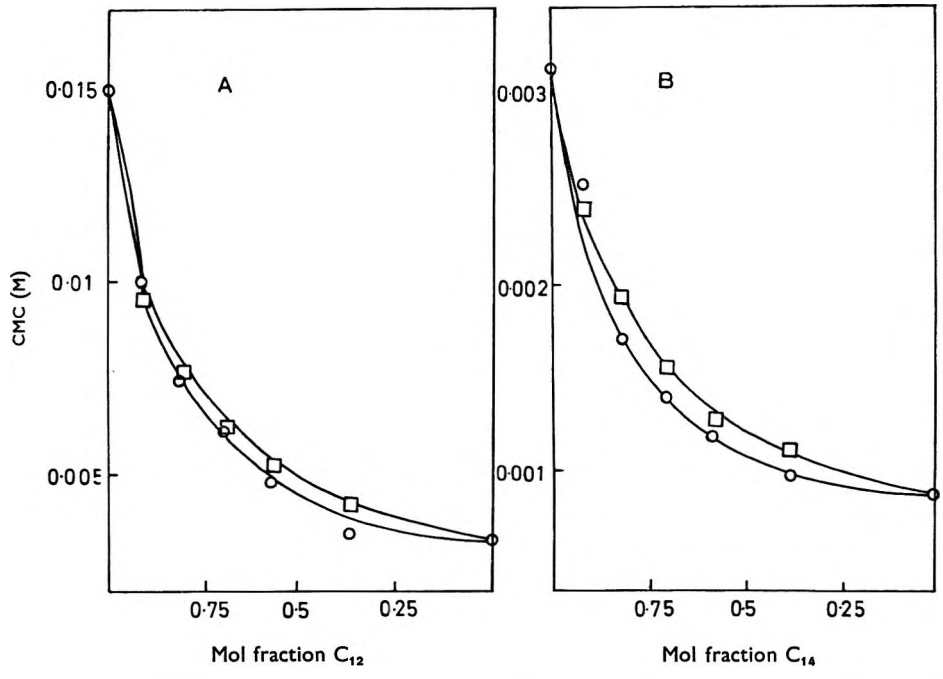

FIG. 1. The CMC at 21° of binary mixtures of cationic surfactants determined by the surface-tension method (circles) compared with calculated values (squares). A. C_{12}/C_{14} mixtures. B. C_{14}/C_{16} mixtures.

The CMC of cetrimide was 2·2 mmol litre^{-1}. The CMC values of the mixtures were always between those of the individual components, although, small amounts of the component with the lower CMC produced a disproportionately large reduction (Klevens, 1948; Lange, 1953 & Shinoda, 1954). The last two authors have examined the CMC values of surfactant mixtures which may be calculated from the values of the individual components and the equation used by Shinoda is:

$$\frac{C_{m1}^{1+Kg}\, x'}{x' + (1 - x') \exp\left[(m_2 - m_1)\, \omega/kT\right]} + \frac{C_{m2}^{1+Kg}\, (1 - x') \exp\left[(m_2 - m_1)\, \omega/kT\right]}{x' + (1 - x') \exp\left[(m_2 - m_1)\, \omega/kT\right]} = C_{mix}^{1+Kg}$$

Where C_{m1}, C_{m2} and C_{mix} are the CMC of the two surfactants and the mixture respectively; x' and $(1 - x')$ are the respective mol fractions; m_1 and m_2 are the numbers of carbon atoms in the paraffin chains; ω is the surface energy change per methylene group passing from the aqueous environment into the micelle and is equal to 1·08 kT; K_g is a constant relating the CMC and the concentration of gegenions. A value of 0·56 for K_g was used (Shinoda, 1954).

Biological measurements

The British Standard method (B.S. 3286: 1960) for "Laboratory Evaluation of Disinfectant Activity of Quaternary Ammonium Compounds by Suspension Test

Procedure" was used for measuring the antibacterial activity of the surfactants and their mixtures. In the particular form of the test adopted, a suspension of a test organism (*Escherichia coli*, NCTC 86) was treated at 21° with a range of concentrations of the surfactants and their mixtures for a fixed time of 15 min so that at least three and preferably four solutions gave survivors in the range 10 to 0·0001%.

Of the two inactivators recommended in the British Standard, 2% lecithin mixed with 3% "Lubrol W", and 10% polysorbate 80, only the polysorbate was satisfactory. The lecithin–Lubrol W inactivator was sometimes lethal. Suspensions of the test organism from subcultures between the 4th and 14th, containing about 100×10^6 organisms per ml were used in the tests and the numbers surviving after treatment with the surfactants were counted by the plate method using a nutrient agar medium (Oxoid CM3). Duplicate plates were used in all counts and an average taken from the results. Plots of log concentration of surfactant against log % survivors gave straight lines (visual estimation) Fig. 2. The error of repeatability lies within ±30%.

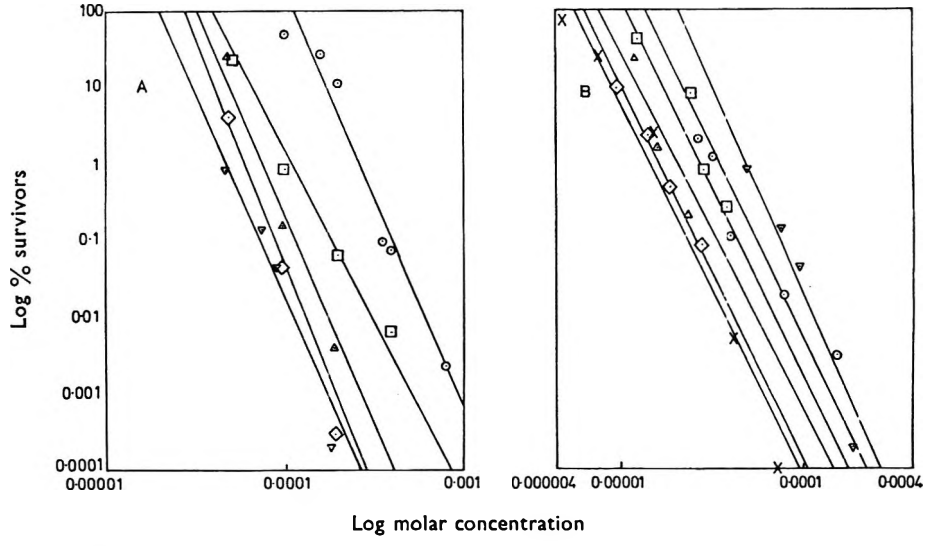

FIG. 2. Effect of concentration of quaternary ammonium compounds on *E. coli*. A, C_{12}/C_{14} mixtures. B, C_{14}/C_{16} mixtures and a ternary mixture.
A. ○ = C_{12}; □ = C_{12}/C_{14}, 0·766/0·234; △ = C_{12}/C_{14}, 0·522/0·478; ◇ = C_{12}/C_{14}, 0·267/0·733; ▽ = C_{14}. B. ▽ = C_{14}; ○ = $C_{12}/C_{14}/C_{16}$, 0·251/0·628/0·121; □ = C_{14}/C_{16}, 0·764/0·236; △ = C_{14}/C_{16}, 0·520/0·480; ◇ = C_{14}/C_{16}, 0·265/0·735; × = C_{16}.

DISCUSSION

One of the ways in which Ferguson's principle may be stated in relation to the toxic effects of materials on bacteria, is that solutions of compounds having the same thermodynamic activity will have equal antibacterial action. For sparingly soluble materials the thermodynamic activity of a solution is given with reasonable accuracy by the ratio of the solution concentration and the concentration of a saturated solution at the same temperature. With surfactants it is convenient to treat the CMC as a solubility limit for the monomolecularly dispersed species (Hartley, 1936), especially when the aggregation number of the micelles is high (Elworthy, Florence & Mac-

farlane, 1968). Light scattering measurements give an aggregation number of 50 for DTAB and higher values for the longer-chain homologues (Debye, 1949). It therefore seems reasonable to calculate the thermodynamic activity of solutions of quaternary ammonium surfactants below the CMC as the ratio of the solution concentration and the CMC. In Table 1 the concentrations of the quaternary ammonium compounds and certain binary and ternary mixtures which kill 99·0 and 99·99% of *E. coli* cells in 15 min at 21° are listed together with related CMC. The latter were derived from the data in Fig. 1. The last two columns of Table 1 compare the thermodynamic activities at the two survivor levels. In almost every case (TTAB values appear slightly low) the thermodynamic activity producing an equivalent biological response is sufficiently close to a constant, bearing in mind the limited accuracy of the antibacterial test, to sustain the Ferguson principle for the systems studied. Thus the antibacterial activity of individual members of the n-alkyl trimethylammonium bromides is linked to their thermodynamic activities and the relation also extends to binary and ternary mixtures.

In comparing biological activity with the surface properties of the antibacterial solutions it is essential to maintain equivalent physical conditions in both sets of measurements. This is relatively easy to do with the physical study but the presence of the cells in the biological measurements almost certainly introduces a variation. Some of the surfactant will be taken up on the cell surfaces and the cells may also release materials which could affect the physical activity of the antibacterial agent by complex formation, precipitation reactions or other means. Reduction in physical activity by adsorption will be less serious if the cell concentration is low and the comparisons are made at low survivor levels where the solution concentrations are high. The results do not provide any indication that the aforesaid factors have a significant effect even for the HTAB system where the solutions are very dilute.

The use of surface concentrations rather than bulk solution concentrations, Weiner & others (1965), is attractive since the mode of action of quaternary ammonium compounds may well involve the cell surface and be analogous to adsorption at the air-water interface. But surface concentrations are difficult to measure and for theoretical reasons the measurements are normally done in the presence of high concentrations of salt (Weiner & Zografi, 1965), which may itself affect the cells. Weiner & others (1965) reported results using bulk concentrations which show a variation in thermodynamic activities of the equitoxic solutions wider than we have found. Their results based on surface concentrations show exceptionally constant thermodynamic activities. However, whether based on bulk or on surface concentrations the thermodynamic activity producing a level of antibacterial activity must always be derived from a ratio involving the latter, and some variation must be accepted. In the present results this is not greater than that expected from the limitations of the biological measurements.

Calculation of the CMC of multi-component systems from data for the individual components is useful since it enables levels of antibacterial activity to be forecast. For example the concentration of a C_{12}/C_{14} mixture (mol fraction C_{12}, 0·522) which gives a 99·99% kill is 0·175mM (Table 1), based on the experimentally determined CMC. The concentration required by calculation of the CMC of this mixture is 0·21mM. The theory also shows that the CMC of multi-component mixtures will always lie between that of the individual components. Since it is linked to antibacterial action, the same will be true of the biological effect of mixtures. Standards for homologue composition of quaternary ammonium surfactants could be set on this basis.

Acknowledgements

We are indebted to Dr. D. Wiseman and other colleagues for advice and many useful discussions during the course of this work.

REFERENCES

ADDERSON, J. E. & TAYLOR, H. (1964). *Proc. 4th Int. Congr. Surf. Activ.*, **2**, 613–619, Brussels.

DEBYE, P. (1949). *J. phys. Colloid Chem.*, **53**, 1–8.

ECANOW, B. & SIEGEL, F. P. (1963). *J. pharm. Sci.*, **52**, 812–813.

ELWORTHY, P. H., FLORENCE, A. T. & MACFARLANE, C. B. (1968). Solubilization by Surface-active Agents, p. 49, London: Chapman and Hall.

HARKINS, W. D. & JORDAN, H. F. (1930). *J. Am. chem. Soc.*, **52**, 1751–1772.

HARTLEY, G. S. (1936). *Aqueous Solutions of Paraffin-Chain Salts*, Paris: Hermann and Cie.

KLEVENS, H. B. (1948). *J. phys. Colloid Chem.*, **52**, 130–148.

LANGE, H. (1953). *Kolloid-Z.*, **131**, 96–103.

LAYCOCK, H. H. (1969). *M. Pharm. thesis*, Univ. of Bradford.

LAYCOCK, H. H. & MULLEY, B. A. (1966). *J. Pharm. Pharmac.*, **18**, *Suppl.*, 9S–11S.

PADDAY, J. F. (1960). *Proc. 3rd Int. Congr. Surf. Activ.*, **1**, 233–238, Cologne.

SHINODA, K. (1954). *J. phys. Chem., Ithaca*, **58**, 541–544.

WEINER, N. D., HART, F. & ZOGRAFI, G. (1965). *J. Pharm. Pharmac.*, **17**, 350–355.

WEINER, N. D. & ZOGRAFI, G. (1965). *J. pharm. Sci.*, **54**, 436–442.

J. Pharm. Pharmac., 1970, **22**, *Suppl.*, 163 S–168 S *Received March* 18, 1970

On the release of drug from hard gelatin capsules

J. M. NEWTON AND G. ROWLEY

Lilly Research Centre Limited, Erl Wood Manor, Windlesham, Surrey, U.K.

The effect of particle size and packing on the *in vitro* release of a water-insoluble hydrophobic drug from hard gelatin capsules has been related to the liquid permeability of powder beds of similar porosities. Drug release and permeability decrease with a decrease in particle size and porosity of the powder bed. A simple moist granulation process transforms a non-permeable powder bed, which allows low drug release, into one with high permeability and high drug release.

The review of the release of drugs from solid dosage forms by Wood (1967), shows that few investigations have been made of the factors affecting the release of drugs from hard gelatin capsules. Differences in biological availability of drugs from capsules, reported by Brice & Hammer (1969) and Glazko, Kinkel & others (1968) can be ascribed to differences in the physical chracteristics of the drug; e.g. crystal form, particle size and the method of formulation. The last effect was demonstrated by Aguiar, Wheeler & others (1968) who were also able to correlate *in vivo* plasma levels of chloramphenicol, administered in capsules of differing formulations, with the results from an *in vitro* dissolution test. Withey & Mainville (1969) reported that differences in the particle size of chloramphenicol altered its release *in vitro* from capsules and they discussed the influence that wetting, deaggregation and packing might have on the drug release. The present report contains details of an investigation of some factors which influence the release of a water-insoluble, hydrophobic drug, ethinamate from hard gelatin capsules and shows one way in which drug release can be improved.

EXPERIMENTAL

Materials

Ethinamate (1-ethynylcyclohexyl carbamate) U.S.N.F., from a single batch of material was graded into size fractions by sieving. A quantity of the unfractionated drug was subjected to fluid energy milling. The resulting powder had a mean particle diameter of 8·3 μm calculated from its specific surface area as determined by the air permeability method of Lea & Nurse (1939). Granules of this micronized ethinamate were prepared by wet granulation with isopropanol. All other chemicals used were of reagent grade.

Methods

Capsule filling. Size No. O hard gelatin capsules (Lilly) were filled using a CAP III capsule filling machine (Tevopharm-Schiedam N.V.). The lowest fill weight for each particle size fraction corresponded to the amount of powder which would occupy the volume of the capsule body without applied pressure. To increase the fill weight for a given size fraction, known weights were applied to the pressure plate to compress the

powder within the capsule body. Each loading was followed by a levelling off with powder until no more powder could be filled into the capsule. By increasing the loading weight, a range of capsules of increasing fill weights was obtained for each size fraction. The capsules were weighed and only those within $\pm 5\%$ of the average fill weight for the filling conditions were retained. The porosity of the bed of powder within the capsule, was calculated as the ratio of the volume of voids to the total capsule volume, assuming that the powder was distributed evenly throughout the capsule shell.

Dissolution testing. This was by the beaker method of Levy & Hayes (1960) at a stirring rate of 45 rev/min. The capsule was held in a spiral of stainless steel wire (0·86 mm d), 5 cm long, 0·8–1·0 cm d with approximately 5 coils per 2 cm. This was held horizontally, 1 cm above a circular loop (5 cm d) of stainless steel wire (1·0 mm d), which was placed centrally at the bottom of a wide necked, round bottom flask containing 1 litre of distilled water. During the test, samples were taken at known time intervals, filtered and the ethinamate in solution determined by refluxing for 2 min with 1% sulphuric acid and estimation of the ammonium salt formed with Nessler's reagent. Allowance was made for the drug removed in the sample volume and results were calculated as a percentage of the total drug originally present. The results are the mean of 8 replicate dissolution tests. The percentage in solution–time curves followed the same general pattern (approximating to an exponential decrease in amount of release with time), hence comparison of different capsules was made at a constant time of 30 min.

Disintegration time of capsules. This was determined by the B.P. disintegration test, but using single capsules, the results being the mean of 5 replicates.

Permeability. The permeability of powder beds of different porosities was measured by the pressure decline method of Dodd, Davis & Pigdeon (1951). A saturated aqueous solution of ethinamate was used as permeating liquid to prevent changes in bed structure due to ethinamate dissolving. It was not possible to obtain a bed of micronized ethinamate through which the liquid would readily permeate without forming channels.

The Kozeny (1927) equation as used by Carman (1937) relates the flow rate of a fluid through a bed of powder, to the characteristics of the bed and the permeating fluid, and can be expressed as

$$Q = \frac{1}{k}\frac{A}{\eta So^2}\frac{\epsilon^3}{(1-\epsilon)^2}\frac{\rho g h}{L} \quad .. \quad .. \quad .. \quad .. \quad (1)$$

where Q = volume rate of flow of liquid through the bed; k = dimensionless constant, known as the Kozeny constant and taken as 5; A = cross sectional area of the powder bed; η = viscosity of the permeating fluid; So = specific surface area per unit volume; ϵ = fractional porosity of the packed powder bed; ρ = density of the permeating fluid; g = acceleration due to gravity; h = drop in fluid head across the powder bed; L = depth of powder bed.

Equation (1) may be written in the form

$$Q = K \rho h \quad .. \quad .. \quad .. \quad .. \quad .. \quad (2)$$

where

$$K = \frac{1}{k}\frac{A}{\eta So^2}\frac{\epsilon^3}{(1-\epsilon)^2}\frac{g}{L} \quad .. \quad .. \quad .. \quad .. \quad (3)$$

Equation (1) may also be arranged in a form equivalent to Darcy's law for isothermal

liquid streamline flow through a porous media as

$$Q = B_0 \frac{A}{\eta} \frac{\rho g h}{L} \quad .. \quad .. \quad .. \quad .. \quad (4)$$

where B_0 = the "permeability coefficient" or permeability. Comparison of equation (2) with equation (4) yields the relation

$$B_0 = \frac{\eta K L}{A g} \quad .. \quad .. \quad .. \quad .. \quad .. \quad (5)$$

In terms of experimental work B_0 can be calculated by employing the values of K, as determined by the method of Dodd and others (1951), in the equation (5).

RESULTS AND DISCUSSION

The percentage of drug released into the solution from the capsule after 30 min is shown as a function of the porosity of the bed of material within the capsule shell in Fig. 1A. The relation obtained is dependent on the particle size of the drug. If dissolution is compared at the same porosity, a larger percentage of drug is released from capsules containing the larger particle size fractions. The larger particle size fractions are not greatly influenced by the packing within the capsules, but as the particle size of drug decreases, packing larger quantities of material into the capsule causes a marked decrease in the percentage of drug released. For the smallest particle size fraction tested, the decrease in drug release took place over a small porosity range and thereafter decreasing porosity had little effect on drug release.

Within the conditions of filling, a larger range of porosities can be obtained as the particle size decreases because of the higher initial voidages associated with finer particles. Reducing the particle size will also decrease the size of pores between the particles which will reduce the ease of access of dissolution media to the powder mass. If this is a significant restriction, the release of drug will be reduced. To obtain a measure of the effect of particle size and packing on the access of dissolution medium to

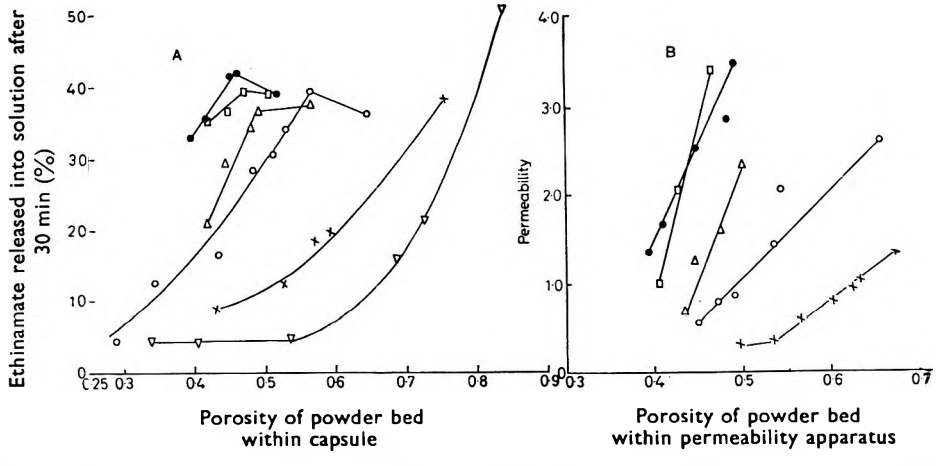

FIG. 1. A. The percentage of drug released after 30 min from capsules containing different particle size fractions of ethinamate packed to give different porosities. B. The liquid permeability ($m^2 \times 10^{11}$) of equivalent particle size fractions at known porosities. ●——● 251–420 μm. □——□ 177–251 μm. △——△ 152–177 μm. ○——○ 125–152 μm. +——+ 66–76 μm. ▽——▽ 8·3 μm.

the powder bed, we applied the liquid permeability method of Dodd & others (1951). The results for the same powders, under packing conditions as near as possible to those within the capsule, are shown in Fig. 1B. The results relate qualitatively to the dissolution results, the larger the particle size and the higher the porosity, the greater is the permeability of the bed: there is not, however, complete correlation. The larger particle sizes show more rapid change in permeability with porosity than the smaller particle sizes, whilst in certain regions of porosity, the reverse is true of drug release. This difference can be attributed to the fact that permeability is not the only factor involved in the dissolution process, the disintegration of the capsule, and the characteristics of the resultant powder mass being also important. The disintegration time of capsules containing 251–420 μm particles is lower than those containing smaller particle sizes and is less influenced by packing (Table 1). Thus, the larger size particle

Table 1. *Porosity of capsule fill* (ϵ) *and disintegration time* (D) *of capsules of ethinamate of different particle size fractions*

Particle size fraction							
251–420 μm		251–420 μm (granules)		124–152 μm		8·3 μm	
ϵ	D (min)	ϵ	D (min)	ϵ	D (min)	ϵ	D (min)
0·515	5·7	0·763	2·7	0·646	7·3	0·833	18·4
0·459	4·6	0·678	3·6	0·531	4·5	0·726	13·75
0·416	4·5	0·604	3·7	0·511	7·75	0·686	17·1
0·403	4·75	0·514	5·0	0·484	6·1	0·485	>30·0
				0·435	5·9		
				0·290	10·6		

systems break up and form a powder mass on the bottom of the beaker which probably has a higher porosity than the powder mass within the capsule. The smaller particles with extended disintegration times, however, do not break up readily and in extreme cases remain virtually in the same structure as that within the capsule. When the mass does not disintegrate readily, permeability will more nearly parallel dissolution, although in extreme cases the very low permeability will only allow dissolution to take place from the outermost surface of the capsule-shaped powder mass which often remains. In these cases increasing the quantity of drug within the capsule will not affect dissolution, e.g. the dissolution results for capsules containing micronized material.

The results from the permeability experiments can be used to determine the specific surface area of different size fractions, under similar packing conditions to those within the capsule, see Table 2. Comparison of these results with those for dissolution leads to the conclusion that, although the specific surface area increases with decrease in particle size, it is not available for dissolution. Studies on the dissolution rates from powdered drugs by Finholt, Kristiansen & others (1966), illustrated that granulation of powders increased the availability of the surface as indicated by dissolution. We prepared granules from micronized material which when dried, were sieved to give the same particle size as the largest individual size fraction of crystals tested, i.e. 251–450 μm. The dissolution and permeability of these two types of material are compared in Fig. 2. The results show the advantage of granulating the

Table 2. *Specific surface area per unit volume (So), of ethinamate size fractions as determined by liquid permeability at different porosities* (ϵ)

Size fraction μm	ϵ	So cm²/cm³	Size fraction μm	ϵ	So cm²/cm³	Size fraction μm	ϵ	So cm²/cm³
251–420	0·491	514	125–152	0·655	1348	251–420 Granulated	0·583	336
	0·482	543		0·543	872		0·565	360
	0·448	484		0·490	1029		0·537	330
	0·409	491		0·471	986		0·523	376
	0·398	490		0·448	1034		0·507	416
177–251	0·468	463		0·674	2070			
	0·428	484		0·633	1914			
	0·408	627		0·626	1940			
152–177	0·501	660	66–76	0·601	1866			
	0·475	701		0·564	1799			
	0·446	676		0·536	2026			
	0·435	880		0·497	1815			

micronized drug. Again, there is a clear relation between dissolution and permeability. The ranges of porosity used in the dissolution tests are higher than those of the permeability tests because the liquid pressure head in the permeability apparatus causes initial compaction of the powder bed. Thus permeabilities of powder beds of granules within the capsules will be even higher than those in Fig. 2. Because there is not a parallel increase in the rate of release of drug from capsules containing granules, we must again conclude that permeability alone does not control dissolution. The similarity of the specific surface areas of crystalline and granulated ethinamate, as determined by liquid permeability (Table 2) again indicates a lack of correlation

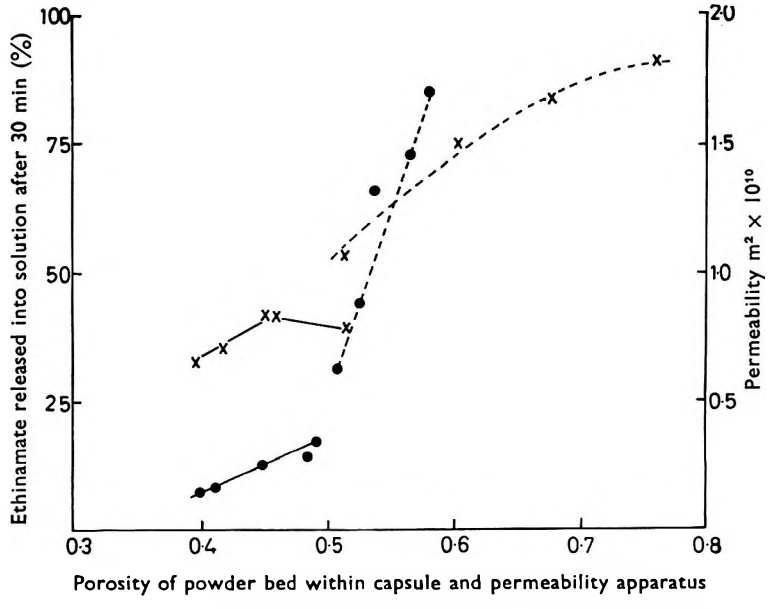

FIG. 2. A comparison of percentage of drug released after 30 min from capsules containing 251–420 μm crystals and 251–420 μm granules of micronized ethinamate, packed to give different porosities, and the liquid permeability of beds of the same samples. —— 251–420 μm crystals. - - - - - - 251–420 μm granules. ● Liquid permeability. × Dissolution.

between permeability and dissolution. As noted previously, the time taken for the capsule to disintegrate under standard conditions does not solely control drug release. The capsules containing the granulated drug had similar disintegration times to those containing crystals of same particle size range see Table 1.

In the presentation of water insoluble hydrophobic drugs in capsules, it is important to ensure that a water permeable mass exists within the capsule and we have demonstrated one method whereby this may be achieved. This is based on capsules filled by one particular process. Capsules filled by alternative processes, especially those in which a slug is formed, may require different formulation methods. To ensure adequate drug release, however, penetration of liquid into the powder mass and its break up into readily available particles is essential.

Acknowledgements

The authors wish to express their thanks to Professor P. H. Elworthy for helpful discussion and Miss R. J. Maidment and Miss F. M. Turford for their technical assistance.

REFERENCES

AGUIAR, A. J., WHEELER, L. M., FUSARI, S. & ZEHNER, J. E. (1968). *J. pharm. Sci.*, **57**, 1844–50

BRICE, G. W. & HAMMER, F. H. (1969). *J. Am. med. Ass.*, **208**, 1189–90.

CARMAN, P. C. (1937). *Trans. Inst. Chem. Eng.*, **15**, 150–66.

DODD, C. G., DAVIS, J. W. & PIDGEON, F. D. (1951). *J. phys. Colloid Chem.*, **55**, 684–98.

FINHOLT, P., KRISTIANSEN, H. SCHMIDT, O. C. & WOLD, K. (1966). *Meddr norsk farm. Selsk.*, **28**, 17–47.

GLAZKO, A. J., KINKEL, A. W., ALEGNANI, W. C. & HOLMES, E. L. (1968). *Clin. Pharmac. Ther.*, **9**, 472–83.

KOZENEY, J. (1927). *Sber. Akad. Wiss. Wien.*, **136**, 271–306.

LEA, F. M. & NURSE, R. W. (1939). *J. Soc. chem. Ind., Lond.*, **58**, 277–83.

LEVY, G. & HAYES, B. A. (1960). *New Eng. J. Med.*, **262**, 1053–8.

WITHEY, R. J. & MAINVILLE, C. A. (1969). *J. pharm. Sci.*, **58**, 1120–6.

WOOD, J. H. (1967). *Pharm. Acta Helv.*, **42**, 129–151.

J. Pharm. Pharmac., 1970, 22, *Suppl.*, 169 S–174 S *Received March* 13, 1970

The absorption, blood concentrations and excretion of pentazocine after oral, intramuscular or rectal administration to man

A. H. BECKETT, P. KOUROUNAKIS*, D. P. VAUGHAN AND M. MITCHARD

Department of Pharmacy, Chelsea College (University of London), Manresa Road, London, S.W.3, U.K.

Blood concentrations, urinary excretion rates and faecal excretion of unchanged drug were measured after oral, intramuscular or rectal administration of pentazocine; *Significant inter-subject variation* was observed. Blood concentration-time curves are related to urinary excretion rates. Relative physiological availabilities by each route were determined.

The urinary excretion of pentazocine in man shows large inter-subject variation and only a relatively small amount of unchanged drug is excreted by this route (Berkowitz & Way, 1969; Beckett, Taylor & Kourounakis, 1970). We have attempted to evaluate the physiological availability† of pentazocine by different routes of administration using an acid urine to prevent reabsorption of unchanged drug in the kidney tubules (Beckett & Tucker, 1967) and have used each subject for a comparative study of different formulations.

Cumulative urinary excretion of unchanged pentazocine is used to assess the relative physiological availability by the different routes.

EXPERIMENTAL

The subjects (I–IV) and procedures of Beckett & others (1970) were used but, in the GLC analysis of pentazocine, dipipanone as well as α-methadol was used as an internal standard.

Pentazocine administration

Oral route. Tablets (Fortral, Bayer) instead of solutions (Beckett & others, 1970) were used. These were taken in a single dose (four tablets of pentazocine HCl equivalent to a total of 88·7 mg base), or as two doses, each equivalent to 88·7 mg base, separated by 2 h.

Intramuscular route. 1 ml of aqueous pentazocine HCl (≡40 mg base) was injected into the *gluteus maximus* muscle.

Rectal route. A suppository (100 mg pentazocine base as lactate in 1·661 g Suppocire AM, Gattefossé—sfpa) was inserted high into the rectum.

* Present address: Faculty of Pharmacy, University of Montreal, Case Postale 6128, Montreal 101, Canada.

† Physiological availability is interpreted as the amount of drug available from the preparation to give a pharmacological or clinical response, whereas, *biological availability* is interpreted as the amount of drug available in a form which can be absorbed.

RESULTS

Urinary and faecal excretion

The 24 h urinary recoveries of unchanged drug for all subjects and routes are presented in Fig. 1. Faecal recoveries of unchanged drug after oral and rectal administration, ranged from 0·1 to 0·8% of the administered dose. Data obtained after oral administration as a solution (Beckett & others, 1970) are included for comparison.

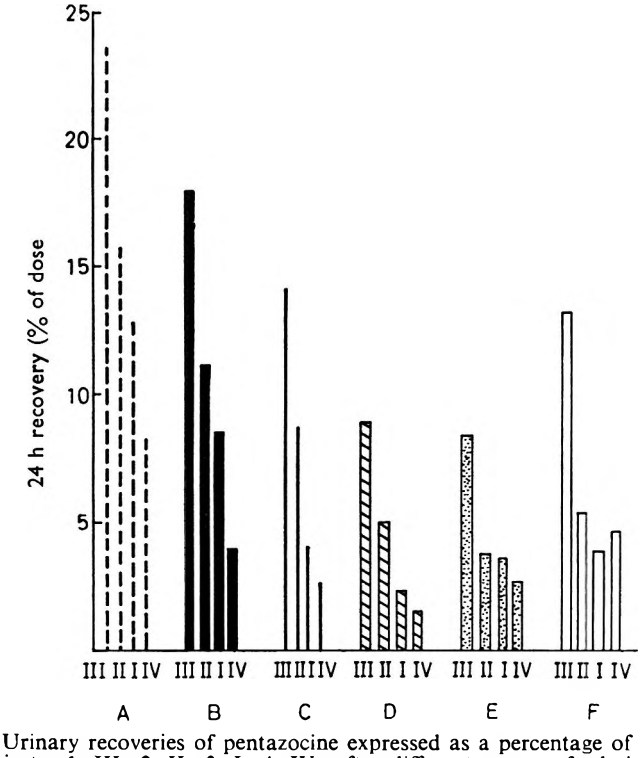

FIG. 1. 24 h Urinary recoveries of pentazocine expressed as a percentage of administered dose from four subjects: 1, III; 2, II; 3, I; 4, IV; after different routes of administration. A, i.v. (24 mg base)*; B, i.m. (40 mg base); C, oral (solution) (88·7 mg base)*; D, oral (tablets) (88·7 mg base); E, suppositories (100 mg base); F, two oral tablet doses (each 88·7 mg base) separated by a period of 2 h.

Concentration of pentazocine in blood and urine

Blood concentrations for successive samples after oral, intramuscular and rectal administration are shown in Fig. 2 as are the urinary excretion rates for two of the four subjects (III and IV); the profiles for I were similar to those of IV whereas those for II were similar to those of III. The blood levels and urinary excretion rates after 2 × 88·7 mg of pentazocine base are shown in Fig. 3. The ratios of the total amount of pentazocine excreted in the urine during a 24 h period after intravenous injection (Beckett & others, 1970) relative to the amount excreted after the other routes of administration, are shown in Table 1. The approximate urinary elimination half lives ($t_{\frac{1}{2}}$) of pentazocine, obtained from semi-logarithmic plots of urinary excretion after the initial absorption phase, and the ratios of the areas under the urinary excretion curves to that under the blood curves (expressed in arbitrary but relative units for each route and subject) are also shown in Table 1.

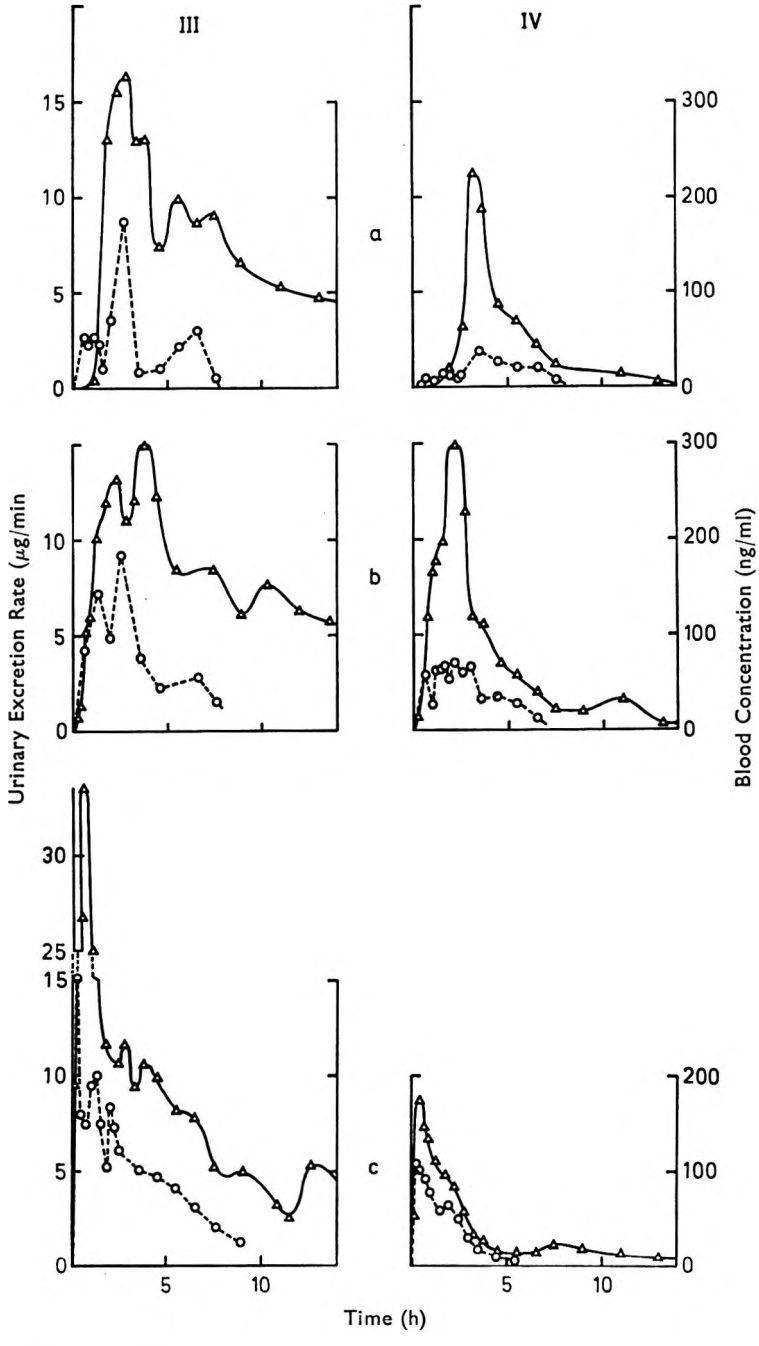

FIG. 2. Urinary excretion rates and the corresponding blood levels of pentazocine after administration of (a) oral tablets (88·7 mg base); (b) suppository (100 mg base) and (c) i.m. injection (40 mg base) to subjects III and IV, under conditions of acidic urinary pH. —△— Urinary excretion rates. —○— Blood concentration.

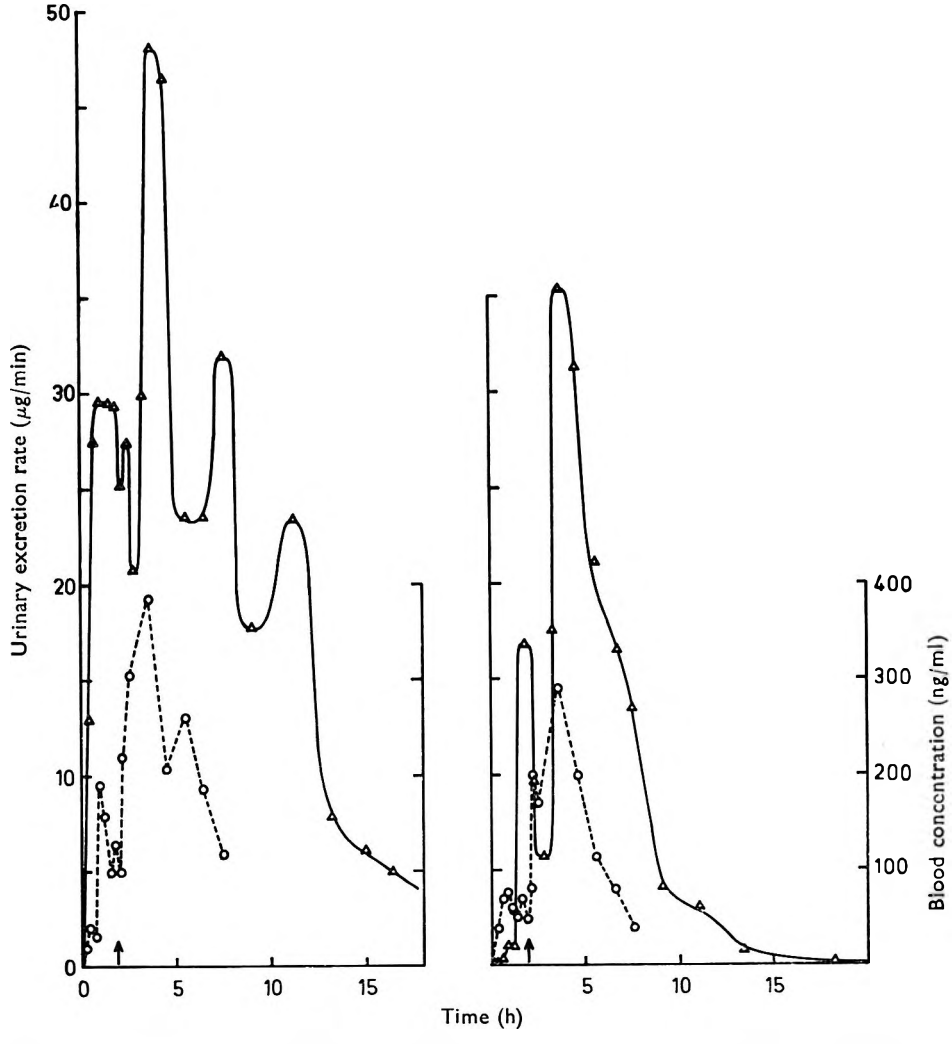

FIG. 3. Urinary excretion rates and the corresponding blood levels of pentazocine after administration of two oral tablet doses (each 88·7 mg base) to subjects III and IV under conditions of acidic urinary pH. —△— Urinary excretion rate. —○— Blood concentration.

DISCUSSION

Figs 2 and 3 indicate that when the urine is acid, blood concentrations are related to urinary excretion rates as with amphetamine (Beckett & others, 1969). Consistent inter-subject variation in blood concentrations and urinary excretion rates was observed for the various routes of administration of pentazocine; for example, subject III always had higher blood concentrations and a greater percentage recovery of unchanged drug in urine than did subject IV for comparable routes (Fig. 1). Thus unlike many other basic drugs, the determination of the relative physiological availability of pentazocine from various pharmaceutical forms must involve studies in each individual.

Two subjects in this study had a smooth urinary excretion curve and blood concentrations that did not fluctuate greatly (I and IV), two showed fluctuations in both

Table 1. *The relative physiological availabilities, half lives and urine excretion curve areas relative to blood curve areas obtained in man after different routes and forms of administration*

	Relative physiological availabilities‡ (RPA) and urinary excretion half lives ($t_{\frac{1}{2}}$ h)								Area under urine excretion curve / Area under blood concentration curve (in arbitrary units)			
	I		II		III		IV					
Route	RPA	$t_{\frac{1}{2}}$	RPA	$t_{\frac{1}{2}}$	RPA	$t_{\frac{1}{2}}$	RPA	$t_{\frac{1}{2}}$	I	II	III	IV
Intravenous* ..	1	2·8	1	2·5	1	6·0	1	1·7	1·25	0·89	1·42	0·63
Intramuscular ..	1·5	3·0	1·4	1·5	1·3	5·2	2·1	1·9	0·71	0·80	0·84	0·67
Oral solution* ..	3·1	2·5	1·8	2·0	1·7	5·5	3·1	1·8†	1·17	0·96	1·42	0·71
Oral tablets ..	5·4	3·2	3·1	2·5	2·6	6·5	5·2	2·3	1·00	1·33	1·54	1·50
Rectal suppository	3·5	3·1	4·1	2·2	2·8	6·4	3·1	2·4†	0·89	1·00	1·00	1·20
Two oral doses	3·2	ND	2·9	ND	1·8	ND	1·7	ND	1·13	1·00	1·30	1·10

† Estimated from a line of best fit because of non-linear terminal part of semi-log graph of excretion/time.

‡ Relative physiological availability ≡

The 24 h urinary excretion of unchanged drug after intravenous administration expressed as a percentage of the dose

The 24 h urinary excretion of drug administered by a different route, or as different formulations, expressed as a percentage of the dose.

* Data from Beckett & others (1970).

ND—Not determined.

aspects (II and III) (Figs 2 and 3). The latter two subjects excreted the greater amount of unchanged drug in the urine (Fig. 1). The similarity of the profiles for blood concentrations and urinary excretion rates (acidic urine) for each of the subjects using the different routes of administration indicates that the fluctuations in blood concentrations are not artifacts arising from sampling or analytical techniques.

Despite the relatively small amount, it is proposed to compare the relative amounts of unchanged drug excreted in the urine (cumulative 24 h) in each subject by each route as a method for assessing the relative physiological availability of pentazocine by each route. This is done because:

(*a*) the areas under the blood curves and urinary excretion curves gave similar ratios for each method of drug administration to each individual (Table 1); (*b*) although the subjects showed variation in the 24 h urinary excretion of pentazocine expressed as a percentage of the administered dose, there was no inter-subject variation between the *relative* physiological availabilities obtained for each route of administration or formulation; (*c*) the large differences in blood concentrations and in the urinary excretion of unchanged drug using different routes of administration cannot be accounted for by a failure to make the drug available for absorption because faecal recoveries of unchanged drug were negligible; (*d*) the apparent urinary elimination half lives ($t_{\frac{1}{2}}$) for pentazocine after intravenous and intramuscular administration are similar to the apparent $t_{\frac{1}{2}}$ values obtained after oral and rectal administration, the $t_{\frac{1}{2}}$ being different for each individual (Table 1); the absorption of pentazocine into the systemic circulation is complete after 2–3 h by oral or rectal routes.

Table 1 shows that changes from intravenous to intramuscular route, to oral solution and then to oral tablet requires an increase in the dose of 1·5, 2–3 and 3–5 times respectively, to obtain similar cumulative urinary excretion profiles and similar

blood levels. Rectal administration shows a greater variation, about twice the dose being required by this route than by mouth using a solution for subjects II and III whereas approximately equal doses are required for subjects I and IV (Fig. 1).

When two doses of pentazocine (each of four tablets = 88·7 mg base) were given 2 h apart there was an increase in the percentage of unchanged drug in the urine compared to that obtained from a single oral tablet dose (Fig. 1). This increase indicates that the percentage of the dose metabolized has been reduced. Substrate inhibition or saturation of the enzymes involved in the transformation of pentazocine may be responsible for the reduction in the percent metabolized. Thus the reduction in apparent biological availability from an oral tablet dose, relative to an oral solution dose (1·7 for *all* subjects, see Fig. 1) may be due to the slow release of pentazocine in the gastrointestinal tract. Slow release implies lower concentrations of pentazocine at the enzymatic sites and hence a greater proportion metabolized.

Unlike some other drugs, e.g. fenfluramine (Brookes, 1968), it is therefore necessary to give different amounts of pentazocine by the different routes to provide similar physiological availabilities from the different formulations.

Acknowledgements

We thank all who participated in the drug trials; the Bayer Products Company, Surbiton, Surrey for supplying pentazocine.

REFERENCES

Beckett, A. H., Salmon, J. A. & Mitchard, M. (1969). *J. Pharm. Pharmac.*, **21**, 251–258.
Beckett, A. H., Taylor, J. F. & Kourounakis, P. (1970). *Ibid.*, **22**, 123–128.
Beckett, A. H. & Tucker, J. F. (1967). *J. Mond. Pharm.*, **3**, 181–202.
Berkowitz, B. & Way, E. L. (1969). *Clin. Pharmac. Ther.*, **10**, 681–689.
Brookes, L. G. (1968). Ph.D. Thesis, University of London.